Diss. ETH Nr. 14129

Structural Aspects of Neuropeptide Y: Implications of the Membrane-bound State for Receptor Recognition and Subtype Selection Studied by NMR

A dissertation submitted to the
Swiss Federal Institute of Technology Zürich
for the degree of
Doctor of Natural Sciences

presented by
Reto Bader
Diplom-Biologe
Universität Bern

born on April 25, 1971
citizen of Olten (Solothurn)

accepted on the recommendation of
Prof. Dr. Gerd Folkers, examiner
Prof. Dr. Annette G. Beck-Sickinger, co-examiner
Dr. Oliver Zerbe, co-examiner

2001

Vorwort

Moderne Molekularbiologie und NMR-Spektroskopie ergänzen sich wunderbar, um Informationen über die Bauweise und die Dynamik von biologischen Makromolekülen zu gewinnen und daraus etwas über ihre Wirkungsweise zu lernen. Mein erster Dank geht an Dr. Oliver Zerbe für das mir geschenkte Vertrauen bei der Besetzung seiner Doktorandenstelle anno 98 und das mir überantwortete Dissertationsthema. Die Methodenvielfalt hätte nicht interdisziplinärer und die Arbeitsatmosphäre freundschaftlicher nicht sein können. Die Schatztruhe oder besser Trickkiste mit NMR-Experimenten ist gross und wird immer voller. Oliver hat sie für mich ein bisschen geöffnet und die Spins vor meinen Augen tanzen lassen. Äs härzlechs Merci!

Der Gegenstand unserer Untersuchungen war ein erst seit Beginn der 80er-Jahre bekanntes Neurohormon, das eine wichtige Rolle bei der Regulation einer Vielfalt von Körperfunktionen spielt. Dass mein Thema in einem derart spannenden Gebiet angesiedelt war, habe ich Prof. Annette Beck-Sickinger zu verdanken. Es war schön, in ihrer Gruppe jederzeit willkommen geheissen worden zu sein!

Ein Grossteil der Arbeit wäre ohne die Mitglieder und das Labor von Prof. Gerd Folkers nicht möglich gewesen. Für die guten Voraussetzungen und die Übernahme des Referats mein bester Dank.

Viel zu meiner Motivation beigetragen haben Prof. Leonardo Scapozza und Dr. Erich Weber. Im Labor konnte ich viel von Erichs Wissen profitieren. Für ihr allgemeines Interesse, die interessanten Diskussionen und natürlich für die sportliche Haltung (indoors and out of doors) beiden ein grosses Dankeschön und grazie!

Drei Personen, die während einer gewissen Zeit näher in das Projekt involviert waren oder noch sind, gebührt meine nächste Anerkennung. Gestartet wurde der Teil über die „Fress"-Verhalten auslösenden Hormone mit dem Molekül Q32 von Dr. Chiara Cabrele. Die vielen Diskurse mit ihr hatten einige

Ideen zur Folge und waren in Bezug auf Nahrungsaufnahme klar antagonistisch wirksam. Gaby Rytz hat es sich zur Aufgabe gemacht, das erwähnte Hormon in Bakterien zu produzieren. Dafür, dass sie den Mut hatte, während ihrer Diplomarbeit von mir überwacht zu werden, und für ihre zahlreichen schönen Resultate mein herzlicher Dank. Mirjam Lerch, meiner Nachfolgerin auf dem Projekt, danke ich für die mannigfaltigen Hilfeleistungen bei der Fertigstellung der Arbeit (inkl. Sätzli und moralische Unterstützung).

Mein Dank geht an Andrea Bettio für die Gastfreundschaft während meines Leipzig-Aufenthalts. Und ohne die Einladungen von und geselligen Abende bei Michaela Dinger, Regula Pohl und Ulrike Krauss wäre die besondere Atmosphäre in der Gruppe Beck-Sickinger sicher nicht zustande gekommen.

Dasselbe gilt natürlich auch in Zürich: Kaffee-Pausen mit Dr. Susanne Gonser und Stefan Reinelt (und auch mal Séverine Dédier) wirkten wunder - nicht nur wegen des Koffein-Nachschubs. Nicht zu vergessen sind die DVD-Abende von Regula Johner und Pierre Schelling. Und Pavel Pospisil möchte ich herzlich danken, dass er mir für das letzte Diss.-Jahr ein Zimmer vermittelt und mich als Zimmernachbar erduldet hat.

Als Instituts-Wichtel sind die Phytos bekannt. Besonders danke ich der Hobby-Confiseurin Karin Winkelmann, Pınar Akbay und Fatima Hilmi für die vielen Gespräche über alles mögliche und unmögliche.

Dank gebührt auch René Bemsel und dem Schalter-Team, Miepie Brändle und Anita Caputo und ihren Kolleginnen für ihre unterstützenden Arbeiten.

Mitverantwortlich für die Wahl meines Diss.-themas ist Dr. Michel Hochuli. Merci für zahlreichen fachlichen Gedankenaustausch und die gemeinsame Zeit in Zürich! Auch Markus Kaufmann gebührt ein besonderer Dank, insbesondere für die Fyrabe-Bier und dafür, dass er mich mehrmals in den Genuss seiner ausgezeichneten Kochkünste kommen liess.

Einige lange Abende in Basel oder Zürich durfte ich mit Michael Marti verbringen und die Gemeinsamkeiten und Unterschiede von Doktoraten in Volkswirtschaft und Naturwissenschaften kennenlernen. Es ganz speziells Merci für aui fründschaftleche Tips!

Schliesslich danke ich meinen Eltern und meiner Familie für die Unterstützung, auf die ich in all meinen Studienjahren stets zählen konnte.

We bear and are borne by a soul we do not know. When the riddle raises itself on two legs without being solved, it is our turn. When the dream picture pinches its own arm without waking, it is us. For we are the riddle no one guesses. We are the fairy-tale trapped in its own image. We are what moves on and on without arriving at understanding.

Jostein Gaarder

Table of Contents

Summary 5
Zusammenfassung 9
Abbreviations 13

Chapter 1:
Introduction 15

1.1. Structure and function of G protein coupled receptors 19
Structural aspects 19
Evolutionary aspects and classification of GPCRs 20
The two-state model of receptor activation 27
The role of lipids in biological membranes 28
Membrane bound pathways for ligand/receptor recognition 33

1.2. Reduced models to study G protein coupled receptors 35
Binding properties of single loops and terminal fragments 36
The role of disulfide bonds for receptor function 37
Split G protein coupled receptors and assembly from fragments 38
Minimum structural requirements for a functional GPCR 39

1.3. NMR spectroscopy of membrane receptors and their ligands 40
NMR of peptide hormones 43
NMR of G protein coupled receptors 48
NMR of ligand/receptor interactions 52

1.4. The structure of Neuropeptide Y: Aims & scopes of this work 55

1.5. References 62

Chapter 2:
Structure and Dynamics of Micelle-bound Neuropeptide Y: Comparison with Unligated NPY and Implications for Receptor Selection **75**

2.1. Introduction 76

2.2. Results 81
Three-dimensional structure of NPY bound to DPC micelles 82
Hydrogen exchange experiments 87
Spin-label studies 88
Probing of the dimerization interface of NPY in aqueous solution 91

2.3. Discussion 103
The structure of NPY in aqueous solution and on DPC micelles 103
Interaction of NPY with a phosphocholine membrane mimetic 107
Biological implications for receptor selection 110

2.4. Conclusion 115

2.5. Materials and Methods 116
Materials 116
Production of ^{15}N-labeled porcine NPY 117
Solid-phase peptide synthesis 118
NMR spectroscopy 119
Structure determination 121
Spin-label experiments 122
Relaxation data analysis 123

2.6. Acknowledgement 125

2.7. References 126

2.8. Supplementary Materials 135

Chapter 3:
The First Selective Agonist for the Neuropeptide YY_5 Receptor Increases Food Intake in Rats **141**

3.1. Introduction 142

3.2. Results 144
[Ala^{31},Aib^{32}]pNPY: Selectivity and agonism at the Y_5 receptor 144
Ala^{31}-Aib^{32}: Key motif for Y_5 receptor selectivity 146
Stimulation of food intake in rats by selective Y_5 receptor activation 147
Structural characterization of [Ala^{31},Aib^{32}]pNPY 150

3.3. Discussion 153

3.4. Materials and Methods 157
Materials 157
Peptide synthesis and purification 157
Cell culture 158
Binding assays 158
cAMP enzyme immunoassays 159
Food intake studies 159
CD spectroscopy 159
NMR spectroscopy 160
Structure calculation 160

3.5. Acknowledgement 161

3.6. Footnotes 161

3.7. References 162

3.8. Supplementary Material 167

Chapter 4:
The Key Motif to Gain High Affinity and Selectivity at the Neuropeptide Y_5 Receptor II: Solution Structure and Dynamics of [Ala^{31},Pro^{32}]-NPY **169**

4.1. Introduction 170

4.2. Results 174
Secondary chemical shifts 175
Interresidual NOEs and coupling constants 178
Three-dimensional structure 180
Topological orientation 182
Amide proton H/D exchange 184
Backbone-dynamics 184

4.3. Discussion 188

4.4. Materials and Methods 196
Materials 196
Peptide synthesis 196
Cloning, expression, and purification of uniformly ^{15}N enriched [Ala^{31}, Pro^{32}]-pNPY 196
CD spectroscopy 197
NMR spectroscopy 198
Spin-label experiment 199
Hydrogen exchange 199
Structure calculation 200
Relaxation data analysis 200

4.5. References 201

4.6. Supplementary Materials 208

Chapter 5:
Towards a Peptide Model Mimicking the Third Extracellular Loop of a Neuropeptide Y Receptor 213

5.1. Introduction 213

5.2. Results and Discussion 217
Characterization of N-acetylated and C-terminally amidated peptides derived from the e3-loops of three Y receptor subtypes 217
Synthesis of a lipopeptide mimicking the third extracellular loop of the Y_1 receptor 222

5.3. Materials and Methods 226
Materials 226
Solid-phase peptide synthesis 227
NMR spectroscopy 228

5.4. References 229

Curriculum Vitae 233
Publications 234

Summary

The present dissertation is concerned with the determination and interpretation of structure-activity-relationships of the neurohormone and -transmitter neuropeptide Y (NPY). NPY is a 36-residue and C-terminally amidated peptide hormone and represents the natural ligand of the NPY family of G protein coupled receptors. This family consists of 6 presently known receptor subtypes, that have been associated with several important physiological effects. As could be shown previously, the selective recognition of the NPY Y_5 receptor, which is involved in the regulation of food intake, is achieved by the introduction of a characteristic dipeptidic key motif in positions 31/32. The presented nuclear magnetic resonance (NMR) studies allow to discuss this phenomenon on a structural basis.

In the first part of this work, native NPY is structurally characterized in solution. For some peptide hormones it is postulated, that binding to the cell membrane, in which the receptors are embedded, is an essential step preceeding receptor recognition. The studies have therefore also been conducted in the presence of dodecylphosphocholine (DPC) micelles, which is a well-known membrane-mimetics in NMR spectroscopy. In order to simplify the resonance assignment procedure with respect to signal overlap and to permit the investigation of dynamics, NPY-glycine (pro-NPY 1-37) was cloned C-terminally fused to decahistidine-tagged ubiquitin. The fusion-protein was expressed while uniformly labeling the nitrogen atoms with the ^{15}N-isotope. The purification strategy was based on Ni^{2+}-affinity chromatography. The conversion of NPY-glycine into the C-terminally amidated NPY was performed by use of the enzyme peptidylglycine-α-amidating monooxygenase. The studies of NPY free in solution focussed on the characterization of its quarternary

structure. A heterodimer was formed consisting of ^{15}N-labeled NPY and ^{14}N-NPY, that contained the spin-label TOAC in position 34. In a [^{15}N,^{1}H]-HSQC experiment it was shown that in the absence of membranes the hydrophobic side of the helix is masked by dimerization in parallel as well as anti-parallel arrangements, however, without involving the C-terminal tetrapeptide. The flexibility of the C-terminal part is supported by ^{15}N-relaxation measurements, so that the C terminus retains the high flexibility observed in aqueous solution. In addition, the question was addressed, whether the N terminus folds back onto the C-terminal helix. Such a tertiary fold had previously been described for the pancreatic polypeptide (PP) and was postulated for all members of the NPY hormone family, known as the „PP fold". However, from the present data such a conformation can clearly be excluded for NPY at the given sample-conditions. Moreover, the structure of membrane-bound NPY was solved based upon distance and dihedral angle restraints, which were estimated from NOE data and scalar coupling constants. Whereas the N terminus is unstructured which is obvious from the low density of inter-residual NOEs, the second half of the molecule is in a regular α-helical conformation. The helical section comprising residues 21-30 could be determined to a very high precision (RMSD for the backbone atoms: 0.23 Å). The comparison with a previously published NPY dimer structure, which was measured in aqueous solution, reveals a conformational change a the C-terminal tetrapeptide. Membrane-integrating spin-labels as well as amide proton-/deuterium-exchange experiments gave evidence for a surface-associated topology on the membrane. Obviously, the association is driven by interactions of the hydrophobic side-chains of the amphipathic α-helix with the phospholipids, which guides the C-terminal tyrosine-amide into a membrane-affiliated position. The global and internal backbone-dynamics of NPY in water and on DPC micelles were characterized by ^{15}N-relaxation-exepriments and quantified by calculation of generalized order parameters following the Lipari-Szabo approach. The N terminus is completely flexible in water as well as in the

membrane-bound state. On the other hand, association to the membrane via the C-terminal segment leads to a strong stabilization of the helical conformation.

The second part of the thesis describes the structural characteristics of a class of NPY-mutants, that exhibit Y_5 receptor selectivity. The comparison of the published solution structure of NPY with the one of the first Y_5 receptor selective agonist, [Ala^{31}, Aib^{32}]-NPY, as described herein, revealed a different conformation in the C-terminal region. The α-helix of NPY is substituted by a 3_{10}-helical turn in the mutant encompassing residues 28 to 31, followed by a flexible C terminus. Very similar receptor-subtype binding profiles are found for analogues, in which the non-biogenic residue aminoisobutyric acid (Aib) is replaced by proline. Once two appropriate point mutations had been introduced into the DNA-sequence of NPY by site-directed mutagenesis the recombinant production of ^{15}N-labeled [Ala^{31}, Pro^{32}]-NPY became possible. NMR-data were then collected in the presence of DPC-micelles under the same conditions used for NPY and compared to them. Although the global fold is very similar to NPY, there are again significant differences in the helical region and at the C terminus, which most probably play a role for the receptor-subtype selective recognition. Very high generalized order parameters between 0.9 and 1 as well as characteristic low scalar coupling constants for residues 21-30 are indicative of an almost rigid helical peptide backbone. On the other hand, the C terminus is clearly more flexible in the mutant than in NPY and is no longer in a regular α-helical conformation. However, the preferred proximity of the C-terminal tyrosine-amide to the membrane still persists. Enlarged proton-/deuterium-exchange rates together with a concomitantly decreased global correlation time suggest a lower affinity to the membrane. It is assumed, that the mutant possesses fewer membrane-anchoring residues. On the other hand, its orientation on the membrane is more well-defined and the reduced-length helical segment is more rigid. The C-terminal hexapeptide can be considered as

a short but nevertheless flexible loop on the membrane surface. It is speculated, that in contrast to NPY, the positions of two basic amino acids, that are known to be essential for receptor binding, are less well-defined and probably display a higher average distance to the membrane.

One of the binding sites of NPY is supposed to be localized in the third extracellular loop of the Y receptors. To study possible interactions between NPY and/or the receptor-subtype selective mutants with this loop, a peptide was synthesized by solid phase synthesis, which comprised the sequence of the third extracellular loop of the Y_1 receptor. Hydrocarbon-chains were coupled to the N and C termini of the peptide in order to anchor the loop-mimicking molecule onto the micelles. A slightly sequence-modified construct was succesfully synthesized and enabled the measurement of 1D ^{1}H-NMR-spectra of satisfactory quality in dodecylphosphocholine micelles. However, NPY did not display any resonance shifts in the presence of the loop-mimicking peptide, suggesting that the ligand does not interact with the isolated receptor fragment.

Zusammenfassung

Die vorliegende Dissertation befasst sich mit der Bestimmung und Interpretation von Struktur-Aktivitäts-Beziehungen des Neurohormons und -transmitters Neuropeptid Y (NPY). NPY ist ein 36 Aminosäuren umfassendes, C-terminal amidiertes Peptidhormon, das den natürlichen Ligand der NPY Familie von G Protein gekoppelten Rezeptoren (Y_n-Rezeptoren) darstellt. Diese Familie besteht aus 6 bis heute identifizierten Rezeptor-Subtypen, die mit verschiedenen physiologisch-bedeutsamen Effekten assoziiert werden. Frühere Arbeiten hatten gezeigt, dass durch die Einführung eines bestimmten Dipeptid-Motivs an Position 31/32 die selektive Erkennung des in der Regulation der Nahrungsaufnahme involvierten NPY Y_5 Rezeptor-Subtypen vermittelt wird. Die hier präsentierten Kernresonanzspektroskopie (NMR)-Studien erlauben es, die Rezeptor-Subtyp Spezifität auf einer strukturellen Basis zu diskutieren.

Im ersten Teil der Arbeit wird das native NPY in Lösung strukturell charakterisiert. Für einige Peptidhormone wird postuliert, dass die Bindung an die Zellmembran, in denen die Rezeptoren eingelagert sind, ein essentieller, der Rezeptorerkennung vorgelagerter Schritt ist. Die Studien wurden deshalb auch in Gegenwart von Dodecylphosphocholin (DPC)-Mizellen, einem in der NMR-Spektroskopie häufig verwendeten Membran-Mimetikum durchgeführt. Um die Resonanzzuordnungen zu vereinfachen und Dynamikuntersuchungen zu ermöglichen, wurde NPY uniform ^{15}N-Isotopen-markiert dargestellt. Dazu wurde NPY-Glycin (Pro-NPY 1-37) C-terminal mit Decahistidin-Ubiquitin als Fusionsprotein kloniert und exprimiert. Die Reinigungsstrategie basierte auf Ni^{2+}-Affinitätschromatographie. Die Konversion von NPY-Glycin zum C-terminalen Amid erfolgte mit dem Enzym Peptidylglycin α-amidierende Mono-

oxygenase. Die Untersuchungen von NPY frei in Lösung konzentrierten sich auf die Bestimmung der Quartärstruktur. Dazu wurde aus ^{15}N-markierten NPY und ^{14}N-NPY, welches das Spinlabel TOAC an Position 34 enthielt, ein Heterodimer hergestellt. Mit einem solchen Sample konnte in einem [^{15}N,^{1}H]-HSQC Experiment gezeigt werden, dass die hydrophobe Seite der Helix in Abwesenheit von Membranen durch Dimerisierung in sowohl paralleler als auch antiparalleler Helix-Anordnung maskiert ist. Davon ausgeschlossen ist allerdings das C-terminale Tetrapeptid. Dadurch erfährt dieses Segment in wässriger Lösung eine erhöhte Flexibilität, wie durch Messung der ^{15}N- Relaxation gezeigt werden konnte. Zudem wurde der Frage nachgegangen, ob der N-Terminus, dem aPP-Fold (Pankreatisches Polypeptid des Vogels) gleichkommend, auf die C-terminale Helix rückfaltet. Diese früher postulierte Rückfaltung liess sich bei den gegebenen Proben-Bedingungen klar ausschliessen. Zudem wurde die Stuktur von Membran-gebundenen NPY aufgrund von Distanz- und Diederwinkeleinschränkungen, die aus NOE Daten und skalaren Kopplungen gewonnen wurden, ermittelt. Während der N Terminus infolge geringer inter-residueller NOE-Dichte keine gut definierte Architektur erkennen lässt, ist die zweite Molekülhälfte in einer regulären α-helikalen Konformation gefaltet, deren dreidimensionale Koordinaten in der Region der Reste 21-31 mit einer sehr hohen Präzision (RMSD für die Rückgratatome: 0.23 Å) bestimmt werden konnten. Der Vergleich mit einer publizierten NPY-Dimer-Struktur, die in wässriger Umgebung gemessen worden war, zeigt eine konformationelle Änderung am C-terminalen Tetrapeptid. Die Ursache hierfür wurde deutlich, nachdem Membran-integrierende Spin-Label und Amidproton/-Deuterium-Austausch-Experimente die Orientierung von NPY auf der Membranoberfläche enthüllten. Offenbar wird die Membran-Assoziation durch die Interaktion von hydrophoben Seitenketten der amphipathischen α-Helix mit den Phospholipiden gesteuert, wodurch das C-

terminale Tyrosin-Amid in einer Membran-zugewandten Position zu liegen kommt. Die globale und interne Rückgrats-Dynamik von NPY auf Mizellen wurde mit ^{15}N-Relaxationsexperimenten charakterisiert und im Rahmen des Lipari-Szabo Ansatzes in Form von Ordnungsparametern quantifiziert. Der N Terminus ist in Wasser und in der Membran-gebundenen Form gleichermassen äusserst flexibel. Dagegen führt die Membran-Assoziation des C-terminalen Bereichs zu einer starken Stabilisierung der helikalen Konformation.

Der zweite Teil der Dissertation beschreibt die strukturellen Merkmale einer Klasse von NPY-Mutanten, die Y_5 Rezeptorsubtyp-Selektivität zeigen. Vom ersten Y_5 Rezeptor-selektiven Agonisten, [Ala^{31}, Aib^{32}]-NPY, wurde die Lösungsstruktur bestimmt. Im Vergleich mit NPY wurde eine Konformationsänderung im C-terminalen Bereich gefunden. Die α-Helix von NPY wird im selektiven Agonisten durch einen 3_{10}-helikalen Turn zwischen den Resten 28-31, gefolgt von einem ungeordneten C Terminus, ersetzt. Gleiche Rezeptorsubtyp-Bindungsprofile werden gefunden, wenn die unnatürliche Aminoisobuttersäure (Aib) durch ein natürliches Prolin substituiert wird. Die rekombinante Herstellung von [Ala^{31}, Pro^{32}]-NPY in ^{15}N-markierter Form wurde möglich, nachdem zwei entsprechende Punktmutationen in der DNA-Sequenz von NPY mit Hilfe von zielgerichteter Mutagenese eingeführt worden waren. Die NMR-Daten wurden diesmal in Gegenwart von DPC-Mizellen unter gleichen Bedingungen wie für NPY erhoben. Der Vergleich mit NPY zeigt, dass es, obwohl die globale Architektur derjenigen von NPY sehr ähnlich sieht, wiederum signifikante Unterschiede im helikalen Bereich und am C Terminus gibt, die demnach wahrscheinlich eine Rolle bei der spezifischen Rezeptorerkennung spielen. Die Reste 21-30, die sich unmittelbar vor der Mutation befinden, zeigen Ordnungsparamter zwischen 0.9 und 1 sowie charakteristisch tiefe skalare Kopplungskonstanten und somit eine beinahe rigide helikale Rückgrats-Konformation an. Anderer-

seits ist der C Terminus der Mutante deutlich flexibler als jener von NPY und nicht mehr α-helikal gefaltet. Dabei wird jedoch die bevorzugte Membrannähe des C-terminalen Tyrosin-Amids nicht aufgegeben. Ausserdem deuten erhöhte Proton-/Deuterium-Austauschraten bei einer gleichzeitig erniedrigten globalen Korrelationszeit eine schwächere Membran-Affinität an. Offenbar bindet die Mutante aufgrund ihrer etwas schlechteren Membranverankerung zwar weniger gut an die Mizelle, kann sich dafür aber im verkürzten helikalen Bereich besser und mit erhöhter Rigidität auf ihr ausrichten. Das C-terminale Hexapeptid andererseits kann als kurze, aber trotzdem flexible Schleife auf der Membranoberfläche betrachtet werden. In dieser sind im Gegensatz zum nativen NPY die beiden für die Rezeptorbindung essentiellen basischen Arginin Aminosäuren weniger genau definiert und möglicherweise in einem grösseren durchschnittlichen Abstand zur Membran positioniert.

Eine Bindungstelle von NPY wird in der dritten extrazellulären Schleife der Y Rezeptoren vermutet. Um allfällige Interaktionen zwischen NPY, bzw. Rezeptor-Subtyp-selektiven Mutanten und der Schleife NMR-spektroskopisch zu charakterisieren, wurden deshalb im letzten Teil der Arbeit Anstrengungen unternommen, die Peptidsequenz der Schleife des Y_1 Rezeptors mittels Peptidfestphasensynthese herzustellen. Durch N- und C-terminale Kupplung von Kohlenwasserstoffketten sollte das Schleifen-imitierende Molekül in die Mizellen verankert werden. Ein leicht sequenz-modfiziertes Konstrukt konnte erfolgreich synthetisiert werden und erlaubte es, in der Gegenwart von Mizellen eindimensionale ^{1}H-Spektren von guter Qualität aufzunehmen. Allerdings wurden bei NPY in der Gegenwart des Schleifen-imitierenden Peptids keinerlei Resonanzverschiebungen beobachtet, was ein starker Hinweis dafür ist, dass der Ligand mit dem Rezeptorfragment nicht interagiert.

Abbreviations

Aib	aminoisobutyric acid
Boc	*tert*-butyloxycarbonyl
cAMP	cyclic adenosyl monophosphate
CCK	cholecystokinin
CD	circular dichroism
COSY	correlation spectroscopy
DIC	*N,N*-diisopropylcarbodiimide
DIPEA	*N*-ethyldiisopropylamine
DM	1,2-dimyristoyl-3-mercaptoglycerol
DMF	*N,N*-dimethylformamide
doxyl	(4,4-dimethyl-3-oxazolidine-N-oxyl)
DPC	dodecyl phosphocholine
e1-3	extracellular loop 1-3
E.COSY	exclusive correlation spectroscopy
EDTA	ethylenediamine tetraacetic acid
EMF	extended model-free formalism
Fmoc	*N*-(9-fluorenyl)methoxycarbonyl
FT	Fourier transformation
GABA	γ-amino butyric acid
HOBt	1-hydroxy-benzotriazole
HPLC	high performance liquid chromatography
HSQC	heteronuclear single-quantum correlation
Hyp	4-*trans*-hydroxyproline

i1-3	intracellular loop 1-3
IPTG	isopropyl-thiogalactopyranoside
$^{3}J_{HN\alpha}$	vicinal spin-spin coupling constant between the backbone H^N proton and the α-proton
$^{3}J_{\alpha\beta}$	vicinal spin-spin coupling constant between the α-proton and one of the β-protons
MES	2-morpholinoethanesulfonic acid
NOE	nuclear Overhauser effect
NOESY	nuclear Overhauser enhancement spectroscopy
$^{15}N\{^{1}H\}$-NOE	heteronuclear Overhauser enhancement of ^{15}N after saturation of ^{1}H
NPY	neuropeptide Y (h, human; p, porcine)
PP	pancreatic polypeptide (a, avian)
PYY	peptide YY
R_1	longitudinal relaxation rate constant
R_2	transverse relaxation rate constant
RMSD	root mean square deviation
SDS	sodium dodecyl sulfate
SMF	simple model-free formalism
SSE	sum-squared error
tBu	*tert*-butyl
TFA	trifluoroacetic acid
TM I-VII	*trans*-membrane helix I - VII
TOAC	4-amino-2,2,6,6-tetramethyl piperidine-1-oxyl-4-carboxylic acid
TOCSY	total correlation spectroscopy
TPPI	time-proportional phase incrementation
Trt	trityl

Chapter 1

Introduction

It was J.N. Langley, studying the effects of curare and nicotine in frog neuromuscular transmission, who was the first scientist to use the term „receptive substances" to describe cellular recognition sites where molecules bind and exert actions on cells (Langley, 1909). A series of discoveries in the subsequent 80 years led to the today known general concepts of cell signaling, which are fundamental to modern biology (for a historical perspective see Lefkowitz, 2000). Essentially, two mechanisms for transduction of extracellular signals (hormones, neurotransmitters, growth factors, odorants, light, etc.) into the cell have evolved. The first is represented by single membrane proteins with an extracelluar ligand-binding and a directly coupled intracellular effector domain. In the second class of signal transduction systems, the intracellular domain of the membrane receptor is coupled to a heterotrimeric guanine nucleotide binding protein (G protein). Upon activation by the receptor, these G proteins act as modulators of effector enzymes (*e.g.* adenylate cyclase, phospholipase C-β), ion channels or transporters, resulting in a tremendous signal amplification (Figure 1.1). Herein, the focus is on the molecular structure and function of G protein coupled receptors. Four break-throughs that led to the identification of the elements constituting this three-component transmembrane signaling system are worth to be high-lightened:

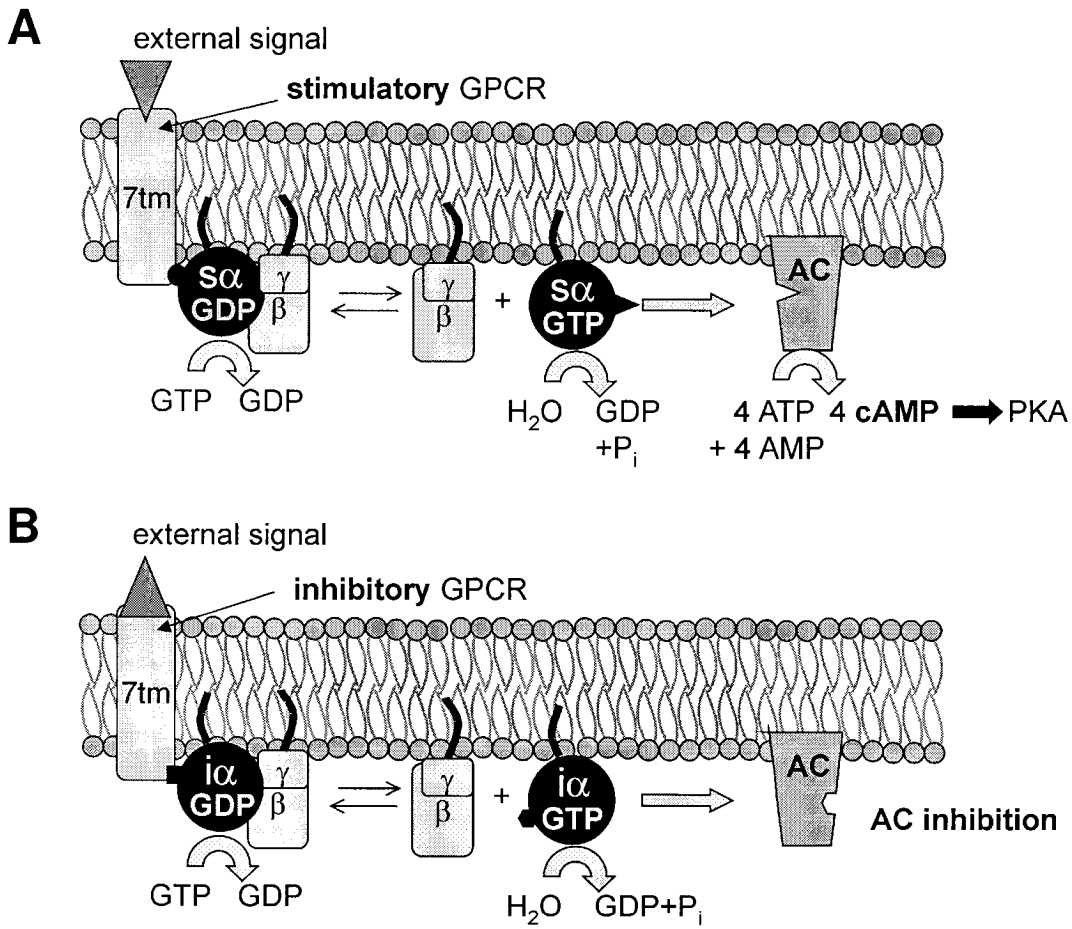

Figure 1.1 G protein coupled receptor mediated activation (A)/inhibition (B) of adenylate cyclase (AC). Binding of an external signal molecule stabilizes the active form of the 7-tm-receptor, resulting in the intracellular binding of a heterotrimeric G protein. This, in turn, stimulates the G_α subunit to exchange its bound GDP for GTP. The activated G_α-GTP complex then dissociates from $G_\beta G_\gamma$ and either stimulates (if G_α is an stimulatory subunit $G_{s\alpha}$, see A) or inhibits (if G_α is an inhibitory subunit $G_{i\alpha}$, see B) AC from synthesizing cyclic AMP. However, these effects are short-lived because the G protein hydrolyzes GTP to GDP+P_i at a rate of 2 to 3 per minute and reverts to its inactive state, again. The figure is according to Voet & Voet (1995).

1. In the mid-sixties E.W. Sutherland had established the first broken cell preparations that allowed him to discover the cyclic AMP producing enzyme adenylate cyclase and to come up with the second-messenger concept. The theory states that a hormone (first messenger) induces the production of a second messenger (*e.g.* cAMP)

which finally effects the cell response. However, Sutherland left us with the question whether the first messenger (hormone) acts directly on the second messenger producing enzyme (adenyl cyclase) or *via* an interconnected molecular entity (Sutherland & Robison, 1966).

2. L. Birnbaumer, G.A. Robison and co-workers not only recognized that several distinct receptors are coupled to one common type of adenylate cyclase (Birnbaumer & Rodbell, 1969) but also postulated the existence of a transducer molecule between the receptors and the cyclase (Rodbell *et al.*, 1971). This has later been discovered to be the family of G proteins, which use GTP hydrolysis to switch between a receptor binding and an adenylate cyclase binding (stimulating or inhibitory) state (Schramm & Selinger, 1984; Gilman, 1987).

3. The close relationship between the hormone and the light stimulated signaling systems was recognized in the mid-eighties by L. Stryer and co-workers (Stryer & Bourne, 1986). Isolation and cloning of the gene encoding bovine rhodopsin gave first evidence for a seven membrane spanning receptor (Nathans & Hogness, 1983). The same topography as well as shared sequence homology between rhodopsin and the β_2-adrenergic receptor, as found in 1986 by Dixon and co-workers (Dixon *et al.*, 1986), led to the speculation, that those two receptors, although activated by completely different stimuli, belong to a probably large gene family. Today, the number of proteins that are classified as belonging to the rhodopsin-like superfamily of GPCRs (family 1, see below) is 569 (rank 4 among all protein families), whereas the number of protein-encoding genes is predicted to be approx. 32'000 (International Human Genome Sequencing Consortium, 2001). Since only 50% of the genes is classified, the GPCR family 1 is therefore presently esti-

mated to be encoded by 1,7 to 4% of the genes in the human genome.

4. Very recently, the crystal structure of rhodopsin in the ground-state has been solved (Palczewski *et al.*, 2000) providing the first atomic resolution structure for a G protein coupled receptor.

GPCR structure studies are of particular importance for pharmaceutical research in the context of the so-called rational drug design. This is a structure-based approach to exploit 3D structure data of a known ligand, a receptor or the complex of both, for the purpose of structure-based drug improvement (by molecular modelling) or even finding new lead compounds (by use of 3D database searching methods such as DOCK). Thereby, new drugs that modulate disease-related cell communication (for a review see: Hubbard, 1997) may be developed. Today, approximately 60% of approved drugs elicit their therapeutic effects by selectively addressing members of the GPCR target family (Müller, 2000).

The present contribution deals with the structural characterization of the first steps in ligand-receptor recognition applying nuclear magnetic resonance spectroscopy (NMR) techniques while studying the neuropeptide Y (NPY)/Y_n-receptor (n=1..5) system. In the introduction general structural and functional aspects of G protein coupled receptor are addressed. In particular, some functional studies revealing prerequisites for structural and functional integrity when modelling the high-molecular weight receptor in its highly heterogeneous and fine-balanced *in vivo* membrane environment are reviewed. An approach that was prosecuted by us aims at using a reduced-size receptor fragment in a membrane-mimeticum and observe binding and structural features by NMR. Finally, some NMR techniques and examples for gaining structural data of ligand-receptor interactions are presented.

To look back to the starting point of the GPCR saga again, I close this section citing E.W. Sutherland's lecture given in 1971 when he received the Nobel Prize in Physiology and Medicine (Sutherland, 1971):

„(...) In conclusion I wish to suggest or plead that all of us exert a small amount of effort to stimulate interest in biological and medical research. A life in research can be a most enjoyable life with many frontiers to explore. In addition, we need research to understand man and his ailments. I believe we are reaching a stage where research will be more and more helpful to man."

1.1. Structure and function of G protein coupled receptors

Structural aspects

Primarily technical problems so far prevented the successful determination of the structure of a G-protein coupled receptor until the very recent publication of Palczewski *et al.* (2000) appeared in SCIENCE. The difficulties are due to insufficient over-expression of the receptor, problems with its purification, concentration, and with the preparation of fully reconstituted receptors in membrane environments. Furthermore, crystallization of membrane proteins is still difficult although considerable progress has been made in that area (Caffrey, 2000). The upper size of about 30-50 kDa that was limiting NMR structure determination until the TROSY methodology was introduced excluded the application of NMR in that area.

Early information about the seven transmembrane architecture of the GPCRs came from hydropathy plots. In this technique a window of about 19 amino acid is moved through the sequence and segments containing (exclusively) hydrophobic residues are identified. This method still serves to identify GPCRs on the gene level. Arseniev *et al.* have used NMR to look at transmembrane-fragments of bacteriorhodopsin in organic solvents and discovered that these fragments form helices of variable stabilities (Pervushin *et al.*, 1994). Cryo-electron microscopy has been used successfully to obtain low-resolution images of rhodopsin (Schertler *et al.*, 1993). From earlier data it was obvious that G protein coupled receptors have in common a central core domain of seven transmembrane helices (TM I ... TM VII) connected by three intracellular (i1, i2, i3) and three extracellular (e1, e2, e3) loops (see Baldwin, 1993, for a review). The cryo-electron micrographs could then reveal the mode in which the transmembrane helices are packed against each other. Other experiments have used site-specific attachment of spin-labels in order to measure selected distances by paramagnetic electron resonances (EPR) (Cornish *et al.*, 1994).

Evolutionary aspects and classification of GPCRs

An amino acid sequence comparison reveals three main families of GPCRs sharing no pairwise sequence homology and hence the three families evolved by molecular convergence. This view is also reflected by the encountered mechanisms through which the receptor switch from the inactive to the active conformation and how they couple to the G proteins. Figure 1.2 schematically depicts morphological differences between the families with respect to nature and localizations of the ligand binding sites and the disulfide bonding pattern (according to Bockaert & Pin, 1999). In the following, structural and functional properties

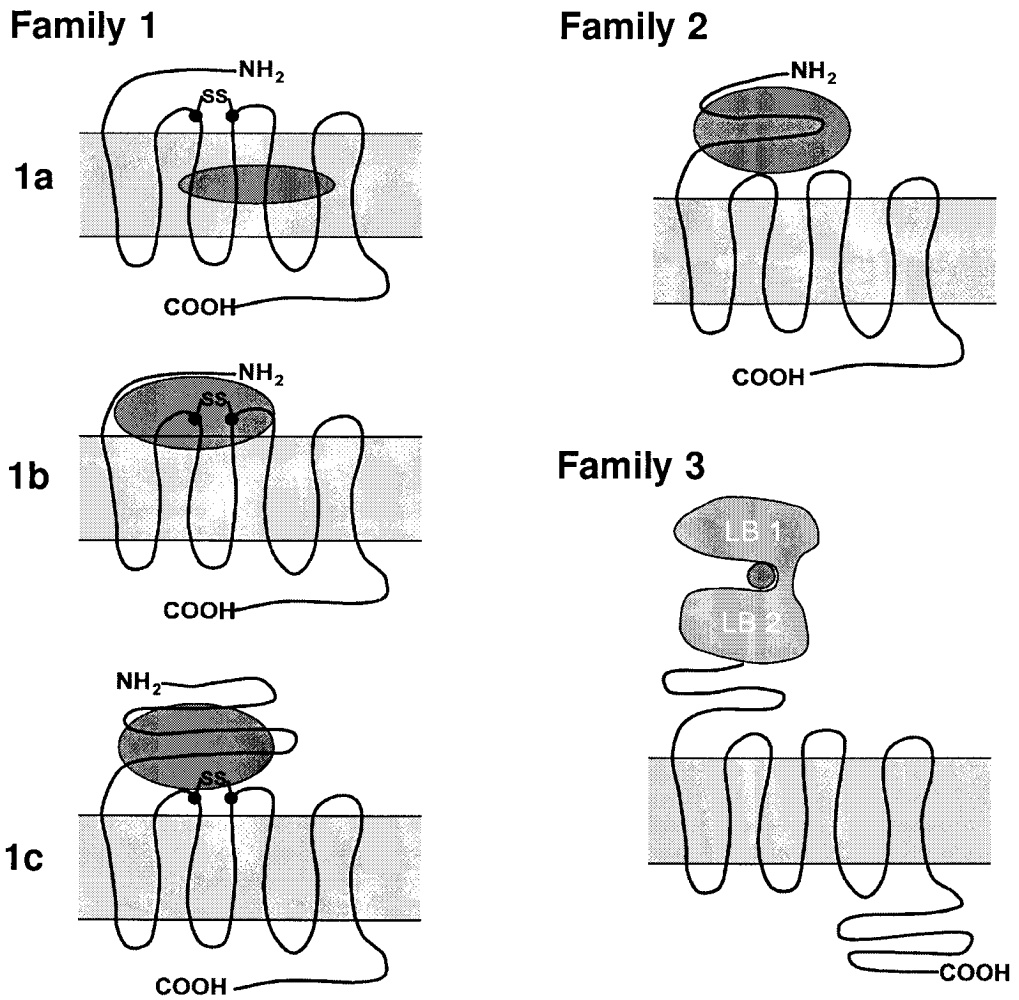

Figure 1.2 GPCRs are classified into three main families (1, 2 and 3). The members of family 1, which contains most GPCRs, possess a characteristic disulfide bridge between e1 and e2. Group 1a contains GPCRs for small ligands including rhodopsin, opioid receptors and β-adrenergic receptors. The binding site (dark grey coloured) is within the seven TMs in the hydrophobic membrane compartment. GPCRs for peptide hormones and in particular NPY are mainly members of family 1b with the ligand binding site including the N-terminal part and the extracellular loops. Group 1c contains receptors for glycoprotein hormones. They are characterized by a large extracellular domain. Family 2 GPCRs have a highly similar morphology like group 1c GPCRs without sharing any sequence homology. Ligands include high molecular weight hormones such as glucagon, secretine, PACAP and PTH. Family 3 contains the metabotropic glutamate receptors (mGluRs), the Ca^{2+} sensing receptors and the GABA-B receptors. These receptors possess a very large extracellular domain constituted of two lobes (ligand binding regions LBR 1 and 2) that close like a Venus' flytrap upon ligand binding. The figure is according to Bockaert & Pin (1999).

are reviewed for each family. Finally, the two-state model of receptor activation, which seems to apply to GPCRs as well as to transmitter-gated ion channels is presented and the role of lipids, forming the membrane environment in which the receptors are embedded, is discussed.

Family 1 GPCRs (the rhodopsin-like type of receptors)

Family 1 contains approximately 90% of all GPCRs including receptors for odorants and other small molecules (family 1a), peptides (family 1b) as well as large glycoprotein hormones (family 1c). The most prominent member of this family is rhodopsin, which is activated by light, thereby making vision possible. In the inactive ground-state, rhodopsin consists of the 40 kD protein opsin and the chromophore 11-*cis*-retinal, which is covalently attached through Lys^{296}. The crystal-structure of rhodopsin at 2.8 Å, which is presently the only available high-resolution structure of a family 1 GPCR, has recently been solved by Palczewski *et al.* (2000) (Figure 1.3).

Besides the organization and packing of the seven transmembrane helix bundle, the structure reveals the presence of two anti parallel β-sheets and a secondary membrane-associated amphiphilic helix. The first strand is located in the N-terminal tail running almost parallel to the expected plane of the (extracellular) membrane. The second one lies within the e2-loop, being part of the chromophore-binding pocket. Cys^{187} in e2 forms a disulfide bond with Cys^{110} at the extracellular end of TM III. This disulfide bond is conserved in all family 1 GPCRs. A short amphiphilic helix, which is clearly distinct from and lying nearly perpendicular to TM VII and therefore parallel to the cytoplasmic membrane, is part of the C-terminal tail.

Upon absorption of a photon the 11-*cis*-retinal isomerizes to all-*trans*-retinal. This alters the shape of the retinal (Grobner *et al.*, 2000), forcing a slower conformational change of the protein moiety including the cyto-

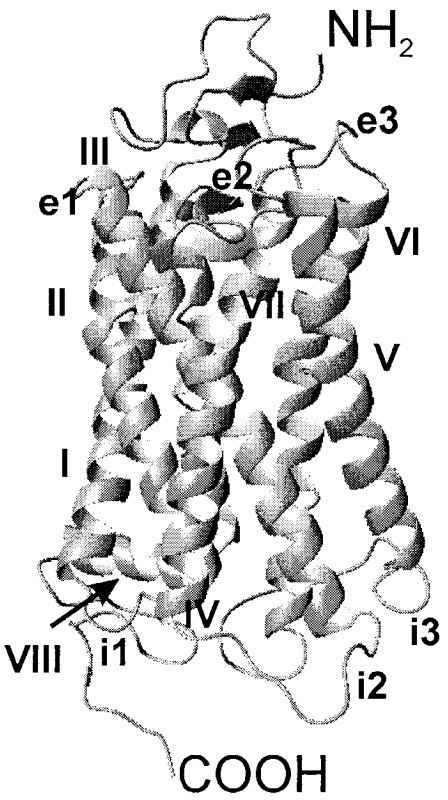

Figure 1.3 Ribbon presentation of rhodopsin according to the X-ray structure of Palczewski *et al.* (2000). The extracellular side is at the top. The oligasaccharides at Asn^2 and Asn^{15} as well as the chromophore 11-*cis*-retinal at Lys^{296} are omitted.

plasmic surface. The activation of opsin leads to the binding of transducin. It is only transient, before the all-*trans*-retinal is hydrolyzed and dissociates from the opsin. Mutagenesis and biochemical analysis showed that the switch from the inactive to the active conformation is associated with a change in the relative orientation of TM III and TM VI. This affects the conformation of the i2 and i3 loops, and by so doing unmasks G protein-binding sites (for reviews see: Bourne, 1997; Wess, 1997). The probably very conserved molecular architecture of the seven-transmembrane receptors suggests that the conformational changes, as described for rhodopsin, also occur in other GPCRs. This is astonishing considering that ligand binding sites show great variability not only between but also within the families.

One concept which came up in the nineties was that dimerization of G protein coupled receptors is required for full functionality. One very compelling evidence for the functional meaning of receptor dimerization is related to the role of dimers in functional rescue. Maggio *et al.* (1993) prepared chimeric (family 1) receptors with the N terminus and TM I - TM V taken from the muscarinic M_3 receptor while TM VI and TM VII up to the C terminus stemmed from the α_2-adrenergic receptor. This receptor was found to be completely inactive, as was the complementary adrenergic-muscarinic chimeric receptor. However, G proteins could be activated upon co-expression of the two chimeras. Functional analysis of mutated type 1 angiotensin receptors (AT1) revealed that Lys^{102} (TM III) and Lys^{199} (TM V) mutants do not bind angiotensin II or different analogues. Co-expression of these two deficient receptors permitted the restoration of a normal binding site. This effect was not due to homologous recombination of the cDNAs but to protein *trans*-complementation (Monnot *et al.*, 1996). A possible role of the dimerization in receptor activation is suggested by Hebert *et al.* (1996), who found that a peptide corresponding to TM VI of the β_2-adrenergic receptor inhibits both receptor dimerization and activation.

Family 2 GPCRs

Family 2 GPCRs are morphologically very similar to family 1c GPCRs (Figure 1.2) although the sequence homology is very low and although they lack the characteristic disulfide bond of family 1 GPCRs. In both types the N-terminal domain plays an important role in ligand binding. The ligands for the family 2 GPCRs are large peptides including the closely related 29-residue peptide glucagon, the 27-residue peptide secretin and the 28-residue vasoactive intestinal peptide (VIP), or the calcium and phosphate ion concentration regulating 32-residue peptide calcitonin and the 84 amino acid peptide parathyroid hormone (PTH).

Recently it has been found that the calcitonin receptor-like receptor (CRLR) requires formation of a heterodimer with a one-TM domain protein in order to become correctly glycosylated and transported to the membrane as well as to obtain its final identity, *i.e.* ligand specificity. Thus, the CRLR is a virtual receptor which generates the calcitonin gene-related peptide (CGRP) receptor when associated with the receptor-activity-modifying protein 1 (RAMP1) and the adrenomedullin receptor in association with RAMP2 (McLatchie *et al.*, 1998).

Family 3 GPCRs (the metabotropic glutamate receptor-like family of GPCRs)

Whereas family 1 and 2 GPCRs bind ligands in pockets formed by their transmembrane helices and/or extracellular loops, the family 3 receptors possess a large extracellular domain which consists of the ligand-binding region (LBR) and the cysteine-rich region. The LBR shares sequence similarity with the bacterial periplasmic binding protein (PBP) and the extracellular regions of both the ionotropic glutamate receptors and the γ-aminobutyric acid $(GABA)_B$ receptor, which is a member of the family 3 GPCRs as well.

Three different crystal structures of the extracellular ligand-binding region of mGluR1, in a complex with glutamate and in two unligated forms, have very recently been determined (Kunishima *et al.*, 2000). The asymmetric unit of all crystal forms contained two molecules of m1-LBR, forming a homodimer covalently connected by an intermolecular disulfide bridge between Cys^{140} of each monomer. Since this cysteine is located in a disordered segment, it probably does not act as a structural scaffold but instead serves to increase the effective concentration of the dimeric form of mGluR1. The global conformations of the ligand-bound (complex) form and one of the two free forms (form I) are substantially different, whereas the other free form (II) and the complex form have

almost identical conformations (Figure 1.4). Obviously, the bi-lobed

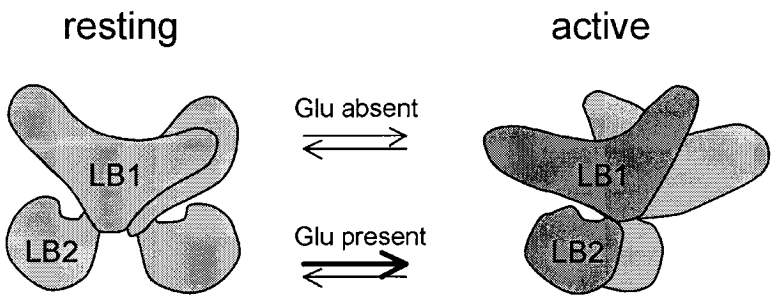

Figure 1.4 Even in the absence of glutamate, the resting and the active state of the m1-LBR are in a dynamic equilibrium between the free interprotomer forms I (resting) and II (active) (top). Glutamate binding (bottom) stabilizes the closed (dark grey coloured) conformation of one of the two protomers. Accordingly, the X-ray structures of the free form II and the complex form reveal very similar global conformations (Kunishima *et al.*, 2000).

architectures in the dimer flexibly change their domain arrangements to form an open or closed conformation, corresponding to a resting and an active conformation. The two conformations are modulated through interactions within the dimer interface which is formed by α-helices packed against each other. Thus, the relative domain arrangements of the dimer in the active state is in dynamic equilibrium with other states and becomes selectively stabilized by glutamate binding. Such a model of receptor activation which is based on the existence of two receptor states, an open (resting) and a closed (active) one, is compatible with the two-state model of receptor activation, originally developed by De Lean *et al.* (1980). Therein, the ligand (glutamate) stabilizes the active state thereby increasing the ratio of closed to open state. This model was originally developed to explain the agonist-specific binding properties of the β-adrenergic receptor (see below).

The two-state model of receptor activation

The predictions of the two-state model of receptor activation and its implications for the analysis of agonist-receptor interactions have been reviewed by Leff (1995). One of the most convincing arguments in favor of the model stems from the ability of GPCRs to exist in a constitutively activated state, *i.e.*, a state which is able to initiate a biochemical response even in the absence of an agonist. Additionally, the concept explains inverse agonism, *i.e.* the existence of ligands that exert a descending agonist concentration-effect curve instead of the ascending one displayed by agonists.

The model states, that in the absence of a ligand, the receptor is in an equilibrium between the resting state (concentration [R]) and the active state (concentration [R^*]), described by the thermodynamic equilibrium constant L=[R]/[R^*] that determines the relative population of receptors in the two states. Accordingly, binding of a ligand (concentration [A]) to the receptor has to be described by two constants K_A = [R][A]/[AR] and K_A^* = [R^*][A]/[AR^*] governing the dissociation constants for the two states. An agonist is defined to have higher affinity to R^* and shifts the equilibrium towards the activated state, whereas an inverse agonist stabilizes the resting state R. On the other hand, ligands with equal affinity for the two receptor states are devoid of agonism or inverse agonism and behave as competitive antagonists, if they are able to displace agonists from the receptor. Irreversible antagonists inactivate either R, R^*, or both. In the two-state model, this is modelled by reducing [R], [R^*] or both, respectively.

The two-state model of GPCRs has been validated using a transgenic mouse model with a myocardial overexpression of β_2-adrenergic receptors. The overexpression was high enough such that a significant population of spontaneously activated receptor (R^*) was present, inducing a

maximal response even in the absence of an agonist (Milano *et al.*, 1994). Moreover, it was shown, that inverse agonists really exist at the β_2-adrenergic receptor (Bond *et al.*, 1995). Very recently, it was shown, that two mutant H_3 receptors display high constitutive activity in rodent brain *in vivo* at medium and high expression levels. Using inverse agonists this activity could be reduced and was regained upon addition of a neutral antagonist (Morisset *et al.*, 2000).

The role of lipids in biological membranes

As mentioned above GPCRs are embedded in membranes and hence the membrane displays an important structural and functional role in these systems.

Cell membranes are widely diverse with respect to their phospholipid composition (according to the different headgroup classes) and to their protein composition (see Table 1.1), Generally, the amphipathic nature of the lipid molecules causes them to form spherical micelles with the aliphatic chains pointing inward, or bilayers, which are bimolecular sheets with the hydrophobic tails sandwiched between the hydrophilic headgroups. Most membrane phospholipids are cylindrically shaped and therefore form bilayers. However, the lipid composition in the two halves of the bilayer may be different. In the human erythrocyte membrane for instance, cholines (*i.e.*, PC and SM) are in the outer half, whereas PE and the negatively charged PS are in the inner half, resulting in a charge difference across the bilayer. ESR studies revealed that phospholipid molecules may transverse - but very rarely - from the monolayer on one side onto the other (called „flip-flop") (Devaux, 1993). Nevertheless, membranes have to be considered as very fluid. This implicates large lateral diffusion coefficients of individual lipid molecules (D) of about 10^{-8}

Table 1.1 Lipid composition of membrane preparations[a]

Source	Chole -sterol	Lipid composition (mole percentage)[b] PC	SM	PE	PI	PS	PG	DPG	PA
net charge	0	0	0	0	-	-	-	2-	-
Human erythrocyte	45	17	17	16	-	6			
Bov. rod outer segm. disk	10	36		40	2	12			
Escherichia coli	0	-		80			15		5
Bacillus subtilis	0	0		30			12		
Sindbis virus	0	26	18	35		20			
Rabbit sarc. reticulum	10	63		17		10			
Rat liver:									
ER, rough	6	55	3	16	8	3	-	-	-
ER, smooth	10	55	12	21	6.7			1.9	
Mitochondria (inner)	<3	45	2.5	25	6	1	2	18	0.7
Mitochondria (outer)	<5	50	5	23	13	2	2.5	3.5	1.3

(a) This table is extracted from Yeagle, 1993

(b) Abbreviations used: ER, endoplasmic reticulum; PC, phosphatidylcholine; SM, sphingomyelin; PE, phosphatidylethanolamine; PI, phosphatidylinositol; PS, phosphatidylserine; PG, phosphatidylglycerol; DPG, diphosphatidylglycerol; PA, phosphatidic acid.

cm^2/sec (Kornberg & McConnell, 1971), rapid rotation about their long axis as well as high flexibility in their hydrocarbon chains. Many (eukaryotic) cell membranes contain cholesterol and glycolipids. Cholesterol orients in the bilayer with its hydroxyl group close to the polar headgroups of the phospholipid molecules. The rigid steroid skeleton interacts with the first few CH_2 groups of the phospholipid hydrocarbon chains, thereby making the membrane less fluid and decreasing the permeability of the bilayer to small water-soluble molecules. Another interesting role

for cholesterol, (glyco-)sphingolipids and lipid-modified signaling molecules has been postulated in the context of vesicular invaginations of the plasma membrane, the so-called caveolae (Okamoto *et al.*, 1998). Together with structural proteins, the caveolins, they form a scaffold onto which many classes of signaling molecules can assemble to generate preassembled signaling complexes, concentrating them within a distinct region of the plasma membrane. Particularly, several G protein coupled receptors, *i.e.* endothelin, bradykinin, muscarinic acetylcholine, and β-adrenergic receptors have been localized to caveolae. In the case of the bradykinin receptor, it is suggested that only the activated receptor undergoes translocation to the caveolae. Since many downstream transducers of GPCRs (*e.g.* G proteins and adenylate cyclase) have also been localized in caveolae, agonist-induced translocation of GPCRs to caveolae membranes may be an essential step in the initiation of signaling cascades. Yet less clear is the function of glycolipids in general. They are exclusively found in the extracellular half of the bilayer, resulting from the addition of sugar groups in the lumen of the Golgi apparatus. Speculations about their role include protection of the membrane from environmental influences (low pH, degradative enzymes) and important structural features in cell-recognition processes as well as charge effects and concentrations of ions like Ca^{2+}. Again, the latter might be relevant in the framework of the Hofmeister effect of salts on the conformational equilibria between inactive and active GPCR conformations (either agonist-bound or free) (Vogel *et al.*, 2001).

Membrane proteins are divided into two classes: the peripheral membrane proteins, with affinity for binding sites on the membrane surface (which are either part of integral membrane proteins or directly belong to the lipids or sugars from the membrane surface), and integral membrane proteins, usually hydrophobic sequences in an α-helical or β-barrel conformation that span the membrane (transmembrane) or penetrate the

membrane from on side (anchor). The membrane spanning peptides and proteins adopt a unique direction by which they cross the membrane, *e.g.* the peptide inserts from the cytosol to the extracellular part in C- to N-terminal direction or *vice versa* but never in both ways (Yeagle, 1993). The oligomerization state of the membrane-spanning or membrane-associated proteins and peptides is mainly determined by three pairwise interactions: protein-protein interactions, lipid-protein interaction and lipid-lipid interactions. If protein-protein or lipid-lipid (*e.g.* in the gel state of the lipids) interactions are favoured over lipid-protein interactions, protein oligomerization is observed. This has been predicted for entropical reasons for a system of hydrophobic helices of transmembrane proteins and lipids (Wang & Pullman, 1991), since lipid-protein contacts are minimized due to restriction in the number of conformations available to the lipid chain upon interaction with the protein surface.

The ester carbonyls of lipids, the phospholipid head groups and water molecules around the lipid head groups present opportunities for dipole-dipole interactions and promote H-bonding with appropriate amino acid side chains. On one hand, favorable enthalpy terms may arise from electrostatic interactions, on the other hand, interactions between the phospholipid headgroup and the membrane protein might entropically be favorable over a highly hydrated phospholipid surface.

There is emerging evidence that amino acid residues do not only display a preference for either the lipidic core of the membrane or the aqueous surrounding (depending on their charge hydrophobicity/polarity and potential for H-bonding), but that also the interfacial region is enriched for specific amino acids (Killian & von Heijne, 2000). White & Wimley (1998) studied the hydrophobic interactions of small water-soluble peptides with the interfacial region of lipid bilayers and found that particularly Trp and Tyr have a special affinity for the interface due to their size, rigidity and aromaticity. Investigations with larger amphip-

athic helices revealed a more or less parallel orientation with respect to the membrane surface with the peptide buried in the interfacial area (Hristova *et al.*, 1999; Mattila *et al.*, 1999). The hydrophilic side-chains extended towards the aqueous environment, the hydrophobic ones penetrated the bilayer. An interesting „snorkeling" mechanism has been proposed for interfacial Lys (Mishra & Palgunachari, 1996): the C_α backbone position is proposed to be localized in the hydrophobic part of the membrane, while the long and flexible positively charged side chains snorkel towards the interface (a similar situation exists for Arg), thereby helping to anchor the amphipathic helix into the lipid bilayer (Killian & von Heijne, 2000).

A preference for tyrosine and tryptophan residues to be located at the termini of transmembrane alpha-helices was also found in multiple- as well as in single-membrane-spanning proteins through a statistical analysis for putative transmembrane alpha-helices. In this investigation data were obtained from a database representing the subset of membrane proteins available in Swiss-Prot (Arkin & Brünger, 1998). Possible functional roles proposed for interfacial aromatic residues include: (a) positioning or anchoring the TM segments in the membrane (Landolt-Marticorena *et al.*, 1993), (b) introducing rigidity to the periphery of TM segments (Tsang & Saier, 1996), (c) allowing vertical mobility of the TM region with respect to the membrane (Pawagi & Deber, 1990), (d) facilitating translocation of the periplasmic portion of protein through the membrane, and (d) acting as determinants of protein orientation (Schiffer *et al.*, 1992).

Yuen *et al.* (2000) studied the influence of aromatic residues at the membrane-water interface on protein-lipid interactions of the adjoining TM segment in micelle-bound bacteriophage M13 coat protein. Previous structural studies by NMR (Papavoine *et al.*, 1998) had resulted in a L-shaped model, consisting of an N-terminal amphipathic surface helix and a micelle-spanning C-terminal helix. Five of the six aromatic residues in

M13 coat protein, namely Tyr^{21}, Tyr^{24}, Trp^{26}, Phe^{42} and Phe^{45} are at or near the membrane-water interface. Polar mutants of Tyr^{24} were found to be less buried in deoxycholate micelles than in the wild-type and exhibited α-helix to β-structure transitions at lower temperatures than those of wild-type or nonpolar mutants. Mutation of Tyr^{21} to Phe exhibited the highest transition temperature. Using a phage viability assay it was found that viable mutants could not be generated with both Tyr^{21} and Tyr^{24} simultaneously mutated. Together with the non-mutatable Trp^{26} they seem to be vital for the positional anchoring of the membrane-spanning helix. They conclude that amphiphilic residues such as Tyr and Trp may be particularly suited for interfacial positioning, as they can effectively bridge the two contrasting environments and suggest a „push-pull" role for interfacial Tyr residues in fine-tuning the positions. In their view, the choice of Tyr is a compromise between anchoring effectivity (for which Phe is more suitable) and maintenance of the dynamics required during the phage life cycle.

Membrane bound pathways for ligand/receptor recognition

Another important role for the lipid membrane, namely as catalyst for peptide-receptor interactions, has been postulated by R. Schwyzer. In his Membrane Compartment Theory (Sargent & Schwyzer, 1986; Schwyzer, 1991; Sargent *et al.*, 1988; Schwyzer, 1986; Schwyzer, 1995a; Schwyzer, 1995b), derived from work on peptides targeting opioid and neurokinin receptors, he states that membrane binding serves to direct residues into the correct compartments (Figure 1.5), thereby pre-positioning them for receptor binding and possibly inducing the conformation required for receptor recognition and selection. Such a membrane-bound pathway would lower the change of entropy upon ligand binding and increase the effective hormone concentration in vicinity of the receptor and finally

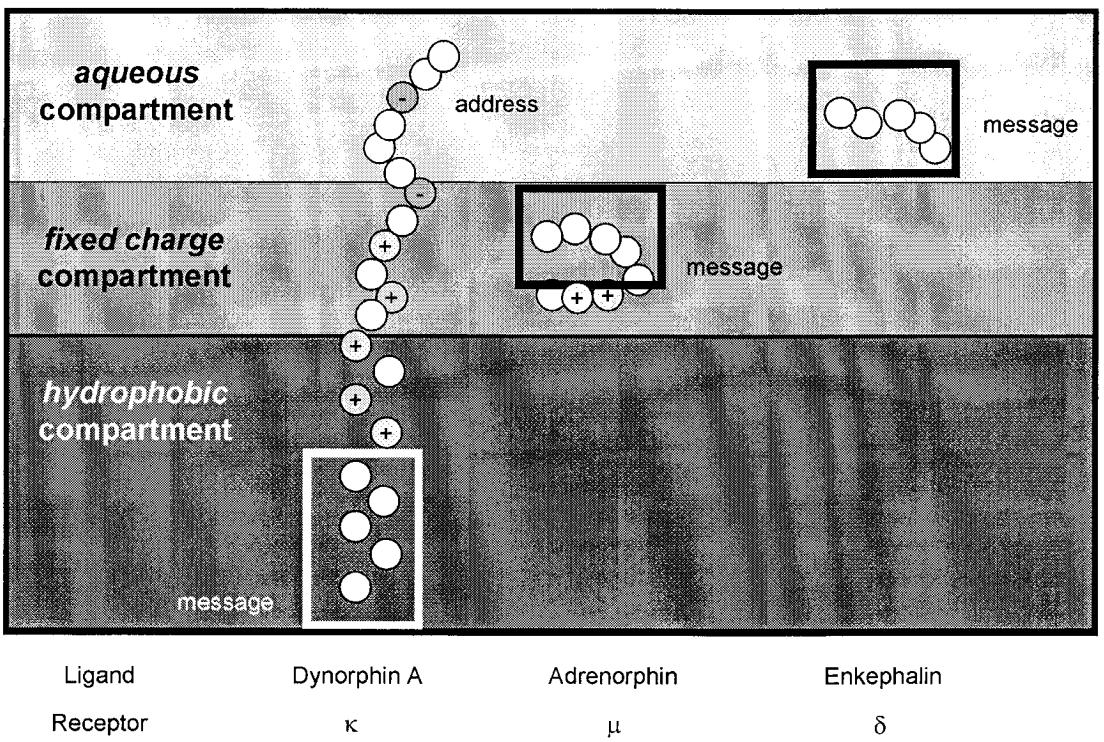

Figure 1.5 R. Schwyzer's Membrane Compartment Theory and message-address concept, applied to the compartment preference by the message of opioid peptides (Schwyzer, 1991; Schwyzer, 1986). Members of a peptide family with identical or similar message sequences (boxed) elicit similar activities but with different selectivities. The selectivity is dominated by the address, which guides the message to a certain receptor (subtype). The neutral and only slightly δ-selective [Leu]-enkephalin is expected to accumulate in both the aqueous and the fixed charge compartment. Electrostatic interactions are guessed to address the strongly μ-selective adrenorphin to the anionic membrane compartment. On the other hand, the strong κ-receptor selection exhibited by dynorphin A is determined by the tendency of its message domain to adopt a perpendicularly oriented α-helical structure in the membrane.

reduces the receptor search to two-dimensional diffusion along the membrane surface.

1.2. Reduced models to study G protein coupled receptors

The size of macromolecular structures that can be determined by NMR has been increased dramatically over the last few years and resonance assignments for molecules as large as approx. 100 kD became possible (Salzmann *et al.*, 1999; Clore & Gronenborn, 1991; Wüthrich, 1998). However, solution structures of very large molecules (with M_r in the range of hundred kDa) have still not been published up to now because their slow overall tumbling leads to very efficient T_2 relaxation. This gives rise to very broad proton resonance lines in non fully-deuterated proteins required to record NOESY spectra. Moreover, the production and functional reconstitution of membrane receptors with associated lipids is still by far not trivial. There are currently severe limitations in obtaining sufficient amounts of receptor for direct study.

One approach to gain structural information of membrane receptors and receptor-ligand interactions by NMR is therefore to reduce the systems in size by splitting it into different fragments. These peptides can possibly be produced by either conventional solid-phase peptide synthesis or alternatively by molecular biology in a straightforward manner and their structure may then be characterized separately. A number of NMR studies on fragments of biologically relevant loops of receptors that fold similarly to the intact system, has been reported and will be discussed in section 1.3. Another approach reported is the modelling of ligand/receptor interactions using structural data combined with information from site-directed mutagenesis studies. Here the focus is on biochemical studies of reduced receptor systems and the *in vivo* assembly of GPCRs from fragments to justify the above mentioned splitting/modelling approach.

Binding properties of single loops and terminal fragments

The question whether peptides representing the cytoplasmic loops of a G protein coupled receptor reflect the structure of the corresponding segment in the parent protein, has been addressed by several laboratories. König *et al.* (1989) designed 14 synthetic peptides comprising all surface regions of rhodopsin. By using a spectroscopic assay that measures the amount of metarhodopsin II-formation caused by G_t (transducin) binding they found that three peptides, corresponding to the second, third and a putative fourth cytoplasmic loop (in the carboxyl-terminal sequence) were able to compete with metarhodopsin II for G_t binding exhibiting K_d values in the 2 μM range. Interestingly, any combination of two out of these three peptides displayed a 15 times higher, synergistic competition effectiveness than when assayed separately. Moreover, for a 14-residue peptide from the C-terminal tail of rhodopsin it was found that it not only binds to the transducin α-subunit (in complex with GDP) but also facilitates its NaF-induced activation of the retinal effector enzyme cyclic GMP phosphodiesterase (cGMP PDE) (Phillips & Cerione, 1994).

Very recently, the complete N-terminal, extracellular part of the parathyroid hormone receptor 1 (PTHR1) has been overexpressed in *Escherichia coli*. After oxidative renaturation from the inclusion bodies and purification, nPTHR (23-191), ligand binding was tested by surface plasmon resonance spectroscopy and isothermal titration calorimetry. Both types of binding assays and one competition assay revealed apparent dissociation constants K_d of 3 - 5 μM, which is 1000 fold lower than the dissociation constant of PTH to membrane-bound full-length PTHR1. The disulfide pattern in nPTHR involving the highly conserved cysteine residues within family 2 GPCRs, was determined by digesting the protein with chymotrypsin followed by RP-HPLC analysis of the resulting fragments

and N-terminal sequencing. Thereby, the linkage pattern was identified and structural homogeneity proven (Grauschopf *et al.*, 2000).

The role of disulfide bonds for receptor function

All members of family 1 GPCRs share two conserved cysteine residues, one in the putative first extracellular loop e1 near the top of the third transmembrane domain TM III and one in e2. It is a common opinion that this pair of cysteines forms a disulfide bond in most or even all family 1 GPCRs (Bockaert & Pin, 1999) being conformationally important during synthesis, expression on the cell surface and/or to maintain normal binding and activation. Mutants of rhodopsin, in which one or both of the cysteines were substituted by alanine, were expressed normally and bound retinal normally, but they exhibited a defect in the stability of the activated intermediate metarhodopsin II (Davidson *et al.*, 1994). The situation is different at the β_2-adrenergic receptor, where 4 extracellular cysteines may form 2 extracellular disulfide bonds between e1 and e2. Noda *et al.* (1994) identified two pairwise linkages each between one of the conserved and one of the additional cysteines, which is therefore distinct from other G protein coupled receptors.

Perlman *et al.* (1995) collected data for the thyrotropin-releasing hormone receptor, based on single and double mutations of the two conserved cysteine residues in e1/e2, and on the effects of the reducing agent dithiothreitol (DTT) on these mutants. High affinity binding of thyrotropin-hormone was decreased by DTT in wild-type receptors (22 fold lower K_i for methyl-thyrotropin), substitution of either of the conserved cysteines decreased TRH binding affinity (4'400/640 fold higher EC_{50} value of TRH for stimulation of inositolphosphate formation), but was not decreased by DTT in mutants in which one of the cysteines was substi-

tuted by alanine and finally, substitution of both cysteines by alanine did not decrease the estimated affinity more than substitution of Cys^{98} alone (4'400 fold). Obviously, the extracellular disulfide bond between the conserved cysteines is necessary to constrain the receptor in a conformation that can attain high affinity binding. However, the maximal extents of stimulation of wild-type and mutated receptors were the same, which is consistent with the suggestion that the efficacies of these receptors are similar. The conserved extracellular disulfide bond is therefore not required for full apparent efficacy in GPCRs.

Split G protein coupled receptors and assembly from fragments

Cysteine scanning mutagenesis and oxidative disulfide cross-linking is a method to map out tertiary interactions in receptors (Falke & Koshland, 1987). This method has recently been adapted to rhodopsin by using split receptor (SR) constructs in which receptors are expressed as non-covalently associated N- and C-terminal fragments (Struthers *et al.*, 1999). A cysteine is introduced into each fragment. If a disulfide bond is formed upon oxidative cross-linking, then the two introduced cysteines are likely to be close in the three-dimensional structure of the native protein, *e.g.* it was shown, that cysteine substitutions at positions 198, 200 and 204 in SR(1-5) exhibited significant cross-linking with a cysteine at position 276 in SR(6-7). Moreover, both SR(1-5:T198C/6-7:F276C) and SR(1-5:V204C/6-7:F276C) but not SR(1-5:N200C/6-7:F276C) reconstituted with 11-*cis*-retinal and showed normal bleaching behavior.

Martin *et al.* (1999) created a series of genes encoding α-mating pheromone receptors of *Saccharomyces cerevisiae* with amino- or carboxyl-terminal truncations at each of the loop regions connecting transmembrane segments. Complementary and noncomplementary pairs of N- and C-

terminal fragments were coexpressed in yeast. The ability of the split receptors to signal in the presence of α-factor was assayed by testing for induction of the yeast pheromone response pathway. From their investigations they concluded: (1) Correct folding of the α-factor receptor does not require a covalent connection between any pair of transmembrane segments that are adjacent in the sequence. (2) Most of the second intracellular loop of the receptor is not required for function. (3) The structure of the receptor cannot, in most cases, tolerate the presence of extra transmembrane segments. (4) None of the truncated fragments of the α-factor receptor can efficiently oligomerize with normal receptors in such a way as to inhibit receptor function.

Minimum structural requirements for a functional GPCR

In their effort to clone the chemokine receptor CCR5, Ling *et al.* (1999) unexpectedly obtained the mutant mCCR5 lacking 72 amino acids (Leu^{36} - Gly^{107}) coding for the first and second putative transmembrane and the first intracellular and extracellular loops of CCR5. The analogous mutation was subsequently constructed for another chemokine receptor CXCR4 resulting in mCXCR4. Thus, both receptors possessed only the last five TMs with the intact N terminus directly connected to the third TM.

Stable surface expression on human embryonic kidney 293 cells of the wild-type and the mutant chemokine receptors, tagged with the hemagglutinin epitope at the N termini was detected by laser confocal microscopy and flow cytometry after immuno-fluorescence staining. The five-TM mutant receptors mediated chemokine-stimulated chemotaxis, Ca^{2+}-influx and activation of pertussis-toxin-sensitive G proteins. They exhib-

ited agonist-dependent internalization and desensitization and were subjected to regulation by GPCR kinases and arrestins.

The data suggest that already the five-TM domain structure may be sufficient for a functional GPCR at least in some cases. Wherever efforts and costs for investigations rise with the molecular size it might be worth to keep this fact in mind.

1.3. NMR spectroscopy of membrane receptors and their ligands

During the last two decades, NMR has become a powerful alternative technique to X-ray crystallography to obtain atomic resolution structures of biological macromolecules. Today, it is mainly applied to proteins in the 2 to 30 kDa range, with a maximum at 8 to 10 kDa (Güntert, 1998). Up to a size of about 6-10 kDa, structure determination is quite straight forward by applying 2D NMR experiments (Ernst *et al.*, 1987), following the sequence-specific sequential resonance assignment methodology developed by Wüthrich and co-workers (Wagner & Wüthrich, 1982b) and finally calculating structures from the NMR derived distance restraints (Williamson *et al.*, 1985; Güntert, 1998) (Figure 1.6). Molecules in the 8-15 kDa (15-25 kDa) range require ^{15}N (^{15}N and ^{13}C) uniform enrichment and may still be handled by heteronuclear resolved 3D/4D NMR. The isotope enriched proteins require new strategies for labelling with ^{15}N and ^{13}C using bacterial expression systems (Kay & Gardner, 1997) and allowed the development of ^{1}H-^{13}C-^{15}N triple resonance experiments for conformation-independent sequential assignments (Ikura *et al.*, 1990). Further-

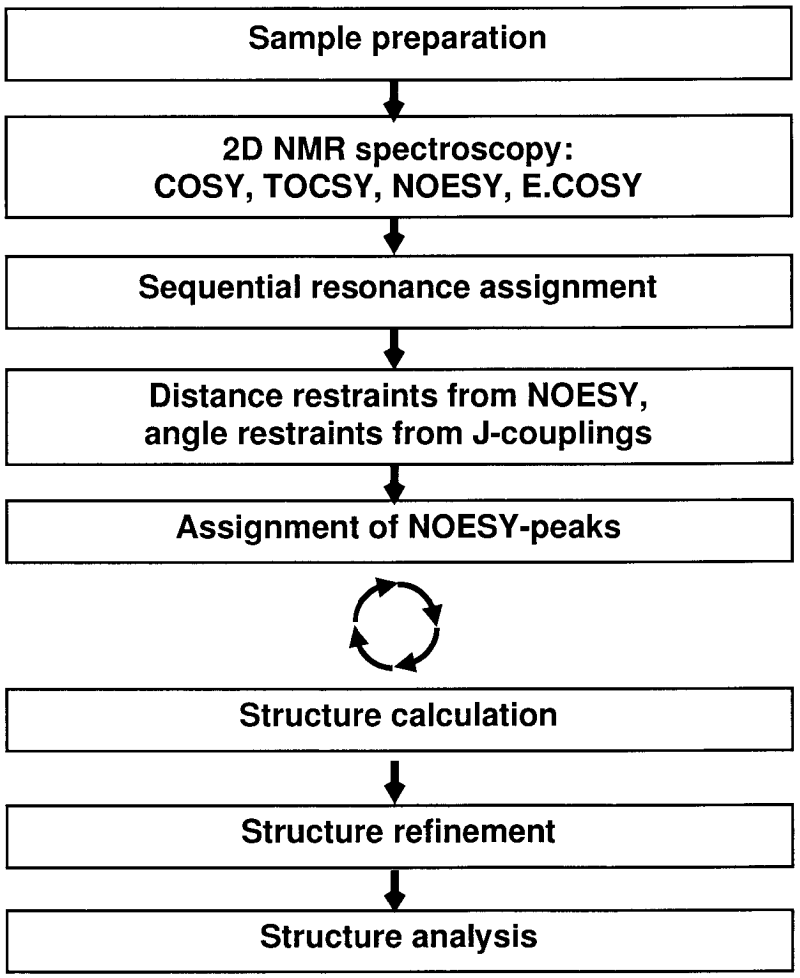

Figure 1.6 Determination of peptide structures by NMR (Wüthrich, 1986)

more, growing bacterial expression in ^2H_2O results in full or partial deuteration of proteins simplifying resonance multiplet structures and sharpening NMR line widths (LeMaster, 1994) and can help to rise limits to 40-50 kDa. For larger proteins, however, rapid transverse relaxation resulting in very broad signals and substantial spectral overlap need transverse relaxation-optimized spectroscopy (TROSY) (Pervushin *et al.*, 1997) and cross-correlated relaxation-enhanced polarization transfer (CRINEPT) (Riek *et al.*, 1999) techniques. The latter two experiments require high degrees of deuteration and very high magnetic fields to fully exploit their advantages.

One of the major advantages of NMR over X-ray crystallography is its applicability to molecules in solution resembling physiological conditions more closely. Furthermore, the proteins do not need to be crystallized, something that is notoriously difficult to achieve especially in the field of membrane proteins. In fact, comparisons between solution and crystal structures have revealed a very high similarity. Although the accuracy of NMR structures (especially for large proteins) is often lower NMR nevertheless is an important complement to X-ray crystallography for proteins that cannot be crystallized rapidly, for investigations into intermolecular interactions in solution, for determination of the dynamics (Peng & Wagner, 1993; Wagner, 1993; Palmer *et al.*, 1996) and investigations of folding pathways (Dobson & Hore, 1998) as well as for the identification of weak ligands and the subsequent rational design of high-affinity ligands for proteins, the so-called SAR (structure/activity relationship) by NMR (Shuker *et al.*, 1996). Finally, a number of proteins or peptides are only partially structured in solution, such as some hormones (one of which is the subject of interest in the present thesis), loops of membrane-spanning receptors or cytoplasmic receptor tails. Such molecules can hardly be crystallized but can readily be characterized with regard to structure and internal mobility by NMR spectroscopy. The following subsections present applications of these techniques and strategies to membrane-bound systems in more detail.

An emerging field whose impact is rising but cannot be exactly predicted for the near future are solid-state NMR investigations using uniformly isotopically labeled proteins. Molecular-size limits are *per se* irrelevant in the solid state. First assignments for a SH3 domain have recently appeared in literature (Pauli *et al.*, 2000) and substantial progress has been made in methodology (for a review see Fu & Cross, 1999). Limitations are severe due to limited dispersion of resonance lines and efficient spin-diffusion pathways.

NMR of peptide hormones

Many drugs mediate their effects by targeting G protein coupled receptors. The identification of structural properties, that are essential for the recognition and/or signalling process, is therefore likely to facilitate the design of non-peptide drugs with improved pharmacological properties (resistance to enzymatic degradation and improved delivery). In some cases, when a ligand acts on several receptor subtypes, the development of subtype-selective drugs could therefore reduce the range of associated side-effects. In a number of peptide systems, structural investigations have been complemented by mutagenesis studies and the introduction of conformational constraints to the peptides. Again, the modified peptides allow for comparative structural as well as biological investigations and hopefully for establishing a relationship between the structure and the biological activity.

The human parathyroid hormone shall serve as an example of a peptide hormone that has been extensively studied in solution. Whereas the 1-34 peptide fragment hPTH(1-34) is fully active and displays both adenyl cyclase (AC) stimulation and protein kinase C activities, the hPTH(1-31)NH_2 has only the AC-stimulating activity but shows full anabolic potency in the ovariectomized rat model of osteoporosis. The NMR structure of hPTH(1-31)NH_2 has recently been determined (Chen *et al.*, 2000) and compared to hPTH(1-34) (Marx *et al.*, 2000) and hPTH(1-37) (Marx *et al.*, 1995) (Figure 1.7) . For all three peptides, a short N-terminal helix followed by a loop and then by a long C-terminal helix, has been found. The atomic resolution structures revealed that the C-terminal helix is stabilized by a defined turn preceeding the helix with Asn^{16} as a N-cap residue. On the other hand, in the structure of hPTH(1-31)NH_2 residues Asp^{30} and Val^{31} appear to provide capping interactions to the C-terminal helix, which might be distracted in favour of nonspecific hydrophobic

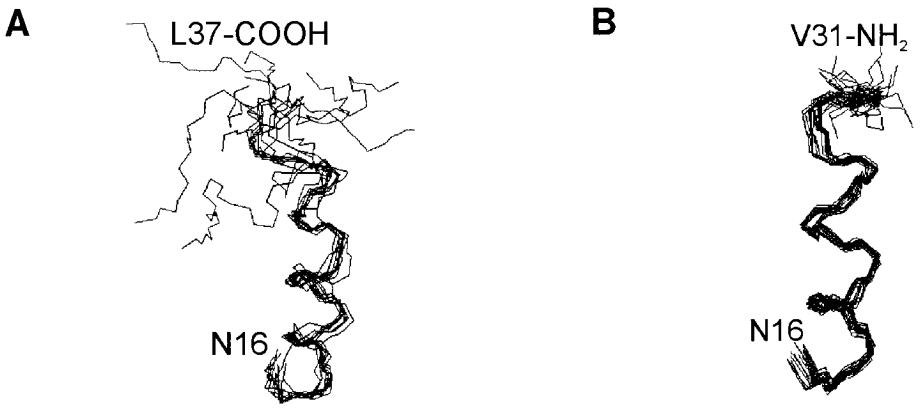

Figure 1.7 Comparison of the well-folded C-terminal helix of hPTH(1-31)NH_2 (A, PDB 1FVY) with that of hPTH(1-37) (B, PDB 1HPH). The backbone atoms of 10 conformers (A) and 30 conformers (B), respectively, are superimposed over residues 16-31.

contacts by the additional (flexible) residues His^{32}, Asn^{33}, Phe^{34} and Val^{35}, Ala^{36}, Leu^{37} in hPTH(1-34) and hPTH(1-37), respectively. It was concluded that capping and side-chain packing interactions might play a major role in the conformational stability of hPTH(1-31)NH_2 and that the existence of well-folded conformations at the C-terminus of PTH-fragments might be an important determinant for the biological activities. Compatible with these structural investigations was the finding that AC stimulating activity was enhanced when the 26-30 region of hPTH(1-31)NH_2 was cyclized in addition to the 18-22 cyclization (Barbier *et al.*, 2000) and the 13-17 cyclization (Condon *et al.*, 2000).

Investigating hormone binding to biological membranes by NMR

In view of the proposed membrane-bound pathway of receptor binding studies of peptide hormones should generally be conducted in the presence of a membrane surface. There are four alternative systems available for mimicking biological membranes: organic solvents, such as chloroform, methanol or trifluoroethanol, detergent micelles, bicelles (Sanders *et al.*, 1993) and small unilamellar phospholipid vesicles

(SUVs)/bilayers. Bicelles and bilayers are composed of true membrane phospholipids with two hydrocarbon chains esterified to a glycerol which in turn is esterified to the phosphate of a polar head group. However, the smallest phospholipid vesicles have the size of a small virus (250-300 Å) with a correlation time in the microsecond time range (Henry & Sykes, 1994). The larger the systems are, the longer their overall correlation time (τ_c) resulting in short transverse relaxation times T_2 and therefore broad lines. As a consequence, proteins tightly bound to bicelles, bilayers or SUVs can only be studied by solid-state NMR techniques. As an alternative, micelles formed from single-tailed lipid or detergent (amphipathic) molecules with molecular weights of the aggregates less than 30 kDa and correlation times in the 10 nanosecond range are well suitable for high-resolution NMR. Moreover, a large number of detergents are commercially available in deuterated form and their physical properties are well characterized (for rev. see: Henry & Sykes, 1994). Since small peripheral membrane proteins and membrane surface-associating peptides (but not necessarily membrane-spanning proteins, see below) are thought to attach to vesicles and micelles in a similar way, as long as the head-groups are identical, the characterization of peptide hormones associated to a micelle surface promises to give relevant information about their interaction with the plasma membrane (Figure 1.8 B). One widely used micelle is dodecylphosphocholine (DPC), a detergent that forms micelles consisting of about 60 molecules above the critical micelle concentration (cmc) of 1.1 mM (Lauterwein *et al.*, 1979). The zwitterionic head group (phosphate and choline) is modeled on phosphatidylcholine, the predominant phospholipid in animal cell membranes. Perdeuterated DPC was developed specifically for NMR purposes and has the advantage of being stable over a wide range of temperatures and pH values and is not expected to be subject to strong ionic strength effects (Brown, 1979).

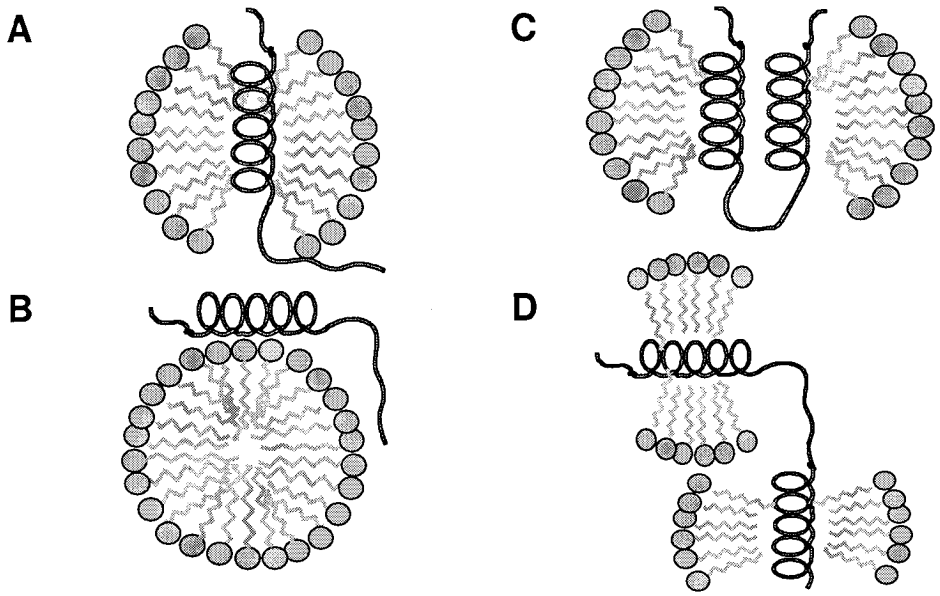

Figure 1.8 Solubilization of membrane proteins by use of detergent micelles. (A) Short hydrophobic, membrane-spanning peptide. (B) Membrane surface associated short amphiphilic peptide. (C) Detergent solubilization of a membrane protein with two transmembrane helices in the native state. (D) Denaturation of a membrane protein by disruption of tertiary interactions. The figure is modified from Henry & Sykes (1994).

Again, the parathyroid hormone shall serve as an example for a peptide studied in a micellar environment. The NMR study of hPTH(1-34) in the presence of dodecylphosphocholine (DPC) micelles clearly demonstrated that the membrane environment induced a higher degree of conformational order, extending and stabilizing both the N- and C-terminal α-helix. In pure water or phosphate buffer with 270 mM NaCl, the two helical domains are separated by a flexible region centered around residues 14/15. A flexible hinge region is also found in DPC micelles, but centered about residues 18 and 19 (Pellegrini *et al.*, 1998b). Interestingly, results from a series of PTH-related protein (PTHrP) mutants that were cyclized through introduction of side-chain lactam bridges have shown that flexibility around residue 19 is required for high biological activity at the PTH1 receptor (Mierke *et al.*, 1997). The 39-residue tuberoinfundibu-

lar peptide (TIP39) is a natural ligand for the PTH2 receptor. The PTH2 receptor shares 51% identity (70% sequence similarity) with the PTH/PTHrP (PTH1) receptor and was initially described as being activated only by PTH and not by PTHrP. Although the sequence alignment of bovine TIP39 with human PTH(1-40) indicates low sequence homology, superposition of helical fragments 5-15 of TIP39 with Ser3-Lys13 of PTH(1-34) (as determined by NMR in the presence of DPC micelles) revealed an almost identical spatial distribution of polar and hydrophobic amino acids. Two exceptions are TIP39(Asp^7)/PTH(Ile^5) and TIP39(Arg^{13})/PTH(Leu^{11}) located in the first and third loop of the N-terminal helix (Piserchio *et al.*, 2000b). These two residues are projecting toward the micelle surface in both structures, as determined by probing with membrane-integrating spin-labels (see below). Together with binding data of N-terminally truncated TIP39 at the PTH1 and PTH2 receptors (Hoare *et al.*, 2000) as well as modelling data (Rolz *et al.*, 1999), it is speculated, that Asp^7 accounts for the selectivity of TIP39 toward the PTH2 receptor.

The topological orientation of peptides on the micelle surface can be determined by enhanced longitudinal and transverse relaxation due to dipolar interactions with paramagnetic molecules in close (less than about 10 Å) vicinity. Doxyl-stearic acid with the spin-label substituted at various positions along the alkyl chain readily incorporate into SDS or DPC micelles. The effect of the spin-label position on the line width of the carbon atoms of the DPC alkyl chain have been determined using ^{13}C NMR and approximate spatial locations within the micelle for the nitroxide moieties of the different spin-labels were deduced from the NMR relaxation rates observed for different nuclei of dodecylphosphocholine (Brown *et al.*, 1981) (Figure 1.9) . Doxyl-stearates have successfully been applied to determine the location and orientation of glucagon (Brown *et al.*, 1981), melittin (Brown *et al.*, 1982), β-peptides of Alzheimer's disease

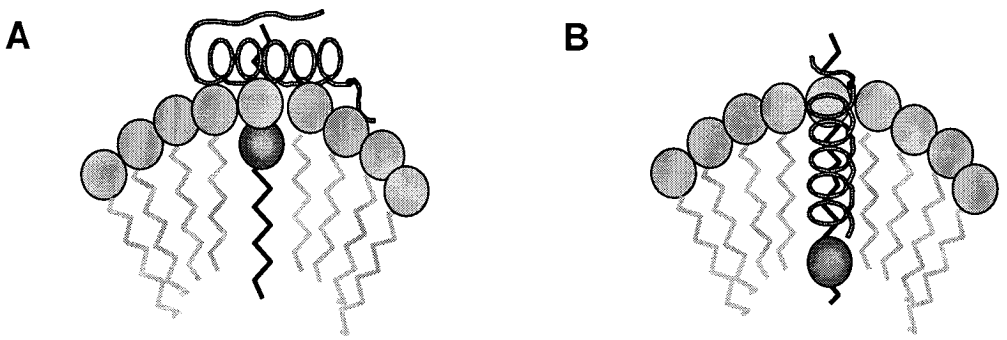

Figure 1.9 Most common membrane-integrating spin-labels (black coloured) are 5-doxyl-stearic acid (A) and 12-doxyl-stearic acid (B) with the nitroxide containing doxyl-groups becoming located in the vicinity of the lipid head-groups or in the center of the micelles, respectively. 5-doxyl-stearic acid is particularly suitable to study surface associating peptides, whereas 12-doxyl-stearic acid is used to identify micelle-integrating residues.

(Shao *et al.*, 1999) and many others relative to the micelle surface. Complementary information about the peptide orientation can be obtained by amide hydrogen exchange measurements at elevated pH. Hydrogen exchange is catalyzed by both acid and base. For solvent accessible, labile backbone hydrogen protons of peptides in aqueous solution at 25°C, exchange is slowest at pH 3 (Wüthrich & Wagner, 1979). At elevated pH, amide proton exchange rates can nevertheless be slow indicating stable hydrogen bond formation or shielding from the surrounding solvent (Wagner & Wüthrich, 1982a). In fact, it has been observed that amide protons from residues at the membrane interface are indeed shielded from solvent and display reduced exchange rates (Shao *et al.*, 1999).

NMR of G protein coupled receptors

G protein coupled receptors are membrane proteins (>200 residues) with seven transmembrane helices. The membrane spanning domains consist of highly hydrophobic sequences of about 20-25 amino acids, con-

nected by alternating extracellular and intracellular loops. Besides the problems in producing sufficient amounts and in purification of membrane proteins, difficulties are also expected from solubilizing them in a medium suitable for NMR. Organic solvents as well as micellar detergents are known to induce folding, and it can *a priori* not be excluded that non-native secondary structure is induced thereby. Moreover, the tertiary structure of proteins with two or more membrane-spanning regions can be disrupted in detergents, and hydrophobic peptides/proteins sometimes form nonnative β aggregates (Figure 1.8). Finally, the correlation time problem implying the size limitation of macromolecular structure determination by NMR, has inspired a search for alternate approaches to gain structural information about membrane proteins. For GPCRs one such approach is to determine the structures of discrete subdomains such as the helices and loops (*vide supra*). The hypothesis is, that the solution structures of these subdomains closely resembles the structures of the corresponding turns of the intact protein. Katragadda *et al.* (2000) very recently examined this hypothesis for loop regions of bacteriorhodopsin from *Halobacterium halobium*. In several crystal structures three of the six loops are well defined. The structures for these three loops (a 23mer, a 15mer and a 24mer) were determined in DMSO and superimposed on the corresponding amino acid sequence in a crystal structure of bacteriorhodopsin (Lücke *et al.*, 1999). Good agreement with rmsd values of around 2 was obtained except at the last two or three residues which are disordered in the solution structure. This result indicates that the loop regions connecting transmembrane helices are stabilized largely by relatively short range interactions and that at least some of the loop regions may contribute to structural stability of bacteriorhodopsin.

It has already been discussed that peptides corresponding to the second and third cytoplasmic loops and the carboxyl-terminal domain have biological activity in solution and are synergistic in their ability to inhibit

the activation of the G protein by light-activated rhodopsin (König *et al.*, 1989), suggesting that these domains form a complex in solution, at least in the presence of the G protein. Yeagle and co-workers solved the solution structures of the three cytoplasmic loops and the carboxyl-terminal domain of rhodopsin both individually (Yeagle *et al.*, 1995a; Yeagle *et al.*, 1995b; Yeagle *et al.*, 1996; Yeagle *et al.*, 1997b) and together in the proposed complex (Yeagle *et al.*, 1997a) using 7 intermolecular NOE constraints. The comparison showed that the ends of the loops are more ordered in the complex than individually supporting the conclusions drawn for the loop peptides of bacteriorhodopsin. Using dipolar interactions between spin labels, distances between specific sites on rhodopsin were measured in both the inactivated (R) and activated (R^*) state (Altenbach *et al.*, 1996; Farrens *et al.*, 1996; Yang *et al.*, 1996). The distances, measured on the complex as determined by NMR, agreed with the distances reported on intact rhodopsin in the activated state R^*. One interesting conclusion drawn from the fact that the readily assembled complex of the four peptides is similar to the activated state of the cytoplasmic face of rhodopsin, is that 11-*cis*-retinal might be considered as an inverse agonist, stabilizing the inactivated state until the absorption of light.

A slightly different approach for the structure determination of the third cytoplasmic loop of the PTH1 receptor was chosen by Mierke *et al.* (1996). They examined a 27-amino acid peptide both in the linear form and cyclized with a octa-methylene linker to maintain a distance of 12 Å. This distance was derived from measurements between transmembrane helices in bacteriorhodopsin. The structure of the peptides was determined in aqueous solution and in the presence of sodium dodecylsulfate (SDS) micelles. Both peptides were unstructured in aqueous solution. In the membrane mimicking system, the peptides maintained a well-defined α-helix at the N-terminus followed by a flexible domain. How-

ever, only in the cyclic analogue, the C-terminal portion was in a turn-like conformation as well.

Work on the characterization of extracellular domains of GPCRs was mainly conducted by Mierke and co-workers for the PTH system (reviewed in Pellegrini & Mierke, 1999b). The extracellular N-terminal region of PTH1 receptor between residues 173-181 had been implicated in ligand binding by results of photoaffinity labelling studies (Zhou *et al.*, 1997). The NMR analysis of PTH1R[168-198], carried out in the presence of DPC micelles, indicated a conformation of three α-helices. From spin-label experiments (*vide supra*) it was concluded that the C-terminal helix, containing seven residues of the first TM helix (TM I) was embedded within the micelle interior, whereas the other two amphipathic helices were found to lie on the micelle surface. It was concluded that in this orientation, many hydrophilic residues point towards the solvent and can be accessed by the ligand to form complementary interactions with polar residues (Pellegrini *et al.*, 1998a). Similarly, Leu^{261}, located in the first extracellular loop e1, was found to cross-link to a Lys^{27} (linked to benzophenone) of PTH (Greenberg *et al.*, 2000). Again, a peptide was designed, which comprises the e1-domain and a sufficient number of amino acids of the adjacent TM helices were added in order to act as anchors. Thereby, the loop or termini were tethered to the lipid environment and provided the naturally occurring topological orientation resulting in the fragment PTH1R(241-285) (Piserchio *et al.*, 2000a). The N terminus exhibited a long loop embedded into the membrane, probably constituting the C-terminal end of TM II. In the loop region of e1, a well-defined α-helix was observed between Leu^{256}-Ile^{264}, lying parallel to the membrane surface. Again, the C-terminal portion (275-284) was in membrane-embedded α-helical conformation. Residue Leu^{261} was found to be located in the middle of the well-defined central helix pointing its side chain towards the membrane. Since the photoreactive PTH(1-34) ana-

logue used in the cross-linking experiments contained a benzophenone (BP) moiety on Lys^{27}, the identification of the lipid-water interface located Leu^{261} as a contact point is therefore not surprising.

NMR of ligand/receptor interactions

The same NOE-based approach used to determine the three-dimensional structures of a single macromolecule can also be applied to identify contact points between a ligand and a receptor. Chen *et al.* (1998) studied the interactions of the 74-residue glycoprotein C5a anaphylatoxin, derived from the fifth component of the complement system upon proteolytic activation, with peptide fragments of the amino-terminal domain of the C5a receptor. He found specific binding of the isolated N-terminal domain (1-34) of C5aR to C5a and to a C5a antagonist analogue. Similarly, Pellegrini & Mierke (1999a) investigated the bimolecular complex of the C-terminal octapeptide of cholecystokinin, CCK-8, with the N-terminus of the CCK(A)-receptor, CCK(A)-R(1-47), including 6-7 amino acids of the first TM helix. The ligand/receptor complex was characterized by unambiguous intermolecular NOEs between Tyr27 and Met28 of CCK-8 and Trp39 of CCK(A)-R(1-47) (Figure 1.10). Interestingly, this alignment was consistent with published mutagenesis studies, but required a different interpretation of recent findings from photoaffinity cross-linking studies.

A disadvantage of the NOE-based approach to identify a ligand binding site is that the experiments and unambiguous assignments of intermolecular NOEs are time consuming and therefore not suitable for screening purposes. In contrast, in the recently introduced drug discovery technique called SAR (structure-activity relationship) by NMR (Shuker *et al.*, 1996) binding of a test compound to specific residues is

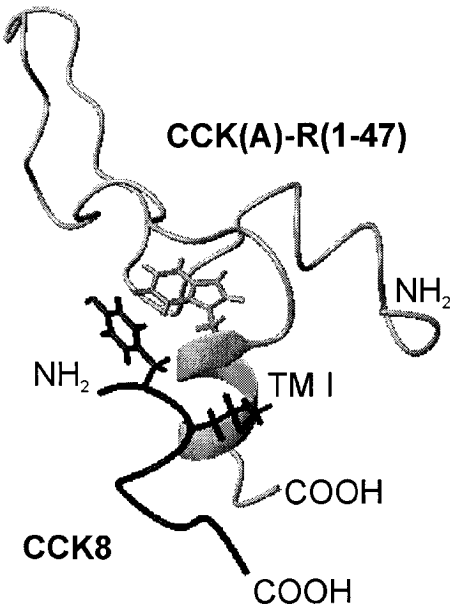

Figure 1.10 The ligand/receptor complex of CCK-8 (black) with the N-terminal fragment of the CCK(A)-receptor (1-47) (grey) in DPC micelles (PDB 1D6G). The TM I segment of the receptor fragment is in helical conformation. Intermolecular NOEs are observed between Tyr27 and Met28 of CCK-8 and Trp39 of CCK(A)-R(1-47) (side-chains are shown only for these residues).

readily recognized by observing changes in the position of the corresponding [^{15}N, ^{1}H]-HSQC-peaks due to chemical shift perturbations. The [^{15}N, ^{1}H]-HSQC-experiment, is very sensitive (required concentrations can be below 0.1 mM) and quickly yields a usually very well dispersed spectrum displaying a single peak for each amide moiety of the backbone of all residues except Pro. The method allows the detection of very weak binding ($K_d > 1$ mM).

Binding of a ligand to a receptor can also be detected through measurement of translational diffusion. The technique is based on the fact that lateral diffusion in solution is strongly size-dependent. If the diffusion coefficient of the ligand in the complex is different enough from the one of the free ligand, pulsed-field gradient-NMR can be applied to suppress the signals of the more rapidly diffusing (smaller) molecules. Alternatively, the change in the diffusion constant may indicate the degree of binding. Compounds with affinity to the target are therefore readily identified from a mixture containing also nonbinding molecules (Bleicher *et al.*, 1998). However, this approach gives no information about the location of the binding site. Alternatively, increased T_2 relaxation leads to

line-broadening of signals upon binding, which is easily detected in 1D experiments. All experiments based upon differential relaxation or changes in diffusion coefficients do not require isotopically enriched material and may therefore be used to screen large libraries.

In the absence of a structure of the drug-target complex, drug design may profit form the knowledge of the conformation of the bound drug/ligand. Although limited to ligands with a $10^{-3} > K_d > 10^{-7}$ M, the transferred NOE (trNOE) experiment allows to measure NOEs that have built up when the ligand was bound to the target between ligand protons by observing the effect on the sharper lines of the unbound molecule in solution (Clore & Gronenborn, 1982). By this procedure it was possible to solve the conformation of a macrolide antibiotic bound to the ribosome (Campbell & Sykes, 1993). Although this method is of limited use for the characterization of the receptor, it nevertheless gives important structural information on the target and is therefore useful in the context of drug design. Recently the first conformation of a peptide ligand, an analogue of the pituitary adenylate cyclase activating peptide (PACAP), bound to its G-Protein coupled receptor was solved using the trNOE experiment (Inooka *et al.*, 2001). They could show that in the receptor-bound state the C-terminal α-helix comprising residues 8-21 is very similar to the one in the micelle-bound state while the N-terminal residues 1-7 adopt a unique β-coil structure only after binding to the receptor. This β-coil forms a hydrophobic patch which seems to be essential for receptor binding and/or activation (Figure 1.11). These findings suggest that PACAP essentially consists of two functional segments, in agreement with the message/address concept by Schwyzer. Whereas the C-terminal α-helix serves to anchor the peptide on the membrane surface, the N terminus gets in contact with the receptor, resulting in a defined β-coil structure and stabilization of the active receptor conformation.

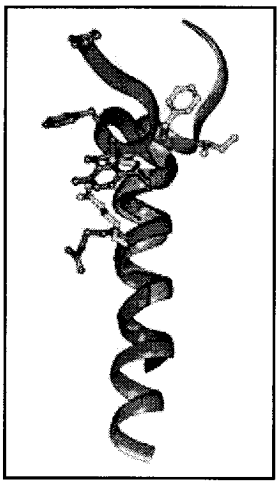

Figure 1.11 Superimposition of the receptor-bound PACAP21 (black) and the micelle-bound PACAP27 (grey), from Inooka *et al.* (2001). The side-chains constituting the hydrophobic patch are indicated as ball-and-stick models.

1.4. The structure of Neuropeptide Y: Aims & scopes of this work

Neuropeptide Y (NPY), peptide YY (PYY) and pancreatic polypeptide (PP) are three very important and closely related endocrine polypeptides. In the circulation, PP is mainly found in the pancreas, PYY in the gut and NPY is released from neuroneal stores. Whereas PP and PYY act as gastrointestinal hormones, NPY is a neurotransmitter of the central and peripheral nervous system. It is a potent vasoconstrictor and has been implicated in anxiety and depression, feeding and obesity, memory retention, neuroneal excitability, endocrine function and metabolism. All these actions are mediated by at least six (so-far identified) NPY receptors that belong to the family 1b of G protein coupled receptors. The typical signaling responses of NPY receptors are similar to those of other G_i/G_o-coupled receptors, *i.e.* inhibition of adenylate cyclase. Other signal transduction pathways including inositol phosphate-dependent and independent mobilization of Ca^{2+} from intracellular stores and activation of a

phospholipase A_2 by NPY receptors have been postulated (for reviews see Gehlert, 1998; Michel *et al.*, 1998).

Today, the NPY Y_1, Y_2, Y_4, and Y_5 receptors have been cloned and characterized. With such cell lines in hand, it became possible to perform ligand binding studies at the different receptor subtypes and to develop potent and selective agonists and antagonists. The essential segments of NPY for receptor recognition have been determined using C- and N-terminal truncated analogues. The significance of each residue was systematically assessed by the single exchange with L-Ala or the corresponding D-isomer. Moreover, single and multiple substitutions of important residues with both natural and unnatural amino acids, and the introduction of conformational constraints by means of special amino acid units, spacer templates or cyclizations and the subsequent affinity measurements of these compounds resulted in a huge amount of affinity data of NPY analogues at the different receptor subtypes (see Cabrele & Beck-Sickinger, 2000).

Structural studies of NPY and NPY analogues that may be related to receptor subtype specificity are important for further optimizations in a more rational way and a deeper understanding of the mechanisms underlying receptor recognition and possibly activation. Due to the above-mentioned difficulties in obtaining sufficient amounts of pure and functionally reconstituted receptor protein, most of the structural studies are limited to the characterization of the unbound ligand. Although the receptor-bound conformations of the ligand are expected to vary from one receptor subtype to another (induced fit) and to be well defined, the presence of residual structure either in aqueous solution or bound to a membrane should reveal structural features that are important in the initial receptor recognition process, as outlined above. Herein, we present NMR studies of NPY and a Y_5 receptor-selective NPY analogue in aqueous solution and when bound to a micelle-forming membrane mimetic.

NMR is perfectly suitable for this kind of studies, since it provides high resolution structures, information about the dynamics and all kind of interactions between the different components of the system under investigation.

The molecular conformation of NPY either in pure water or in the presence of organic solvents like trifluoroethanol, hexafluoroisopropanol and even DMSO has been controversially discussed in the literature. Table 1.2 summarizes a representative set of those NMR studies. The presented tertiary structures can essentially be grouped into two classes of structural models. The first class is composed of models that closely resemble the tertiary fold derived from the crystal structure of dimeric avian pancreatic polypeptide (aPP) (Blundell *et al.*, 1981) (Figure 1.12). It

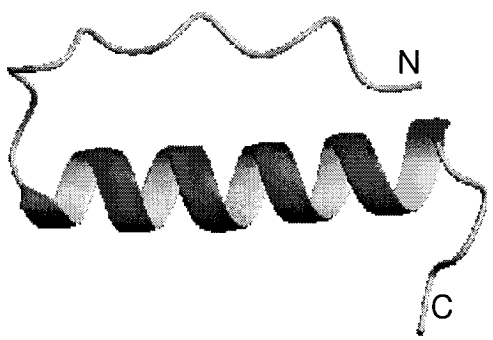

Figure 1.12 Ribbon presentation of the crystal structure of avian pancreatic polypeptide (PDB accession code 1PPT).

is characterized by an α-helix involving residues 14-31 connected *via* a β-turn to an N-terminal polyproline II helix and is referred to as the PP-fold. The NMR data, which lead to these models, were collected on NPY in water and in DMSO, as well as [Leu31, Pro34]-NPY in DMSO (Table 1.2, references 1-3). The second class comprises structures based on NMR data of NPY in water and trifluoroethanol (TFE) (Table 1.2, references 4-7). In this type of model, the N-terminal tail is fully flexible, whereas residues 11-36 in water and residues 19-34 in TFE are in an α-helical conformation (Figure 1.13). Moreover, the data obtained in TFE were indicative of a NPY monomer (Mierke *et al.*, 1992). On the other hand, Cowley *et al.*

Table 1.2 NMR studies on NPY and NPY analogues

Peptide	Conditions	Structural characterization	Reference
hNPY	H_2O, pH 3.1, 37°C	aPP-like fold	Darbon *et al.*, 1992
NPY, [Ahx5-17]NPY	DMSO	hairpin, C terminus orientated towards N terminus	Boulanger *et al.*, 1995
[Leu31, Pro34]NPY	DMSO, 27°C	aPP-like fold	Khiat *et al.*, 1998
pNPY	H_2O, pH 3.1, 37°C	α-helix 11-36, flexible N terminus	Saudek & Pelton, 1990
hNPY	TFE	α-helix 19-34, flexible N terminus	Mierke *et al.*, 1992
pNPY	H_2O, 0.05 M acetic acid pH 3.2, 37°C	dimer (handshake model), α-helix 11-36, N terminus unstructured	Cowley *et al.*, 1992
hNPY	H_2O, pH 3.1, 37°C	antiparallel dimer, α-helix 11-36, flexible N terminus	Monks *et al.*, 1996
hNPY	H_2O/Tris pH 7.2, 25°C	dimer - monomer equilibrium	Nordmann *et al.*, 1999
NPY(1-9)/ NPY(1-14)/ NPY(1-25)	0-50% TFE	random coil/random coil/13% α-helix	Chu *et al.*, 1995
NPY (13-36)	30% HFP, 15°C, pH 3.1	monomer, α-helix	Arvidsson *et al.*, 1994
[L17, Q19, A20, E23, L28, L31]NPY(13-36)	20% TFE, pH 3.7, 20°C	α-helix, antiparallel dimer	Barden, 1995
NPY (13-36)	DMSO, 25°C	α-helix 30-36, wide loop 17-22	Labelle *et al.*, 1997
Ac[Leu(28,31)]NPY(24-36)	40% TFE, 4-20°C	α-helix 25-35, trimer/tetramer	Barnham *et al.*, 1999
cyclic [Lys28-Glu32] NPY Ac-25-36	30% TFE, 35°C	hairpin, C terminus orientated towards N terminus	Rist *et al.*, 1996

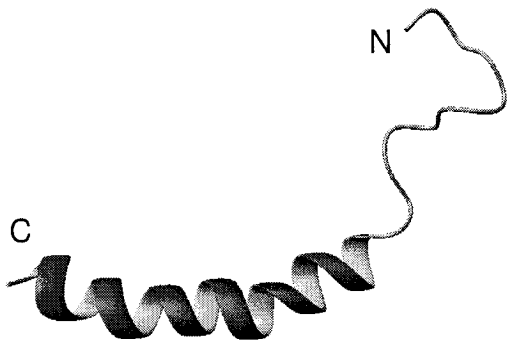

Figure 1.13 Ribbon presentation of one representative NMR structure of neuropeptide Y according to Monks *et al.* (1996) (PDB accession code 1RON).

(1992) and Monks *et al.* (1996) observed intermolecular NOEs for NPY in aqueous solution whose origin could only be explained by the proposition of a dimeric model, in which the two NPY molecules interact *via* side-chains of their α-helices and are aligned in an anti-parallel fashion. However, the authors reported different sets of intermolecular NOEs and therefore also proposed different models to fulfil the derived distance restraints (Figure 1.14 A, B). Based on investigations by CD spectroscopy,

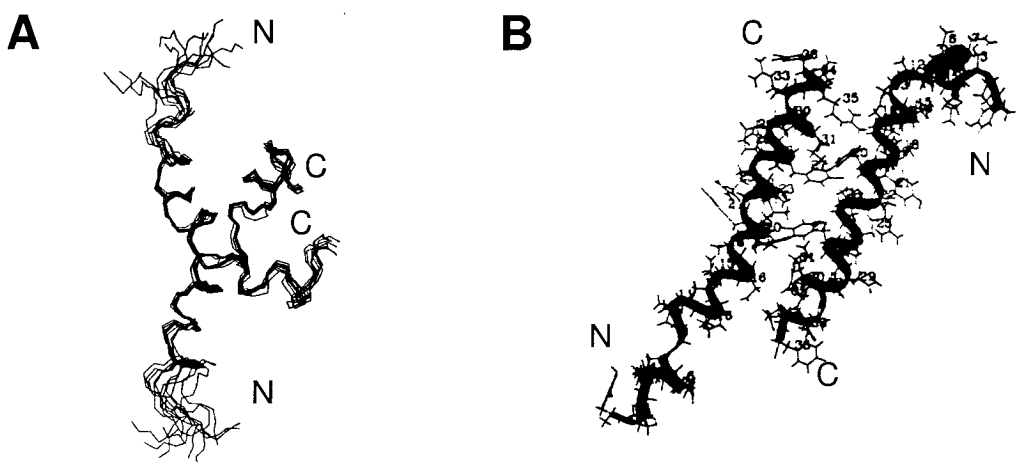

Figure 1.14 The proposed quarternary structures of dimeric NPY. (A) „Handshake model" by Cowley *et al.* (1992). Superposition of the best 12 structures of the dimer, fitted for minimal rmsd of their main chain atoms in the residues 13-33. Only residues 10-36 are shown. (B) Anti-parallel helix arrangement according to Monks *et al.* (1996). Only the helical residues are well defined; the orientation of the N termini relative to the helices varies greatly. Both figures stem from the original publications.

Nordmann *et al.* (1999) suggested that the PP-fold conformation might exist at low concentrations, but that at concentrations needed for NMR studies, the dimer is the most abundant form. This is in agreement with the K_d of dimerization, which was determined to be 1.6 μM (Cowley *et al.*, 1992). Nordmann postulates, that dimerization is accompanied by an unfolding of the polyproline helix.

Several authors dealt with the conformation of NPY fragments. N-terminal segments are not only completely inactive in biological assays, but are also unstructured in 0-50% TFE up to a length of at least 14 residues. 13% helical content is observed in NPY(1-25) (Chu *et al.*, 1995). Whereas the affinity for analogues of N-terminally truncated NPY analogues drops to the micromolar range at the Y_1 and Y_5 receptors, NPY(13-36), NPY(18-36) and NPY(22-36) still exhibit subnanomolar affinities for the Y_2 receptor (Beck-Sickinger & Jung, 1995). In 30% hexafluoroisopropanol NPY(13-36) is completely α-helical and monomeric (Arvidsson *et al.*, 1994). The same molecule is characterized by a helical C-terminal fragment Leu^{30}-Tyr^{36} and a wide loop from Leu^{17} to Ser^{22} in DMSO (Labelle *et al.*, 1997). [Leu^{17}, Gln^{19}, Ala^{20}, Glu^{23}, Leu^{28}, Leu^{31}]NPY(13-36) (ANA-NPY) forms a well-defined helix between residues Leu^{24}-Tyr^{36} in 20% TFE. A second helix extends from Asp^{16} to Glu^{23}. Two monomers are arranged in an anti-parallel orientation associated at an interface in the segment Leu^{24}-Tyr^{36} (Barden, 1995). The potent Y_2 receptor agonist Ac[$Leu^{28,31}$]NPY(24-36) is unstructured and monomeric in aqueous solution at 5-20°C. In 40% TFE at 20°C it forms a well-defined helix (encompassing residues 25-35) and associates to form a tetramer, which is in contrast to many peptides in aqueous TFE (Barnham *et al.*, 1999). The C-terminal dodecapeptide of NPY was cyclized between residues 28 and 32 by lactamization upon replacement of Leu^{28} and Thr^{32} by Lys and Glu, respectively. Cyclo-(28/32) Ac-[Lys^{28}-Glu^{32}] NPY showed a more than 100-fold increase in affinity compared to the C-terminal linear dode-

capeptide and revealed full agonistic properties. The NMR structures as determined in 30% TFE revealed a major difference between the inactive linear and the active cyclic peptide in the orientation of the C-terminal amino acids Arg^{35}-Tyr^{36}-NH_2. Whereas for the linear peptide this dipeptide is part of the helix, in the case of the cyclic derivative the last two residues are involved in a bend which orients the C terminus towards the N terminus (Rist *et al.*, 1996).§

Chapter 2 of the present work focusses on the structural characterizations of NPY in aqueous solution and in a membrane environment. Differences in the two states are outlined and their implications for receptor recognition are discussed. Special attention is given to the existence and role of NPY dimers, the widely discussed „PP-fold", that is proposed for all members of the NPY family of peptide hormones, the binding mode and interactions with a membrane as well as dynamical aspects of membrane binding. The results are in agreement with a membrane-bound pathway of receptor recognition.

The subjects of chapters 3 and 4 are devoted to the development and structural characterization of the first Y_5 receptor-selective agonist. Differences in the dynamics of the C-terminal part of the selective analogue compared to NPY as well as in the membrane binding mode are observed and suggested to play a role for the selective binding at the Y_5 receptor.

Finally, chapter 5 describes first steps in the synthesis and sample preparation of a lipopeptide mimicking the third extracellular loop of a Y receptor. The rationale for studying the structure of a single loop and its possible interactions with NPY is discussed.

1.5. References

Altenbach, C., Yang, K., Farrens, D. L., Farahbakhsh, Z. T., Khorana, H. G. & Hubbell, W. L. (1996). Structural features and light-dependent changes in the cytoplasmic interhelical E-F loop region of rhodopsin: a site-directed spin- labeling study. *Biochemistry* **35,** 12470-12478.

Arkin, I. T. & Brünger, A. T. (1998). Statistical analysis of predicted transmembrane α-helices. *Biochim. Biophys. Acta* **1429,** 113-128.

Arvidsson, K., Jarvet, J., Allard, P. & Ehrenber, A., (1994). Solution structure by ^{1}H and dynamics by natural abundance of ^{13}C NMR of a receptor recognising peptide derived from a C-terminal fragment of neuropeptide Y. *J.Biomol. NMR* **4,** 653-672.

Baldwin, J. M. (1993). The probable arrangement of the helices in G protein-coupled receptors. *EMBO J.* **12,** 1693-1703.

Barbier, J. R., MacLean, S., Morley, P., Whitfield, J. F. & Willick, G. E. (2000). Structure and activities of constrained analogues of human parathyroid hormone and parathyroid hormone-related peptide: implications for receptor-activating conformations of the hormones. *Biochemistry* **39,** 14522-14530.

Barden, J. A. (1995). Structure of prejunctional receptor binding analog of human neuropeptide Y dimer ANA-NPY. *Biochem. Biophys. Res. Com.* **215,** 264-271

Beck-Sickinger, A. G. & Jung, G. (1995). Structure-activity relationships of neuropeptide Y analogues with respect to Y_1 and Y_2 receptors. *Biopolymers* **37,** 123-142.

Birnbaumer, L. & Rodbell, M. (1969). Adenyl cyclase in fat cells. II. Hormone receptors. *J. Biol. Chem.* **244,** 3477-3482.

Bleicher, K., Lin, M., Shapiro, M. J. & Wareing, J. R. (1998). Diffusion edited NMR: Screening compound mixtures by affinity NMR to detect binding ligands to vancomycin. *J. Org. Chem.* **63,** 8486-8490.

Blundell, T. L., Pitts, J. E., Tickle, I. J., Wood, S. P. & Wu, C.-W. (1981). X-ray analysis (1.4 Å resolution) of avian pancreatic polypeptide: small globular protein hormone. *Proc. Natl Acad. Sci. USA,* **78,** 4175-4179.

Bockaert, J. & Pin, J. P. (1999). Molecular tinkering of G protein-coupled receptors: an evolutionary success. *EMBO J.* **18,** 1723-1729.

Bond, R. A., Leff, P., Johnson, T. D., Milano, C. A., Rockman, H. A., McMinn, T. R., Apparsundaram, S., Hyek, M. F., Kenakin, T. P. & Allen, L. F. (1995). Physiological effects of inverse agonists in transgenic mice with myocardial overexpression of the β_2-adrenoceptor. *Nature* **374,** 272-276.

Boulanger, Y., Chen, Y., Commodari, F., Senécal, L., Laberge, AM., Fournier, A. & St-Pierre, S. (1995) Structural characterication of neuropeptide tyrosine (NPY) and its agonist analog [Ahx$^{5-17}$]NPY by NMR and molecular modeling. *Int. J. Peptide Protein Res.* **45**, 86-95

Bourne, H. R. (1997). How receptors talk to trimeric G proteins. *Curr. Opin. Cell Biol.* **9**, 134-142.

Brown, L. R. (1979). Use of fully deuterated micelles for conformational studies of membrane proteins by high resolution 1H nuclear magnetic resonance. *Biochim. Biophys. Acta* **557,** 135-148.

Brown, L. R., Bosch, C. & Wüthrich, K. (1981). Location and orientation relative to the micelle surface for glucagon in mixed micelles with dodecylphosphocholine: EPR and NMR studies. *Biochim. Biophys. Acta* **642,** 296-312.

Brown, L. R., Braun, W., Kumar, A. & Wüthrich, K. (1982). High resolution nuclear magnetic resonance studies of the conformation and orientation of melittin bound to a lipid-water interface. *Biophys. J.* **37,** 319-328.

Cabrele, C. & Beck-Sickinger, A. G. (2000). Molecular characterization of the ligand-receptor interaction of the neuropeptide Y family. *J. Pept. Sci.* **6,** 97-122.

Caffrey, M. (2000). A lipid's eye view of membrane protein crystallization in mesophases. *Curr. Opin. Struct. Biol.* **10,** 486-497.

Campbell, A. P. & Sykes, B. D. (1993). The two-dimensional transferred nuclear Overhauser effect: theory and practice. *Annu. Rev. Biophys. Biomol. Struct.* **22,** 99-122.

Chen, Z., Xu, P., Barbier, J. R., Willick, G. & Ni, F. (2000). Solution structure of the osteogenic 1-31 fragment of the human parathyroid hormone. *Biochemistry* **39,** 12766-12777.

Chen, Z., Zhang, X., Gonnella, N. C., Pellas, T. C., Boyar, W. C. & Ni, F. (1998). Residues 21-30 within the extracellular N-terminal region of the C5a receptor represent a binding domain for the C5a anaphylatoxin. *J. Biol. Chem.* **273,** 10411-10419.

Chu, S. S., Velde, D. V., Shobe, D., Balse, P. & Doughty, M. B. (1995) Conformational properties of the proline region of porcine neuropeptide Y by CD and ^{1}H-NMR spectroscopy. *Biopolymers* **53**, 583-593

Clore, G. M. & Gronenborn, A. M. (1982). Theory and applications of the transferred nuclear Overhauser efect to the study of the conformations of small ligands bound to proteins. *J. Magn. Reson.* **48**, 402-417.

Clore, G. M. & Gronenborn, A. M. (1991). Structures of larger proteins in solution: three- and four-dimensional heteronuclear NMR spectroscopy. *Science* **252**, 1390-1399.

Condon, S. M., Morize, I., Darnbrough, S., Burns, C. J., Miller, B. E., Uhl, J., Burke, K., Jariwala, N., Locke, K., Krolikowski, P. H., Kumar, N. V. & Labaudiniere, R. F. (2000). The bioactive conformation of human parathyroid hormone. Structural evidence for the extended helix postulate. *J. Am. Chem. Soc.* **122**, 3007-3014.

Cornish, V. W., Benson, D. R., Altenbach, C. A., Hideg, K., Hubbell, W. L. & Schultz, P. G. (1994). Site-specific incorporation of biophysical probes into proteins. *Proc. Natl Acad. Sci. U S A* **91**, 2910.

Cowley, D. J., Hoflack, J. M., Pelton, J. T. & Saudek, V. (1992). Structure of neuropeptide Y dimer in solution. *Eur. J. Biochem.* **205**, 1099-1106.

Darbon, H., Bernassau, J.-M., Deleuze, C., Chenu, J., Roussel, A. & Cambillau, C. (1992). Solution conformation of human neuropeptide Y by 1H nuclear magnetic resonance and restrained molecular dynamics. *Eur. J. Biochem.* **209**, 765 - 771.

Davidson, F. F., Loewen, P. C. & Khorana, H. G. (1994). Structure and function in rhodopsin: replacement by alanine of cysteine residues 110 and 187, components of a conserved disulfide bond in rhodopsin, affects the light-activated metarhodopsin II state. *Proc. Natl Acad. Sci. USA* **91**, 4029 - 4033.

De Lean, A., Stadel, J. M. & Lefkowitz, R. J. (1980). A ternary complex model explains the agonist-specific binding properties of the adenylate cyclase-coupled β-adrenergic receptor. *J. Biol. Chem.* **255**, 7108-7117.

Devaux, P. F. (1993). Lipid transmembrane asymmetry and flip-flop in biological membranes and in lipid bilayers. *Curr. Opin. Struct. Biol.* **3**, 489 - 494.

Dixon, R. A., Kobilka, B. K., Strader, D. J., Benovic, J. L., Dohlman, H. G., Frielle, T., Bolanowski, M. A., Bennett, C. D., Rands, E. & Diehl, R. E. (1986). Cloning of the

gene and cDNA for mammalian β-adrenergic receptor and homology with rhodopsin. *Nature* **321,** 75-79.

Dobson, C. M. & Hore, P. J. (1998). Kinetic studies of protein folding using NMR spectroscopy. *Nat. Struct. Biol.* **5,** 504-507.

Ernst, R. R., Bodenhausen, G. & Wokaun, A. (1987). *The Principles of Nuclear Magnetic Resonance in One and Two Dimensions*, Clarendon Press, Oxford.

Falke, J. J. & Koshland, D. E., Jr. (1987). Global flexibility in a sensory receptor: a site-directed cross-linking approach. *Science* **237,** 1596-1600.

Farrens, D. L., Altenbach, C., Yang, K., Hubbell, W. L. & Khorana, H. G. (1996). Requirement of rigid-body motion of transmembrane helices for light activation of rhodopsin. *Science* **274,** 768-770.

Fu, R. & Cross, T. A. (1999). Solid-state nuclear magnetic resonance investigation of protein and polypeptide structure. *Annu. Rev. Biophys. Biomol. Struct.* **28,** 235-268.

Gehlert, D. R. (1998). Multiple receptors for the pancreatic polypeptide (PP-fold) family: physiological implications. *Proc. Soc. Exp. Biol. Med.* **218,** 7-22.

Gilman, A. G. (1987). G proteins: transducers of receptor-generated signals. *Annu. Rev. Biochem.* **56,** 615-649.

Grauschopf, U., Lilie, H., Honold, K., Wozny, M., Reusch, D., Esswein, A., Schafer, W., Rucknagel, K. P. & Rudolph, R. (2000). The N-terminal fragment of human parathyroid hormone receptor 1 constitutes a hormone binding domain and reveals a distinct disulfide pattern. *Biochemistry* **39,** 8878-8887.

Greenberg, Z., Bisello, A., Mierke, D. F., Rosenblatt, M. & Chorev, M. (2000). Mapping the bimolecular interface of the parathyroid hormone (PTH)-PTH1 receptor complex: spatial proximity between Lys(27) (of the hormone principal binding domain) and Leu(261) (of the first extracellular loop) of the human PTH1 receptor. *Biochemistry* **39,** 8142-8152.

Grobner, G., Burnett, I. J., Glaubitz, C., Choi, G., Mason, A. J. & Watts, A. (2000). Observations of light-induced structural changes of retinal within rhodopsin. *Nature* **405,** 810-813.

Güntert, P. (1998). Structure calculation of biological macromolecules from NMR data. *Q. Rev. Biophys.* **31,** 145-237.

Hebert, T. E., Moffett, S., Morello, J. P., Loisel, T. P., Bichet, D. G., Barret, C. & Bouvier, M. (1996). A peptide derived from a β2-adrenergic receptor transmembrane domain inhibits both receptor dimerization and activation. *J. Biol. Chem.* **271,** 16384-16392.

Henry, G. D. & Sykes, B. D. (1994). Methods to study membrane protein structure in solution. *Methods Enzymol.* **239,** 515-535.

Hoare, S. R., Clark, J. A. & Usdin, T. B. (2000). Molecular determinants of tuberoinfundibular peptide of 39 residues (TIP39) selectivity for the parathyroid hormone-2 (PTH2) receptor. N-terminal truncation of TIP39 reverses PTH2 receptor/PTH1 receptor binding selectivity. *J. Biol. Chem.* **275,** 27274-27283.

Hristova, K., Wimley, W. C., Mishra, V. K., Anantharamiah, G. M., Segrest, J. P. & White, S. H. (1999). An amphipathic α-helix at a membrane interface: a structural study using a novel X-ray diffraction method. *J. Mol. Biol.* **290,** 99-117.

Hubbard, R. E. (1997). Can drugs be designed? *Curr. Opin. Biotechnol.* **8,** 696-700.

Ikura, M., Kay, L. E. & Bax, A. (1990). A novel approach for sequential assignment of ^{1}H, ^{13}C, and ^{15}N spectra of proteins: heteronuclear triple-resonance three-dimensional NMR spectroscopy. Application to calmodulin. *Biochemistry* **29,** 4659-4667.

Inooka, H., Ohtaki, T., Kitahara, O., Ikegami, T., Endo, S., Kitada, C., Ogi, K., Onda, H., Fujino, M. & Shirakawa, M. (2001). Conformation of a peptide ligand bound to its G-protein coupled receptor. *Nat. Struct. Biol.* **8,** 161-165.

International Human Genome Sequencing Consortium (2001). Initial sequencing and analysis of the human genome. *Nature* **409,** 860-921.

Katragadda, M., Alderfer, J. L. & Yeagle, P. L. (2000). Solution structure of the loops of bacteriorhodopsin closely resembles the crystal structure. *Biochim. Biophys. Acta* **1466,** 1-6.

Kay, L. E. & Gardner, K. H. (1997). Solution NMR spectroscopy beyond 25 kDa. *Curr. Opin. Struct. Biol.* **7,** 722-731.

Khiat, A., Labelle, M. & Boulanger, Y. (1998). Three-dimensional structure of the Y1 receptor agonist [Leu^{31},Pro^{34}]NPY as determined by NMR and molecular modeling. *J. Peptide Res.* **51,**317-322.

Killian, J. A. & von Heijne, G. (2000). How proteins adapt to a membrane-water interface. *Trends Biochem. Sci.* **25,** 429-434.

König, B., Arendt, A., McDowell, J. H., Kahlert, M., Hargrave, P. A. & Hofmann, K. P. (1989). Three cytoplasmic loops of rhodopsin interact with transducin. *Proc. Natl Acad. Sci. USA* **86,** 6878-6882.

Kornberg, R. D. & McConnell, H. M. (1971). Lateral diffusion of phospholipids in a vesicle membrane. *Proc. Natl Acad. Sci. U S A* **68,** 2564-2568.

Kunishima, N., Shimada, Y., Tsuji, Y., Sato, T., Yamamoto, M., Kumasaka, T., Nakanishi, S., Jingami, H. & Morikawa, K. (2000). Structural basis of glutamate recognition by a dimeric metabotropic glutamate receptor. *Nature* **407,** 971-977.

Labelle, M., St-Pierre, S., Savard, R. & Boulanger, Y. (1997). Solution structure of neuropeptide tyrosine 13-36, a Y2 receptor agonist, as determined by NMR. *Eur. J. Biochem.* **246,** 780-785.

Landolt-Marticorena, C., Williams, K. A., Deber, C. M. & Reithmeier, R. A. (1993). Non-random distribution of amino acids in the transmembrane segments of human type I single span membrane proteins. *J. Mol. Biol.* **229,** 602-608.

Langley, J. N. (1909). On the contraction of muscle, chiefly in relation to the presence of "receptive" substances. Pt. IV. The effect of curari and of some other substances on the nicotine response of the sartorius and gastrocnemius muscles of the frog. *J. Physiol.* **39,** 235-295.

Lauterwein, J., Bosch, C., Brown, L. R. & Wüthrich, K. (1979). Physicochemical studies of the protein-lipid interactions in melittin-containing micelles. *Biochim. Biophys. Acta* **556,** 244-264.

Leff, P. (1995). The two-state model of receptor activation. *Trends Pharmacol. Sci.* **16,** 89-97.

Lefkowitz, R. J. (2000). The superfamily of heptahelical receptors. *Nat. Cell Biol.* **2,** E133-136.

LeMaster, D. M. (1994). Isotope labeling in solution protein assignment and structural analysis. *Progr. NMR Spectr.* **26,** 371 - 419.

Ling, K., Wang, P., Zhao, J., Wu, Y. L., Cheng, Z. J., Wu, G. X., Hu, W., Ma, L. & Pei, G. (1999). Five-transmembrane domains appear sufficient for a G protein-coupled receptor: functional five-transmembrane domain chemokine receptors. *Proc. Natl Acad. Sci. USA* **96,** 7922-7927.

Lücke, H., Schobert, B., Richter, H. T., Cartailler, J. P. & Lanyi, J. K. (1999). Structure of bacteriorhodopsin at 1.55 A resolution. *J. Mol. Biol.* **291,** 899-911.

Maggio, R., Vogel, Z. & Wess, J. (1993). Coexpression studies with mutant muscarinic/adrenergic receptors provide evidence for intermolecular "cross-talk" between G-protein-linked receptors. *Proc. Natl Acad. Sci. USA* **90,** 3103-3107.

Martin, N. P., Leavitt, L. M., Sommers, C. M. & Dumont, M. E. (1999). Assembly of G protein-coupled receptors from fragments: identification of functional receptors with discontinuities in each of the loops connecting transmembrane segments. *Biochemistry* **38,** 682-695.

Marx, U. C., Adermann, K., Bayer, P., Forssmann, W. G. & Rösch, P. (2000). Solution structures of human parathyroid hormone fragments hPTH(1-34) and hPTH(1-39) and bovine parathyroid hormone fragment bPTH(1-37). *Biochem. Biophys. Res. Commun.* **267,** 213-220.

Marx, U. C., Austermann, S., Bayer, P., Adermann, K., Ejchart, A., Sticht, H., Walter, S., Schmid, F. X., Jaenicke, R., Forssmann, W. G. & Rösch, P. (1995). Structure of human parathyroid hormone 1-37 in solution. *J. Biol. Chem.* **270,** 15194-15202.

Mattila, K., Kinder, R. & Bechinger, B. (1999). The alignment of a voltage-sensing peptide in dodecylphosphocholine micelles and in oriented lipid bilayers by nuclear magnetic resonance and molecular modeling. *Biophys. J.* **77,** 2102-2113.

McLatchie, L. M., Fraser, N. J., Main, M. J., Wise, A., Brown, J., Thompson, N., Solari, R., Lee, M. G. & Foord, S. M. (1998). RAMPs regulate the transport and ligand specificity of the calcitonin-receptor-like receptor. *Nature* **393,** 333-339.

Michel, M. C., Beck-Sickinger, A., Cox, H., Doods, H. N., Herzog, H., Larhammar, D., Quirion, R., Schwartz, T. & Westfall, T. (1998). XVI. International Union of Pharmacology recommendations for the nomenclature of neuropeptide Y, peptide YY, and pancreatic polypeptide receptors. *Pharmacol. Rev.* **50,** 143-150.

Mierke, D. F., Maretto, S., Schievano, E., DeLuca, D., Bisello, A., Mammi, S., Rosenblatt, M., Peggion, E. & Chorev, M. (1997). Conformational studies of mono- and bicyclic parathyroid hormone-related protein-derived agonists. *Biochemistry* **36,** 10372-10383.

Mierke, D. F., Royo, M., Pellegrini, M., Sun, H. & Chorev, M. (1996). Peptide mimetic of the third cytoplasmic loop of the PTH/PTHrP Receptor. *J. Am. Chem. Soc.* **118,** 8998-9004.

Milano, C. A., Allen, L. F., Rockman, H. A., Dolber, P. C., McMinn, T. R., Chien, K. R., Johnson, T. D., Bond, R. A. & Lefkowitz, R. J. (1994). Enhanced myocardial func-

tion in transgenic mice overexpressing the β_2-adrenergic receptor. *Science* **264,** 582-586.

Mishra, V. K. & Palgunachari, M. N. (1996). Interaction of model class A1, class A2, and class Y amphipathic helical peptides with membranes. *Biochemistry* **35,** 11210-11220.

Monks, S.A., Karagianis, G., Howlett, G.J. & Norton, R.S. (1996) Solution structure of human neuropeptide Y. *J. Biomol. NMR* **8**, 379-390.

Monnot, C., Bihoreau, C., Conchon, S., Curnow, K. M., Corvol, P. & Clauser, E. (1996). Polar residues in the transmembrane domains of the type 1 angiotensin II receptor are required for binding and coupling. Reconstitution of the binding site by co-expression of two deficient mutants. *J. Biol. Chem.* **271,** 1507-1513.

Morisset, S., Rouleau, A., Ligneau, X., Gbahou, F., Tardivel-Lacombe, J., Stark, H., Schunack, W., Ganellin, C. R., Schwartz, J. C. & Arrang, J. M. (2000). High constitutive activity of native H_3 receptors regulates histamine neurons in brain. *Nature* **408,** 860-864.

Müller, G. (2000). Towards 3D structures of G protein-coupled receptors: A multidisciplinary approach. *Curr. Med. Chem.* **7,** 861-888.

Nathans, J. & Hogness, D. S. (1983). Isolation, sequence analysis, and intron-exon arrangement of the gene encoding bovine rhodopsin. *Cell* **34,** 807-814.

Noda, K., Saad, Y., Graham, R. M. & Karnik, S. S. (1994). The high affinity state of the β_2-adrenergic receptor requires unique interaction between conserved and non-conserved extracellular loop cysteines. *J. Biol. Chem.* **269,** 6743-6752.

Nordmann, A., Blommers, M.J., Fretz, H., Arvinte, T. & Drake, A.F. (1999) Aspects pf the molecular structure and dynamics of neuropeptide Y. *Eur. J. Biochem.* **261**, 216-226

Okamoto, T., Schlegel, A., Scherer, P. E. & Lisanti, M. P. (1998). Caveolins, a family of scaffolding proteins for organizing "preassembled signaling complexes" at the plasma membrane. *J. Biol. Chem.* **273,** 5419-5422.

Palczewski, K., Kumasaka, T., Hori, T., Behnke, C. A., Motoshima, H., Fox, B. A., Le Trong, I., Teller, D. C., Okada, T., Stenkamp, R. E., Yamamoto, M. & Miyano, M. (2000). Crystal structure of rhodopsin: A G protein-coupled receptor. *Science* **289,** 739-745.

Palmer, A. G., III., Williams, J. & McDermott, A. (1996). Nuclear magnetic resonance studies of biopolymer dynamics. *J. Phys. Chem.* **100,** 13293 - 13310.

Papavoine, C. H., Christiaans, B. E., Folmer, R. H., Konings, R. N. & Hilbers, C. W. (1998). Solution structure of the M13 major coat protein in detergent micelles: a basis for a model of phage assembly involving specific residues. *J. Mol. Biol.* **282,** 401-419.

Pauli, J., van Rossum, B., Forster, H., de Groot, H. J. & Oschkinat, H. (2000). Sample optimization and identification of signal patterns of amino acid side chains in 2D RFDR spectra of the α-spectrin SH3 domain. *J. Magn. Reson.* **143,** 411-416.

Pawagi, A. B. & Deber, C. M. (1990). Ligand-dependent quenching of tryptophan fluorescence in human erythrocyte hexose transport protein. *Biochemistry* **29,** 950-955.

Pellegrini, M., Bisello, A., Rosenblatt, M., Chorev, M. & Mierke, D. F. (1998a). Binding domain of human parathyroid hormone receptor: from conformation to function. *Biochemistry* **37,** 12737-12743.

Pellegrini, M. & Mierke, D. F. (1999a). Molecular complex of cholecystokinin-8 and N-terminus of the cholecystokinin A receptor by NMR spectroscopy. *Biochemistry* **38,** 14775-14783.

Pellegrini, M. & Mierke, D. F. (1999b). Structural characterization of peptide hormone/receptor interactions by NMR spectroscopy. *Biopolymers* **51,** 208-220.

Pellegrini, M., Royo, M., Rosenblatt, M., Chorev, M. & Mierke, D. F. (1998b). Addressing the tertiary structure of human parathyroid hormone-(1-34). *J. Biol. Chem.* **273,** 10420-10427.

Peng, J. & Wagner, G. (1993). Protein mobility from multiple ^{15}N relaxation parameters. *In Nuclear Magnetic Resonance Probes of Molecular Dynamics*, Tycko R. ed., Kluwer Academic Publishers, Dordrecht.

Perlman, J. H., Wang, W., Nussenzveig, D. R. & Gershengorn, M. C. (1995). A disulfide bond between conserved extracellular cysteines in the thyrotropin-releasing hormone receptor is critical for binding. *J. Biol. Chem.* **270,** 24682-24685.

Pervushin, K., Riek, R., Wider, G. & Wüthrich, K. (1997). Attenuated T_2 relaxation by mutual cancellation of dipole-dipole coupling and chemical shift anisotropy indicates an avenue to NMR structures of very large biological macromolecules in solution. *Proc. Natl Acad. Sci. USA* **94,** 12366-12371.

Pervushin, K. V., Orekhov, V., Popov, A. I., Musina, L. & Arseniev, A. S. (1994). Three-dimensional structure of (1-71)bacterioopsin solubilized in methanol/chloroform and SDS micelles determined by ^{15}N-^{1}H heteronuclear NMR spectroscopy. *Eur. J. Biochem.* **219,** 571-583.

Phillips, W. J. & Cerione, R. A. (1994). A C-terminal peptide of bovine rhodopsin binds to the transducin α-subunit and facilitates its activation. *Biochem. J.* **299,** 351-357.

Piserchio, A., Bisello, A., Rosenblatt, M., Chorev, M. & Mierke, D. F. (2000a). Characterization of parathyroid hormone/receptor interactions: structure of the first extracellular loop. *Biochemistry* **39,** 8153-8160.

Piserchio, A., Usdin, T. & Mierke, D. F. (2000b). Structure of tuberoinfundibular peptide of 39 residues. *J. Biol. Chem.* **275,** 27284-27290.

Riek, R., Wider, G., Pervushin, K. & Wüthrich, K. (1999). Polarization transfer by cross-correlated relaxation in solution NMR with very large molecules. *Proc. Natl Acad. Sci. U S A* **96,** 4918-4923.

Rist, B., Zerbe, O., Ingenhoven, N., Scapozza, L, Peers, C., Vaughan, P. F. T., McDonald, R. L., Wieland, H. A., Beck-Sickinger, A. G. (1996). Modified, cyclic dodecapeptide analog of neuropeptide Y is the smalles full agonist at the human Y_2 receptor. *FEBS Letters* **394,** 169-173.

Rodbell, M., Birnbaumer, L., Pohl, S. L. & Krans, H. M. (1971). The glucagon-sensitive adenyl cyclase system in plasma membranes of rat liver. V. An obligatory role of guanylnucleotides in glucagon action. *J. Biol. Chem.* **246,** 1877-1882.

Rolz, C., Pellegrini, M. & Mierke, D. F. (1999). Molecular characterization of the receptor-ligand complex for parathyroid hormone. *Biochemistry* **38,** 6397-6405.

Salzmann, M., Pervushin, K., Wider, G., Senn, H. & Wüthrich, K. (1999). [^{13}C]-constant-time [^{15}N,^{1}H]-TROSY-HNCA for sequential assignments of large proteins. *J. Biomol. NMR* **14,** 85-88.

Sanders, C. R., Hare, B. J., Howard, K. & Prestegard, J. H. (1993). Magnetically-oriented phospholipid micelles as a tool for the study of membrane-associated molecules. *Prog. NMR Spectr.* **26,** 421-444.

Saudek, V. & Pelton, J. T. (1990). Sequence-specific ^{1}H NMR assignment and secondary structure of neuropeptide Y in aqueous solution. *Biochemistry* **29,** 4509-4515.

Sargent, D. F., Bean, J. W. & Schwyzer, R. (1988). Conformation and orientation of regulatory peptides on lipid membranes. Key to the molecular mechanism of receptor selection. *Biophys. Chem.* **31,** 183-193.

Sargent, D. F. & Schwyzer, R. (1986). Membrane lipid phase as catalyst for peptide-receptor interactions. *Proc. Natl Acad. Sci. U S A* **83,** 5774-5778.

Schertler, G. F., Villa, C. & Henderson, R. (1993). Projection structure of rhodopsin. *Nature* **362,** 770-772.

Schiffer, M., Chang, C. H. & Stevens, F. J. (1992). The functions of tryptophan residues in membrane proteins. *Protein Eng.* **5,** 213-214.

Schramm, M. & Selinger, Z. (1984). Message transmission: receptor controlled adenylate cyclase system. *Science* **225,** 1350-1356.

Schwyzer, R. (1986). Molecular mechanism of opioid receptor selection. *Biochemistry* **25,** 6335-6342.

Schwyzer, R. (1991). Peptide-membrane interactions and a new principle in quantitative structure-activity relationships. *Biopolymers* **31,** 785-792.

Schwyzer, R. (1995a). 100 years lock-and-key concept: are peptide keys shaped and guided to their receptors by the target cell membrane? *Biopolymers* **37,** 5-16.

Schwyzer, R. (1995b). In search of the 'bio-active conformation' - is it induced by the target cell membrane? *J. Mol. Recognit.* **8,** 3-8.

Shao, H., Jao, S., Ma, K. & Zagorski, M. G. (1999). Solution structures of micelle-bound amyloid β-(1-40) and β-(1- 42) peptides of Alzheimer's disease. *J. Mol. Biol.* **285,** 755-773.

Shuker, S. B., Hajduk, P. J., Meadows, R. P. & Fesik, S. W. (1996). Discovering high-affinity ligands for proteins: SAR by NMR. *Science* **274,** 1531-1534.

Struthers, M., Yu, H., Kono, M. & Oprian, D. D. (1999). Tertiary interactions between the fifth and sixth transmembrane segments of rhodopsin. *Biochemistry* **38,** 6597-6603.

Stryer, L. & Bourne, H. R. (1986). G proteins: a family of signal transducers. *Annu. Rev. Cell Biol.* **2,** 391-419.

Sutherland, E. W. (1971). Nobelpriset i fysiologi eller medicin 1971: hormoners verkningsmekanism skisserad. *Lakartidningen* **68,** 4991-4995.

Sutherland, E. W. & Robison, G. A. (1966). The role of cyclic-3',5'-AMP in responses to catecholamines and other hormones. *Pharmacol. Rev.* **18,** 145-161.

Tsang, S. & Saier, M. H., Jr. (1996). A simple flexible program for the computational analysis of amino acyl residue distribution in proteins: application to the distribution of aromatic versus aliphatic hydrophobic amino acids in transmembrane α-helical spanners of integral membrane transport proteins. *J. Comput. Biol.* **3,** 185-190.

Voet, D. & Voet, J. G. (1995). *Biochemistry, 2nd ed.*, John Wiley & Sons, Inc., New York.

Vogel, R., Fan, G. B., Sheves, M. & Siebert, F. (2001). Salt Dependence of the Formation and Stability of the Signaling State in G Protein-Coupled Receptors: Evidence for the Involvement of the Hofmeister Effect. *Biochemistry* **40,** 483-493.

Wagner, G. (1993). NMR relaxation and protein mobility. *Curr. Opin. Struct. Biol.* **3,** 748 - 754.

Wagner, G. & Wüthrich, K. (1982a). Amide protein exchange and surface conformation of the basic pancreatic trypsin inhibitor in solution. Studies with two-dimensional nuclear magnetic resonance. *J. Mol. Biol.* **160,** 343-361.

Wagner, G. & Wüthrich, K. (1982b). Sequential resonance assignments in protein ^{1}H nuclear magnetic resonance spectra. Basic pancreatic trypsin inhibitor. *J. Mol. Biol.* **155,** 347-366.

Wang, J. & Pullman, A. (1991). Do helices in membranes prefer to form bundles or stay dispersed in the lipid phase? *Biochim. Biophys. Acta* **1070,** 493-496.

Wess, J. (1997). G-protein-coupled receptors: molecular mechanisms involved in receptor activation and selectivity of G-protein recognition. *FASEB J.* **11,** 346-354.

White, S. H. & Wimley, W. C. (1998). Hydrophobic interactions of peptides with membrane interfaces. *Biochim. Biophys. Acta* **1376,** 339-352.

Williamson, M. P., Havel, T. F. & Wüthrich, K. (1985). Solution conformation of proteinase inhibitor IIA from bull seminal plasma by ^{1}H nuclear magnetic resonance and distance geometry. *J. Mol. Biol.* **182,** 295-315.

Wüthrich, K. (1998). The second decade - into the third millenium. *Nat. Struct. Biol.* **5,** 492-495.

Wüthrich, K. (1986). *NMR of Proteins and Nucleic Acids*, Wiley, New York.

Wüthrich, K. & Wagner, G. (1979). Nuclear magnetic resonance of labile protons in the basic pancreatic trypsin inhibitor. *J. Mol. Biol.* **130,** 1-18.

Yang, K., Farrens, D. L., Altenbach, C., Farahbakhsh, Z. T., Hubbell, W. L. & Khorana, H. G. (1996). Structure and function in rhodopsin. Cysteines 65 and 316 are in proximity in a rhodopsin mutant as indicated by disulfide formation and interactions between attached spin labels. *Biochemistry* **35,** 14040-14046.

Yeagle, P. L. (1993). *The membranes of cells,* Academic Press, San Diego.

Yeagle, P. L., Alderfer, J. L. & Albert, A. D. (1995a). Structure of the carboxy-terminal domain of bovine rhodopsin. *Nat. Struct. Biol.* **2,** 832-834.

Yeagle, P. L., Alderfer, J. L. & Albert, A. D. (1995b). Structure of the third cytoplasmic loop of bovine rhodopsin. *Biochemistry* **34,** 14621-14625.

Yeagle, P. L., Alderfer, J. L. & Albert, A. D. (1996). Structure determination of the fourth cytoplasmic loop and carboxyl terminal domain of bovine rhodopsin. *Mol. Vis.* **2,** 12.

Yeagle, P. L., Alderfer, J. L. & Albert, A. D. (1997a). Three-dimensional structure of the cytoplasmic face of the G protein receptor rhodopsin. *Biochemistry* **36,** 9649-9654.

Yeagle, P. L., Alderfer, J. L., Salloum, A. C., Ali, L. & Albert, A. D. (1997b). The first and second cytoplasmic loops of the G-protein receptor, rhodopsin, independently form β-turns. *Biochemistry* **36,** 3864-3869.

Yuen, C. T., Davidson, A. R. & Deber, C. M. (2000). Role of aromatic residues at the lipid-water interface in micelle-bound bacteriophage M13 major coat protein. *Biochemistry* **39,** 16155-16162.

Zhou, A. T., Bessalle, R., Bisello, A., Nakamoto, C., Rosenblatt, M., Suva, L. J. & Chorev, M. (1997). Direct mapping of an agonist-binding domain within the parathyroid hormone/parathyroid hormone-related protein receptor by photoaffinity crosslinking. *Proc. Natl Acad. Sci. U S A* **94,** 3644-3649.

Chapter 2

Structure and Dynamics of Micelle-bound Neuropeptide Y: Comparison with Unligated NPY and Implications for Receptor Selection[1]

The biological importance of the neuropeptide Y (NPY) has steered a number of investigations about its solution structure over the last 20 years. Here, we focus on the comparison of the structure and dynamics of NPY free in solution to when bound to a membrane mimetic, dodecylphosphocholine (DPC) micelles, as studied by 2D ^{1}H NMR spectroscopy. Both, free in solution and in the micelle-bound form, the N-terminal segment (Tyr1-Glu15) is shown to extend like a flexible tail in solution. This is not compatible with the PP-fold model for NPY that postulates backfolding of the flexible N terminus onto the C-terminal helix. The correlation time (τ_c) of NPY in aqueous solution, 5.5 (±1.0) ns at 32°C, is only consistent with its existence in a dimeric form. Exchange contributions especially enhancing transverse relaxation rates (R_2) of residues located on one side of the C-terminal helix of the molecule are supposed to originate from dimerization of the NPY molecule. The dimerization interface was directly probed by looking at ^{15}N-labeled NPY/spin-labeled

[1]published in: Bader, R., Bettio, A., Beck-Sickinger, A.G. & Zerbe, O. (2001). *J. Mol. Biol.*, **305**, 307-329.

[TOAC34]-[^{14}N]-NPY heterodimers and revealed both parallel and anti-parallel alignment of the helices. The NMR-derived three-dimensional structure of micelle-bound NPY at 37°C and pH 6.0 is similar but not identical to that free in solution. The final set of 17 lowest-energy DYANA structures is particularly well defined in the region of residues 21-31, with a mean pairwise RMSD of 0.23 Å for the backbone heavy atoms and 0.85 Å for all heavy atoms. The combination of NMR relaxation data and CD measurements clearly demonstrates that the α-helical region Ala18-Thr32 is more stable, and the C-terminal tetrapeptide becomes structured only in the presence of the phosphocholine micelles. The position of NPY relative to the DPC micelle surface was probed by adding micelle integrating spin labels. Together with information from ^{1}H,^{2}H exchange rates, we conclude that the interaction of NPY with the micelle is promoted by the amphiphilic α-helical segment of residues Tyr21-Thr32. NPY is located at the lipid-water interface with its C-terminal helix parallel to the membrane surface and penetrates the hydrophobic interior only *via* insertions of a few long aliphatic or aromatic side-chains. From these data we can demonstrate that the dimer interface of neuropeptide Y is similar to the interface of the monomer binding to DPC-micelles. We speculate that binding of the NPY monomer to the membrane is an essential key step preceeding receptor binding, thereby pre-orientating the C-terminal tetrapeptide and possibly inducing the bio-active conformation.

2.1. Introduction

Neuropeptide Y (NPY), a 36-residue, C-terminally amidated polypeptide hormone and neurotransmitter, is a member of the NPY family of

regulatory peptides that includes the endocrine peptides, peptide YY and pancreatic polypeptide (PP) (Larhammar, 1996a). It was first isolated from porcine brain (Tatemoto *et al.*, 1982) and has shown to be the most abundant neuropeptide in the mammalian central nervous system (Gray & Morley, 1986), but is also widely expressed in the peripheral nervous system (Dumont *et al.*, 1992).

NPY has been implicated in various physiological responses including cardiovascular regulation and the control of food intake: sympathetic NPY has a vasopressor effect, reflecting direct vasoconstriction of blood vessels and potentiation of the noradrenaline-evoked response (Grundemar & Hakanson, 1993). On the other hand, central administration has demonstrated the potency of NPY as an orexigenic agent (Stanley & Leibowitz, 1985). In fact, NPY is the only known peptide that can cause animals to eat until they are obese (Inui, 1999).

The variety of physiological effects attributed to NPY is the result of its activity at a heterogeneous population of at least six receptor subtypes, termed Y_1-y_6, all of which have been cloned, except for Y_3 (Michel *et al.*, 1998). Y receptors belong to the rhodopsin-like superfamily of G protein-coupled receptors. Their activation leads to the inhibition of adenylate cyclase and an increase in intracellular calcium concentration. Sequence comparisons show that receptors Y_1, Y_4, and y_6 are more closely related to each other than to the receptors Y_2, and Y_5 (Larhammar, 1996b). Recently, Wraith *et al.* (2000) proposed, based on combined information from chromosomal localizations and sequence-based analysis, that two local gene duplication events of an ancestral gene gave rise to Y_1, Y_2, and Y_5, followed by large-scale (chromosomal or genome) duplication events. This may have resulted in three subfamilies of Y receptors, which contain the $Y_1/Y_4/y_6$, the Y_2, and the Y_5 receptor, respectively.

Several observations suggest that the C-terminal tetrapeptide of NPY

is a key interaction site with the receptors: (i) the single substitution of Arg35 to Ala leads to a complete loss of affinity at all cloned receptor subtypes; (ii) exchange of Arg33 is not tolerated at receptor subtypes Y_1 and Y_4 and significantly reduces binding to Y_2 and Y_5 receptors; and (iii) the negatively charged, free carboxlic group at the C terminus prevents it from binding to all receptor subtypes (Hoffmann *et al.*, 1996; Beck-Sickinger & Jung, 1995; Beck-Sickinger *et al.*, 1994; Cabrele & Beck-Sickinger, 2000; McCrea *et al.*, 2000).

Although the individual receptor subtypes obviously share the C terminus of NPY as one common recognition site, amino acid substitutions in this region have subtype-specific effects on binding affinity. Whereas [Pro34]-substituted analogues loose affinity only at the Y_2-receptor (Fuhlendorff *et al.*, 1990; Grandt *et al.*, 1994; Wieland *et al.*, 1995), it was recently found that [Ala31, Aib32]-NPY is a selective agonist at the Y_5-receptor (Cabrele *et al.*, 2000).

The N terminus is essential for activity only at the Y_1 and the Y_5-receptor, at both of which the affinity of the endogenously formed NPY (3-36) drops to the micromolar range. However, all N-terminal segments such as NPY (1-12) or NPY (1-24) were completely inactive (Beck-Sickinger & Jung, 1995; Cabrele & Beck-Sickinger, 2000).

The molecular conformation of NPY has been discussed in the literature both extensively and controversially. Essentially, two types of structural models have been proposed. The first is based on NMR data of NPY (Darbon *et al.*, 1992) and [Leu31, Pro34]-NPY (Khiat *et al.*, 1998) and resembles closely the secondary-structure model (Allen *et al.*, 1987) derived from the crystal structure of dimeric avian pancreatic polypeptide (aPP) in the presence of Zn^{2+} (Blundell *et al.*, 1981). It is characterized by an α-helix involving residues 14-31 connected *via* a β-turn to an N-terminal polyproline II helix and is referred to as PP-fold. The second is

based upon NMR data of human (Monks *et al.*, 1996) and porcine NPY (Cowley *et al.*, 1992) with NOE constraints whose origin could only be explained by the proposition of a dimeric model, in which the two NPY molecules interact *via* side-chains of their α-helices and are aligned in an anti-parallel fashion. In this type of model, at least residues 1-9 of the N-terminal tail are fully flexible.

Recently, Nordmann *et al.* (1999) concluded, based on their investigations by CD-spectroscopy, that the monomer form can adopt a PP-fold conformation at low concentrations, but that at concentrations usually used for NMR the dimer is the most abundant form. They suggest that dimerization goes hand in hand with an unfolding of the polyproline helix.

Obviously, structure elucidation of a peptide hormone in solution in the absence of the target receptor can deliver only very limited insight into the bioactive conformation. Furthermore, since the work of Schwyzer and co-workers (Schwyzer, 1986, 1995a; Sargent *et al.*, 1988) on peptides targeting opioid and neurokinin receptors, there is emerging evidence that interactions of peptide hormones with the cell membrane form a key step required for receptor subtype recognition and selection. Such membrane association increases the effective hormone concentration in vicinity of the receptor and reduces the receptor search to two-dimensional diffusion along the membrane surface. Moreover, special conformations due to interactions with the membrane as well as specific orientations and functional compartmentalizations in the membrane-solution interphase may be induced. The 28-residue hybrid brain natriuretic peptide analogue pBNP1, which is essentially unstructured in aqueous solution, may serve as an example of the former. When bound to DPC micelles it adopts four turn-like structures and hydrophobic, rather than electrostatic, interactions are postulated to be responsible for the initial folding of the peptide at the membrane-mimetic surface (Carpenter *et al.*, 1997). Moroder

and co-workers synthesized a lipophilic cholecystokinin adduct (DM-CCK) by linking a fully active CCK analogue to 1,2-dimyristoyl-3-mercaptoglycerol. In contrast to the parent CCK peptide, DM-CCK inserted rapidly into phospholipid bilayers. Although the receptor association rate of the lipo-CCK peptide was lower than that of the unmodified CCK, the data nevertheless confirmed that lateral penetration of receptor structures is possible (Moroder *et al.*, 1993).

In view of such a two-step receptor recognition process, consisting of pre-adsorption of the ligand to the membrane with subsequent lateral diffusion to the receptor followed by receptor recognition, we have compared the structure and dynamics of NPY free in solution to that when bound to DPC-micelles, as studied by NMR spectroscopy. The membrane was modeled through the zwitterionic detergent phosphatidylcholine, which is the predominant phospholipid in animal cell membranes (Henry & Sykes, 1994). Thus, it can be expected to resemble closely the natural receptor environment, albeit forming a system which is still amendable to investigations by high-resolution NMR.

Herein, we demonstrate that NPY associates to DPC-micelles mainly through hydrophobic rather than electrostatic interactions. Thereby, the α-helical conformation, which is already present in the NPY dimer in aqueous solution, is significantly stabilized. The peptide is located at the lipid-water interface parallel to the membrane surface and does not penetrate the hydrophobic core. The N terminus remains flexible and does not interact with the micelle. The implications of the orientation and conformation of NPY when bound to DPC micelles to receptor recognition are discussed and compared with the findings of structure-affinity and structure-activity relationship studies derived from NPY analogues.

2.2. Results

Although it is well known that with increasing acidity the α-helical content of NPY decreases and it adopts a less ordered conformation (Nordmann *et al.*, 1999), NMR measurements of free NPY were performed at slightly acidic pH (3.1) conditions in order to reduce backbone amide proton exchange, improve solubility and allow comparison of our data with published work. Furthermore, we and others observed that the H^N and H^α chemical shifts of some residues located in the α-helical region are highly concentration dependent. This is due to NPY's self-association (*vide infra*), which has shown to be pH independent with a K_d of 1.6(±0.6) μM (Cowley *et al.*, 1992). In this study experiments to characterize the dimerization interface were performed at a total concentration of 4 mg/ml peptide at which 97% of NPY is dimeric. In contrast, 300 mM aqueous DPC solutions, corresponding to a 5 mM concentration of micelles (Henry & Sykes, 1994), allowed us to obtain homogenous samples of 3 mM NPY at pH=6.0. Moreover, at that pH value only residues Ser3 and Lys4 were seriously affected by H^N exchange broadening. 1D NMR spectra were identical with respect to line width and chemical shifts in the concentration range between 0.15 mM to 3 mM NPY and 150 mM to 300 mM DPC, therefore excluding self-association effects. All 2D NMR measurements were performed at these high DPC concentrations, well beyond the critical micelle concentration of 1.1 mM and at micelle/peptide ratios well above unity, which has been shown to improve significantly the quality of NMR spectra (McDonnell & Opella, 1993). The samples were completely stable for several months, as checked by 1D and 2D NMR experiments.

Three-dimensional structure of NPY bound to DPC micelles

NMR sequence-specific resonance assignment was largely based upon the methodology developed by Wüthrich and coworkers (Wüthrich, 1986). However, the usual homonuclear scalar and dipolar coupling data were supplemented by extensive use of a 200 ms-mixing-time NOE-relayed [^{15}N,^{1}H]-HSQC experiment. By so doing, sequential amide protons displaying characteristic short distances in NOESY spectra could be efficiently assigned and problems due to overlapping amide proton resonances were nicely resolved through dispersion of the signals along the chemical shift of the attached ^{15}N nucleus (Figure 2.1) . The

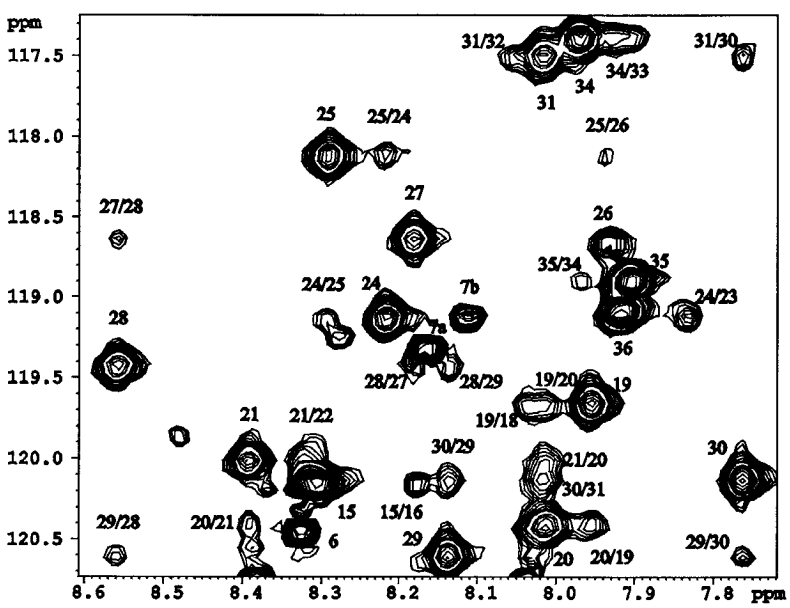

Figure 2.1 Region of a 200 ms NOE-relayed [^{15}N,^{1}H]-HSQC spectrum of porcine NPY in 300 mM DPC/H_2O at pH 6.0 and 37°C showing intraresidue and sequential (*i*, *i*+1 or *i*, *i*-1) ^{15}N,H^N cross-peaks, that were particularly useful for the sequential assignment of the spin systems. Pro8 is found in both *trans* and *cis* conformation resulting in two different chemical shift combinations for the preceeding Asn7 as denoted by (a) and (b), respectively.

sequential assignment of the flexible N-terminal residues was performed by using a homonuclear NOESY spectrum obtained at 150 ms mixing time where intraresidual and some of the sequential H^N_{i+1}/H^α_i and

H^N_{i+1}/H^β_i NOEs were strong. Side-chain assignments were completed by combined use of a 14 ms TOCSY and 150 ms as well as 75 ms NOESY spectra measured in 90% $H_2O/^2H_2O$ and in 99.9% ^2H_2O. The complete ^1H and backbone ^{15}N NMR assignments for porcine NPY bound to DPC micelles are tabulated in the Supplementary Material. ^{15}N resonances of pNPY in aqueous solution were assigned very similarly again using a NOE-relayed [^{15}N,^1H]-HSQC experiment supported by the shifts of the amide resonances as published by Monks *et al.* (1996).

Interestingly, the H^α resonances of pNPY bound to DPC micelles are very similar to those found by Monks *et al.* (1996) for human NPY, in which leucine 17 is replaced by a methionine residue. A downfield shift for the H^α resonance of >0.1 ppm was observed only for Asn7, upfield shifts of >0.1 ppm for residues Pro2, Asp6, Glu10, Asp11, Ala18, Ser22, and Arg25. When comparing ^{15}N resonances of pNPY bound to DPC micelles with the ^{15}N resonances of pNPY in aqueous solution as tabulated in the Supplementary Material, upfield shifts of >1 ppm were found for residues Leu17, Ser22, Tyr27, Ile28, and the C-terminal hexapeptide, whereas most of the backbone ^{15}N resonances of the N-terminal residues shifted downfield by >1 ppm. Finally, the deviations of the H^N chemical shifts (secondary chemical shifts), that were shown to be directly correlated with hydrogen bond strengths and α-helix bending (Kuntz *et al.*, 1991; Zhou *et al.*, 1992) show a similar pattern for pNPY on DPC micelles and in aqueous solution. However, they adopt larger values and extend further out to the C terminus in the former. In both cases, they display the 3-4 repeat periodicity, which is characteristic for bent amphiphilic α-helices. The low-field shifts of Leu17, Tyr21 and Ile28 of NPY on DPC micelles may either be indicative of strong intramolecular hydrogen bonding or be due to a proximity with polar headgroups of the micellar surface. Taken together, these data provide first evidence that the secondary structure of NPY does not change at the N terminus and in the N-ter-

minal part of the α-helix upon binding to DPC-micelles. Upfield shifts of C-terminal ^{15}N and H^N resonances relative to the values for NPY in aqueous solution, however, suggest that the helical conformation of the micelle-bound form is stabilized towards the C terminus. For the tertiary structure analysis, NOESY spectra were measured in water and ^2H_2O at a mixing time of 75 ms. Nearly complete assignment of these spectra was achieved. However, due to severe spectral overlap, some short-range and medium-range NOEs involving C-terminal residues could neither be unambiguously assigned nor properly integrated, i.e. H^N 33/H^α 33, H^N 33/H^α 32, H^N 36/H^α 32, H^N 35/H^α 35, H^N 35/H^α 34 and H^N 35/H^α 32.

Further constraints for the backbone dihedral angle ϕ were derived from scalar $^3J_{HN\alpha}$ coupling constants. Those were derived from inverse Fourier transformation of in-phase NOESY peaks involving H^N protons (Szyperski *et al.*, 1992). Values for residues 3-12, 26-28 and 32-36 are in the range of 6-8 Hz and for residues 20-25 and 29-31 are smaller than 6.0 Hz (arrows in Figure 2.2) , which is indicative of α-helical conformation.

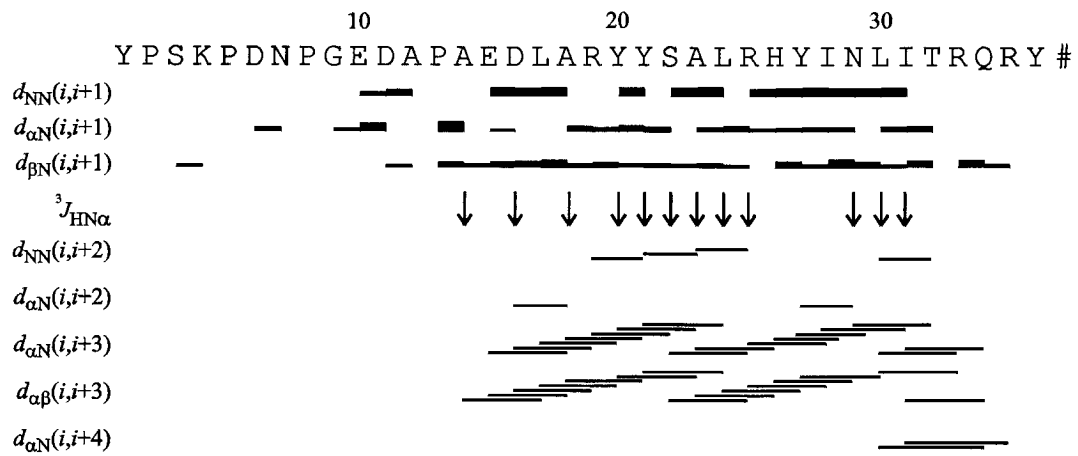

Figure 2.2 Summary of the meaningful distance constraints as derived from the unambiguosly assigned inter-residue NOEs between the backbone H^N, H^α and H^β of NPY bound to DPC micelles. The NOE intensities between protons belonging to sequential residues are reflected by the thickness of the lines. Values of $^3J_{HN\alpha}$<6 Hz are indicated by ↓. # denotes the C-terminal amide.

All four proline residues (residues 2, 5, 8, and 13) showed strong $d_{\alpha\delta}$ and no $d_{\alpha\alpha}$ NOE connectivities, which is only consistent with a *trans* conformation of the Xxx-Pro peptide bond. However, peak splitting of Asn7, as evident from the [^{15}N,^{1}H]-HSQC spectrum at peptide/DPC ratios of 1:2000 (300 mM DPC), 1:1000 (150 mM DPC) as well as 1:300 (300 mM DPC) reveals, that Pro8 adopts both *trans*, and to minor extent, *cis* conformations (Figure 2.1). Figure 2.2 shows a summary of the intra- and inter-residual NOE connectivities for NPY on DPC micelles. From the pattern of NOEs, the peptide can be divided into two main segments: The N-terminal segment from Tyr1-Pro13 is in extended conformation, the set of $d_{\alpha N}(i, i+3)$, $d_{\alpha\beta}(i, i+3)$ and $d_{\alpha N}(i, i+4)$ NOEs observed between residues Ala14-Tyr36 is characteristic for an α-helical structure. The sequential $H^{N}_{i+1}/H^{\alpha}_{i}$ NOE-derived upper distance limit for Asp16-Glu15 was too short to be simultaneously fullfilled with the set of NOEs that are characteristic for helical structures. Since investigations of the dynamics show (*vide infra*), that this segment is in an equilibrium between random coil and helical structure, we felt justified to not use this constraint in the structure calculations.

Some 30 low-energy three-dimensional structures were generated using a total of 105 intra-residual, 92 sequential and 147 medium-range (i-j=2, 3, 4) meaningful upper-limit distance restraints and 145 dihedral angle restraints. Structures were calculated with molecular dynamics in torsion angle space utilizing a simulated annealing protocol as implemented in the program DYANA (Güntert *et al.*, 1997), followed by an energy minimization with the AMBER (Weiner *et al.*, 1986) force field. From the set of 30 computed DYANA structures, the 17 lowest NMR-energy term structures were absent of distance violations larger than 0.1 Å. Statistical information on the structure calculation is provided in the Supplementary Material.

The residue-specific atomic root mean square deviations (RMSD) for

backbone heavy atoms monotonically decreased from 22.7 at Tyr1 to 2.3 at Pro13. In the Ala14-Tyr36 region, the RMSD was <1.6 for all residues. This segment was largely -helical among all computed structures (Figure 2.3).

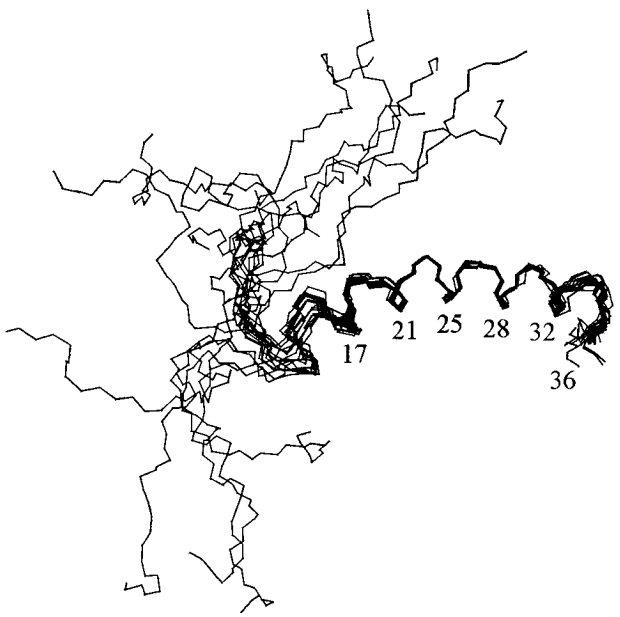

Figure 2.3 Backbone atoms (C^{α}, N and C) of 17 minimized structures for NPY bound to micelles. The structures are superimposed over the backbone heavy atoms of residues Tyr21-Ile31.

Best convergence of the resulting structures was observed for the region between Tyr21 and Ile31 with RMSD of 0.23(±0.18) Å for the backbone heavy atoms and 0.85(±0.23) Å for all heavy atoms. For the C-terminal pentapeptide, the corresponding values were 0.64(±0.46) Å, and 2.05(±0.54) Å, respectively.

In most of the structures, $H^{N}_{i+4} \rightarrow CO_i$ hydrogen bonds were observed in the helix between residues Tyr20-Arg35. Additionally, an $H^{N}_{i+4} \rightarrow CO_i$ hydrogen bond was present between Ala14 and Ala18, an $H^{N}_{i+3} \rightarrow CO_i$ between Asp16 and Arg19, as well as an $H^{N}_{i+2} \rightarrow CO_i$ hydrogen bond between Pro13 and Glu15. The ϕ and ψ angles for residue Ala14 are consistent with the presence of a classical γ-turn in half of the computed structures.

The results from the tertiary structure calculation agreed with the suggestions based upon NOE patterns and chemical shift analysis. Further-

more, the partitioning of the molecule into well-structured and flexible parts are supported by results from NMR relaxation measurements, as described below.

Hydrogen exchange experiments

Proton-deuterium exchange experiments have long been used to prove that amide protons are involved in hydrogen bonds or are shielded from solvent access to a large extent (Wagner *et al.*, 1982). Recently, these experiments have also been recognized to be an appropriate tool to determine the residues involved in binding of peptides to membranes. Amide protons from residues at the interface are shielded from solvent and display largely reduced exchange rates (Shao *et al.*, 1999). Altered exchange kinetics at the micelle-water interface are also obvious from the fact that good-quality amide signals in protons spectra could be measured at pH 6.0, at which large linewidths of amide protons of NPY free in solution excludes observation of these resonances. This fact may be attributed to an altered apparent pH in the vicinity of the DPC headgroups possibly complemented by different exchange mechanisms and has been observed by others.

For measurement of exchange rates a protonated ^{15}N-pNPY sample containing DPC-d_{38} was dissolved in $^{2}H_2O$ and 2D [^{15}N,^{1}H]-HSQC spectra were recorded at different time intervals, thereby monitoring the disappearance of the ^{15}NH peaks. Nearly all peaks in the 2D [^{15}N,^{1}H]-HSQC had vanished after ten minutes, with exception of the signals of Leu24, Arg25, Tyr27, Ile28 and Ile31 (Figure 2.4). The only signal remaining after 40 minutes corresponded to Ile28. From these results we conclude that the leucine and isoleucine residues are anchored to the DPC micelle possibly *via* penetration of their long aliphatic side-chains into the hydrophobic

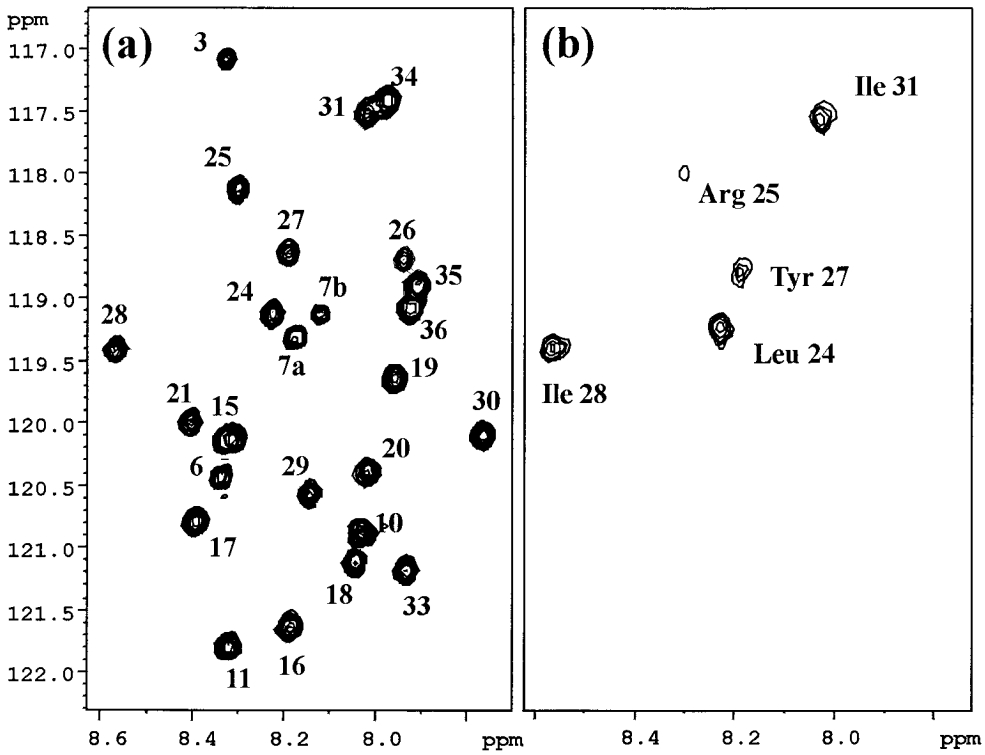

Figure 2.4 Expansion of [^{15}N,^{1}H]-HSQC spectra for NPY in DPC solution, (a) at 310 K in presence of 90% H_2O/10% $^{2}H_2O$, and (b) ten minutes after addition of $^{2}H_2O$ to a lyophilized sample.

interior. Furthermore, the amphipathic helix of NPY is located at the micelle surface with the hydrophobic side facing towards the micelle surface and the most persistent contacts are made by residues in the C-terminal half of the helix.

Spin-label studies

Further evidence for the exact orientation of pNPY residues with respect to the micelle surface was derived from experiments utilizing spin-labels such as 12-doxyl-stearic acid, 5-doxylstearic acid and 5-doxyl-stearic acid methyl ester. All of these compounds contain doxyl head-groups, a cyclic nitroxide with unpaired electrons, which is bound to the

aliphatic chain carbon in position 12 or 5, respectively. Unpaired electrons lead to dramatically accelerated longitudinal and transverse relaxation rates of protons in spatial proximity *via* highly efficient spin, electron relaxation. This effect depends on the distance between the spin-label and the protons and is nicely observed as loss of signal intensity in [^{15}N,^{1}H]-HSQC spectra for amide protons separated by less than about 10 Å from the spin label. Using mixed micelles of SDS with the different spin-labels it could be clearly demonstrated that the doxyl group of the 12-doxyl-stearic acid is located close to the center of the hydrophobic core, whereas the 5-doxyl-stearic acid particularly broadens the resonances from SDS carbon atoms 1-3 which are in vicinity to the micelle surface (Papavoine *et al.*, 1994; Jarvet *et al.*, 1997).

The effects of the spin-labels on the ^{15}NH signal intensities were quantified by comparing the volumes of backbone [^{15}N,^{1}H]-HSQC peaks both in the presence and in the absence of the spin-labels. All signal intensities remained constant after addition of one or two molecules of 12-doxyl-stearic acid per micelle, thereby proving that no residues of NPY become embedded into the hydrophobic core of the micelle (data not shown). On the other hand, in the presence of 5-doxyl- stearic acid, the ratio of signal volumes from experiments performed in the presence of the spin-label to those from a control sample without spin-label decreased monotonically from the N-terminal Ser3 to Ala14, which is the first residue of the α-helical segment (Figure 2.5(a)). Moreover, a 3-4 periodicity is observed for the signal intensities of the residues that are located in the helix, with Leu17, Tyr20, Tyr21, Leu24, Arg25, Ile28, Asn29, Thr32, Tyr36 being more affected by the spin-label than their neighbouring residues. This provides further evidence that the helix of NPY is located at the lipid-water interphase with its C-terminal helix parallel to the membrane.

Interestingly, signal intensities from residues, which are reduced to the highest extent in the presence of 5-doxyl-stearic acid, can selectively

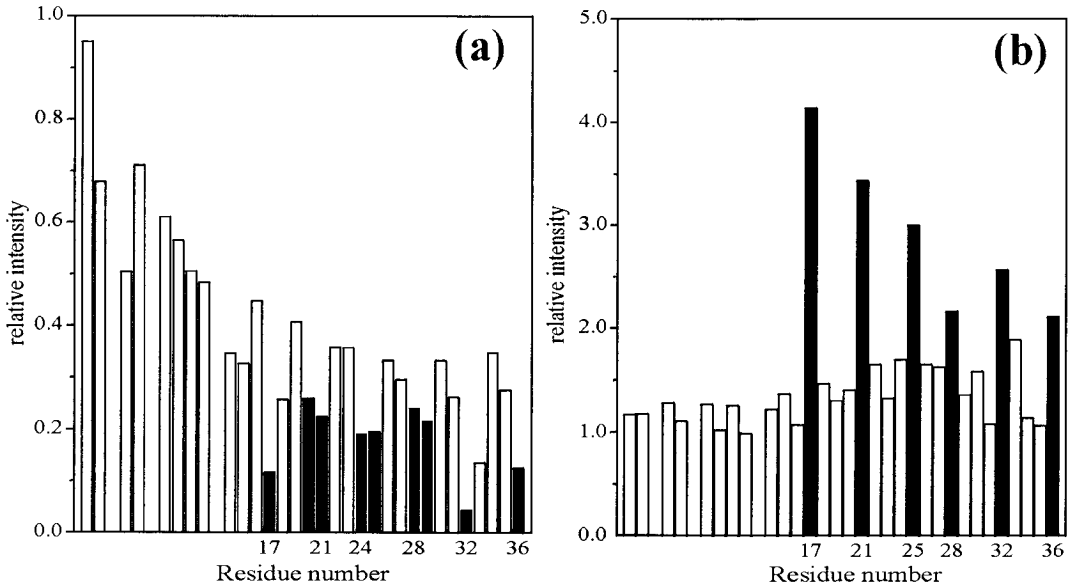

Figure 2.5 Relative signal intensities in [^{15}N,^{1}H]-HSQC spectra of NPY in DPC solution (a) in the presence of the spin-labeled 5-doxylstearic acid with respect to a reference spectrum without spin-labeled stearic acid, and (b) in the presence of spin-labeled 5-doxylstearic acid plus 5 mM $CaCl_2$ and 150 mM NaCl with respect to a reference spectrum with only the presence of spin-labeled stearic acid and 150 mM NaCl.

be regained upon addition of 5 mM calcium chloride/150 mM sodium chloride (Figure 2.5(b)), but not upon addition of solely sodium chloride. NPY contains a number of positively charged residues in the C-terminal helix. In order to exclude the possibility that these residues directly interact with the negatively charged carboxy-function from the stearic acid thereby forcing these residues into spatial proximity to the spin label and that it is this interaction, which is inhibited by Ca^{2+}, we also used the spin-label 5-doxyl-stearic acid methylester. However, nearly identical results were derived from these control experiments and hence we believe that the orientation of NPY on the membrane is not significantly influenced through the spin-label.

Probing of the dimerization interface of NPY in aqueous solution

Two models for the NPY dimer have been proposed, both based on the observation of 24, although different, intersubunit NOEs (Cowley *et al.*, 1992; Monks *et al.*, 1996). The models exhibited large differences, but were consistent in the way that two NPY molecules interact through their helices in an anti-parallel alignment. However, we felt that characterization of the dimerization interface using NOEs is difficult for two reasons. First, the spectral region containing the long aliphatic side-chains responsible for the contacts is heavily overlapped, making unambiguous assignments of intersubunit-NOEs difficult. Second, even when such assignments can be made, data interpretation is complicated by the monomer-dimer equilibrium.

To circumvent these problems we have probed the dimerization interface of two NPY molecules by measuring the distance-dependent effect of a spin-label placed within one monomer subunit onto transverse relaxation of the other monomeric subunit. The spin-labeled pNPY derivative, which has Gln34 replaced by the nitroxide free radical containing TOAC-residue and has ^{15}N nuclei at natural abundance was mixed in threefold excess to ^{15}N-enriched NPY. Therefore, ^{15}N-labeled NPY is most likely complexed to [TOAC34]-NPY, and [^{15}N,^{1}H]-HSQC spectra should reveal spin-label-induced relaxation effects in the formed heterodimers, thereby largely avoiding problems with interpretation due to the monomer-dimer equilibrium. The final monomer concentration was 1 mM. For two reasons we feel entitled to believe that the presence of a TOAC-group in the pNPY/[TOAC34]-NPY heterodimer does not influence the conformation of the dimer. First [^{15}N,^{1}H]-HSQC spectra of the homodimer and the heterodimer at a total monomer concentration of 1 mM display identical peak positions. Minor chemical shifts (by about one linewidth in both dimensions) were observed only for the cross-peaks of Asp11 and Asp16.

Second, as estimated from NMR relaxation data (*vide infra*), the C-terminal tetrapeptide is highly flexible, such that a persistent and specific interaction of the TOAC-group with any residue on the associated NPY-molecule is unlikely.

Surprisingly, the most dramatic signal reductions in the spin-label experiments could be localized at Ala14, Ile28 and Thr32 (Figure 2.6). In

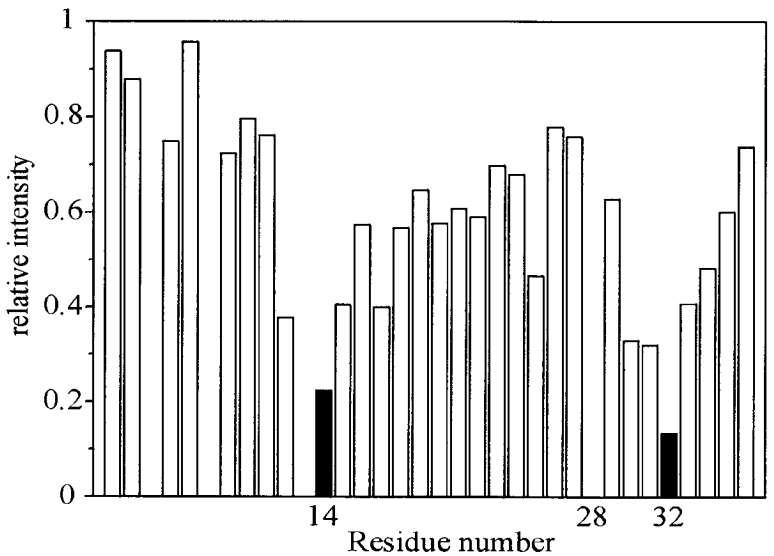

Figure 2.6 Signal intensities in [^{15}N,^{1}H]-HSQC spectra of NPY in aqueous solution at pH 3.1 in the presence of the spin-labeled [TOAC34]-NPY/^{15}N-labeled NPY (3:1) relative to a reference spectrum of pure ^{15}N-labeled NPY. The total NPY concentration was 1 mM.

the central part of the helix, minor effects were observed at Leu17 and Tyr21. No signal reductions were found for the N-terminal residues Ser3-Asp11, and the C-terminal tetrapeptide is characterized by a continuously decreasing influence of the spin-label towards Tyr36. This result is inconsistent with any of the so-far proposed models for the NPY dimer. According to Monks and co-workers, the intramolecular distance between Ala14 and Leu30 is more than 20 Å. Therefore, it is impossible in the anti-parallel arrangement that these residues are simultaneously affected by the spin-label. Instead, the data would rather favour the

"hand-shake" model by Cowley and co-workers. However, the set of intermolecular NOEs that were used for their dimer structure calculation do not explain the obviously close proximity between Ala14 and Gln34, but instead of it would imply a contact between Gln34 and Leu24, which cannot be supported by our data.

We therefore conclude that at least two self-association modes for NPY exist, a parallel and an anti-parallel arrangement. The latter would place [TOAC34] such that the signal intensity of Ala14 is reduced, whereas the former causes signal reductions at residues Leu30-Thr32. In fact, in the parallel arrangement of the monomeric units, intersubunit NOEs in the NMR spectra could not be distinguished from medium and short-range intrasubunit NOEs.

For both types of self-association, the parallel as well as the anti-parallel arrangement of the helices, we propose a single set of residues that build the dimerization interface, namely Leu17, Tyr21, Leu24, Ile28, Leu30, Ile31, and Thr32. All these residues are located on the hydrophobic side of the amphiphilic helix. It is exactly these residues that exhibit significantly enhanced ^{15}N transverse relaxation rates R_2 (see below), as well as slow H^N $^1H,^2H$ exchange of the backbone amide hydrogen atoms (Saudek & Pelton, 1990).

Determination of the motional parameters by the Model-Free approach

The motional behaviour of NPY in the self-associated form and when bound to DPC micelles was also characterized by measuring ^{15}N R_1 and R_2 relaxation rates and $^{15}N\{^1H\}$-NOE data for 1 mM NPY in the presence of 300 mM DPC at pH 6.0 and in aqueous solution at pH 3.1. Figure 2.7 presents the values of R_1, R_2 and the heteronuclear NOE determined at 500 MHz. In the case of NPY bound to DPC micelles, the peaks of Ser3 and Lys4 are too broad due to fast H^N exchange rates at pH 6.0 and inten-

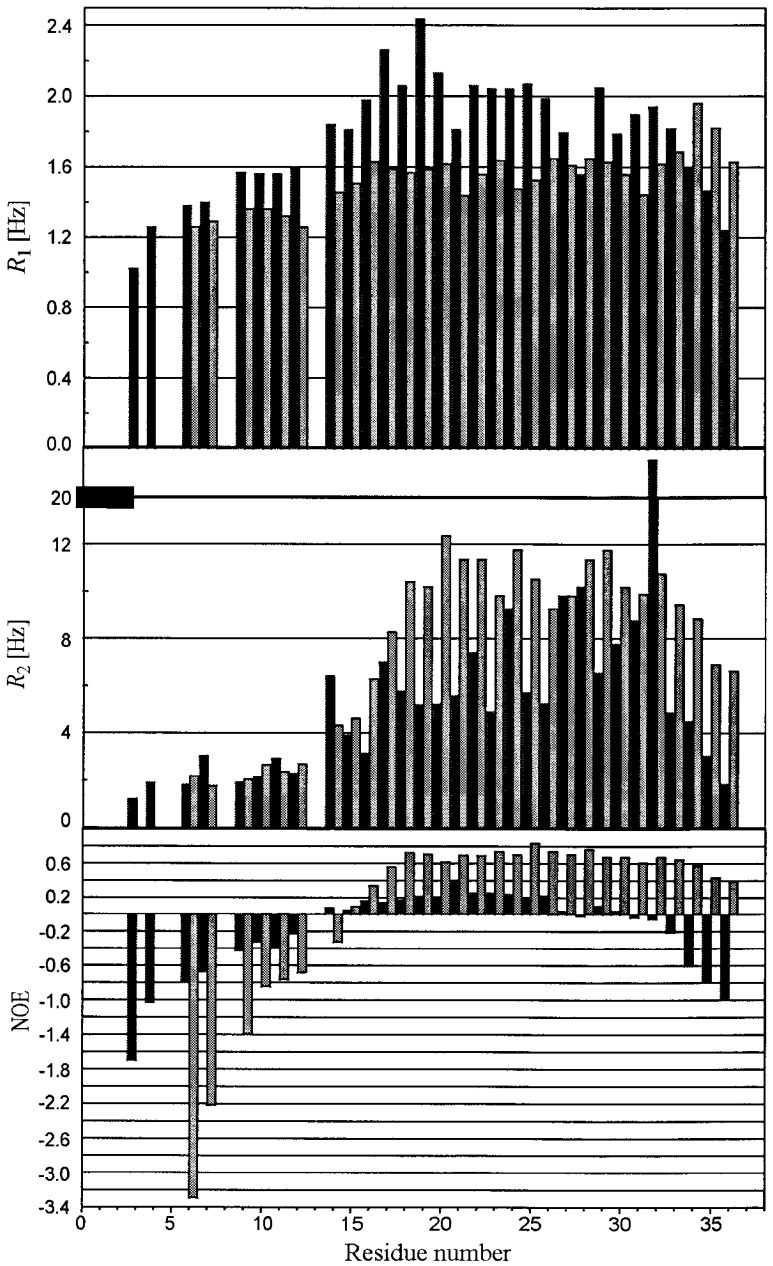

Figure 2.7 Plots of the relaxation rate constants $R_1(^{15}N)$, $R_2(^{15}N)$ and the $^{15}N\{^1H\}$-NOEs for NPY bound to DPC micelles (shaded bars) and in aqueous solution (black bars) versus the amino acid sequence, determined at 500 MHz.

sities are therefore too low to perform reliable integrations. Thus, data for Ser3 and Lys4 are omitted from the analysis. The average uncertainty for the sample containing DPC is 3.4% (R_1) and 5.8% (R_2) at 500 MHz, and 17.5% (R_1) and 18.3% for R_2 at 600 MHz. Unfortunately, for technical reasons we removed the sample between the two duplicate experiments con-

ducted to measure the reproducibility of the data at 600 MHz resulting in systematically lowered volume integrals. However, the experiments for the relaxation series were recorded without interruption and fitting of three-parameter single-exponential functions to the experimental data was possible with very small residuals. Therefore, we used both 500 and 600 MHz data to derive relaxation rate constants for the subsequent estimation of motional parameters in order to statistically improve our estimates. For the NOE at 500 MHz, the uncertainty was estimated by the standard deviation of the baseplane noise and was set to 10.0% for all residues. The corresponding values for the sample in aqueous solution are 3.5% for R_1, 2.5% for R_2, and 3.4% for the NOE at 500 MHz, and 8.5% for R_2 at 600 MHz.

A complete summary of the relaxation parameters for NPY in aqueous solution and on DPC micelles is provided in the Supplementary Material.

At 500 MHz, the average R_1 values for the N-terminal residues Asp6-Asp11 of NPY on DPC micelles are 1.31±0.05 Hz, between residues Ala14-Arg33, it is 1.57(±0.07) Hz, and at the C-terminal tripeptide, it monotonically decreases from 1.96 to 1.63 Hz. A nearly monotonic increase is observed for R_2 at the N-terminal Asp6-Asp16 from 2.17 to 6.29 Hz, whereas the values are very uniform between Leu17-Arg33 with an average of 10.42(±1.13) Hz and only slightly diminished at Arg35 (6.90 Hz) and Tyr36 (6.62 Hz). The heteronuclear NOE is strictly monotonically increasing between Asp6 and Leu17 from -3.30 to 0.56. It is >0.60 for all residues Ala18-Arg33 with an average of 0.70±0.06 and decreases at the C-terminal tripeptide towards 0.39 (Figure 2.7, shaded bars).

In order to get more detailed insights into the dynamics of NPY bound to DPC micelles, we determined the motional parameters from the relaxation data according to the Model-Free Approach (Lipari & Szabo,

1982a,b; Clore *et al.*, 1990). The procedure has been applied successfully to a large variety of (mainly smaller) proteins in the last years and was shown to be an appropriate tool to derive site-specific information on internal dynamics similar to the *B*-factors known in crystallography, albeit with the advantage of additionally supplying information on the timescales of these motions. The analysis reveals the correlation time for overall tumbling, the generalized order parameters and effective correlation times for internal motions on one (SMF) or two different (EMF) timescales. The Lipari-Szabo model has recently been used to interpret ^{15}N relaxation data of peptides in the presence of micelles (Papavoine *et al.*, 1997) and to characterize a dimerization interface (Pfuhl *et al.*, 1999).

For NPY on DPC-micelles, a first estimate of the overall isotropic rotational correlation time was determined from the average value of R_2/R_1 of selected nuclei. For residues exhibiting no internal motions, the theoretical NOE is approximately 0.86 assuming a correlation time τ_c of 9 ns, which corresponds to a mass of around 20 kDa at 310 K (Daragan & Mayo, 1997). For residues Ala18-Arg33 the $^{15}N\{^1H\}$-NOEs exceeded the value of 0.60. Therefore, internal motions in pNPY/DPC are limited in the helical region of Ala18-Arg33 and R_2/R_1 is only function of the global correlation time τ_c (Kay *et al.*, 1989). At 500 and 600 MHz, the average values are $(R_2/R_1)_{500}$=6.75±0.73 and $(R_2/R_1)_{600}$=8.17±1.05 and correspond to values for τ_c of 9.2(±0.6) ns and 8.6(±0.7) ns, respectively, which match each other sufficiently closely. We followed the statistical approach to the selection of the internal motional parameters S^2_e, S^2_s, S^2_f, and R_{ex} as outlined by Mandel *et al.* (1995), which is described in Materials and Methods in more detail. In the initial phase the five different models proposed by Mandel *et al.* (1995) were fitted to the five experimental relaxation parameters R_1, R_2, and $^{15}N\{^1H\}$-NOE, determined at 500 MHz, and R_1, R_2, determined at 600 MHz for each residue while the global correlation time τ_c was kept constant at the initial estimate of 8.9 ns. Once the appro-

priate model had been selected for each residue, the overall rotational correlation time and the internal motional parameters for each spin were optimized simultaneously. Because the relaxation data of the N-terminal residues Asp6 and Asn7 could not be explained by any of the proposed models, they were excluded from the final calculation. The results from the fitting procedure are listed in Table 2.1. The final value of τ_c was

Table 2.1 Parameters of backbone dynamics for pNPY on DPC micelles[a]

residue	S^2	dS^2	τ_e [ps]	$d\tau_e$ [ps]	S_s^2	dS_s^2	S_f^2	dS_f^2	R_{ex}	dR_{ex}	$\chi^{2\,b}$
Gly 9	0.06	0.02	635	47	0.07	0.02	0.83	0.03			1.38
Glu 10	0.11	0.01	776	40	0.14	0.02	0.76	0.02			0.39
Asp 11	0.09	0.01	839	40	0.12	0.02	0.71	0.02			1.57
Ala 12	0.13	0.01	823	37	0.18	0.01	0.69	0.02			4.33
Ala 14	0.27	0.01	855	31	0.35	0.02	0.78	0.01			3.77
Glu 15	0.28	0.01	1218	25	0.39	0.02	0.73	0.01			2.10
Asp 16	0.44	0.02	1356	95	0.56	0.03	0.79	0.02			3.38
Leu 17	0.63	0.04	1300	293	0.79	0.04	0.80	0.02			0.71
Ala 18	0.82	0.02									2.66
Arg 19	0.83	0.02									3.83
Tyr 20	0.82	0.03	70	25					2.09	0.72	0.64
Tyr 21	0.76	0.03							1.69	0.78	3.69
Ser 22	0.82	0.02	31	23							4.83
Ala 23	0.85	0.03									3.51
Leu 24	0.78	0.03							1.70	0.75	3.28
Arg 25	0.81	0.03									1.24
His 26	0.79	0.03									5.83
Tyr 27	0.84	0.03									3.71

Table 2.1 Parameters of backbone dynamics for pNPY on DPC micelles[a]

residue	S^2	dS^2	τ_e [ps]	$d\tau_e$ [ps]	S_s^2	dS_s^2	S_f^2	dS_f^2	R_{ex}	dR_{ex}	$\chi^{2\,b}$
Ile 28	0.88	0.03									1.52
Asn 29	0.86	0.03	55	34							4.37
Leu 30	0.82	0.02									4.59
Ile 31	0.76	0.03	51	18							1.66
Thr 32	0.86	0.05									3.79
Arg 33	0.80	0.02	67	23							5.83
Gln 34	0.64	0.04	1829	349	0.70	0.04	0.92	0.03			0.06
Arg 35	0.46	0.03	1674	162	0.55	0.03	0.83	0.02			0.42
Tyr 36	0.46	0.02	1439	117	0.59	0.03	0.79	0.02			3.11

a. The parameters are obtained applying the following models: (1) S_2, (2) S_2, $\tau_e=\tau_f$, (3) S_2, R_{ex}, (4) S_2, $\tau_e=\tau_f$, R_{ex}, (5) S^2_f, S^2, $\tau_e=\tau_f$.
b. χ^2 values are calculated as the sum-squared error residuals. The theoretical values for the 95% confidence interval of the χ^2-distribution are 9.49, 7.81, and 5.99 for one, two, and three motional parameters, respectively.

8.96(±0.1) ns, only slightly different from the initial guess.

Fast ^1H, ^2H exchange and order parameters smaller than 0.2 up to residue Ala12 indicate that the N terminus extends freely into the aqueous phase surrounding the micelle. It has often been recognized that relaxation data from residues of flexible parts of the molecule cannot be fitted to the simple Lipari-Szabo model but require a (extended) model that includes contributions from slow internal motions on the nanosecond time scale (EMF). The necessity of such a model for fitting of residues Gly9-Leu17 strongly supports the view that the N-terminal motions are mainly uncorrelated to overall tumbling. However, Schurr *et al.* (1994) could show that data from molecules with pronounced anisotropic tumbling may, when interpreted with the EMF formalism, reveal slow internal motions even in the absence of such motions. Taking into account that

the micelle is approximately globularly shaped and that binding of the (much smaller) pNPY to it is unlikely to change overall tumbling dramatically, we suggest that reorientation of the complex is still isotropic, a view that has recently been supported by Papavoine *et al.* (1997) in their analysis of the M13 phage coat protein gVIIIp on SDS micelles. Because a structural model for the NPY-micelle complex is presently not available, we did not attempt to test for anisotropy. NPY on micelles is most rigid between Ala18 and Arg33 with S^2=0.82±0.04 (Figure 2.8). Remarkably,

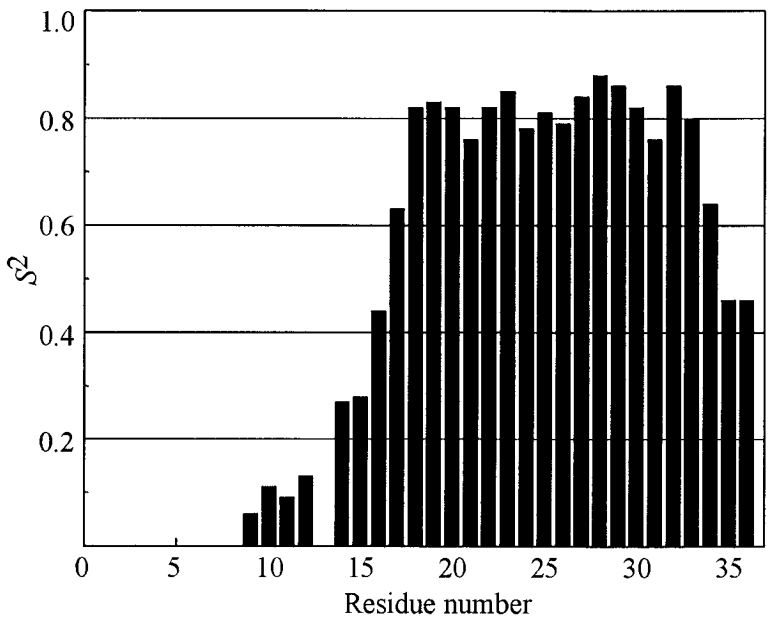

Figure 2.8 Model-free order paramters S^2 for NPY in DPC solution from ^{15}N spin relaxation measurements as a function of the protein sequence.

the order parameters at the C-terminal turn, that are between 0.46 and 0.64, clearly indicate, that the C terminus has residual structure. Papavoine discovered that the micelle-spanning helix in M13 coat protein gVIIIp/SDS is much more stable than the surface-associated helix, as is obvious from the generalized order parameters of 0.96 and 0.51, respectively. Our value of 0.82 is therefore much closer to that found for the micelle spanning hydrophobic helix 2 of the M13 coat protein (S^2=0.96±0.03), and indicates that the helix of NPY is unusally rigid com-

pared to other secondary helices. Furthermore, Papavoine and co-workers reported slow internal motions for the surface associated helix, which are strictly absent in the helical region of pNPY. Instead, we observe small chemical exchange contributions (1.7-2.1 Hz) for residues Tyr20, Tyr21, and Leu24.

For NPY in aqueous solution the R_1 values at 500 MHz monotonically increase at Ser3-Asp16 from 1.02 to 1.98 Hz. Between Leu17 and Asn29 the adopted values range from 2.26 to 1.99 Hz with exceptions of Tyr21, Tyr27, and Ile28, which have significantly diminished longitudinal relaxation rates (1.56-1.81 Hz). R_1 is 1.79-1.82 Hz at Leu30-Arg33 and monotonically decreases towards the C terminus to 1.24 Hz. The mean R_2 value for the N-terminal residues Ser3-Ala12 is 2.14(±0.60) Hz. The R_2 values adopted at Ala14-Gln34 can essentially be grouped into two classes: (i) Ala14-Ala23, Arg25, His26, Asn29 with an average R_2 of 5.53(±1.18) Hz, and (ii) Leu24, Tyr27, Ile28, Leu30, and Ile31 with a significantly enhanced mean R_2 of 9.15(±0.96) Hz, and finally Thr32 with R_2=22.22 Hz. The heteronuclear NOE increases at Ser3-Glu15 from -1.70 to 0.04, adopts a mean value of 0.22±0.07 between residues Asp16-His26, is around 0 at Tyr27, Ile28, Leu30, and Ile31, 0.10 at Asn29, and decreases at the C-terminal pentapeptide from -0.06 to -1.0 (Figure 2.7, black bars).

Because NPY in aqueous solution is expected to be structurally most rigid in a range of residues similar to the one observed for NPY on DPC micelles, a first estimate of the overall isotropic rotational correlation time was determined from the average value of R_2/R_1 of residues Ala18-Arg33 as well, which was $(R_2/R_1)_{500}$=4.04±2.33. The high standard deviation results mainly from a few residues with enhanced transverse relaxation rates R_2. Since a reliable estimation of the overall tumbling time would not be possible using this inaccurate value, we calculated the 20% trimmed mean value of R_2/R_1 of residues Ala18-Arg33, neglecting the contributions of residues Arg19, Ala23, Tyr27, Ile28, Ile31, and Thr32.

Thereby, we obtained $(R_2/R_1)_{500}$=3.20±0.73, corresponding to τ_c of 5.5(±1.0) ns. This value is consistent with the presence of NPY as a dimer at 32°C (Daragan & Mayo, 1997). However, severe line-broadening concomitant with substantial changes of chemical shift values for certain protons is observed when the concentration is increased up to 4 mM, which indicates that NPY forms also higher aggregates. Moreover, after one week of NMR measurements at 305 K, a number of additional weak peaks appeared in the [^{15}N,^{1}H]-HSQC spectrum, showing that the sample is not completely stable, either due to irreversible self-aggregation or degradation effects in aqueous solution.

Many of the nuclei exhibit small or even negative NOEs. Residues experiencing internal motions on a timescale from 100 ps to nanoseconds are usually identified by heteronuclear NOEs smaller than 0.65 (Kay *et al.*, 1989). This applies to all residues of unligated NPY. Moreover, due to its elongated structure, rotational diffusion is expected to be anisotropic, which may be further complicated by dimerization. The latter additionally leads to different chemical environments for nuclei at the interface contributing to exchange. Altogether, the motional behaviour of unligated NPY is expected to be very complex, with some processes leading to similar effects on relaxation rates. Taking into account that the number of experimental data points used in the fitting procedure is only four, and that uncertainties in the data are substantial, the complex motional behaviour cannot be unambiguously assigned into the contributions made by the different mechanisms without heavy overinterpretation. We therefore decided to not interpret the relaxation data according to a motional model but rather based our conclusions on the raw data.

Increased values of R_2 are found for residues Leu17 to Thr32 accompanied by positives values for the heteronuclear NOE at Leu17-His26 but small NOEs at Tyr27-Thr32. Without explicit calculations of order parameters it is evident from the data that the helix is most rigid in this region.

Importantly, R_2 values for the C-terminal tetrapeptide are similar to those of the transition region preceeding the α-helix (residues Ala12 to Asp16) and the heteronuclear NOE is negative. We conclude therefore, that the C-terminal tetrapeptide is largely unstructured, an observation that is inconsistent with the structural data by Monks *et al.* (1996), in which the α-helix extends to the last residue. In contrast, pNPY bound to DPC micelles is displaying large R_2 values and positive NOE for the tetrapeptide. An important question to be answered from the relaxation data is whether the N terminus folds back onto the C-terminal helix. A monotonic decay of the heteronuclear NOE and a monotonic decrease of the R_2 values indicates that the N terminus is fully flexible. Back-folding of N-terminal residues onto the helix should restrict the motions of residues involved in making the contacts and would therefore be incompatible with a monotonic decrease of NOE/decrease of R_2. Furthermore, a bimodal behaviour of relaxation data would be expected for the backfolding case. To conclude we state that:

(1) Unligated NPY is structured between residues Leu17-Thr32 and unstructured at the C-terminal tetrapeptide. It predominantly forms a dimer in solution at concentrations of 1 mM or even below, exhibiting chemical exchange processes resulting in enhanced transverse relaxation rates R_2 mainly involving residues Leu24, and Tyr27, Ile28, Leu30-Thr32. No backfolding of N-terminal residues onto the C-terminal helix occurs.

(2) NPY bound to DPC micelles is structurally similar to unligated NPY. However the C-terminal α-helix is much more stable and extends to the last residue. Again, backfolding of N-terminal residues can be excluded.

2.3. Discussion

The tertiary and quarternary structures of NPY in aqueous solution and on DPC micelles

In the present study we have carefully chosen sample conditions, such as pH and temperature, to allow a structural study of NPY interacting with a membrane model under conditions that should match physiological conditions as close as possible. The set of NOE-derived distance restraints are completely devoid of data that would arise from back-folding of the N terminus onto the α-helix, as postulated for the PP-fold of NPY (Darbon *et al.*, 1992; Khiat *et al.*, 1998), nor do we see any evidence for a dimer arrangement in a "handshake-type" fashion as postulated by Cowley *et al.* (1992), or the anti-parallel alignment-mode favoured by Monks *et al.* (1996). Indeed, line-widths, proton and ^{15}N chemical shifts are concentration independent, clearly showing that NPY is monomeric in the presence of DPC micelles.

A careful comparison of the H secondary chemical shift data with the values published for porcine NPY (Saudek & Pelton, 1990) and human NPY (Monks *et al.*, 1996) reveals striking similarities for Tyr1-Ile31, but significant low field shifts are observed for the H^N chemical shifts of Leu17, Tyr21 and Ile28. We propose that the similarity of the H^α chemical shifts indicates similar secondary structures for the segment Tyr1-Ile31 in aqueous solution and on DPC micelles, whereas the differences in some of the H^N chemical shifts are due to a close proximity with polar headgroups of the micellar surface in the presence of DPC. This interpretation is supported by the observation of similar backbone ^{15}N resonances for the residues located in the α-helix in aqueous solution and on DPC micelles. On the other hand, the H^α, and even more pronounced the H^N

and the ^{15}N resonances at the C-terminal pentapeptide Thr32-Tyr36 tend to shift upfield upon addition of DPC, which is indicative of helix formation or helix stabilization.

Overall, the three-dimensional structure calculated for NPY on DPC micelles at pH 6 is similar to the previously reported ones for human NPY (Monks *et al.*, 1996) and porcine NPY (Cowley *et al.*, 1992) in aqueous solution at slightly acidic pH conditions, but different from the PP-fold structure proposed by Darbon *et al.* (1992). It consists of an unstructured N terminus comprising residues Tyr1-Pro13 followed by an α-helix spanning residues Ala14-Tyr36. The helix is best defined between residues Asp16-Arg33 and is probably in an equilibrium between helical and partially unfolded structures at the capping turns Pro13-Glu15 and Gln34-Tyr36. In fact, the partitioning of the molecule into structured and more flexible parts as evident from the DYANA calculations is nicely reflected by the motional order parameters that were determined from ^{15}N relaxation measurements. Generalized order parameters S^2 with values larger than 0.75 are observed only for the segment Ala18-Arg33, whereas Glu15-Leu17 and Gln34-Tyr36 are characterized by values between 0.28 and 0.64 and additionally exhibit significant internal motions on the nanosecond time-scale with τ_e>1.2 ns. We attribute these slow motions to the transitions between partially unstructured conformations and the α-helix (Orekhov *et al.*, 1999). At Gly9-Ala12, S^2 values are steadily increasing from 0.06 to 0.13, with effective internal correlation times between 635 and 839 ps. Here, the highly uncorrelated slow internal motions are interpreted as random diffusion of the N terminus in the aqueous environment of the micelle.

Surprisingly, the precision of the solution structure proposed by Monks *et al.* (1996) is much more uniform throughout the whole α-helical segment comprising Ala12-Tyr36. Although the presence of averaged $^3J_{HN\alpha}$ coupling constants indicates that the helix is not completely stable

the RMSD values for the backbone atoms are low throughout this segment. However, the analysis of our relaxation data, obtained for ^{15}N-labeled pNPY at 1 mM in aqueous solution, clearly shows that the molecule is highly flexible, exhibiting motions on different time-scales. Internal motions manifested by negative values of the heteronuclear NOE and smaller R_2 rates are very pronounced at the N terminus, data that are completely incompatible with a back-folding of the N terminus onto the C-terminal helix commonly described as the PP-fold. Even in the helical region the relaxation data imply residual flexibility, presumably resulting from transitions between helical and partially unfolded conformations. The global correlation time, as estimated from a 20% trimmed mean value of R_2/R_1 of residues Ala18-Arg33, is consistent with the presence of NPY as a dimer. Obviously, monomeric NPY is expected to tumble anisotropically due to its elongated shape. However, dimerization and partial unfolding both contribute to a more globular shape so that the correlation time for overall reorientation may not be too far away from that expected for a globular protein. It has been shown theoretically that folding of an isolated helix in water is thermodynamically unfavourable (Zimm & Bragg, 1959), which means that a linear oligopeptide containing less than 40 residues is unable to adopt a stable helical conformation without additional interactions. It was argued that mutual contacts between the helices of the monomers significantly stabilize the α-helix in NPY. As noted by Nordmann *et al.* (1999) the presence of a positive charge on His26 at pH<4, as chosen in the previous NMR studies, affects dimerization and therefore the α-helical content. They observed in CD spectra that the helical content of NPY substantially increases by shifting the pH from 4 to 8. Unfortunately, the solubility of NPY even at pH 6 (together with largely increased H^N exchange rates) is so little that spectra with qualities sufficient to derive structural constraints from them cannot be recorded. In addition to dimer stabilization at elevated pH, association to DPC

micelles obviously favours helix promotion, as determined from CD measurements at pH 6 in the presence and absence of DPC (Figure 2.9).

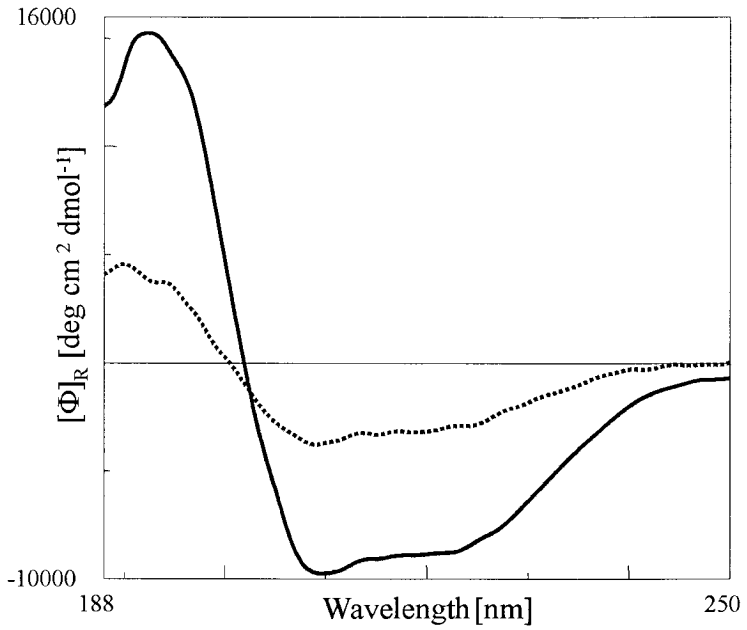

Figure 2.9 CD spectra of 50 µM pNPY in aqueous solution (---) and in 300 mM DPC (-) at pH 6.0 and 37°C. The ellipticity is expressed as the mean-residue molar ellipticity.

A lot of speculation about the physiological significance of NPY self-association has occurred. However, the rather large K_d value, which was determined to be 1.6(±0.6) µM by fluorescence studies (Cowley *et al.*, 1992), already indicates that NPY exists as a monomer at physiological concentrations (Minakata *et al.*, 1989). Moreover, probing the dimerization interface with a spin-labeled [TOAC34]-NPY analogue revealed that NPY does not arrange exclusively in form of an an anti-parallel dimer, which had previously been postulated from intersubunit NOEs (Cowley *et al.*, 1992; Monks *et al.*, 1996) but rather exists as a mixture of dimers with parallel and anti-parallel alignment of the helices. In this context it is interesting to note that Monks and co-workers observed a doubling of the signals for the imidazole ring protons of His26 and the aromatic protons of Tyr20 and Tyr27 of both human and porcine NPY in aqueous solution

in a 2:1 ratio. Coalescence was achieved at 75°C and could be reversed upon cooling to 37°C. Based on our data, we speculate that the signal doubling is due to the two different self-association modes. The apparent unspecifity in the arrangement supports the view that at most the dimer may have some implications for storage when present in high concentrations. In fact, our data show that in the presence of DPC micelles NPY no longer form dimers, but rather associates to the membrane as discussed below.

Interaction of NPY with a phosphocholine membrane mimetic

Interestingly, binding of NPY to the membrane surface is accompanied by a conformational reorientation of the C-terminal pentapeptide (Figure 2.10). It is this particular segment that is believed to contain resi-

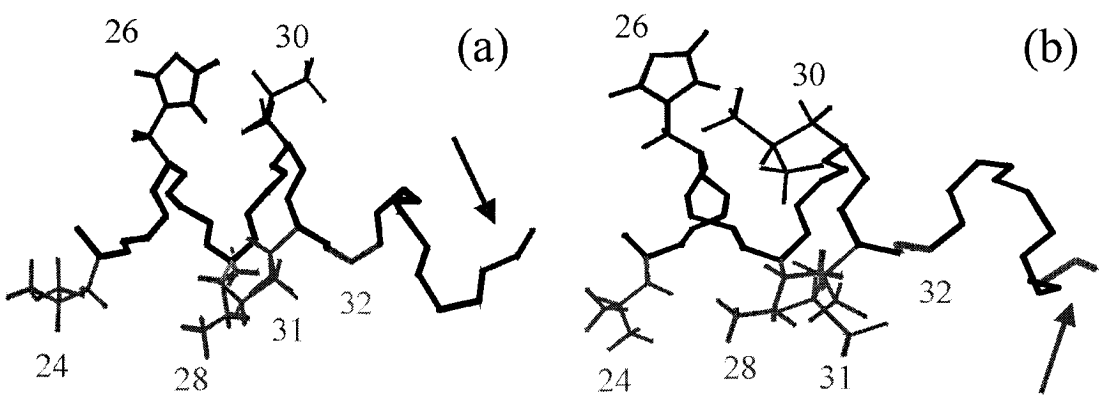

Figure 2.10 One representive energy-minimized DYANA structure displaying residues Leu24-Tyr36 of NPY (a) in aqueous solution as determined by Monks *et al.* (1996), and (b) bound to DPC micelles, using the backbone atoms (C^{α}, N and C) and side-chain atoms (with RMSD<1.0 Å) as indicated. The aqueous surrounding is at the top, and the surface of the micelle is at the bottom (light grey-coloured). The arrows point to a difference in the relative position of the C-terminal Tyr residue between NPY in aqueous solution and NPY in DPC solution.

dues which directly interact with the receptor, presumably through electrostatic interactions involving Arg33 and/or Arg35 (Beck-Sickinger & Jung, 1995). We therefore propose that membrane interactions are relevant for the subsequent receptor selection. In order to yield a structurally more detailed understanding of the mechanism of interaction of NPY with a membrane, we determined the orientation of the hormone relative to DPC micelles. Proximity to a spin-label located near the transition region between hydrophobic and ionic compartment of the micelles mostly affected intensities of crosspeaks from a [^{15}N,^{1}H]-HSQC of residues Leu17, Tyr20, Tyr21, Leu24, Ile28, Asn29, Ile31, Thr32, and Tyr36. Such a regular pattern, reflecting a 3-4 periodicity had also been described for motilin in SDS micelles (Jarvet *et al.*, 1997). It was interpreted such that the helix is oriented parallel to the micelle surface with the side containing residues that experience the most pronounced signal reductions facing the micelle surface. In agreement with this view, we were unable to observe line broadening of amide resonances when using a spin-label that is placed near the hydrophobic core of the micelle. Secondly, $^{1}H^{N}$, $^{2}H^{N}$ exchange at 310 K was complete within 40 minutes for all residues with the exception of Ile28. For only a few residues, namely Leu24, Arg25, Tyr27, Ile28, and Ile31, signals were still present after ten minutes. Altogether, these data strongly indicate that NPY remains in vicinity of the micelle surface. Neither the α-helix nor the N terminus penetrate the hydrophobic interior. Moreover, we clearly find that the amphipathic helix arranges parallel to the membrane with the hydrophobic residues facing towards the micelle surface. It becomes evident now, that the latter are the same residues that were shown to make intermolecular contacts in the dimer interface, as determined by spin-label and relaxation experiments. It has already been published, based on $^{1}H^{N}$, $^{2}H^{N}$ exchange measurements, that dimerization is due to hydrophobic interactions between tyrosine and isoleucine side-chains (Cowley *et al.*, 1992). We conclude,

that in the presence of a phosphocholine lipid membrane, interactions of these side-chains with the hydrophobic compartment of the membrane are favoured over hydrophobic packing in the dimer. Wherever our membrane model approximates biological conditions sufficiently well, the dimer is not expected to be physiologically relevant for the binding to a membrane receptor. One limitation of our membrane model is concerned with the net charge of the headgroups. DPC contains both negative and positive charges on the headgroups. Phosphatidylserine in contrast is negatively charged, others may even be neutral. It is expected that the exact lipid composition of the membrane, together with other factors influencing the membrane potential, are important for fine regulation of affinity to the membrane; we have therefore initiated research in that area.

The net charge of NPY at pH 6-7 is +1 or +2, depending on the protonation state of His26. However, the helical region Leu17-Tyr36, that comes into closest contact with the membrane surface, contains four to five positive charges, whereas five negative and two positive charges are present in the flexible N terminus. Thus, our observation that the positively charged helix associates to the membrane with the hydrophobic side facing the surface of the micelle, onto which positive and negative charges of the headgroups mutually compensate, supports the view that absorption is mainly due to hydrophobic forces. Addition of Ca^{2+} in millimolar concentrations in the presence of physiological NaCl concentrations significantly and specifically reduced the effect of the spin-label on the signals of the hydrophobic residues that are identified to mediate membrane association. No shifts of NPY $^{1}H^{N}$ or ^{15}N resonances were observed upon addition of Ca^{2+}, thereby excluding complexation of NPY by Ca^{2+}. The signals of the helical residues were still significantly more broadened than those of the N-terminal. We speculate, that Ca^{2+} is concentrated in the ionic surface compartment (Swairjo *et al.*, 1995), resulting

in a positive net charge of the micelle and electrostatic repulsion of the positively charged helix. Moreover, our results indicate that besides the hydrophobic force that promotes binding of NPY to the helix, the exact orientation of the peptide relative to the membrane might additionally depend on the local electropotential. The electrostatics in the surroundings of a receptor are dependent on the precise composition of the membrane, the electric and membrane dipole moment (Schwyzer, 1991), and may therefore be difficult to calculate. It is evident that these parameters might vary from one receptor subtype to another and may even be influenced by charges from receptor residues (Schoch & Sargent, 1980).

Biological implications for receptor selection

Figure 2.11 shows a hypothetical model for the mechanism of receptor selection and binding preceeding receptor activation involving: (1) intracellular storage and release, followed by; (2) membrane association, and finally; (3) receptor selection and binding.

(1) Inspired by data from the crystal structure of avian pancreatic polypeptide, a homologue of NPY, which had been successfully solved in the presence of Zn^{2+} and which revealed that PP exists as a dimer under these conditions, it has been speculated that the storage form of this peptide in membrane-enclosed granules reflects either an aggregated or even crystalline state (Blundell *et al.*, 1981). Similarly, after release into the synaptic cleft, concentrations are still high, such that the dimer is expected to persist to predominate. Chang *et al.* (1980) compared chicken plasma levels of avian PP with its self-association constant and estimated a 50-60% content of the dimer in the dimer- monomer equilibrium. Based on the suggestion that the hydrophobic residues involved in the self-association of glucagon and insulin are also forming contacts with their respective

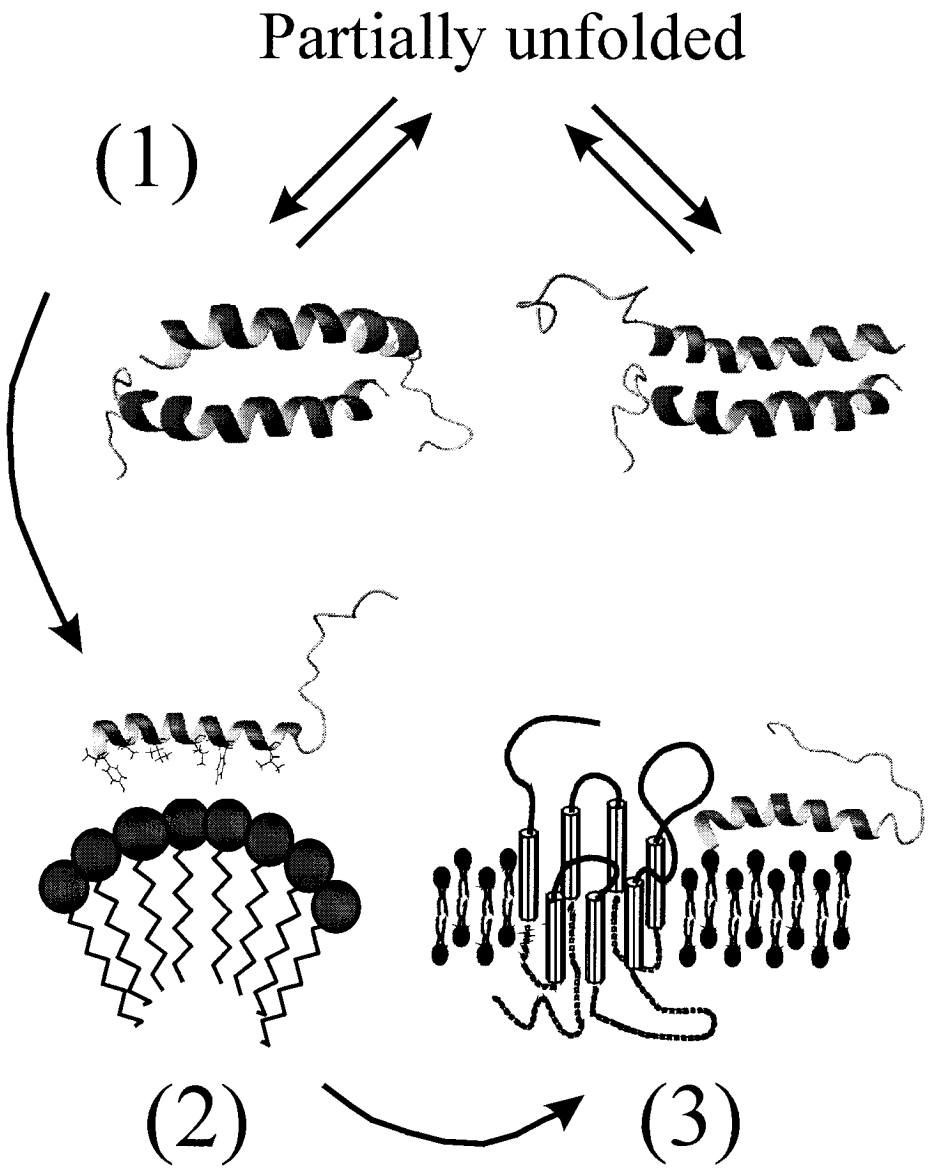

Figure 2.11 Proposed three-step model of receptor selection for NPY (see the text).

membrane receptors, they proposed a three-step equilibrium between monomeric peptide, dimeric peptide and the receptor-bound monomer. Based upon our NMR data for NPY in aqueous solution, we extend and modify this model in the following way: in the absence of a receptor or a membrane, NPY undergoes self-association involving hydrophobic residues of the α-helix. This is energetically conceivable, since it helps to bury hydrophobic surface residues which would otherwise have been exposed

to solvent. Experiments utilizing a spin-labeled NPY-analogue established for the first time that both anti-parallel and parallel arrangements exist in the dimer. In both dimer arrangements the C-terminally located spin-label does not affect N-terminal residues from the associated molecule. The view that the N terminus is completely flexible in aqueous solution is additionally supported by our relaxation as well as by published structural data (Monks *et al.*, 1996).

(2) We could demonstrate association to phosphocholine micelles through hydrophobic residues. We postulate that the main task of the hydrophobic residues responsible for self-association in aqueous solution at sufficiently high concentrations, is association with the membrane rather than receptor binding. This view was originally developed by Schwyzer in his Membrane Compartments Theory (Schwyzer, 1986, 1991, 1995a). The theory states that the target cell membrane influences receptor selection of regulatory peptides by guiding important residues into the appropriate compartment(s), i.e. the hydrophobic, the fixed-charge and/or the aqueous compartment of the membrane. Furthermore, preferred conformations and orientations are induced. This implies that the fit of the ligand to its receptor, which defines the receptor requirements, needs to be complemented by a set of membrane requirements for optimal ligand-receptor interactions (membrane-assisted receptor selection). Two observations count for our view that the accumulation and orientation of the α-helix of NPY on the membrane influences receptor binding at the Y_1-receptor. (i) Single amino acid substitutions by alanine revealed that, in the C-terminal helical region encompassing Arg19-Thr32, residues sensitive and residues insensitive to mutations are distributed non-randomly but form a pattern of 1-2 sensitive followed by 2-3 insensitive positions. Important residues include Tyr20, Leu24, Tyr27, and Ile31, Thr32, and Tyr36. Arg33 and Arg35 are the most sensitive positions and are supposed to be directly required for receptor binding (Beck-

Sickinger & Jung, 1995). The observed pattern causes all relevant positions to point to one side of the helix, which we were able to identify as the membrane interface. (ii) The same authors reported that substitution of three helical residues His26-Ile28 of the N-terminally acetylated NPY fragment Arg25-Tyr36-NH_2, by only one or two alanine residues results in a small decrease of α-helical conformation but a strong decrease in receptor binding. They concluded, that not only the α-helical stretch itselt, but also its particular orientation and amphiphilicity may be required and are responsible for providing the conformational prerequisites of residues Arg33-Tyr36-NH_2, for receptor binding (Jung *et al.*, 1991).

Interestingly, the proximity of the spin-label from 5-doxylstearate located at the hydrophobic/ionic compartment interphase with the C-terminal Tyr36-amide residue indicates that the C terminus is oriented towards the micelle surface (Figure 2.10). The conformational difference found between the C-terminal turn in aqueous solution and on DPC micelles supports our view that Tyr36-amide serves as an anchor to the membrane, thereby stabilizing the helix at the C terminus, restricting the conformational space and possibly inducing the bio-active conformation (Schwyzer, 1995a,b). Interestingly, upon substitution of the C-terminal Tyr36-amide by the Phe-amide the affinity remains in the nanomolar range at both the Y_1 and the Y_2 receptor (Beck-Sickinger *et al.*, 1994). The positioning of these residues relative to the membrane interface can be explained using thermodynamic arguments. Wimley & White (1996) have determined the whole-residue free energies of transfer of amino acid residues from water to the palmitoyloleoylphosphatidylcholine (POPC) interface. Values of Tyr, Phe and Trp are -0.94, -1.13, and -1.85 kcal/mol, respectively. Based on these free energies of transfer, the aromatic residues Tyr, Phe and Trp should accumulate at the water-membrane interface to the largest extent compared to the other residues, an

hypothesis which is fully supported by the observed occurence of Tyr-amide at the interface.

We speculate that partitioning of the hydrophobic Tyr36-amide at the interface, together with anchoring of the helix to the membrane *via* residues Ile31/Thr32 provides the proper positioning/pre-orientation of Arg33-Arg35 relative to the membrane, such that receptor recognition is facilitated. This may further explain why the C-terminal amide group is essential for receptor binding and why the negatively charged carboxylate C terminus is not tolerated (Hoffmann *et al.*, 1996). Proper positioning of the segment Arg33-Arg35 is also reflected in the intolerance of substitution of Gln34 by Pro34 at the Y_2 (Fuhlendorff *et al.*, 1990) and of Ile31-Thr32 by Ala31-Aib32 at all other except the Y_5-receptor (Cabrele *et al.*, 2000).

(3) As a consequence of accumulation of the ligand on the membrane surface, only two-dimensional rather than three-dimensional diffusion to the receptor is required, which is relevant considering the low density of the receptors on the target cell membranes (80,000-100,000 receptors/cell) (Fabry *et al.*, 2000). Whether NPY exhibits major conformational changes upon binding to a receptor is still unclear, as is the functional role of the fully flexible N terminus, which was shown to be essential for agonism at the Y_1 and the Y_5 receptor. The presence and uniform distribution of four proline residues and four negative charges between Tyr1-Ala14 might prevent it from folding into α-helical conformation. In addition, Glu15-Asp16 may constitute an N-cap of the helix.

In contrast, the C-terminal tetrapeptide is already rather rigid when bound to DPC micelles, even in the absence of a receptor. Clearly, receptor-subtype specific interactions could give rise to small conformational changes or reorientations of the helix on the membrane. However, it is the membrane-associated conformation of the ligand that is first recognized

by the receptor (Moroder, 1997). This statement has recently been supported by the work of Pellegrini & Mierke (1999), who structurally characterized the molecular complex of the C-terminal octapeptide of cholecystokinin and the N terminus of the cholecystokinin A receptor on DPC micelles by means of NMR data.

2.4. Conclusion

In this work we have structurally characterized neuropeptide Y free in solution and in the membrane-bound form. We found that peptide-lipid interactions replace the non-specific contacts observed in the unligated dimer. Both arise from a distribution of hydrophobic residues on one side of the C-terminal helix which we consider to be required for correct positioning on the membrane surface. By so doing, residues are partitioned into the correct compartment and are pre-oriented for receptor binding.

The presented results envision a new approach for the design of receptor-subtype selective agonists of hormone peptides. The approach is based upon deconvolution of binding into contributions of residues due to membrane association and the correct positioning of the hormone on the membrane surface and into contributions due to forming correct receptor contacts. We have found it sometimes very difficult to rationalize the effects of mutations onto biological activities, as expressed by IC_{50} values, at the different receptor subtypes when taking only residues of the receptor likely to interact with NPY and residues from the hormone itself into account. A detailed understanding of features that determine the membrane-binding mode enables us to design NPY mutants in which membrane-anchoring is changed. Residues that make contacts with the

receptor will be differently pre-positioned and it thus becomes possible to investigate the influence of such mutations on receptor-subtype selectivity. However, a prerequisite of this approach is a detailed understanding of the receptor-hormone interaction. We are presently working on the development of such a model.

2.5. Materials and Methods

Materials

$^{15}NH_4Cl$ was purchased from Martek (Columbia, USA), deuterated DPC-d_{38} (99%-d), and methanol-d_3 were ordered from Cambridge Isotope Laboratories (Andover, Massachusets, USA). 5-Doxylstearic acid, 5-doxylstearic acid methyl ester and 12-doxylstearic acid were bought from Aldrich (Buchs, Switzerland).

The *N*-(9-fluorenylmethoxycarbonyl, Fmoc)-protected natural amino acid residues were purchased from Alexis (Läufelingen, Switzerland). Side-chain protecting groups were: *tert*-butyl for Asp, Glu, Ser, Thr, and Tyr, Boc for Lys, trityl for Asn, Gln and His, 2,2,5,7,8-pentamethylchroman-6-sulphonyl (Pmc) for Arg. The 4-(2',4'-dimethoxyphenyl-Fmoc-aminomethyl)-phenoxy (Rink Amide)-resin was obtained from Novabiochem (Läufelingen, Switzerland). *N*-hydroxybenzotriazole (HOBt), *O*-(7-azabenzotriazol-1-yl)-1,1,3,3-tetramethyluronium hexafluorophosphate (HATU) and *N*-diisopropylethylamine (DIPEA) were purchased from Fluka (Buchs, Switzerland). *N*, *N*'-diisopropylcarbodiimide (DIC) was bought from Aldrich (Buchs, Switzerland).

Production of ^{15}N-labeled porcine NPY (pNPY)

For the production of uniformly ^{15}N-labeled NPY we followed the strategy previously described by Khono *et al.* (1998). In his approach, shorter peptides are expressed as proteins fused to N-terminally decahistidine-tagged yeast ubiquitin (Ub). After expression and purification of the fusion protein, the desired peptide is cleaved off with a hexahistidine-tagged ubiquitin hydrolase (YUH). In order to produce the C-terminal amidated form of pNPY an additional gly codon was introduced, which after production of the corresponding peptide, was converted to an amide function through the peptidylglycine α-amidating enzyme. The required plasmids pUBK19 and pYUHK20b for cloning of the fusion protein and for the production of YUH were received as a generous gift from Dr T. Kohno (Mitsubishi Kasei Institute of Life Sciences, Tokyo, Japan).

The synthesized DNA encoding for pNPY, followed by a codon for the additional glycine as well as two stop codons and the appropriate *Sal* I cleavage site, was cloned into pUBK19 as outlined by Kohno and co-workers. The resultant plasmid pUBK19/NPY-G was transformed into *Escherichia coli* strain DH5α and the sequence confirmed using dideoxy-sequencing. Expression of uniformly ^{15}N-labeled H_{10}Ub-NPY-G was performed in *E. coli* strain BL21 (DE3) at 37°C on M9 minimal medium, supplemented with trace elements as described by Khono, and with $^{15}NH_4Cl$ as the sole nitrogen source. Induction of expression was done at A_{600}=0.7 by addition of 0.4 mM IPTG and cultivated for another ten hours.

Isolation, purification and refolding was done according to the protocol by Kohno *et al.* (1998), and the final yield was 20-30 mg/l of uniformly ^{15}N-labeled fusion protein. Following cleavage with ubiquitin hydrolase for four hours, the mixture was separated on a Ni^{2+}-NTA-Agarose column (Qiagen, Basel, Switzerland). A subsequent Sep-Pak Plus C_{18} cartridge served to desalt the eluate (Waters, Rupperswil, Switzerland) with increasing acetonitrile concentrations in 10% steps. Reversed-phase HPLC analyses (column C-18, 3×125 mm, 5 µm, flow 0.6 ml/min, gradient 20% acetonitrile to 70% acetonitrile in water/trifluoroacetic acid (100:0.1) within 30 minutes) indicated that NPY-G eluted with 40% acetonitrile and that the purity was >95%.

The α-amidation of the C terminus of NPY-G was performed using peptidylglycine α-amidating enzyme (EC 1.14.17.3; Unigene Laboratories, Fairfield, NJ., USA). The reaction mixture contained 30 mM MES/NaOH (pH 5.5), 0.001% (v/v) Triton X-100, 1% (v/v) ethanol, 5 mM KI, 10 µg/ml bovine liver catalase (Sigma, Buchs, Switzerland), 0.5 µM $CuSO_4$, 1.5 mM sodium ascorbate, 1-2

mg/ml NPY-G, and 15,000 units/ml of peptidylglycine α-amidating enzyme, and was incubated for 2.5-3 hours at 37°C. Again, desalting was achieved using Sep-Pak Plus C_{18} cartridges.

Completeness of the reaction and purity of the NPY fraction were checked by electrospray ionization mass spectrometry (SSQ710, Finnigan, San Jose, CA) and reversed-phase HPLC. The final yield of pure and uniformly labeled ^{15}N-pNPY was 2.5 mg/l culture.

Solid-phase peptide synthesis

pNPY containing ^{15}N nuclei, only at natural abundance was used for structure determination in the presence of DPC micelles, and was prepared by solid-phase peptide synthesis using Fmoc (9-fluorenylmethoxycarbonyl) protection group strategy on a robot system (Syro, MultiSynTech, Bochum). In order to obtain the peptide amide, 4-(2',4'-dimethoxyphenyl-Fmoc-aminomethyl)phenoxy resin was used, anchored to a polymer matrix consisting of polystyrene-1% divinylbenzene (30 mg, 15 μmol). A double coupling procedure with tenfold excess Fmoc-amino acid, HOBt, DIC in DMF (2×40 minutes) was chosen during peptide chain assembly. Fmoc-deprotection was achieved by 40% piperidine in DMF for three minutes, 20% piperidine for seven minutes and 40% piperidine for five minutes. The peptide amides were cleaved from the resin with trifluoroacetic acid/thioanisole/thiocresol 90/5/5 within three hours and subsequently precipitated using diethyl ether. The product was lyophilized from water and purified and characterized by reversed-phase HPLC and electron spray ionisation mass spectrometry. Due to the lower reactivity of the amino and carboxy groups of TOAC, the introduction of this residue and of the following arginine residue in the peptide sequence was performed manually using a different protocol: the couplings were performed twice each time using three equivalents of Fmoc-amino acid, three equivalents of HATU (*O*-(7-azabenzotriazol-1-yl)-1,1,3,3-tetramethyluronium hexafluorophosphate); the total reaction time of a single coupling was four hours. All other steps and conditions of the synthesis were performed as described for pNPY. The peptide amide was cleaved from the resin with trifluoroacetic acid/anisole/cresol 90/5/5 within three hours and precipitated using diethyl ether. After drying under nitrogen flow, the product was dissolved in aqueous ammonia (pH 9) for three hours, lyophilized and char-

acterized by reversed-phase HPLC and electron spray ionisation mass spectrometry.

NMR spectroscopy

The sample used for structure elucidation of pNPY when bound to DPC micelles was approximately 3.0 mM pNPY (not enriched in ^{15}N) in 90% H_2O/10% ^2H_2O at pH=6.0. The concentration of deuterated d_{38}-DPC was 300 mM. For relaxation measurements uniformly ^{15}N enriched (>99%) pNPY at a concentration of 1.0 mM, pH=6.0 together with 300 mM d_{38}-DPC was used. Data were recorded at 310 K. Dynamics of unligated pNPY were measured with 1.0 mM pNPY at pH=3.1 and 305 K. Structural data were measured on a Bruker DRX-600 operating at proton frequencies of about 600.13 MHz and nitrogen frequencies of about 60.81 MHz. The relaxation data (R_1, R_2 and NOE) were recorded at 50.68 MHz for both unligated pNPY and pNPY/DPC. In addition R_1 and R_2 data for pNPY/DPC and R_2 data for unligated pNPY were recorded at 60.81 MHz. Spectra were processed with the Bruker XWINNMR-2.1 software and transferred into the XEASY (Bartels *et al.*, 1995) program for inspection and data interpretation. Integration of peak volumes was performed within the program SPSCAN. Homonuclear 2D spectra for structure elucidation of pNPY bound to DPC micelles were recorded in pure-absorption mode using TPPI-States quadrature detection in the indirect dimension. For the sequential resonance assignments a presat. 2QF-COSY (Rance *et al.*, 1983), a presat. clean-TOCSY (Griesinger *et al.*, 1988) with a mixing time of 14 ms, and a 150 ms NOESY (Macura & Ernst, 1980; Kumar *et al.*, 1980) with watergate-type solvent suppression (Piotto *et al.*, 1992) for assignment purposes were measured. NOESY experiments, from which the upper limits for the structure calculation were extracted were recorded with mixing times of 75 ms in 90% H_2O/10% ^2H_2O and in 99.9% ^2H_2O, and incorporated the filter scheme of Otting for zero-quantum suppression (Otting, 1990). Data matrices comprised 10 ppm (F2) * 8.4 ppm (F1), 2048 complex (F2)*512 complex time domain data points (F1) corresponding to $t2_{max}$=341 ms and $t1_{max}$=102 ms and were zero-filled once and weighted by 70° shifted sine-bell window functions prior to the 2D Fourier-transformation (FT). After processing the digital resolution along ω2 was approx. 1.4 Hz and 5.3 Hz along ω1. The baselines were improved by applying a fifth order polynomial baseline correction as implemented in XWINNMR.

Scalar $^3J_{HN\alpha}$ coupling constants were derived from inverse Fourier transformation of in-phase NOESY peaks involving H^N protons (Szyperski *et al.*, 1992). Values from $^3J_{\alpha\beta}$ were extracted from an E.COSY experiment (Griesinger *et al.*, 1987).

For assignment purposes of the [^{15}N,^{1}H]-correlation map a [^{1}H,^{1}H] NOE-relayed [^{15}N,^{1}H]-HSQC experiment with a mixing time of 150 ms was performed (Gronenborn *et al.*, 1989). Therein, water suppression was achieved by incorporation of spin-lock purge pulses (Messerle *et al.*, 1989).

Proton, nitrogen correlation maps were derived from [^{15}N,^{1}H]-HSQC experiments. These and the subsequently described relaxation experiments utilized pulsed-field gradients for coherence selection and quadrature detection with square-shaped gradients of 25 G/cm/1ms for labeling nitrogen coherences. The gradients were followed by delays of 200 µs to allow to recover from gradients. Furthermore, the sensitivity enhancement element of Rance and Palmer was added to the standard sequences (Palmer *et al.*, 1991a; Kay *et al.*, 1992a), together with water-flip back methodology (Grzesiek & Bax, 1993).

Relaxation measurements were performed using proton-detected versions of Carr-Purcell-Meiboom-Gill (Meiboom & Gill, 1958), inversion-recovery (Vold *et al.*, 1968) and ^{15}N{^{1}H} steady-state heteronuclear Overhauser effect (Noggle & Schirmer, 1971) sequences (Dayie & Wagner, 1994). We found it problematic to incorporate schemes that aim at restoring water magnetization along +z at the end of the sequence into relaxation experiments. Depending on the specific relative durations of relaxation delay and radiation damping times, water restoring may largely differ within a series of experiments. Therefore, we preferred to destroy water magnetization, keeping in mind that some problems may occur for amide protons involved in very fast exchange with water. In all experiments the effective $t1$ delay period was set to zero for the first increment in order to yield zero phase correction in the indirect dimension. Cross-correlation effects during the relaxation delays of R_1 experiments were removed by applying a series of 90° proton pulses separated by 5 ms (Kay *et al.*, 1992b). Phase-cycling in these experiments was performed such that the steady-state ^{15}N magnetization was subtracted (Sklenar *et al.*, 1987). The spin-echo delay period in the R_2 experiments was set to 1 ms. In all of the experiments the proton carrier frequency was placed onto the water line (4.63 ppm at 310 K/4.68 ppm at 305 K) and the nitrogen transmitter at 116.3 ppm. Proton chemical shifts were referenced relative to the water line at the chosen temperature ($\delta[H_2O]$=7.83-T/96.9 ppm) and nitrogen shifts were referenced indirectly to liquid NH_3 (Live *et al.*, 1984). The hard

pulses on the proton channel were applied at a RF field of $\gamma B_1/2\pi$=40.2 KHz and at 13.0 KHz on the nitrogen channel. Decoupling the ^{15}N nucleus during acquisition was performed by using the WALTZ-16 composite pulse sequence (Levitt *et al.*, 1982) applied at a field strength of 1.25 kHz. All ^{15}N,^{1}H experiments were performed with data matrices of 15 ppm (^{1}H) * 30 ppm (^{15}N) spectral widths with 2048(F2)*150(F1) complex time domain data points. Data were extended once in F1 by linear prediction, zero-filled and processed with 70° shifted sine-bell window functions in ω2 and ω1 prior to the 2D FT. During processing of all heteronuclear spectra a digital low-pass filter was applied to reduce the residual water line (Marion *et al.*, 1989).

For R_1 and R_2 experiments, recycle delays of 2.2 s and for the $^{15}N\{^{1}H\}$-NOE delays of 3.2 seconds were applied. For R_1 and R_2 experiments 16 scans were accumulated for each increment and 64 scans for each increment in the $^{15}N\{^{1}H\}$-NOE. The R_1 series used the following relaxation delays: 0.03, 0.12, 0.21, 0.76, 1.23, 1.99 and 3.00 seconds. The R_2 series was run with the following delay settings: 0.002, 0.02, 0.04, 0.08, 0.14, 0.2, 0.4, 0.6, 1.0 seconds for unligated pNPY and 0.004, 0.012, 0.02, 0.04, 0.1, 0.2, 0.4, 0.6 seconds for pNPY/DPC. Buildup of the NOE was achieved through a pulse train of 120 degree pulses separated by 5 ms over a period of three seconds.

Structure determination

Distance restraints were obtained from NOESY spectra recorded with a mixing time of 75 ms either in 90% H_2O/10% $^{2}H_2O$ or in 99.9% $^{2}H_2O$. In the case of severe spectral overlap, when deconvolution of a peak volume into the contributions of the degenerate protons was impossible, the corresponding NOEs were excluded from the set used for the structure calculations. Finally, 954 NOE cross-peaks from the spectra recorded in 90% H_2O/10% $^{2}H_2O$ and 99.9% $^{2}H_2O$ were used to generate the input of upper-limit distance restraints for the structure calculations. Additional conformational restraints were inferred from $^{3}J_{HN\alpha}$ scalar coupling constants derived from the splitting of the in-phase doublets of NOESY peaks involving amide protons (Szyperski *et al.*, 1992). However, only those 12 scalar couplings were included whose values did not lie within the region between 6 and 8 Hz, values that are commonly interpreted to indicate rotationally averaged torsion angles. Where possible, $^{3}J_{\alpha\beta}$ coupling constants were determined from the passive couplings of $H^{\alpha,\beta}$ cross-peaks found in the E.COSY

spectrum recorded in 99.9% ^2H_2O. Again, torsion angle restraints derived from these couplings were excluded, if the combination of corresponding $^3J_\alpha\beta_2$ and the $^3J_\alpha\beta_3$ values indicated that the χ^1 torsion angle fluctuates more than ±30° around a given value (Nagayama & Wüthrich, 1981). Only Arg25 was found to have a pattern consistent with a non-averaged χ^1 torsion angle. For residues 29 and 33, only one of the two passive coupling constants could be extracted.

On the basis of the above-mentioned distance restraints and scalar coupling constants, a systematic analysis of the local conformation around the C atom of each residue, including the dihedral angles ϕ, ψ, χ^1, and χ^2, was performed using the macro HABAS (Güntert *et al.*, 1989), as implemented in the program DYANA (Güntert *et al.*, 1997). The final input (including only meaningful restraints) for structure calculations consisted of 344 upper distance limits and 145 dihedral angle constraints. Stereospecific assignments were obtained for the CH_2 of Arg33 only. The final DYANA calculation was performed with 100 randomized starting structures, and the 30 DYANA conformers with the lowest target function values were further refined with the program OPAL (Luginbühl *et al.*, 1996) using the AMBER91 all-atom force field (Weiner *et al.*, 1986). During the energy- minimization the peptide was immersed in a 6 Å thick shell of explicit water molecules using a dielectric constant ε=1.

From the calculated structures only those 17 energy-minimized conformers were selected to represent the NMR structure, that had NMR energies less than 3 kcal/mol after refinement. The quality of the final structures was assessed using the program PROCHECK-NMR (Laskowski *et al.*, 1996). In the range of the well-defined residues Glu15-Tyr36, 91.3% occupy the most favoured regions of Ramachandran space and none are found in disallowed regions. The flexible N terminus was not subjected to the quality assessment. The conformers were analyzed and Figures were prepared with the program MOLMOL (Koradi *et al.*, 1996). The NMR ensemble has been deposited in the Research Collaboratory for Structural Bioinformatics PDB code 1F8P.

Spin-label experiments

For the samples used in the spin-label experiments on DPC micelles, lyophilized, uniformly labeled ^{15}N-labeled NPY was dissolved to a final concentration of 0.2 mM in 300 mM DPC-d_{38} in 250 µl of 90% H_2O/10% ^2H_2O. The pH was adjusted to 6.0 with small aliquots of 0.1 M NaOH. Spin-labeled stearic acid or

stearic acid methyl ester were solubilized in methanol-d_3 at a concentration of 0.3 M. From these stock solutions, aliquots were added the sample to yield a final concentration of the spin label of 5 mM corresponding to approximately one spin-label per micelle, assuming about 56 DPC molecules per micelle (Lauterwein *et al.*, 1979). Reference spectra lacking the spin-labels were recorded at identical conditions, however, the spin-labeled compound was not replaced by unlabeled stearic acid or stearic acid methyl ester. To characterize the dimerization interface in aqueous solution, lyophilized, uniformly labeled ^{15}N-labeled NPY and [TOAC34]-NPY were dissolved to final concentrations of 0.25 and 0.75 mM, respectively, in 250 µl of 90% H_2O/10% ^2H_2O and the pH was adjusted to 3.1 with 0.1 M NaOH. The reference spectrum contained pure ^{15}N-labeled pNPY at a concentration of 1 mM. [^{15}N,^{1}H]-HSQC spectra were recorded as outlined above. Reductions in signal intensities due to close proximity to the spin-label were quantified by calculating the ratio of peak volumes in spectra from the sample containing the respective spin-labeled compound to peak volumes derived from the reference spectra (*vide supra*).

Relaxation data analysis

Relaxation rate constants R_1 and R_2 and NOE enhancements, which were calculated from the peak volumes in the [^{15}N,^{1}H]-HSQC spectra, were determined by fitting three-parameter single-exponential functions to the experimental data using the Levenberg-Marquardt algorithm (Press *et al.*, 1992). The uncertainties in the measured peak volumes were estimated by repeating the experiments at T=210 ms for R_1 and T=140 ms for R_2. Assuming that peak volumes are normally distributed and that the standard deviation is the same for all peaks in the duplicate measurements, the standard deviation of the differences can be divided by $2^{1/2}$ to yield the uncertainty in the peak volumes themselves. Uncertainties in the relaxation rates were then obtained from the covariance matrix of the non-linear fitting algorithm. For the NOE, uncertainties in the peak volumes were estimated by the standard deviation of the baseplane noise in the spectra. Uncertainties of the NOE values were obtained by propagating the uncertainties in the peak volumes (Nicholson *et al.*, 1992).

Interpretation of the relaxation parameters using the model-free approach (Lipari & Szabo, 1982a,b; Clore *et al.*, 1990) was performed using the Modelfree (version 4.01) software package (Palmer *et al.*, 1991b; Mandel *et al.*, 1995).

For membrane-bound NPY we could follow previously published protocols (Mandel *et al.*, 1995; Papavoine *et al.*, 1997). The initial overall rotational correlation time was estimated using the mean value of R_2/R_1, including only residues with an NOE>0.6, for which it is unlikely that fast internal motions make significant contributions to the R_1 and R_2 relaxation rates. Isotropic global diffusion was assumed and is justified by the work by Papavoine *et al.* (1997). Five combinations of one, two or three model-free parameters were tested to optimally describe the measured relaxation data in steps of increasing complexity, while keeping the initial estimate of the overall correlation time fix: (1) S^2; (2) S^2, τ_e; (3) S^2, R_{ex}; (4) S^2, τ_e, R_{ex}; and (5) S^2_f, S^2_s, τ_e. Since we had estimates for the experimental uncertainties in the relaxation parameters, we optimized the values of the model-free parameters by calculating the spectral density function as given for the selected model and predicting the expected relaxation parameters, and finally optimizing the sum-squared-error residual (SSE). An initial grid search of internal motional parameters was performed prior to SSE least squares fitting: S^2, S^2_s, and S^2_f were varied from 0 to 1 in steps of 0.05; τ_e from 0 to 2 ns in steps of 100 ps; and R_{ex} from 0 to 10 Hz in steps of 0.5 Hz.

The SSE for each spin is distributed as a χ^2-statistic with $m=k-l$ degrees of freedom, where k is the number of measured relaxation parameters and l is the number of fitted model-free parameters, only if assuming that the relaxation data have a normal distribution. Thus, in order to prove the statistical relevance of any selected model, the quality of the fit between the experimental data and the theoretical model was assessed by comparing the minimized SSE, after optimization of the model-free parameters, with the $\alpha=0.05$ critical value of the simulated distributions of the SSE for each spin. The simulation of the distributions was performed using the Monte Carlo procedure generating a 500 randomly distributed synthetic data sets (Palmer *et al.*, 1991b). A model was accepted, when the minimized SSE was contained in the 95% quantile of the simulated SSE, or was replaced by a more complex model, otherwise, where the parameters of the simpler model were a subset of the parameters of the second, more complex model (Mandel *et al.*, 1995). The minimized SSE of the simpler model M_1 was compared with the minimized SSE of the more complex model M_2 using an F-statistic with m_1 and m_2 degrees of freedom ($m_1<m_2$) (Mandel *et al.*, 1995). Since the distribution of this F-statistic is exactly the same as the theoretical F-distribution with m_1 and m_2 degrees of freedom, only if the relaxation data are normally distributed, the calculated F-statistic was compared with the 95% critical value of the F-statistic obtained from the simulated data. An improvement in the fit to

the more complicated model M_2 is significant, and not due to a random statistical reduction of the SSE, if the F-value is greater than the critical value.

Once the appropriate models had been chosen for each spin, the overall correlation time was optimized simultaneously with the motional parameters for all residues using Brent's univariate method (Press *et al.*, 1992). During the initial grid search for the rotational correlation time, τ_c was varied from 6 to 12 ns in steps of 0.5 ns. Uncertainties were estimated using 500 Monte Carlo simulations. Because the optimized value for the rotational correlation time remained very close to its initial estimate, we saw no need for doing a further round of model selection and optimization.

2.6. Acknowledgement

We gratefully acknowledge helpful discussions concerning molecular biology by Dr E. Weber and the group of Prof. G. Folkers. We thank Dr M.J.J. Blommers for general interest and helpful discussions and Dr P. Güntert for software support. G. Rytz recorded the CD spectra and Dr T. Khono has supplied us with the plasmids pUBK19 and pYUHK20b and had added helpful tips for the involved molecular biology. The pNPY DNA sequence was derived from a hNPY DNA construct kindly provided by Dr R. Kammerer. Fmoc-TOAC-OH was donated by Prof. C. Toniolo and Dr. F. Formaggio. The financial supports by the ETH Zürich (grant no. 0 20 439-97) and the Swiss National Foundation (grant no. 31-05081.97) are kindly acknowledged.

2.7. References

Allen, J., Novotny, J., Martin, J. & Heinrich, G. (1987). Molecular structure of mammalian neuropeptide Y: analysis by molecular cloning and computer-aided comparison with crystal structure of avian homologue. *Proc. Natl Acad. Sci. USA* **84**, 2532-2536.

Bartels, C., Xia, T.-h., Billeter, M., Güntert, P. & Wüthrich, K. (1995). The program XEASY for computer-supported spectral analysis of biological macromolecules. *J. Biomol. NMR* **6**, 1- 10.

Beck-Sickinger, A. G. & Jung, G. (1995). Structure-activity relationships of neuropeptide Y analogues with respect to Y_1 and Y_2 receptors. *Biopolymers* **37**, 123-142.

Beck-Sickinger, A. G., Wieland, H. A., Wittneben, H., Willim, K. D., Rudolf, K. & Jung, G. (1994). Complete L-alanine scan of neuropeptide Y reveals ligands binding to Y_1 and Y_2 receptors with distinguished conformations. *Eur. J. Biochem.* **225**, 947-958.

Blundell, T. L., Pitts, J. E., Tickle, I. J., Wood, S. P. & Wu, C.-W. (1981). X-ray analysis (1.4 Å resolution) of avian pancreatic polypeptide: Small globular protein hormone. *Proc. Natl Acad. Sci. USA* **78**, 4175-4179.

Cabrele, C. & Beck-Sickinger, A. G. (2000). Molecular characterisation of the ligand receptor interactions of the NPY/PP peptide family. *J. Peptide Sci.* **6**, 97-122.

Cabrele, C., Langer, M., Bader, R., Wieland, H. A., Doods, H. N., Zerbe, O. & Beck-Sickinger, A. G. The first selective agonist at the neuropeptide Y Y_5-receptor increases food intake in rats. *J. Biol. Chem.* **275**, 36043-36048.

Carpenter, K. A., Wilkes, B. C., De Lean, A., Fournier, A. & Schiller, P. W. (1997). Hydrophobic forces are responsible for the folding of a highly potent natriuretic peptide analogue at a membrane mimetic surface: an NMR study. *Biopolymers* **42**, 37-48.

Chang, P. J., Noelken, M. E. & Kimmel, J. R. (1980). Reversible dimerization of avian pancreatic polypeptide. *Biochemistry* **19**, 1844-1849.

Clore, G. M., Driscoll, P. C., Wingfield, P. T. & Gronenborn, A. M. (1990). Analysis of the backbone dynamics of interleukin-1 beta using two-dimensional inverse detected heteronuclear ^{15}N-^{1}H NMR spectroscopy. *Biochemistry* **29**, 7387-7401.

Cowley, D. J., Hoflack, J. M., Pelton, J. T. & Saudek, V. (1992). Structure of neuropeptide Y dimer in solution. *Eur. J. Biochem.* **205**, 1099-1106.

Daragan, V. A. & Mayo, K. H. (1997). Motional model analysis of protein and peptide dynamics using ^{13}C and ^{15}N NMR relaxation. *Prog. Nucl. Magn. Reson. Spectrosc.* **31**, 63-105.

Darbon, H., Bernassau, J. M., Deleuze, C., Chenu, J., Roussel, A. & Cambillau, C. (1992). Solution conformation of human neuropeptide Y by ^{1}H nuclear magnetic resonance and restrained molecular dynamics. *Eur. J. Biochem.* **209**, 765-771.

Dayie, K. T. & Wagner, G. (1994). Relaxation rate measurements for ^{15}N-^{1}H groups with pulsed-field gradients and preservation of coherence pathways. *J. Magn. Reson. A* **111**, 121-126.

Dumont, Y., Martel, J. C., Fournier, A., St-Pierre, S. & Quirion, R. (1992). Neuropeptide Y and neuropeptide Y receptor subtypes in brain and peripheral tissues. *Prog. Neurobiol.* **38**, 125-167.

Fabry, M., Langer, M., Rothen-Rutishauser, B., Wunderli-Allenspach, H., Höcker, H. & Beck-Sickinger, A. G. (2000). Monitoring of the Internalization of Neuropeptide Y on Neuroblastoma Cell Line SK-N-MC. *Eur. J. Biochem.* **267,** 5631-5637.

Fuhlendorff, J., Gether, U., Aakerlund, L., Langeland-Johansen, N., Thogersen, H., Melberg, S. G., Olsen, U. B., Thastrup, O. & Schwartz, T. W. (1990). [Leu31, Pro34]neuropeptide Y: a specific Y_1 receptor agonist. *Proc. Natl Acad. Sci. USA* **87**, 182-186.

Grandt, D., Feth, F., Rascher, W., Reeve, J. R., Jr., Schlicker, E., Schimiczek, M., Layer, P., Goebell, H., Eysselein, V. E. & Michel, M. C. (1994). [Pro34]peptide YY is a Y_1-selective agonist at peptide YY/neuropeptide Y receptors. *Eur. J. Pharmacol.* **269**, 127-132.

Gray, T. S. & Morley, J. E. (1986). Neuropeptide Y: anatomical distribution and possible function in mammalian nervous system. *Life Sci.* **38**, 389-401.

Griesinger, C., Soerensen, O. W. & Ernst, R. R. (1987). Practical aspects of the E.COSY technique. Measurement of scalar spin-spin coupling constants in peptides. *J. Magn. Reson.* **75**, 474-492.

Griesinger, C., Otting, G., Wüthrich, K. & Ernst, R. R. (1988). Clean TOCSY for ^{1}H spin system identification in macromolecules. *J. Am. Chem. Soc.* **110**, 7870-7872.

Gronenborn, A. M., Bax, A., Wingfield, P. T. & Clore, G. M. (1989). A powerful method of sequential proton resonance assignment in proteins using relayed $^{15}N,^{1}H$ multiple quantum coherence spectroscopy. *FEBS Lett.* **243**, 93-98.

Grundemar, L. & Hakanson, R. (1993). Multiple neuropeptide Y receptors are involved in cardiovascular regulation. Peripheral and central mechanisms. *Gen. Pharmacol.* **24**, 785-796.

Grzesiek, S. & Bax, A. (1993). The importance of not saturating H_2O in protein NMR. application to sensitivity enhancement and NOE measurements. *J. Am. Chem. Soc.* **115**, 12593-12594.

Güntert, P., Braun, W., Billeter, M. & Wüthrich, K. (1989). Automated stereospecific ^{1}H NMR assignments and their impact on the precision of protein structure determinations in solution. *J. Am. Chem. Soc.* **111**, 3997-4004.

Güntert, P., Mumenthaler, C. & Wüthrich, K. (1997). Torsion angle dynamics for NMR structure calculation with the new program DYANA. *J. Mol. Biol.* **273**, 283-298.

Henry, G. D. & Sykes, B. D. (1994). Methods to study membrane protein structure in solution. *Methods Enzymol.* **239**, 515-535.

Hoffmann, S., Rist, B., Videnov, G., Jung, G. & Beck-Sickinger, A. G. (1996). Structure-affinity studies of C-terminally modified analogs of neuropeptide Y led to a novel class of peptidic Y_1 receptor antagonist. *Regul. Pept.* **65**, 61-70.

Inui, A. (1999). Neuropeptide Y feeding receptors: are multiple subtypes involved? *Trends Pharmacol. Sci.* **20**, 43-46.

Jarvet, J., Zdunek, J., Damberg, P. & Gräslund, A. (1997). Three-dimensional structure and position of porcine motilin in sodium dodecyl sulfate micelles determined by ^{1}H NMR. *Biochemistry* **36**, 8153-8163.

Jung, G., Beck-Sickinger, A. G., Dürr, H., Gaida, W. & Schnorrenberg, G. (1991). α-helical, small molecular size analogues of neuropeptide Y: Structure-activity-relationships. *Biopolymers* **31**, 613-619.

Kay, L. E., Torchia, D. A. & Bax, A. (1989). Backbone dynamics of proteins as studied by ^{15}N inverse detected heteronuclear NMR spectroscopy: application to staphylococcal nuclease. *Biochemistry* **28**, 8972-8979.

Kay, L. E., Keifer, P. & Saarinen, T. (1992a). Pure absorption gradient enhanced heteronuclear single-quantum correlation spectroscopy with improved sensitivity. *J. Am. Chem. Soc.* **114**, 10663-10665.

Kay, L. E., Nicholson, L. K., Delaglio, F., Bax, A. & Torchia, D. A. (1992b). Pulse sequences for removal of the effects of cross correlation between dipolar and chemical-shift anisotropy relaxation mechanisms on the measurement of heteronuclear T_1 and T_2 values in proteins. *J. Magn. Reson.* **97**, 359-375.

Khiat, A., Labelle, M. & Boulanger, Y. (1998). Three-dimensional structure of the Y_1 receptor agonist [Leu31, Pro34]NPY as determined by NMR and molecular modeling. *J. Pept. Res.* **51**, 317-322.

Kirby, D. A., Boublik, J. H. & Rivier, J. E. (1993). Neuropeptide Y: Y_1 and Y_2 affinities of the complete series of analogues with single D-residue substitutions. *J. Med. Chem.* **36**, 3802-3808.

Kohno, T., Kusunoki, H., Sato, K. & Wakamatsu, K. (1998). A new general method for the biosynthesis of stable isotope-enriched peptides using a decahistidine-tagged ubiquitin fusion system: an application to the production of mastoparan-X uniformly enriched with ^{15}N and $^{15}N/^{13}C$. *J. Biomol. NMR* **12**, 109-121.

Koradi, R., Billeter, M. & Wüthrich, K. (1996). MOLMOL: a program for display and analysis of macromolecular structures. *J. Mol. Graph.* **14**, 51-55.

Kumar, A., Ernst, R. R. & Wüthrich, K. (1980). A two-dimensional nuclear Overhauser enhancement (2D NOE) experiment for the elucidation of complete proton-proton cross-relaxation networks in biological macromolecules. *Biochem. Biophys. Res. Comm.* **95**, 1-6.

Kuntz, I. D., Kosen, P. A. & Craig, E. C. (1991). Amide chemical shifts in many helices in peptides and proteins are periodic. *J. Am. Chem. Soc.* **113**, 1406-1408.

Larhammar, D. (1996a). Evolution of neuropeptide Y, peptide YY and pancreatic polypeptide. *Regul. Pept.* **62**(1), 1-11.

Larhammar, D. (1996b). Structural diversity of receptors for neuropeptide Y, peptide YY and pancreatic polypeptide. *Regul. Pept.* **65**, 165-174.

Laskowski, R. A., Rullmannn, J. A., MacArthur, M. W., Kaptein, R. & Thornton, J. M. (1996). AQUA and PROCHECK-NMR: programs for checking the quality of protein structures solved by NMR. *J. Biomol. NMR* **8**, 477-486.

Lauterwein, J., Bösch, C., Brown, L. R. & Wüthrich, K. (1979). Physicochemical studies of the protein-lipid interactions in melittin-containing micelles. *Biochim. Biophys. Acta* **556**, 244-264.

Levitt, M. H., Freeman, R. & Frenkiel, T. (1982). Broadband heteronuclear decoupling. *J. Magn. Reson.* **47**, 328-330.

Lipari, G. & Szabo, A. (1982a). Model-free approach to the interpretation of nuclear magnetic resonance relaxation in macromolecules. 1. Theory and range of validity. *J. Am. Chem. Soc.* **104**, 4546-4559.

Lipari, G. & Szabo, A. (1982b). Model-free approach to the interpretation of nuclear magnetic resonance relaxation in macromolecules. 2. Analysis of experimental results. *J. Am. Chem. Soc.* **104**, 4559-4570.

Live, D. H., Davis, D. G., Agosta, W. C. & Cowburn, D. (1984). Observation of 1000-fold enhancement of ^{15}N NMR via proton-detected multiple-quantum coherences: Studies of large peptides. *J. Am. Chem. Soc.* **106**, 6104-6105.

Luginbühl, P., Güntert, P., Billeter, M., Wüthrich, K. (1996). The new program OPAL for molecular dynamics simulations and energy refinements of biological macromolecules. *J. Biomol. NMR* **8**, 136-146.

Macura, S. & Ernst, R. R. (1980). Elucidation of cross-relaxation in liquids by two-dimensional NMR spectroscopy. *Mol. Phys.* **41**, 95-117.

Mandel, A. M., Akke, M. & Palmer, A. G., 3rd. (1995). Backbone dynamics of *Escherichia coli* ribonuclease HI: correlations with structure and function in an active enzyme. *J. Mol. Biol.* **246**, 144-163.

Marion, D., Ikura, M. & Bax, A. (1989). Improved solvent suppression in one- and two-dimensional NMR spectra by convolution of time-domain data. *J. Magn. Reson.* **84**, 425- 430.

McCrea, K., Wisialowski, T., Cabrele, C., Church, B., Beck-Sickinger, A. G., Kraegen, E. & Herzog, H. (2000). 2-36[K^4,RYYSA$^{19-23}$]PP a novel Y_5-receptor preferring ligand with strong stimulatory effect on food intake. *Regul. Pept.* **87**, 47-58.

McDonnell, P. A. & Opella, S. J. (1993). Effect of detergent concentration on multidimensional solution NMR spectra of membrane proteins in micelles. *J. Magn. Reson. B* **102**, 120-125.

Meiboom, S. & Gill, D. (1958). Modified spin-echo method for measuring nuclear spin relaxation rates. *Rev. Sci. Instrum.* **29**, 688-691.

Messerle, B. A., Wider, G., Otting, G., Weber, C. & Wüthrich, K. (1989). Solvent suppression using a spin lock in 2D and 3D NMR spetroscopy with H_2O Solutions. *J. Magn. Reson.* **85**, 608-613.

Michel, M. C., Beck-Sickinger, A., Cox, H., Doods, H. N., Herzog, H., Larhammar, D., Quirion, R., Schwartz, T. & Westfall, T. (1998). XVI. International Union of Pharmacology recommendations for the nomenclature of neuropeptide Y, peptide YY, and pancreatic polypeptide receptors. *Pharmacol. Rev.* **50**, 143-150.

Minakata, H., Taylor, J. W., Walker, M. W., Miller, R. J. & Kaiser, E. T. (1989). Characterization of amphiphilic secondary structures in neuropeptide Y through the design, synthesis, and study of model peptides. *J. Biol. Chem.* **264**, 7907-7913.

Monks, S. A., Karagianis, G., Howlett, G. J. & Norton, R. S. (1996). Solution structure of human neuropeptide Y. *J. Biomol. NMR* **8**, 379-390.

Moroder, L. (1997). On the mechanism of hormone recognition and binding by the CCK-B/gastrin receptor. *J. Pept. Sci.* **3**, 1-14.

Moroder, L., Romano, R., Guba, W., Mierke, D. F., Kessler, H., Delporte, C., Winand, J. & Christophe, J. (1993). New evidence for a membrane-bound pathway in hormone receptor binding. *Biochemistry* **32**, 13551-13559.

Nagayama, K. & Wüthrich, K. (1981). Structural interpretation of vicinal proton-proton coupling constants $^3J_{H\alpha H\beta}$ in the basic pancreatic trypsin inhibitor measured by two-dimensional *J*-resolved NMR spectroscopy. *Eur. J. Biochem.* **115**, 653-657.

Nicholson, L. K., Kay, L. E., Baldisseri, D. M., Arango, J., Young, P. E., Bax, A. & Torchia, D. A. (1992). Dynamics of methyl groups in proteins as studied by proton-detected ^{13}C NMR spectroscopy. Application to the leucine residues of staphylococcal nuclease. *Biochemistry* **31**, 5253-5263.

Noggle, J. H. & Schirmer, R. E. (1971). *The nuclear Overhauser Effect: Chemical Applications*, Academic Press, New York.

Nordmann, A., Blommers, M. J., Fretz, H., Arvinte, T. & Drake, A. F. (1999). Aspects of the molecular structure and dynamics of neuropeptide Y. *Eur. J. Biochem.* **261**, 216-226.

Orekhov, V. Y., Korzhnev, D. M., Diercks, T., Kessler, H. & Arseniev, A. S. (1999). ^1H-^{15}N NMR dynamic study of an isolated α-helical peptide (1-36)-bacteriorhodopsin reveals the equilibrium helix-coil transitions. *J. Biomol. NMR* **14**, 345-356.

Otting, G. (1990). Zero-quantum suppression in NOESY and experiments with a z-filter. *J. Magn. Reson.* **86**, 496-508.

Palmer, A. G., Cavanagh, J., Wright, P. E. & Rance, M. (1991a). Sensitivity improvement in proton-detected two-dimensional heteronuclear correlation NMR spectroscopy. *J. Magn. Reson.* **93**, 151-170.

Palmer, A. G., Rance, M. & Wright, P. E. (1991b). Intermolecular motion of a zinc finger DNA-binding domain from xfin characterized by proton-detected natural abundance ^{13}C heteronuclear NMR spectroscopy. *J. Am. Chem. Soc.* **113**, 4371-4380.

Papavoine, C. H., Konings, R. N., Hilbers, C. W. & van de Ven, F. J. (1994). Location of M13 coat protein in sodium dodecyl sulfate micelles as determined by NMR. *Biochemistry* **33**, 12990-12997.

Papavoine, C. H., Remerowski, M. L., Horstink, L. M., Konings, R. N., Hilbers, C. W. & van de Ven, F. J. (1997). Backbone dynamics of the major coat protein of bacteriophage M13 in detergent micelles by ^{15}N nuclear magnetic resonance relaxation measurements using the model-free approach and reduced spectral density mapping. *Biochemistry* **36**, 4015-4026.

Pellegrini, M. & Mierke, D. F. (1999). Molecular complex of cholecystokinin-8 and N-terminus of the cholecystokinin A receptor by NMR spectroscopy. *Biochemistry* **38**, 14775-14783.

Pfuhl, M., Chen, H. A., Kristensen, S. M. & Driscoll, P. C. (1999). NMR exchange broadening arising from specific low affinity protein self-association: analysis of nitrogen-15 nuclear relaxation for rat CD2 domain 1. *J. Biomol. NMR* **14**, 307-320.

Piotto, M., Saudek, V. & Sklenar, V. (1992). Gradient-tailored excitation for single-quantum NMR spectroscopy of aqueous solutions. *J. Biomol. NMR* **2**, 661-665.

Press, W. H., Teukolsky, S. A., Vetterling, W. T. & Flannery, B. P. (1992). *Numerical Recipes. The art of scientific computing, 2nd ed.*, Cambridge University Press, Cambridge.

Rance, M., Sørensen, O. W., Bodenhausen, G., Wagner, G., Ernst, R. R. & Wüthrich, K. (1983). Improved spectral resolution in COSY ^{1}H spectra of proteins via double-quantum filtering. *Biochem. Biophys. Res. Commun.* **117**, 479-485.

Sargent, D. F., Bean, J. W. & Schwyzer, R. (1988). Conformation and orientation of regulatory peptides on lipid membranes. Key to the molecular mechanism of receptor selection. *Biophys. Chem.* **31**, 183-193.

Saudek, V. & Pelton, J. T. (1990). Sequence-specific ^{1}H NMR assignment and secondary structure of neuropeptide Y in aqueous solution. *Biochemistry* **29**, 4509-4515.

Schoch, P. & Sargent, D. F. (1980). Quantitative analysis of the binding of melittin to planar lipid bilayers allowing for the discrete-charge effect. *Biochim. Biophys. Acta* **602**, 234-247.

Schurr, J. M., Babcock, H. P. & Fujimoto, B. S. (1994). A test of the model-free formulas. Effects of anisotropic rotational diffusion and dimerization. *J. Magn. Reson. B* **105**, 211-224.

Schwyzer, R. (1986). Molecular mechanism of opioid receptor selection. *Biochemistry* **25**, 6335-6342.

Schwyzer, R. (1991). Peptide-membrane interactions and a new principle in quantitative structure-activity relationships. *Biopolymers* **31**, 785-792.

Schwyzer, R. (1995a). 100 years lock-and-key concept: are peptide keys shaped and guided to their receptors by the target cell membrane? *Biopolymers* **37**, 5-16.

Schwyzer, R. (1995b). In search of the 'bio-active conformation'--is it induced by the target cell membrane? *J. Mol. Recognit.* **8**, 3-8.

Shao, H., Jao, S., Ma, K. & Zagorski, M. G. (1999). Solution structures of micelle-bound amyloid β-(1-40) and β-(1-42) peptides of Alzheimer's disease. *J. Mol. Biol.* **285**, 755-773.

Sklenar, V., Torchia, D. & Bax, A. (1987). Measurement of carbon-13 longitudinal relaxation using ^{1}H detection. *J. Magn. Reson.* **73**, 375-379.

Stanley, B. G. & Leibowitz, S. F. (1985). Neuropeptide Y injected in the paraventricular hypothalamus: a powerful stimulant of feeding behavior. *Proc. Natl Acad. Sci. USA* **82**, 3940-3943.

Swairjo, M. A., Concha, N. O., Kaetzel, M. A., Dedman, J. R. & Seaton, B. A. (1995). Ca^{2+}-bridging mechanism and phospholipid head group recognition in the membrane-binding protein annexin V. *Nat. Struct. Biol.* **2**, 968-974.

Szyperski, T., Güntert, P., Otting, G. & Wüthrich, K. (1992). Determination of scalar coupling constants by inverse Fourier transfomation of in-phase multiplets. *J. Magn. Reson.* **99**, 552-560.

Tatemoto, K., Carlquist, M. & Mutt, V. (1982). Neuropeptide Y--a novel brain peptide with structural similarities to peptide YY and pancreatic polypeptide. *Nature* **296**, 659-660.

Vold, R. L., Waugh, J. S., Klein, M. P. & Phelps, D. E. (1968). Measurement of spin-relaxation rates in complex systems. *J. Chem. Phys.* **48**, 3831-3832.

Wagner, G. & Wüthrich, K. (1982). Amide proton exchange rates and surface conformation of the basic pancreatic inhibitor in solution. *J. Mol. Biol.* **160**, 343-361.

Weiner, P. K., Kollman, P. A., Nguyen, D. T. & Case, D. A. (1986). An all-atom force field for simulations of proteins and nucleic acids. *J. Comput. Chem.* **7**, 230-252.

Wieland, H. A., Willim, K. & Doods, H. N. (1995). Receptor binding profiles of NPY analogues and fragments in different tissues and cell lines. *Peptides* **16**, 1389-1394.

Wimley, W. C. & White, S. H. (1996). Experimentally determined hydrophobicity scale for proteins at membrane interfaces. *Nat. Struct. Biol.* **3**, 842-848.

Wraith, A., Törnsten, A., Chardon, P., Harbitz, I., Chowdhary, B. P., Andersson, L., Lundin, L. G. & Larhammar, D. (2000). Evolution of the neuropeptide Y receptor family: Gene and chromosome duplications deduced from the cloning and mapping of the five receptor subtype genes in pig. *Genome Res.* **10**, 302-310.

Wüthrich, K. (1986). *NMR of Proteins and Nucleic Acids*, Wiley, New York.

Zhou, N. E., Zhu, B.-Y., Sykes, B. D. & Hodges, R. S. (1992). Relationship between amide proton chemical shifts and hydrogen bonding in amphipathic alpha-helical peptides. *J. Am. Chem. Soc.* **114**, 4320-4326.

Zimm, B. H. & Bragg, J. K. (1959). Theory of the phase transition between helix and random coil in polypeptide chains. *J. Chem. Phys.* **31**, 526-535.

2.8. Supplementary Materials

Table S1

Chemical shifts for porcine NPY on DPC micelles[a]

Residue	N	H^N	H^α	H^β	others
Tyr 1	-	-	4.51	3.04, 3.21	δH 7.21, 7.21; εH 6.89, 6.89
Pro 2	-		4.32	1.93, 2.07	γCH_2 1.97, 1.97; δCH_2 3.32, 3.70
Ser 3	117.1	8.32	4.45	3.88, 4.03	
Lys 4	124.0	8.22	4.66	1.70, 1.87	γCH_2 1.47, 1.47; δCH_2 1.71, 1.71; εCH_2 3.00, 3.00
Pro 5	-		4.43	1.93, 2.29	γCH_2 2.02, 2.02; δCH_2 3.66, 3.79
Asp 6	120.3	8.32	4.52	2.60, 2.64	
Asn 7[b]	119.1	8.17	5.00	2.66, 2.81	δNH_2 6.86, 7.60
Pro 8	-		4.42	1.93, 2.26	γCH_2 2.01, 2.01; δCH_2 3.65, 3.74
Gly 9	109.3	8.34	3.95, 3.95		
Glu 10	120.9	8.03	4.15	1.92, 2.07	γCH_2 2.24, 2.24
Asp 11	121.8	8.32	4.60	2.59, 2.68	
Ala 12	125.7	8.12	4.60	1.36	
Pro 13	-		4.43	1.93, 2.29	γCH_2 2.02, 2.02; δCH_2 3.66, 3.77
Ala 14	124.0	8.37	4.26	1.43	
Glu 15	120.2	8.31	4.26	2.03, 2.10	γCH_2 2.30, 2.30
Asp 16	121.6	8.19	4.46	2.63, 2.69	
Leu 17	120.8	8.38	4.18	1.80, 1.84	γH 1.65; δCH_3 0.94, 1.00
Ala 18	121.1	8.05	4.05	1.54	
Arg 19	119.7	7.95	4.12	1.76, 1.86	γCH_2 1.46, 1.50; δCH_2 3.12, 3.15; εNH 7.33
Tyr 20	120.5	8.01	4.45	3.10, 3.15	δH 7.04, 7.04; εH 6.80, 6.80
Tyr 21	120.0	8.39	4.32	3.19, 3.19	δH 7.07, 7.07; εH 6.78, 6.78
Ser 22	114.5	8.33	4.03	3.98, 3.98	
Ala 23	125.0	7.84	4.25	1.66	
Leu 24	119.1	8.22	4.18	1.88, 1.88	γH 1.82; δCH_3 0.99, 1.01
Arg 25	118.2	8.30	3.79	1.73, 1.86	γCH_2 1.46, 1.59; δCH_2 3.08, 3.08; εNH 7.41
His 26	118.7	7.94	4.34	3.18, 3.30	δ^2H 6.42; ε^1H 8.42
Tyr 27	118.7	8.19	4.18	3.06, 3.06	δH 7.13, 7.13; εH 6.86, 6.86
Ile 28	119.4	8.56	3.75	2.02	γCH_2 1.25, 1.79; γCH_3 0.94; δCH_3 0.85
Asn 29	120.6	8.14	4.44	2.78, 2.94	δNH_2 6.89, 7.56
Leu 30	120.1	7.77	4.03	1.80, 1.80	γH 1.62; δCH_3 0.84, 0.84
Ile 31	117.6	8.02	3.93	2.03	γCH_2 1.29, 1.74; γCH_3 0.95; δCH_3 0.86
Thr 32	111.7	8.07	4.18	4.41	γCH_3 1.33
Arg 33	121.2	7.93	4.18	1.95, 1.73[c]	γCH_2 1.61, 1.61; δCH_2 3.18, 3.18; εNH 7.26
Gln 34	117.4	7.98	4.16	2.12, 2.12	γCH_2 2.38, 2.38; εNH_2 6.78, 7.42
Arg 35	118.9	7.92	4.17	1.65, 1.65	γCH_2 1.39, 1.47; δCH_2 3.08, 3.08; εNH 7.38
Tyr 36	119.1	7.93	4.57	2.85, 3.16	δH 7.14, 7.14; εH 6.81, 6.81
NH_2	107.4	7.03, 7.30			

[a] 3mM in 300mM DPC/90% H_2O/10% ^2H_2O at 37°C and pH 6.0. Chemical shifts are referenced to the water frequency at 37°C (4.63 ppm). ^{15}N chemical shifts are referenced to liquid $^{15}NH_3$ via the proton chemical shift scale.

[b] Chemical shifts are given for Pro8 in trans conformation.

[c] Stereospecifically assigned resonances. For the CβH resonances, the first chemical shift is for $H\beta^2$ (pro-*R*), and the second for $H\beta^3$ (pro-*S*) (IUPAC-IUB, 1970).

Table S2

Chemical shifts for porcine NPY in aqueous solution[a]

Residue	N	H^N
Tyr 1	-	-
Pro 2	-	
Ser 3[b]	116.8	8.37
Lys 4[b]	124.1	8.26
Pro 5	-	
Asp 6[b]	119.9	8.41
Asn 7[b]	120.1	8.26
Pro 8	-	
Gly 9[b]	108.3	8.26
Glu 10	119.0	8.03
Asp 11	119.4	8.34
Ala 12	124.7	7.87
Pro 13	-	
Ala 14	123.5	8.33
Glu 15	118.1	8.43
Asp 16	119.8	8.05
Leu 17	122.4	8.01
Ala 18	121.4	8.06
Arg 19	118.0	7.82
Tyr 20	120.5	7.84
Tyr 21	119.0	8.24
Ser 22	115.4	8.05
Ala 23	125.0	8.01
Leu 24	119.8	8.07
Arg 25	118.6	7.90
His 26	117.3	8.03
Tyr 27	120.6	8.12
Ile 28	120.7	8.15
Asn 29	121.0	8.16
Leu 30	121.8	7.93
Ile 31	119.1	7.96
Thr 32	116.0	7.93
Arg 33	122.0	7.98
Gln 34	120.3	8.12
Arg 35	121.3	8.14
Tyr 36	120.8	8.02
NH_2	108.2	7.03, 7.42

[a] 1mM in 90% H_2O/10% ^2H_2O at 32°C and pH 3.1. Chemical shifts are referenced to the water frequency at 32 °C (4.68 ppm). ^{15}N chemical shifts are referenced to liquid $^{15}NH_3$ via the proton chemical shift scale.

[b] Splitting of peaks due to cis-trans isomerisms of the proline residues. Chemical shifts are given for the major forms.

Table S3

^{15}N relaxation parameters for porcine NPY on DPC micelles[a]

Magnetic field	500 MHz						600 MHz			
Residue	R_1 [Hz]	$\sigma(R_1)$	R_2 [Hz]	$\sigma(R_2)$	NOE	σ_{NOE}	R_1 [Hz]	$\sigma(R_1)$	R_2 [Hz]	$\sigma(R_2)$
Asp 6	1.26	0.04	2.17	0.23	-3.29	0.33	1.39	0.21	1.84	0.88
Asn 7	1.29	0.03	1.76	0.20	-2.21	0.22	1.40	0.17	1.95	0.83
Gly 9	1.36	0.03	2.06	0.15	-1.39	0.14	1.50	0.19	2.35	0.68
Glu 10	1.36	0.03	2.63	0.11	-0.85	0.08	1.36	0.13	2.69	0.69
Asp 11	1.32	0.02	2.34	0.13	-0.76	0.08	1.38	0.11	2.64	0.46
Ala 12	1.26	0.02	2.68	0.09	-0.68	0.07	1.35	0.09	3.14	0.35
Ala 14	1.46	0.03	4.33	0.13	-0.33	0.03	1.41	0.14	5.41	0.47
Glu 15	1.51	0.02	4.63	0.11	0.08	0.01	1.62	0.21	4.18	0.79
Asp 16	1.63	0.05	6.29	0.20	0.34	0.03	1.65	0.24	7.58	0.57
Leu 17	1.59	0.05	8.26	0.34	0.56	0.06	1.50	0.24	9.17	1.43
Ala 18	1.57	0.04	10.42	0.76	0.73	0.07	1.47	0.24	9.80	1.35
Arg 19	1.59	0.06	10.20	0.31	0.71	0.07	1.57	0.25	11.76	1.52
Tyr 20	1.62	0.06	12.35	0.76	0.61	0.06	1.46	0.25	13.33	1.60
Tyr 21	1.44	0.06	11.36	0.77	0.70	0.07	1.35	0.28	10.64	2.15
Ser 22	1.56	0.04	11.36	0.77	0.69	0.07	1.40	0.31	12.82	1.97
Ala 23	1.64	0.06	9.80	0.67	0.74	0.07	1.51	0.24	12.35	1.52
Leu 24	1.48	0.06	11.76	0.83	0.70	0.07	1.30	0.33	11.24	1.64
Arg 25	1.53	0.06	10.53	0.78	0.83	0.08	1.42	0.38	12.35	4.57
His 26	1.65	0.09	9.26	0.43	0.74	0.07	1.62	0.37	10.64	1.81
Tyr 27	1.61	0.07	9.80	0.77	0.70	0.07	1.31	0.36	13.16	2.08
Ile 28	1.65	0.07	11.36	0.77	0.76	0.08	1.51	0.29	11.36	1.81
Asn 29	1.63	0.06	11.76	0.83	0.67	0.07	1.45	0.32	13.51	1.83
Leu 30	1.56	0.04	10.20	0.73	0.67	0.07	1.36	0.25	9.71	1.60
Ile 31	1.45	0.09	9.90	0.69	0.60	0.06	1.40	0.27	10.31	1.49
Thr 32	1.62	0.12	10.75	0.92	0.67	0.07	1.26	0.55	11.76	1.80
Arg 33	1.69	0.06	9.43	0.36	0.65	0.06	1.51	0.24	11.36	1.68
Gln 34	1.96	0.07	8.85	0.31	0.57	0.06	1.59	0.27	9.35	1.31
Arg 35	1.82	0.06	6.90	0.24	0.44	0.04	1.63	0.23	6.29	1.50
Tyr 36	1.63	0.05	6.62	0.18	0.39	0.04	1.72	0.17	7.19	0.52

[a] 1mM in 300mM DPC/90% H_2O/10% ^2H_2O at 37°C and pH 6.0. No results are available for the N-terminal residues Ser 3 and Lys 4 because of fast H^N exchange.

Table S4

^{15}N relaxation parameters for porcine NPY in aqueous solution[a]

Magnetic field	500 MHz						600 MHz	
Residue	R_1 [Hz]	$\sigma(R_1)$	R_2 [Hz]	$\sigma(R_2)$	NOE	σ_{NOE}	R_2 [Hz]	$\sigma(R_2)$
Ser 3	1.02	0.02	1.20	0.03	-1.70	0.06	1.21	0.07
Lys 4	1.26	0.03	1.89	0.04	-1.03	0.05	2.22	0.13
Asp 6	1.38	0.03	1.80	0.03	-0.80	0.05	2.04	0.10
Asn 7	1.40	0.04	3.02	0.06	-0.67	0.05	3.30	0.20
Gly 9	1.57	0.03	1.93	0.04	-0.43	0.05	2.12	0.11
Glu 10	1.56	0.03	2.13	0.03	-0.33	0.05	2.41	0.11
Asp 11	1.56	0.04	2.91	0.06	-0.39	0.05	3.77	0.26
Ala 12	1.60	0.06	2.27	0.05	-0.24	0.05	1.78	0.17
Ala 14	1.84	0.07	6.41	0.16	0.07	0.05	7.63	0.64
Glu 15	1.81	0.06	3.91	0.11	0.04	0.05	3.91	0.38
Asp 16	1.98	0.05	3.13	0.06	0.15	0.05	3.10	0.20
Leu 17	2.26	0.07	6.99	0.15	0.13	0.05	10.75	0.92
Ala 18	2.06	0.07	5.75	0.13	0.17	0.05	6.10	0.41
Arg 19	2.44	0.08	5.18	0.11	0.21	0.05	4.52	0.29
Tyr 20	2.13	0.07	5.21	0.11	0.20	0.05	5.52	0.49
Tyr 21	1.81	0.09	5.56	0.22	0.39	0.05	8.62	0.74
Ser 22	2.06	0.08	7.41	0.16	0.25	0.05	7.75	0.60
Ala 23	2.04	0.07	4.88	0.12	0.25	0.05	4.95	0.39
Leu 24	2.04	0.08	9.26	0.26	0.23	0.05	10.53	0.89
Arg 25	2.07	0.07	5.71	0.13	0.18	0.05	6.02	0.51
His 26	1.99	0.07	5.24	0.11	0.22	0.05	5.81	0.37
Tyr 27	1.80	0.05	9.80	0.29	0.03	0.05	14.29	1.02
Ile 28	1.56	0.09	10.20	0.42	-0.02	0.05		
Asn 29	2.05	0.07	6.54	0.13	0.10	0.05	7.94	0.76
Leu 30	1.79	0.10	7.75	0.42	0.03	0.05		
Ile 31	1.90	0.13	8.77	0.23	-0.03	0.05		
Thr 32	1.94	0.13	22.22	0.99	-0.06	0.05	37.04	16.46
Arg 33	1.82	0.07	4.85	0.14	-0.21	0.05	5.29	0.59
Gln 34	1.59	0.05	4.48	0.08	-0.60	0.05	4.98	0.32
Arg 35	1.47	0.03	3.02	0.05	-0.79	0.05	3.42	0.15
Tyr 36	1.24	0.03	1.84	0.03	-0.99	0.05	2.43	0.10

[a] 1mM in 90% H_2O/10% ^2H_2O at 32°C and pH 3.1. A minimal uncertainty of 0.05 was assumed for the NOE data at 500 MHz. The signals of Ile28, Leu30, and Ile31 in the spectra obtained at 600 MHz were too weak to be properly integrated.

Table S5

Statistical information for the micelle-bound pNPY structure calculation

Distance restraints	Total	344
	Intra-residual	105
	Inter-residual	239
	Sequential (i - j = 1)	92
	Medium (i - j = 2, 3, 4)	147
RMSD[a] (Å)	Glu15-Tyr36 backbone[b]	0.67 ± 0.30
	Glu15-Tyr36 all heavy atoms	1.84 ± 0.39
	Tyr21-Ile31 backbone	0.23 ± 0.18
	Tyr21-Ile31 all heavy atoms	0.85 ± 0.23
Structure check[c] (Average %)	Glu15-Tyr36	91.3
	Tyr1-Tyr36	72.2
NOE constraint violations	Number ≥ 0.1 Å	0.41 ± 0.60
	Maximum (Å)	0.11 ± 0.01
Dihedral angle constraint violations	Number ≥ 2.5 degrees	0.18 ± 0.38
	Maximum	1.70 ± 0.77
AMBER energies (kcal/mol)[d]	Total	-1583 ± 158
	Van der Waals	139 ± 33
	Electrostatic	-1692 ± 137

[a] Atomic root mean square deviation calculated by superimposing the corresponding region of the 17 minimized structures referenced by the mean coordinates.

[b] N, Cα, C′ atoms.

[c] Percentage of the ϕ, φ angles falling within the allowed Ramachandran regions for the 17 refined structures.

[d] AMBER energies are given as the sum of solute-solute and solute-water interactions. Energies of water-water interactions are neglected.

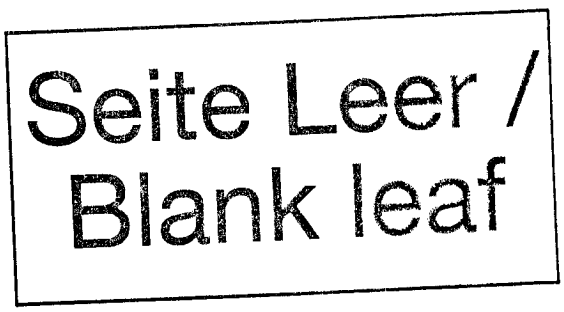
Seite Leer /
Blank leaf

Chapter 3

The First Selective Agonist for the Neuropeptide YY_5 Receptor Increases Food Intake in Rats[1]

The first Y_5 receptor-selective analog of neuropeptide Y (NPY), [Ala^{31},Aib^{32}]NPY, has been developed and biologically characterized. Using competition binding assays on cell lines that express different Y receptors, we determined the affinity of this analog to be 6 nM at the human Y_5 receptor, >500 nM at the Y_1 and Y_2 receptors, and >1000 nM at the Y_4 receptor. Activity studies performed *in vitro* using a cAMP enzyme immunoassay, and *in vivo* using food intake studies in rats, showed that the peptide acted as an agonist. Further peptides obtained by the combination of the Ala^{31}-Aib^{32} motif with chimeric peptides containing segments of NPY and pancreatic polypeptide displayed the same selectivity and even higher affinity (up to 0.2 nM) for the Y_5 receptor. *In vivo* administration of the new Y_5 receptor-selective agonists significantly stimulated feeding in rats. The NMR solution structures of NPY and [Ala^{31},Aib^{32}]NPY showed a different conformation in the C-terminal region, where the α-helix of NPY was substituted by a more flexible, 3_{10}-helical turn structure.

[1]published in: Cabrele, C., Langer, M., Bader, R., Wieland, H.A., Doods, H.N., Zerbe, O. & Beck-Sickinger A. G. (2000). *J. Biol. Chem.*, **275**, 36043-36048.

3.1. Introduction

Neuropeptide Y (NPY), a 36-residue peptide amide, is a member of the pancreatic polypeptide (PP) hormone family that also includes PP and peptide YY (PYY) (Tatemoto *et al.*, 1982). NPY is expressed in the central and peripheral nervous systems and is one of the most abundant neuropeptides in the brain. Several important physiological activities, such as induction of food intake, inhibition of anxiety, increase in memory retention, presynaptic inhibition of neurotransmitter release, vasoconstriction, and regulation of ethanol consumption, have been attributed to NPY (Grundemar & Bloom, 1997; Thiele *et al.*, 1998). Especially, the role of NPY in feeding is of major interest because NPY receptor antagonists are potential anti-obesity drug candidates. Many studies have established the strong central influence of NPY in feeding behavior; for example, injection of NPY into the hypothalamus increases food intake (Levine & Morley, 1984; Stanley & Leibowitz, 1985), and high NPY levels are correlated with leptin deficiency (Erickson *et al.*, 1996), the hormone that is secreted by adipocytes and regulates body weight and energy balance (Dallongeville *et al.*, 1998; Wang *et al.*, 1998). Furthermore, NPY knockout can reduce obesity in leptin-deficient mice (named *ob/ob* mice) (Erickson et al., 1996).

Five distinct Y receptor subtypes that bind NPY, PYY, and PP with different affinities have been identified, cloned, and characterized (Michel *et al.*, 1998). They all belong to the superfamily of the G-protein-coupled receptors and are referred to as Y_1, Y_2, Y_4, Y_5, and Y_6. From studies conducted using partly selective agonists and antagonists, antisense approaches, and knockout techniques, the Y_1 and Y_5 receptors have been suggested to mediate the stimulatory effect of NPY on food intake (Inui, 1999; Bischoff & Michel, 1999). NPY, PYY, [Leu^{31},Pro^{34}]NPY, and three N-terminally truncated analogs, NPY-(2-36), NPY-(3-36), and PYY-(3-36),

have been shown to increase food intake. The rank order of potency of the agonists suggests that the Y_5 receptor is most likely involved in food intake (Inui, 1999; Gerald *et al.*, 1996). However, it has also been shown that both Y_1 and Y_5 receptor antagonists can inhibit NPY-induced food intake (Wieland *et al.*, 1998; Criscione *et al.*, 1998). One limitation of the agonists currently used for *in vivo* studies is the lack of receptor selectivity; NPY and PYY bind to the receptors Y_1, Y_2, and Y_5 with high affinity, the analog [Leu^{31},Pro^{34}]NPY has high affinity for the Y_1, Y_4, and Y_5 receptors, whereas N-terminal fragments are potent at the Y_2 as well as at the Y_5 receptor (Michel et al., 1998; Gerald et al., 1996; Wieland et al., 1998). [D-Trp^{32}]NPY has been described in literature as a weak Y_5 receptor-selective agonist with orexigenic properties (Gerald et al., 1996), but antagonism against NPY-induced increase in food intake has been observed as well (Balasubramaniam *et al.*, 1994; Small *et al.*, 1997). Furthermore, binding affinity studies on [D-Trp^{32}]NPY at the Y receptors have shown significant Y_2 receptor affinity in addition to its affinity for the Y_5 receptor (Gerald *et al.*).

Because highly specific tools to investigate the Y_5 receptor activity are still missing, we have focused our work on the design of NPY receptor agonists with both high affinity and selectivity for the Y_5 subtype. It is well established that the C-terminal part of NPY represents the interaction site with the Y receptors and that amino acid exchange is poorly tolerated in the region 33-36 (Eckard *et al.*, 2001); therefore, we induced a conformational change within the peptide region that mediates receptor binding by introducing the β-turn-inducing dipeptide Ala-Aib (aminoisobutyric acid) (Möhle *et al.*, 1997) into positions 31-32 of NPY and some peptides that contain segments of NPY and PP (NPY/PP chimeras). The [Ala^{31},Aib^{32}]-modified peptides showed high selectivity for the Y_5 receptor. Furthermore, *in vitro* and *in vivo* studies clearly proved their NPY receptor agonism as well as stimulation of food intake.

The solution structure of [Ala^{31},Aib^{32}]pNPY was investigated by CD and two-dimensional NMR. By comparison with the NMR structure of human NPY (hNPY) determined by Monks and co-workers (Monks *et al.*, 1996), a significant conformational change of the C-terminal fragment 28-36 was observed; although in the native peptide the α-helix extends up to residue 36, the α-helical motif of [Ala^{31},Aib^{32}]pNPY ends with a 3_{10}-helical turn between residues Ile^{28} and Ala^{31} followed by a flexible C terminus. Considering the binding properties of this NPY analog, this structural modification seems to be the key for Y_5 receptor selectivity.

3.2. Results

[Ala^{31},Aib^{32}]pNPY: Selectivity and agonism at the Y_5 receptor

Table 3.1 Amino acid sequences of hNPY and hPP and of the Y_5 receptor-selective analogs[a]

Peptide	Sequence
hNPY	YPSKPDNPGEDAPAEDMARYYSALRHYINLITRQRY-NH_2
[Ala^{31},Aib^{32}]-pNPY	YPSKPDNPGEDAPAEDLARYYSALRHYINLABRQRY-NH_2
[hPP^{1-17},Ala^{31},Aib^{32}]hNPY	APLEPVYPGDNATPEQMARYYSALRHYINLABRQRY-NH_2
[cPP^{1-7},NPY^{19-23},Ala^{31},Aib^{32},Gln^{34}]hPP	GPSQPTYPGDNATPEQMARYYSALRRYINMABRQRY-NH_2
hPP	APLEPVYPGDNATPEQMAQYAADLRRYINMLTRPRY-NH_2

a. Aib is indicated by the letter B in the peptide sequence

The peptide was synthesized by solid-phase technique and purified by preparative HPLC. Electrospray ionization mass spectrometry and

analytical HPLC confirmed peptide purity and identity. The amino acid sequence is shown in Table 3.1

[Ala^{31},Aib^{32}]pNPY bound to the Y_5 receptor with an IC_{50} of 6 nM, whereas values in the range of 500 to 1000 nM were observed at the other receptors (Table 3.2). Accordingly, [Ala^{31},Aib^{32}]pNPY turned out to be

Table 3.2 Pharmacological properties of hNPY, hPP,Aib-containing peptides, PYY-(3-36), and [D-Trp^{32}]hNPY

Peptide	Affinity IC_{50} ± S.E. [nM]				Inhibition of cAMP production EC_{50} ± S.E. hY_5 [nM]
	hY_1	hY_2	hY_4	hY_5	
hNPY	0.23 ± 0.01	0.04 ± 0.01	5.8 ± 3.5	0.6 ± 0.2	18.5 ± 6.6
[Ala^{31},Aib^{32}]-pNPY	>700	>500	>1,000	6.0 ± 2.4	98 ± 48
	(>117)	(>83)	(>167)	(1)	
[hPP$^{1-17}$,Ala^{31},Aib^{32}]hNPY	>1,000	>500	170 ± 23	0.92 ± 0.10	n.d.
	(>1,087)	(>543)	(185)	(1)	
[cPP$^{1-7}$,NPY$^{19-23}$,Ala^{31},Aib^{32},Q^{34}]hPP	530 ± 140	>500	51 ± 5	0.24 ± 0.06	17.0 ± 6.9
	(2,208)	(>2,083)	(212)	(1)	
hPP	170 ± 10	>1,000	0.06 ± 0.02	1.4[a]	n.d.
PYY-(3-36)	760 ± 160[b]	0.03±0.01[a]	15[a]	17[a]	n.d.
[D-Trp^{32}]hNPY	>1,000	29 ± 11	>1,000	35[a]	n.d.

a. See Gerald *et al.*
b. See Möhle *et al.*, 1997.

highly selective as well as to have high affinity for the Y_5 receptor.

To further characterize the newly developed Y_5 receptor-selective ligand, we investigated its ability to activate the receptor. Signal transduction of NPY-activated Y receptors is mediated by G_i protein coupling, which leads to the inhibition of the enzyme adenylyl cyclase (Michel et al., 1998). As shown in Table 3.2 and Figure 3.1, [Ala^{31},Aib^{32}]pNPY inhib-

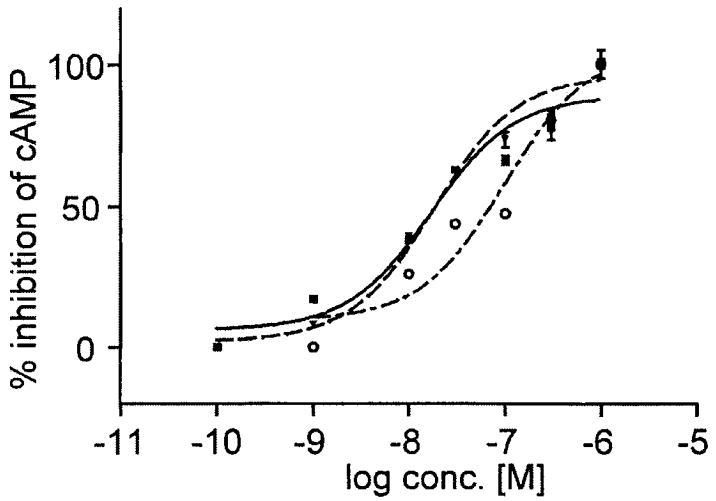

Figure 3.1 Inhibition of forskolin-stimulated cAMP production in BHK cells. Inhibitory effect of pNPY (---), [Ala^{31},Aib^{32}]-pNPY (-·-·-) and [cPP^{1-7}, NPY^{19-23},Ala^{31},Aib^{32},Gln^{34}]hPP (—). [cPP^{1-7},NPY^{19-23},Ala^{31},Aib^{32},Gln^{34}]hPP is slightly more potent than pNPY and 5-fold more effective than [Ala^{31},Aib^{32}]-pNPY, which correlates nicely with the receptor binding.

ited the forskolin-stimulated production of intracellular cAMP in a dose-dependent manner. Taking into account that the analog was 10-fold less potent in binding and 5-fold less potent in activating the Y_5 receptor than NPY, a good correlation between affinity and activity was found for NPY and [Ala^{31},Aib^{32}]pNPY.

The pharmacological profile of [Ala^{31},Aib^{32}]pNPY has all the features that are required for a peptide to be referred to as a highly selective, full agonist at the Y_5 receptor, which makes it a very interesting tool for studying the biological functions that have been attributed or speculated to be related to the Y_5 receptor.

Ala^{31}-Aib^{32}: Key motif for Y_5 receptor selectivity

To further improve receptor affinity, we designed several new peptides based on sequences of PP/NPY chimeras that have been identified

to bind to the Y_5 receptor with picomolar affinity (Cabrele *et al.*, 2001). The PP/NPY chimeras were modified by the introduction of the Ala-Aib dipeptide at positions 31-32. These analogs will be referred to as the Ala-Aib-containing PP/NPY chimeras hereafter. All peptides were prepared by solid-phase peptide synthesis; the sequences are shown in Table 3.1.

As already observed for [Ala^{31},Aib^{32}]pNPY, the Ala-Aib-containing PP/NPY chimeras were selective at the Y_5 receptor as well. At this receptor, the analog [cPP$^{1-7}$,NPY$^{19-23}$,Ala^{31},Aib^{32},Gln^{34}]hPP turned out to be 25-fold more potent than [Ala^{31},Aib^{32}]pNPY (0.24 nM *versus* 6.0 nM) and 3-fold more potent than the native ligand NPY (0.24 nM *versus* 0.6 nM). Furthermore, its selectivity for the Y_5 receptor was improved in comparison with that of [Ala^{31},Aib^{32}]pNPY (2208:1 *versus* > 117:1 relative to the Y_1 receptor, > 2083:1 *versus* > 83:1 relative to the Y_2 receptor, and 212:1 *versus* > 167:1 relative to the Y_4 receptor).

Signal transduction assays confirmed that the ligands described above were agonists at the Y_5 receptor. In particular, [cPP$^{1-7}$,NPY$^{19-23}$,Ala^{31},Aib^{32},Gln^{34}]hPP was at least as efficient as NPY itself in activating the receptor (Figure 3.1).

Accordingly, a new class of Y_5 receptor selective ligands has been developed in which receptor selectivity is provided by the sequence motif Ala^{31}-Aib^{32}.

Stimulation of food intake in rats by selective Y_5 receptor activation

To investigate the *in vivo* potency of [Ala^{31},Aib^{32}]pNPY in stimulating food intake through activation of the Y_5 receptor, the selective agonist was administered centrally to rats at three different doses (0.2, 2.0, and 6.0 nmol), and food intake was subsequently monitored over an 8-h span

(first, at 1 h and then every 2 h). The results showed a dose-dependent stimulatory effect on food intake in rats treated with the NPY analog compared with the control animals (Figure 3.2*a*). One hour after administration, the peptide, although inactive at the low dose of 0.2 nmol, induced an 8- and 10-fold increase in food intake at the higher doses of 2.0 and 6.0 nmol, respectively. After 4 h, even the dose of 0.2 nmol provoked a significant increase in food intake. The stimulation of food intake induced by [Ala^{31},Aib^{32}]pNPY remained significant even 8 h after administration; accordingly, the in food intake increased 3-fold at a dose of 0.2 nmol, 4-fold at 2.0 nmol, and 5-fold at 6.0 nmol as compared with unstimulated consumption. After 24 h, the rats treated with [Ala^{31},Aib^{32}]pNPY ate like the control animals.

The same experiment was performed with the most active and selective analog, [cPP^{1-7},NPY^{19-23},Ala^{31},Aib^{32},Gln^{34}]hPP (Figure 3.2*b*). In this case, even the low dose of 0.2 nmol showed a significant effect even after 1 h: 1.89 ± 0.3 g of food intake of the treated rats in contrast to 0.12 ± 0.09 g of the control animals. The effect becomes more and more evident with the time. After 8 h rats, treated with 0.2 nmol of [cPP^{1-7}, NPY^{19-23},Ala^{31},Aib^{32},Gln^{34}]hPP had consumed 16.19 ± 0.74 g, whereas control animals had eaten 2.36 ± 0.57 g of food. Interestingly, the effect was still pronounced 24 h after injection.

The efficacy of [Ala^{31},Aib^{32}]pNPY and [cPP^{1-7},NPY^{19-23},Ala^{31},Aib^{32},Gln^{34}]hPP on the stimulation of food intake was compared with that of NPY and [hPP^{1-17},Ala^{31},Aib^{32}]NPY. As expected from the binding affinity data, [hPP^{1-17},Ala^{31},Aib^{32}]NPY and NPY induced a higher amount of food intake in comparison with [Ala^{31},Aib^{32}]pNPY but a lower effect than [cPP^{1-7},NPY^{19-23},Ala^{31},Aib^{32},Gln^{34}]hPP, as depicted in Figure 3.2*c*.

The results of the *in vivo* feeding experiments clearly show that selec-

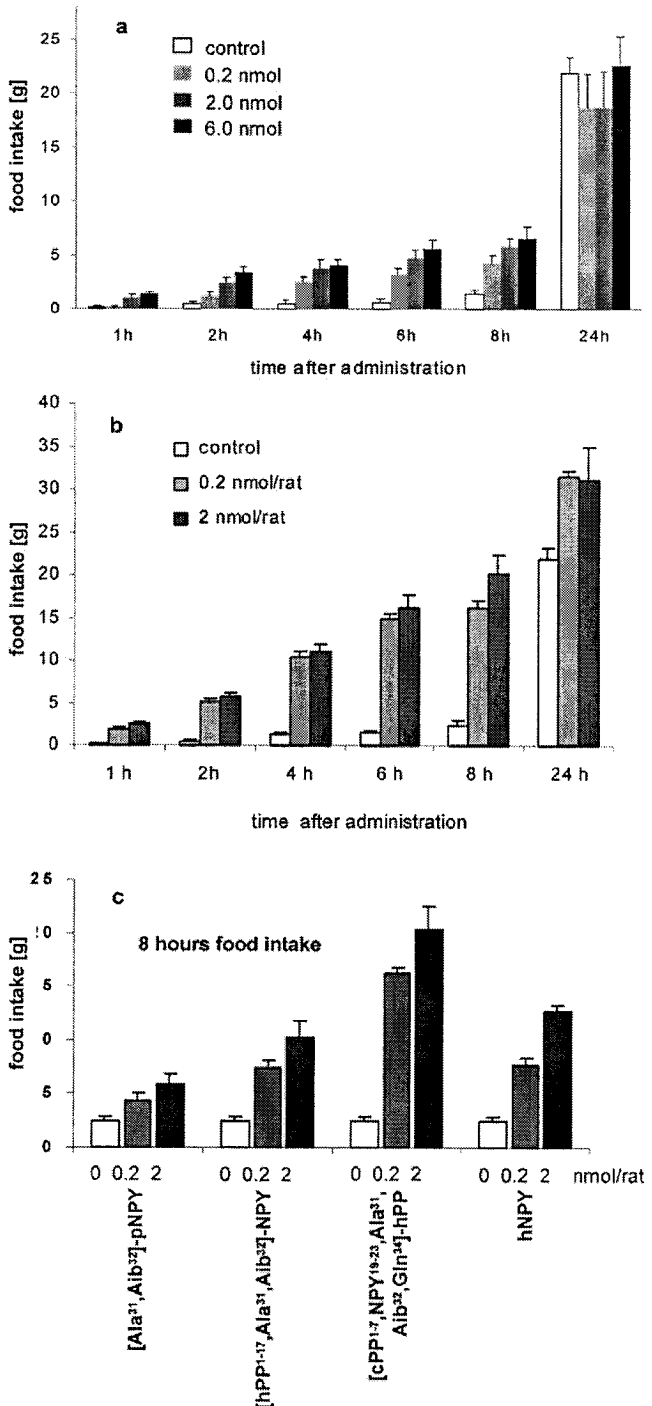

Figure 3.2 Effect of NPY and of the Y_5 receptor-selective analogs on food intake. *a,* dose-dependent stimulation of food intake in rats treated with [Ala^{31},Aib^{32}]NPY *(a);* or *b,* treated with [cPP$^{1-7}$,NPY$^{19-23}$,Ala^{31},Aib^{32},Gln^{34}]-hPP. *c,* comparison of the dose-dependent stimulation of food intake induced by [Ala^{31},Aib^{32}]pNPY, [hPP$^{1-17}$,Ala^{31}, Aib^{32}]-NPY, [cPP$^{1-7}$, NPY$^{19-23}$, Ala^{31}, Aib^{32}, Gln^{34}]hPP, and hNPY within 8 h shows that food intakes correlates with affinity for the hY_5 receptor.

tive activation of the Y_5 receptor influences food intake in a positive manner. Furthermore, Y_5 receptor mediated stimulation of food intake depends on the administered dose of the orexigenic agent. The analog [cPP$^{1-7}$,NPY$^{19-23}$,Ala^{31},Aib^{32},Gln^{34}]hPP, which shows a significantly higher affinity than hNPY itself, turned out to increase feeding ~2.5-fold more effectively than hNPY, which correlates nicely with the increase in affinity.

Structural characterization of [Ala^{31},Aib^{32}]pNPY

The solution structure of [Ala^{31},Aib^{32}]pNPY was investigated by CD and two-dimensional NMR spectroscopy. Figure 3.3 shows the CD spec-

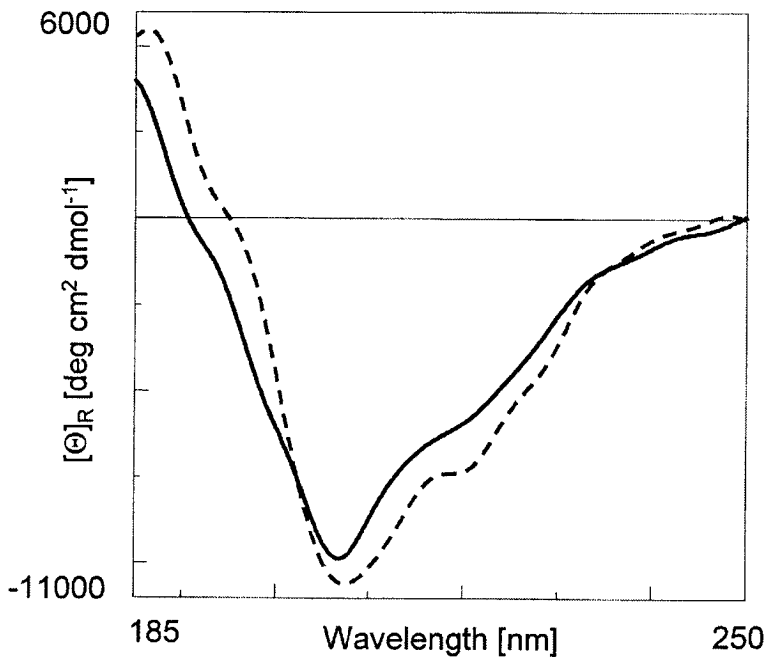

Figure 3.3 CD spectra of pNPY (---) and [Ala^{31},Aib^{32}]pNPY (—) in water at the concentration of 30 µM, pH 3.2, and 20 °C. Differences in the CD spectra at 220 nm suggest a change in the helicity of the peptides.

trum of the pNPY analog compared with the wild-type peptide at pH 3.2. The CD spectrum of pNPY displayed the typical features of an α-helix

with two negative bands at 220 and 208 nm and a positive band at 186 nm. The CD spectrum of the analog was characterized by a decrease in intensity, especially of the positive band and of the negative band at 220 nm. By measuring the ellipticity at 220 nm, using the equation of Chen *et al.* (1974), the fractional helix content was calculated to be approximately 16 and 20% for the modified and the native pNPY, respectively. Accordingly, the substitutions of Ile^{31} with Ala and Thr^{32} with Aib led to a reduction of helicity of about 20%. Furthermore, the change in the shape of the CD curve indicates a partially different conformation of [Ala^{31},Aib^{32}]pNPY. A comparison with the CD spectra of known structures suggests an increase in β-turn or 3_{10}-helix in the analog (Woody, 1985; Toniolo *et al.*, 1996).

To gain a more detailed understanding of the structural differences between [Ala^{31},Aib^{32}]NPY and NPY, we used two-dimensional NMR. Distance constraints used for the structure calculation were generated from 200-ms NOESY spectra of the 2 mM sample at pH 3.2 and 37 °C. Based on the hydrogen bonding pattern, it was concluded that the NPY analog is α-helical in peptide region 15-31 with a mean pairwise root-mean-square difference of 0.95 Å for the backbone heavy atoms. The N terminus showed no preferred conformation in solution (Figure 3.4).

In addition, the following observations support the view that the helix is significantly destabilized toward the C terminus. (*a*) The lack of a significant number of medium range NOEs within the C-terminal pentapeptide indicates that this segment is flexible. (*b*) An $i, i + 3$ hydrogen bond between residues 28 and 31 (Figure 3.5) in the absence of the corresponding $i, i + 4$ reveals the presence of a 3_{10}- instead of an α-helical turn. (*c*) The chemical shift deviations of the $C_\alpha H$ resonances (Wishart *et al.*, 1992) from the corresponding random coil values were smaller in peptide region 25-30 when compared with NPY (Monks *et al.*, 1996), with the $C_\alpha H$ resonance of His^{26} very close to its random coil value. (*d*) All of the $^3J_{NH\alpha}$

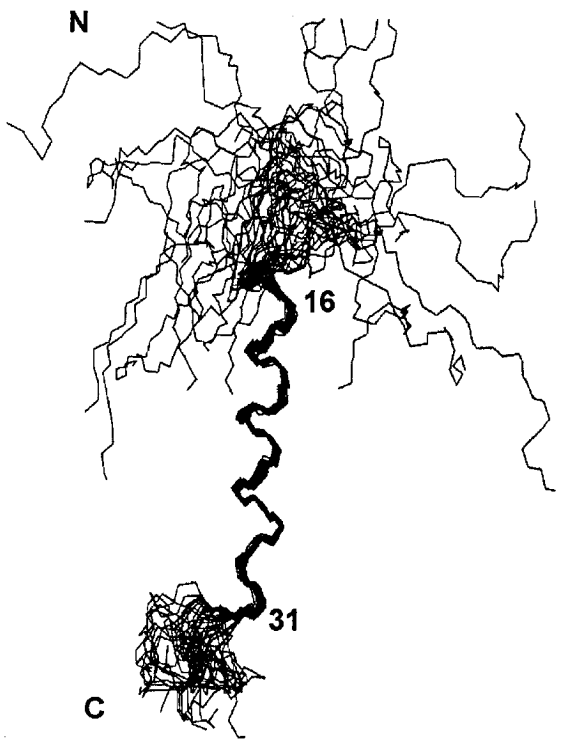

Figure 3.4 Solution structure of [Ala^{31},Aib^{32}]-pNPY. The 30 lowest energy structures with DYANA target function values below 0.8 indicating good agreement with standard length of bonds and angles and compatibility with the NMR constraints are superimposed over the backbone heavy atoms of residues 15-31.

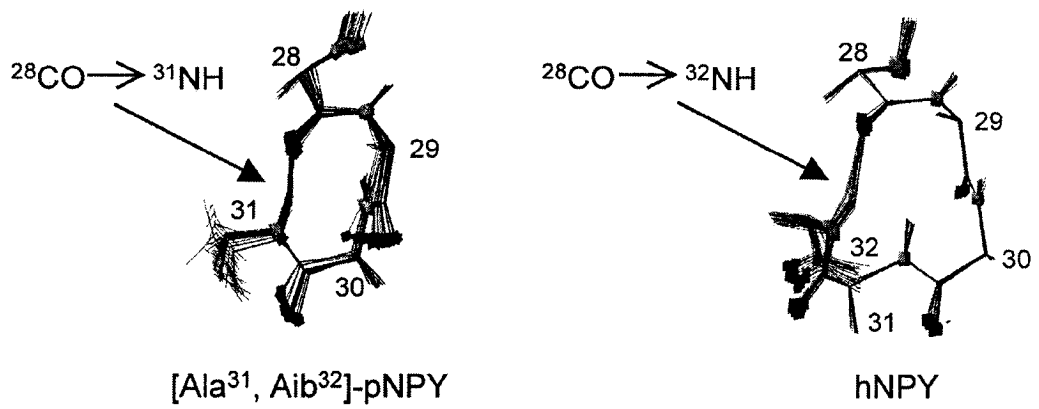

Figure 3.5 Hydrogen bond pattern over residues 28-32 of [Ala^{31},Aib^{32}]pNPY and hNPY. Left, the 30 structures of the analog with the lowest DYANA target function are superimposed over the backbone heavy atoms of residues 28-31. Right, the structure of hNPY according to the NMR data of Monks and co-workers (Monks *et al.*, 1996) is reported. The arrows indicate the presence of the *i*, *i* + 3 hydrogen bond in [Ala^{31},Aib^{32}]pNPY and of the *i*, *i* + 4 bond in hNPY.

coupling constants of residues 24-31 and 33-36 were around 7 Hz, which was the value found for rotationally averaged ϕ-backbone angles. In con-

trast, five $^3J_{NH\alpha}$ coupling constants in peptide region 14-23 were found to be smaller than 6 Hz, clearly showing that the N-terminal part of the helix is more stable. Interestingly, the intermolecular NOEs, as previously proposed for the dimer structure of hNPY (Monks *et al.*, 1996; Cowley *et al.*, 1992), were not detected in this work.

3.3. Discussion

Obesity has become one of the most common health disorders over the past two decades (Kordik & Reitz, 1999; Flier & Maratos-Flier, 1998; Strader *et al.*, 1998). Several medical problems, such as hypertension, cardiovascular diseases, type II diabetes and some forms of cancer, have been correlated with increased body weight . In the past few years, important advances have been made in understanding the mechanisms involved in food intake and energy homeostasis. It became evident that a key role in the regulation of food intake is played by the adipocyte-derived peptide hormone leptin and its receptor (Zhang *et al.*, 1994). Leptin levels are correlated with fat mass; accordingly, high levels of this hormone reduce food intake and body weight and stimulate metabolism. Lack of leptin or its receptor in mutant mice (*ob/ob* and *db/db* mice) induces hyperphagia, obesity, decreased energy expenditure, diabetes, and infertility (Chen *et al.*, 1996; Lee *et al.*, 1996; Chua *et al.*, 1996). Leptin regulates the hypothalamic expression of several neuropeptides (Flier & Maratos-Flier, 1998), among them NPY. It has been shown that *ob/ob* mice are characterized by an overproduction of NPY in the hypothalamus (Erickson *et al.*, 1996), whereas administration of leptin inhibits NPY secretion. Because of its stimulatory effect on food intake, NPY and its

receptor are interesting targets for drug design against obesity. Accordingly, it is important to understand the mechanisms that underlie NPY-stimulated food intake. Among the currently identified NPY receptor subtypes, the Y_1 and Y_5 receptors are the most likely candidates to mediate the orexigenic action of NPY (Inui, 1999; Bischoff & Michel, 1999). However, many doubts still remain, as several results obtained with different methods are contradictory. Wahlestedt and co-workers (Wahlestedt *et al.*, 1993) observed no effect on food intake after administration of Y_1 receptor antisense oligonucleotides, in contrast to the data of Lopez-Valpuesta and co-workers (Lopez-Valpuesta *et al.*, 1996) who found inhibition of NPY-induced feeding. On the other hand, administration of antisense oligonucleotides directed against the Y_5 receptor reduced NPY-induced food intake (Schaffhauser *et al.*, 1997). The knockout studies conducted so far have given unexpected results. Mice with both Y_1 or Y_5 receptor knockout gene exhibited mild obesity, although some differences were observed; the Y_1 receptor-deficient animal showed increased body weight without a change in food intake, mild hyperinsulemia, an elevated basal level of plasma insulin, and an absence of NPY-mediated vasoconstriction (Kushi *et al.*, 1998; Pedrazzini *et al.*, 1998), whereas the Y_5 receptor-deficient mice presented hyperphagia (Marsh *et al.*, 1998). Inhibition of NPY-induced feeding was produced by both Y_1 and Y_5 receptor-selective nonpeptide antagonists (Wieland *et al.*, 1998; Criscione *et al.*, 1998; Hipskind *et al.*, 1997; Kanatani *et al.*, 1996). On the other hand, NPY receptor agonists like [Leu^{31},Pro^{34}]NPY, NPY-(2-36), or NPY-(3-36) stimulated food intake (Gerald *et al.*, 1996). However, these peptides are not selective for one receptor, with [Leu^{31},Pro^{34}]NPY displaying equal affinity to the Y_1 and the Y_5 receptors. In addition, N-terminally truncated analogs are ligands for both Y_2 and Y_5 receptors. Although the Y_2 receptor does not seem to mediate the NPY-induced stimulation of food intake, other actions regulated by this receptor can be elicited, which

might interfere with the activation of the Y_5 receptor, thereby providing a complex and unclear physiological response. Unfortunately, the use of [D-Trp^{32}]NPY did not give unambiguous results. Gerald and co-workers (Gerald *et al.*, 1996) observed cAMP inhibition and stimulation of food intake mediated by the Y_5 receptor and concluded that this peptide is a weak Y_5 receptor-selective agonist *in vitro* and *in vivo*. In contrast, antagonism of NPY-induced stimulation of food intake by [D-Trp^{32}]NPY was found by Balasubramaniam and co-workers (Balasubramaniam *et al.*, 1994) and by Small and co-workers (Small *et al.*, 1997). In view of these observations, it must be stated that the *in vivo* profile of this analog of NPY is not well defined. Furthermore, binding potency at the Y receptors was in the order of Y2 ≅Y5 >>Y1,Y4 (Table 3.2).

In this work, we have presented the first Y_5 receptor-selective ligands with subnanomolar affinity: [Ala^{31},Aib^{32}]pNPY and the Ala-Aib-containing PP/NPY chimeras. The common sequence element Ala^{31}-Aib^{32} represents the key motif for receptor selectivity. The nonproteinogenic amino acid Aib has already been reported able to change the conformation within a peptide sequence, because no C_α-H is available to form appropriate hydrogen bonds (Möhle *et al.*, 1997). Circular dichroism studies on [Ala^{31},Aib^{32}]pNPY revealed reduced α-helical content compared with NPY. The solution structure obtained by two-dimensional NMR and molecular dynamics confined the destabilization of the helix at the C-terminal end encompassing residues 32-36, for which the peptide conformation is apparently not well defined. Interestingly, the presence of an *i*, *i*+3 hydrogen bond between residues 28 and 31 and the absence of the corresponding *i*, *i* + 4 bond suggests that the α-helix motif ends with a 3_{10}-helical turn.

The *in vivo* feeding profile of the newly developed Y_5 receptor-selective agonists confirms that this receptor subtype is involved in the stimulation of food intake, and the potency in stimulation of feeding correlates

nicely with the *in vitro* affinity to the Y_5 receptor. The most effective analog, [cPP$^{1-7}$,NPY$^{19-23}$,Ala^{31},Aib^{32},Gln^{34}]hPP, turned out to be ~2.5-fold more potent that hNPY and accordingly thus far is the most potent stimulator of food intake. Although more aspects remain to be investigated, our results show that the Y_5 receptor certainly plays a decisive role in the complex system that controls hunger. For NPY, as well as for the equally or less potent analogs, the feeding behavior turned back to normal after 24 h, and no difference was found in the food intake of mice with and without injections; this may be because of the proteolytic cleavage of peptides or because of the uptake of the ligand receptor complex by internalization. In contrast, the effect of [cPP$^{1-7}$,NPY$^{19-23}$,Ala^{31},Aib^{32},Gln^{34}]hPP with respect to feeding was still strong even 24 h after injection.

Until now, combined Y_1/Y_5 or Y_2/Y_5 ligands have been used to characterize Y_5 receptor activity. Our new compounds provide highly interesting tools and allow, for the first time, this receptor to be selectively targeted with affinities that are as potent as or even 2.5-fold more active than hNPY. Furthermore, radio- or fluorescence-labeled analogs of [Ala^{31},Aib^{32}]pNPY might be useful for Y_5 receptor specific assays, for receptor localization and investigation of receptor expression in normal and pathogenic brain structures.

The Y_5 receptor is speculated to be involved in epilepsy, sexual behavior, and circadian rhythm by activation or deactivation of special neurons in the hypothalamus or hippocampus (Bischoff & Michel, 1999). The Ala-Aib-containing agonists, with high affinity and selectivity for the Y_5 receptor, can contribute to the elucidation of the (patho)physiological relevance of this receptor subtype. Accordingly, we have already demonstrated that the Y_5 receptor is important for food intake, and further anticipated activities, such as epileptic seizures, are currently subject to investigation.

3.4. Materials and Methods

Materials

N^{α}-Fmoc amino acids were purchased from Alexix and Novabiochem (Läufelfingen, Switzerland). Diisopropylcarbodiimide was obtained from Aldrich. Hydroxybenzotriazole, piperidine, trifluoroacetic acid, thioanisole, thiocresol, ethanedithiol, and trimethylbromosilane were purchased from Fluka (Buchs, Switzerland). All material used for cell culture was purchased from Life Technologies, Inc. [^{3}H]propionyl-NPY was purchased from Amersham Pharmacia Biotech.

Peptide synthesis and purification

The peptides were synthesized by Fmoc/*tert*-butyl solid-phase strategy with an automated multiple peptide synthesizer (Syro MultiSynTech, Bochum, Germany), starting from 4-(2',4'-dimethoxyphenyl-fluorenylmethoxycarbonyl-aminomethyl)-phenoxyacetamido-norleucylaminomethyl resin (30 mg, 0.45 µmol/mg) (Rist *et al.*, 1998). Each Fmoc-amino acid (10-fold excess) was introduced by double coupling (twice for 36 min) using *in situ* activation with diisopropylcarbodiimide and hydroxybenzotriazole. Fmoc removal was carried out with piperidine in dimethylformamide (15 min). Cleavage from the resin and amino acid side chain deprotection were accomplished in one step with 90% trifluoroacetic acid in the presence of 10% scavengers (thioanisole and thiocresol 1:1) for 3 h. For cleavage of the methionine-containing peptides, ethanedithiol was added to the cleavage mixture. The peptides were precipitated from ice-cold diethyl ether and collected by centrifugation, resuspended in ether, and centrifuged again. This procedure was repeated four times. The crude peptides were dissolved in *tert*-butanol/water (3/1 w/w), frozen, and lyophilized. The methionine-containing peptides were subsequently treated with trifluoroacetic acid/trimethylbromosilane/ethanedithiol (96/2.4/1.6 v/v, 30 min) to reduce the methionine sulfoxide (Beck & Jung, 1994) and then precipitated from ice-cold ether as described above. The lyophilized peptides were purified by preparative HPLC using a Nucleosil C-18 column (6 µm, 25 × 30 mm, Waters), 0.1%

trifluoroacetic acid in water, and 0.1% trifluoroacetic acid in acetonitrile as the eluting system. The pure products were characterized by analytical HPLC performed on a LiChrospher RP-18 column (5 µm, 3 × 125 mm, Merck KG, Darmstadt, Germany) and by electrospray ionization mass spectrometry (Finnigan). The peptides were dissolved in diluted HCl (0.5 mM), frozen, and lyophilized; this procedure was repeated twice to obtain the corresponding hydrochloride salts.

Cell culture

BHK cells transfected with hY_1,hY_2,hY_4 receptor cDNA and HEK293 cells transfected with the hY_5 receptor were cultured as described previously (Wieland *et al.*, 1998). SMS-KAN cells (hY_2 receptor) were grown in Dulbecco's modified Eagle's medium/nutrient mix F12 1:1 with 15% fetal calf serum, 4 mM glutamine, and 1% nonessential amino acids (Ingenhoven & Beck-Sickinger, 1997). Cells were grown to confluency at 37 °C and 5% CO_2.

Binding assays

Cells were resuspended in incubation buffer (Minimum Essential Medium with Earl's salts containing 0.1% bacitracin, 50 µM pefabloc SC, and 1% bovine serum albumin). 200 µl of the suspension containing ca. 440,000 cells were incubated with 25 µl of a 10 nM solution of [^{3}H]propionyl-NPY and 25 µl of a 10 µM solution of NPY or analog. Nonspecific binding was defined in the presence of 1 µM cold NPY. After 1.5 h at room temperature, the incubation was terminated by centrifugation at 2,000 × *g* and 4 °C for 5 min. The pellets were then washed once with phosphate-buffered saline by centrifugation, resuspended in phosphate-buffered saline, and mixed with the scintillation mixture. Radioactivity was determined using a beta-counter.

cAMP enzyme immunoassays

Cells grown to confluency were resuspended in cAMP buffer (145 mM NaCl, 1 mM $MgSO_4$, 5 mM KCl, 10 mM HEPES, 0.5% bovine serum albumin, 10 mM glucose, 0.1 mM 3-isobutyl-1-methylxanthine, pH 7.4). 1.5 million cells were incubated with 40 µl of a 1.5 mM solution of forskolin and different concentrations of peptides for 1 h at 37 °C. Incubation was stopped by adding 100 µl of a 1 M solution of HCl. Cell lysis was done by freezing followed by centrifugation, and the supernatant was diluted 1:30. The intracellular amount of cAMP was determined using a cAMP enzyme immunoassay (Biotrak). Reactions were performed according to the protocol of the manufacturer, and optical density was determined at 450 nm.

Food intake studies

Adult male rats weighing between 340 and 400 g were housed individually and maintained on a 12:12 h light-dark cycle beginning at 6 a.m. (Wieland *et al.*, 1998). Tap water and standard laboratory chow were available throughout. After 1 week of habituation to their new housing conditions, the animals were anesthetized with sodium pentobarbital for the placement of stainless steel guide cannulae. Bilateral guide cannulae were placed 1 mm above the paraventricular nucleus according to the stereotaxic coordinates (Paxinos *et al.*, 1985): AP, -1.8; L, 0.5; V, 7.0. Guide cannulae were maintained in place on the skull with small metal screws and dental acrylic cement. Cannulae were closed with a stainless steel stylet when not in use. Rats were allowed to recover for 1 week and were adapted to the injection procedure. On the day of the experiments, drugs were injected between 8 and 9 a. m. For each experiment, eight rats were used, and for each dose a different group of rats was used.

CD spectroscopy

The CD spectra were recorded on a JASCO model J720 spectropolarimeter over the range of 185-250 nm at 20 °C under a N_2 atmosphere. The peptides were dissolved in water at a concentration of 60 µM. The pH was lowered to 3.2 by the

addition of small aliquots of a 0.12 M solution of HCl followed by dilution with water to obtain a concentration of 30 μM. Each measurement was performed four times using a sample cell with constant temperature and with a path of 0.02 cm. The response time was set to 2 s at a scan speed of 20 nm/min, a sensitivity range of 10 millidegrees, and a step resolution of 0.2 nm. The CD spectrum of the solvent was subtracted from the CD spectra of the peptide solutions to eliminate the interference from cell, solvent, and optical equipment. High frequency noise was reduced by means of a low-path Fourier transform filter. The values for the mean residue molar ellipticity $[\Phi]_R$ are expressed in $deg/cm^2/dmol^{-1}$.

NMR spectroscopy

NMR samples were prepared by dissolving the peptide in 90% H_2O, 10% D_2O (v/v) or 99.9% D_2O. The pH was adjusted to 3.2 by adding small aliquots of 0.1 M solutions of HCl or DCl. All experiments were measured on a 2 mM concentrated sample, unless stated otherwise, at 37 °C on a Bruker DRX600 spectrometer. The proton resonances were assigned according to the standard sequential assignment procedure (Wüthrich, 1986) using data from DQF-COSY, 80 ms TOCSY, and 200 ms NOESY spectra recorded on both the 4 and 2 mM samples in 90% H_2O, 10% D_2O and in 99.9% D_2O. Additional torsion angle constraints were introduced from $^3J_{\alpha\beta}$ coupling constants extracted from an exclusive COSY experiment recorded in 99.9% D_2O.

Structure calculation

Upper limits for the structure calculation were taken from the volume integrals of NOESY peaks from all experiments recorded at 2 mM concentration. $^3J_{NH\alpha}$ coupling constants were determined from the splitting of the in-phase doublets of NOESY peaks involving amide protons (Szyperski *et al.*, 1992), but only those couplings were included that were indicative of non-rotationally averaged torsion angles. From all unambiguously assigned NOESY peaks, 14 $^3J_{\alpha\beta}$ coupling constants and 5 $^3J_{NH\alpha}$ coupling constants (<6 Hz), 274 meaningful upper distance limits, as well as 158 ϕ, ψ, χ^1, and χ^2 torsion angle restraints, were derived. The calculation was performed by restrained molecular dynamics in

torsion angle space using a simulated annealing protocol as implemented in the program DYANA (Güntert *et al.*, 1997). Figs. 3.4 and 3.5 were generated using MOLMOL (Koradi *et al.*, 1996).

3.5. Acknowledgement

We are grateful to S. Schacherl-Schmid, E. Schilling, and F. Raible for skilled technical assistance and to our colleagues at Novo Nordisc (S. Hjort, J. S. Rasmussen, and C. Stidsen) for contributions of cDNAs and cells lines.

3.6. Footnotes

This work was supported by the Swiss National Foundation (Grant 31-05081.97) and the Federal Institute of Technology (ETH) of Zurich (TH project no. 0 20 218-96).

This paper is dedicated to Prof. Horst Kessler, LTU, Munich, on the occasion of his 60th birthday.

The atomic coordinates and the structure factors (code 1FVN) have been deposited in the Protein Data Bank, Research Collaboratory for Structural Bioinformatics, Rutgers University, New Brunswick, NJ (http://www.rcsb.org/).

3.7. References

Balasubramaniam, A., Sheriff, S., Johnson, M. E., Prabhakaran, M., Huang, Y., Fischer, J. E. & Chance, W. T. (1994). [D-TRP^{32}]neuropeptide Y: a competitive antagonist of NPY in rat hypothalamus. *J. Med. Chem.* **37,** 811-815.

Beck, W. & Jung, G. (1994). *Lett. Pept. Sci.* **1,** 31-37.

Bischoff, A. & Michel, M. C. (1999). Emerging functions for neuropeptide Y_5 receptors. *Trends Pharmacol. Sci.* **20,** 104-106.

Cabrele, C., Wieland, H. A., Langer, M., Stidsen, C. & Beck-Sickinger, A. G. (2001). Y-Receptor Affinity Modulation by the Design of Pancreatic Polypeptide/Neuropeptide Y Chimera Led to Y_5-Receptor Ligands with Picomolar Affinity. *Peptides,* in press.

Chen, H., Charlat, O., Tartaglia, L. A., Woolf, E. A., Weng, X., Ellis, S. J., Lakey, N. D., Culpepper, J., Moore, K. J., Breitbart, R. E., Duyk, G. M., Tepper, R. I. & Morgenstern, J. P. (1996). Evidence that the diabetes gene encodes the leptin receptor: identification of a mutation in the leptin receptor gene in *db/db* mice. *Cell* **84,** 491-495.

Chen, Y. H., Yang, J. T. & Chau, K. H. (1974). Determination of the helix and beta form of proteins in aqueous solution by circular dichroism. *Biochemistry* **13,** 3350-3359.

Chua, S. C., Chung, W. K., Wu-Peng, X. S., Zhang, Y., Liu, S. M., Tartaglia, L. & Leibel, R. L. (1996). Phenotypes of mouse diabetes and rat fatty due to mutations in the OB (leptin) receptor. *Science* **271,** 994-996.

Cowley, D. J., Hoflack, J. M., Pelton, J. T. & Saudek, V. (1992). Structure of neuropeptide Y dimer in solution. *Eur. J. Biochem.* **205,** 1099-1106.

Criscione, L., Rigollier, P., Batzl-Hartmann, C., Rueger, H., Stricker-Krongrad, A., Wyss, P., Brunner, L., Whitebread, S., Yamaguchi, Y., Gerald, C., Heurich, R. O., Walker, M. W., Chiesi, M., Schilling, W., Hofbauer, K. G. & Levens, N. (1998). Food intake in free-feeding and energy-deprived lean rats is mediated by the neuropeptide Y_5 receptor. *J. Clin. Invest.* **102,** 2136-2145.

Dallongeville, J., Fruchart, J. C. & Auwerx, J. (1998). Leptin, a pleiotropic hormone: physiology, pharmacology, and strategies for discovery of leptin modulators. *J. Med. Chem.* **41,** 5337-5352.

Eckard, C. P., Cabrele, C., Wieland, H. A. & Beck-Sickinger, A. G. (2001). Molecular characterisation of NPY receptors using synthetic peptides and anti-receptor antibodies. *Molecules,* in press.

Erickson, J. C., Hollopeter, G. & Palmiter, R. D. (1996). Attenuation of the obesity syndrome of *ob/ob* mice by the loss of neuropeptide Y. *Science* **274,** 1704-1707.

Flier, J. S. & Maratos-Flier, E. (1998). Obesity and the hypothalamus: novel peptides for new pathways. *Cell* **92,** 437-440.

Gerald, C., Walker, M., Branchek, T. & Weinshank, R. U. S. Patent WO96/16542 PCT/US95/15646.

Gerald, C., Walker, M. W., Criscione, L., Gustafson, E. L., Batzl-Hartmann, C., Smith, K. E., Vaysse, P., Durkin, M. M., Laz, T. M., Linemeyer, D. L., Schaffhauser, A. O., Whitebread, S., Hofbauer, K. G., Taber, R. I., Branchek, T. A. & Weinshank, R. L. (1996). A receptor subtype involved in neuropeptide-Y-induced food intake. *Nature* **382,** 168-171.

Grundemar, L. & Bloom, S. R. e. (1997). *Neuropeptide Y and Drug Development,* pp. 1-39, Academic Press, San Diego.

Güntert, P., Mumenthaler, C. & Wüthrich, K. (1997). Torsion angle dynamics for NMR structure calculation with the new program DYANA. *J. Mol. Biol.* **273,** 283-298.

Hipskind, P. A., Lobb, K. L., Nixon, J. A., Britton, T. C., Bruns, R. F., Catlow, J., Dieckman-McGinty, D. K., Gackenheimer, S. L., Gitter, B. D., Iyengar, S., Schober, D. A., Simmons, R. M., Swanson, S., Zarrinmayeh, H., Zimmerman, D. M. & Gehlert, D. R. (1997). Potent and selective 1,2,3-trisubstituted indole NPY Y-1 antagonists. *J. Med. Chem.* **40,** 3712-3714.

Ingenhoven, N. & Beck-Sickinger, A. G. (1997). Fluorescent labelled analogues of neuropeptide Y for the characterization of cells expressing NPY receptor subtypes. *J. Recept. Signal Transduct. Res.* **17,** 407-418.

Inui, A. (1999). Neuropeptide Y feeding receptors: are multiple subtypes involved? *Trends Pharmacol. Sci.* **20,** 43-46.

Kanatani, A., Ishihara, A., Asahi, S., Tanaka, T., Ozaki, S. & Ihara, M. (1996). Potent neuropeptide Y Y1 receptor antagonist, 1229U91: blockade of neuropeptide Y-induced and physiological food intake. *Endocrinology* **137,** 3177-3182.

Koradi, R., Billeter, M. & Wüthrich, K. (1996). MOLMOL: a program for display and analysis of macromolecular structures. *J. Mol. Graph.* **14,** 51-55, 29-32.

Kordik, C. P. & Reitz, A. B. (1999). Pharmacological treatment of obesity: therapeutic strategies. *J. Med. Chem.* **42,** 181-201.

Kushi, A., Sasai, H., Koizumi, H., Takeda, N., Yokoyama, M. & Nakamura, M. (1998). Obesity and mild hyperinsulinemia found in neuropeptide Y-Y_1 receptor- deficient mice. *Proc. Natl Acad. Sci. U S A* **95,** 15659-15664.

Lee, G. H., Proenca, R., Montez, J. M., Carroll, K. M., Darvishzadeh, J. G., Lee, J. I. & Friedman, J. M. (1996). Abnormal splicing of the leptin receptor in diabetic mice. *Nature* **379,** 632-635.

Levine, A. S. & Morley, J. E. (1984). Neuropeptide Y: a potent inducer of consummatory behavior in rats. *Peptides* **5,** 1025-1029.

Lopez-Valpuesta, F. J., Nyce, J. W., Griffin-Biggs, T. A., Ice, J. C. & Myers, R. D. (1996). Antisense to NPY-Y_1 demonstrates that Y_1 receptors in the hypothalamus underlie NPY hypothermia and feeding in rats. *Proc. R. Soc. Lond. B. Biol. Sci.* **263,** 881-886.

Marsh, D. J., Hollopeter, G., Kafer, K. E. & Palmiter, R. D. (1998). Role of the Y_5 neuropeptide Y receptor in feeding and obesity. *Nat. Med.* **4,** 718-721.

Michel, M. C., Beck-Sickinger, A., Cox, H., Doods, H. N., Herzog, H., Larhammar, D., Quirion, R., Schwartz, T. & Westfall, T. (1998). XVI. International Union of Pharmacology recommendations for the nomenclature of neuropeptide Y, peptide YY, and pancreatic polypeptide receptors. *Pharmacol. Rev.* **50,** 143-150.

Möhle, K., Gussmann, M. & Hofmann, H. J. (1997). Structural and energetic relations between beta turns. *J. Comput. Chem.* **18,** 1415-1430.

Monks, S. A., Karagianis, G., Howlett, G. J. & Norton, R. S. (1996). Solution structure of human neuropeptide Y. *J. Biomol. NMR* **8,** 379-390.

Paxinos, G., Watson, C., Pennisi, M. & Topple, A. (1985). Bregma, lambda and the interaural midpoint in stereotaxic surgery with rats of different sex, strain and weight. *J. Neurosci. Methods* **13,** 139-143.

Pedrazzini, T., Seydoux, J., Kunstner, P., Aubert, J. F., Grouzmann, E., Beermann, F. & Brunner, H. R. (1998). Cardiovascular response, feeding behavior and locomotor activity in mice lacking the NPY Y1 receptor. *Nat. Med.* **4,** 722-726.

Rist, B., Entzeroth, M. & Beck-Sickinger, A. G. (1998). From micromolar to nanomolar affinity: a systematic approach to identify the binding site of CGRP at the human calcitonin gene-related peptide 1 receptor. *J. Med. Chem.* **41,** 117-123.

Schaffhauser, A. O., Stricker-Krongrad, A., Brunner, L., Cumin, F., Gerald, C., Whitebread, S., Criscione, L. & Hofbauer, K. G. (1997). Inhibition of food intake by neuropeptide Y Y_5 receptor antisense oligodeoxynucleotides. *Diabetes* **46,** 1792-1798.

Small, C. J., Morgan, D. G., Meeran, K., Heath, M. M., Gunn, I., Edwards, C. M., Gardiner, J., Taylor, G. M., Hurley, J. D., Rossi, M., Goldstone, A. P., O'Shea, D., Smith, D. M., Ghatei, M. A. & Bloom, S. R. (1997). Peptide analogue studies of the hypothalamic neuropeptide Y receptor mediating pituitary adrenocorticotrophic hormone release. *Proc. Natl Acad. Sci. U S A* **94,** 11686-11691.

Stanley, B. G. & Leibowitz, S. F. (1985). Neuropeptide Y injected in the paraventricular hypothalamus: a powerful stimulant of feeding behavior. *Proc. Natl Acad. Sci. U S A* **82,** 3940-3943.

Strader, C. D., Hwa, J. J., Van Heek, M. & Parker, F. M. (1998). Novel molecular targets for the treatment of obesity. *Drug Discov. Today* **3,** 250-256.

Szyperski, T., Güntert, P., Otting, G. & Wüthrich, K. (1992). Determination of scalar coupling constants by inverse Fourier transfomation of in-phase multiplets. *J. Magn. Reson.* **99,** 552-560.

Tatemoto, K., Carlquist, M. & Mutt, V. (1982). Neuropeptide Y- a novel brain peptide with structural similarities to peptide YY and pancreatic polypeptide. *Nature* **296,** 659-660.

Thiele, T. E., Marsh, D. J., Ste Marie, L., Bernstein, I. L. & Palmiter, R. D. (1998). Ethanol consumption and resistance are inversely related to neuropeptide Y levels. *Nature* **396,** 366-369.

Toniolo, C., Polese, A., Formaggio, F., Crisma, M. & Kamphuis, J. (1996). Circular dichroism spectrum of a peptide 3_{10}-helix. *J. Am. Chem. Soc.* **118,** 2744-2745.

Wahlestedt, C., Pich, E. M., Koob, G. F., Yee, F. & Heilig, M. (1993). Modulation of anxiety and neuropeptide Y-Y_1 receptors by antisense oligodeoxynucleotides. *Science* **259,** 528-531.

Wang, J., Liu, R., Hawkins, M., Barzilai, N. & Rossetti, L. (1998). A nutrient-sensing pathway regulates leptin gene expression in muscle and fat. *Nature* **393,** 684-688.

Wieland, H. A., Engel, W., Eberlein, W., Rudolf, K. & Doods, H. N. (1998). Subtype selectivity of the novel nonpeptide neuropeptide Y Y_1 receptor antagonist BIBO 3304 and its effect on feeding in rodents. *Br. J. Pharmacol.* **125,** 549-555.

Wishart, D. S., Sykes, B. D. & Richards, F. M. (1992). The chemical shift index: a fast and simple method for the assignment of protein secondary structure through NMR spectroscopy. *Biochemistry* **31,** 1647-1651.

Woody, R. W. (1985) in *The Peptides* (Hruby, V. J., ed) Vol. 7, pp. 15-114, Academic Press, New York.

Wüthrich, K. (1986). *NMR of Proteins and Nucleic Acids*, Wiley, New York.

Zhang, Y., Proenca, R., Maffei, M., Barone, M., Leopold, L. & Friedman, J. M. (1994). Positional cloning of the mouse obese gene and its human homologue. *Nature* **372,** 425-432.

3.8. Supplementary Material

Table S1

Chemical shifts for [Ala31,Aib32]NPY[a,b]

Residue	H^N	H^α	H^β	others
Tyr 1	-	4.01	2.99, 3.15	δH 7.12, 7.12; εH 6.88, 6.88
Pro 2		4.51	1.91, 2.29	γCH_2 1.97, 1.97; δCH_2 3.59, 3.75
Ser 3	8.33	4.44	3.85, 3.85	
Lys 4	8.22	4.56	1.68, 1.79	γCH_2 1.41, 1.41; δCH_2 1.67, 1.67; εCH_2 2.98, 2.98
Pro 5		4.38	1.88, 2.25	γCH_2 1.98, 1.98; δCH_2 3.61, 3.77
Asp 6	8.40	4.61	2.72, 2.76	
Asn 7	8.21	4.87	2.63, 2.79	δNH_2 6.84, 7.50
Pro 8		4.38	1.94, 2.24	γCH_2 1.96, 1.96; δCH_2 3.33, 3.68
Gly 9	8.29	3.89, 3.89		
Glu 10	7.97	4.32	1.96, 2.09	γCH_2 2.40, 2.40
Asp 11	8.31	4.68	2.74, 2.85	
Ala 12	7.96	4.53	1.32	
Pro 13		4.35	1.87, 2.28	γCH_2 1.99, 1.99; δCH_2 3.61, 3.73
Ala 14	8.24	4.18	1.38	
Glu 15	8.25	4.24	2.02, 2.05	γCH_2 2.41, 2.41
Asp 16	8.16	4.60	2.78, 2.78	
Leu 17	8.01	4.17	1.61, 1.69	γH 1.62; δCH_3 0.81, 0.88
Ala 18	8.02	4.15	1.41	
Arg 19	7.83	4.11	1.72, 1.72	γCH_2 1.47, 1.54; δCH_2 3.12, 3.12; εNH 7.10; ηNH_2 6.81
Tyr 20	7.81	4.38	2.92, 2.98	δH 6.84, 6.84; εH 6.67, 6.67
Tyr 21	8.08	4.32	2.95, 3.04	δH 7.10, 7.10; εH 6.80, 6.80
Ser 22	8.02	4.23	3.86, 3.92	
Ala 23	7.96	4.22	1.41	
Leu 24	7.83	4.14	1.53, 1.53	γH 1.55; δCH_3 0.79, 0.83
Arg 25	7.85	4.09	1.71, 1.71	γCH_2 1.49, 1.56; δCH_2 3.10, 3.10; εNH 7.08; ηNH_2 6.79
His 26	8.05	4.55	3.10, 3.19	δ^2H 7.11; ε^1H 8.55
Tyr 27	8.08	4.44	2.95, 3.01	δH 7.05, 7.05; εH 6.77, 6.77
Ile 28	7.99	3.96	1.77	γCH_2 1.11, 1.44; γCH_3 0.83; δCH_3 0.80
Asn 29	8.17	4.61	2.75, 2.82	δNH_2 6.84, 7.50
Leu 30	8.01	4.17	1.57, 1.57	γH 1.53; δCH_3 0.80, 0.80
Ala 31	8.05	4.11	1.33	
Aib 32	7.95		1.41; 1.44	
Arg 33	7.72	4.17	1.76, 1.88	γCH_2 1.62, 1.62; δCH_2 3.15, 3.15; εNH 7.12
Gln 34	7.97	4.20	1.99, 2.04	γCH_2 2.33, 2.33; εNH_2 6.75, 7.36
Arg 35	7.94	4.18	1.64, 1.64	γCH_2 1.37, 1.42; δCH_2 3.07, 3.07; εNH 7.04; ηNH_2 6.78
Tyr 36	7.91	4.55	2.86, 3.10	δH 7.11, 7.11; εH 6.78, 6.78
NH_2				7.01, 7.36

[a] 2 mM, 90% H_2O/10% ^2H_2O at 37°C and pH 3.2. Chemical shifts are referenced to the water frequency at 37°C (4.63 ppm).

[b] Splitting of peaks due to cis-trans isomerisms of the proline residues. Chemical shifts are given for the major forms.

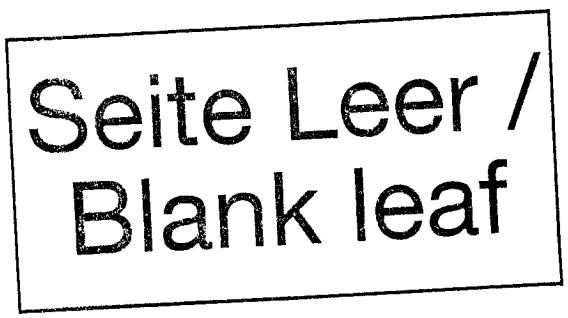
Seite Leer /
Blank leaf

Chapter 4

The Key Motif to Gain High Affinity and Selectivity at the Neuropeptide Y_5 Receptor II: Solution Structure and Dynamics of [Ala^{31},Pro^{32}]-NPY[1]

The structure of [Ala^{31}, Pro^{32}]-NPY, a neuropeptide Y mutant with high affinity and selectivity for the NPY Y_5 receptor [Cabrele, C., Wieland, H. A., Stidsen, C., Beck-Sickinger, A. G., *accompanying paper*], has been characterized in the presence of the membrane mimetic dodecylphosphocholine (DPC) micelles using high resolution NMR techniques. The overall topology closely resembles the fold of the previously described Y_5 receptor-selective agonist [Ala^{31}, Aib^{32}]-NPY [Cabrele, C., Langer, M., Bader, R., Wieland, H. A., Doods, H. N., Zerbe, O., and Beck-Sickinger, A. G. (2000) *J. Biol. Chem.* 275, 36043 – 36048]. Similar to wild-type neuropeptide Y (NPY) and [Ala^{31}, Aib^{32}]-NPY, the N-terminal residues Tyr^1 to Asp^{16} are disordered in solution. Starting from residue Leu^{17} an α-helix extends towards the C terminus. The decreased density of medium-range NOEs for the C-terminal residues resulting in larger RMSD values for the backbone atoms of Ala^{31} to Tyr^{36} indicates that the α-helix has become interrupted through the [Ala^{31}, Pro^{32}]-mutation. This finding is further supported by ^{15}N-relaxation data through which we

[1]Bader, R., Rytz, G., Lerch, M., Beck-Sickinger, A.G. & Zerbe, O., **in preparation**.

can demonstrate that the well-defined α-helix is restricted to residues 17-31 with the C-terminal tetrapeptide displaying increased flexibility compared to NPY. Surprisingly, increased generalized order parameter as well as decreased $^3J_{HN\alpha}$ scalar coupling constants reveal that the central helix is stabilized in comparison to wild-type NPY. Micelle-integrating spin-labels were used to probe the mode of association of the helix with the membrane mimetic. The Y_5 receptor-selective mutant and NPY share a similar orientation, which is parallel to the lipid surface. However, signal reductions due to efficient electron, nuclear spin relaxation were much less pronounced for the surface-averted residues in [Ala^{31}, Pro^{32}]-NPY when compared to wild-type DPC-bound NPY. Only the signals of residues Asn^{29} and Leu^{30} were significantly more reduced in the mutant. The postulation of a different membrane binding mode of [Ala^{31}, Pro^{32}]-NPY is further supported by the faster H/D exchange at the C-terminal amide protons. We conclude that arginine residues 33 and 35, which are believed to be directly involved in forming contacts to basic receptor residues at the membrane-water interface, are no longer fixed in a well-defined conformation close to the membrane surface in [Ala^{31},Pro^{32}]-NPY.

4.1. Introduction

Neuropeptide Y (NPY) is a 36-residue, C-terminally amidated polypeptide hormone (Tatemoto, 1982). At least four Y receptor subtypes (Y_1, Y_2, Y_4 and Y_5), all belonging to the rhodopsin-like family of G-protein coupled receptors and located in the central and/or peripheral nervous system (Dumont *et al.*, 1992), are activated by NPY (Michel *et al.*,

1998). In the brain, NPY is the most abundant neuropeptide and has been implicated in several regulatory functions (Gehlert, 1998). Injection of NPY directly into the paraventricular nucleus of the hypothalamus of satiated, brain-cannulated rats produced a large, dose-dependent increase in food intake (Stanley & Leibowitz, 1985). Especially the possible pharmacological role of hypothalamic NPY for the regulation of food-uptake and hence its influence on obesity has steered a number of pharmacological investigations using peptide analogs, receptor gene-knock-out animals and receptor-specific antagonists. These lead to the suggestion that the Y_1 and Y_5 receptors are important in mediating the effects of NPY on food intake in rats (for a rev. see Gehlert, 1999). In order to characterize each of the two potential "feeding receptor subtypes" individually we focus our efforts on the development of potent and selective agonists and antagonists for the individual receptor subtypes. Selective or partially selective antagonists have been available for both Y_1 and Y_5 receptor subtypes for some time and could be shown to inhibit NPY-induced food intake (Criscione *et al.*; 1998, Kanatani *et al.*, 1998; Rudolf *et al.*, 1994; Wieland *et al.*, 1998). However, we recently presented the first selective agonists at the Y_5 receptor, which indeed turned out to stimulate food intake in rats (Cabrele *et al.*, 2000). A series of NPY mutants and chimeras of NPY and pancreatic polypeptide (PP), another hormone of high sequence homology to NPY which is targeting similar receptors, were designed and proven to be Y_5 receptor-selective as long as they contained the [Ala^{31}, Xxx^{32}]-motif (Cabrele *et al.*, *accompanying paper*). Mutants in which Thr^{32} was replaced by Aib, Pro or Hyp bound selectively to the Y_5 receptor with a good affinity (in the nM range), whereas the introduction of D-proline lead to a drastic loss of affinity.

In an attempt to understand the spatial properties required for Y_5 receptor selectivity, we previously determined the solution structure of [Ala^{31}, Aib^{32}]-NPY (Cabrele *et al.*, 2000). The solution structure of wild-

type NPY itself has been described in literature both by Darbon *et al.* (1992), and by Monks *et al.* (1996). Both publications agree that only the C-terminal part of NPY forms a stable α-helix whereas the N terminus is much more disordered. However, Darbon *et al.* propose a polyproline II helix for the N-terminal part that bends back onto the C-terminal helix. This structural feature was described in the crystal structure of avian polypeptide (aPP) by Blundell and co-workers (Blundell *et al.*, 1981) for the first time and hence became known as the PP fold. In contrast, Monks postulates that the N terminus is fully flexible. We recently have supported the latter view based upon arguments from ^{15}N relaxation data (Bader *et al.*, 2001). Comparison of the conformation of [Ala^{31}, Aib^{32}]-NPYto that of wild-type NPY revealed a significant change in the C-terminal part of the peptide, which is known to be a key interaction site at all known Y-receptors (Beck-Sickinger & Jung, 1995, Cabrele & Beck-Sickinger, 2000). Based upon NOE-derived distance restraints it was found that the mutant adopts a 3_{10}-helical turn between residues 28 and 31, followed by a flexible C terminus. This is in contrast to the solution structure of NPY by Monks in which a regular α-helix extends to the C-terminal end. On the other hand, recent studies of the dynamics of NPY in aqueous solution clearly demonstrated increased flexibility of N-H bond vectors in the C-terminal tetrapeptide compared to those within the central part of the helix (between residues 16-32) (Bader *et al.*, 2001).

Assuming a pathway that requires a membrane-association step prior to receptor binding (Moroder *et al.*, 1993; Sargent & Schwyzer, 1986; Schwyzer, 1986; Schwyzer, 1986), it was suggested, that the determination of the structure of the hormones in the presence of a membrane mimetic gives biologically relevant insight into the peptide conformation which is encountered by the receptor during the initial contact. We used micelles formed by the zwitterionic dodecylphosphocholine (DPC) to model the membrane. DPC is the detergent that presents the predomi-

nant constituent of animal cell membranes (Henry & Sykes, 1994). It has been designed especially for solution NMR purposes (Lauterwein *et al.*, 1979) and is assumed to give structural results that are in agreement with those obtained using bilayers, at least in the case of surface-associated polypeptides (Opella, 1997). As described by Opella *et al.* (1994) using a high excess of detergent well above the critical micelle concentration prevents the formation of different states of aggregates. This yields rather well resolved spectra, whose signal dispersion is even increased due to the polar and charged headgroups.

During our investigations on NPY bound to DPC micelles we noticed that the C-terminal conformation was slightly rearranged so that Tyr^{36} is placed close to the membrane-water interface. Moreover, the α-helix became significantly stabilized as evident from generalized order parameter larger than 0.8 for residues Ala^{18}-Arg^{33}. The membrane-anchoring residues were identified by experiments utilizing micelle-integrating spin-labels such as 5- or 12-doxylstearate. In 5-doxylstearate a paramagnetic label is placed in vicinity of the polar headgroups (Brown *et al.*, 1981) and hence all resonances closer than about 10 Å to the spin-label are significantly broadened through efficient spin, electron relaxation. Thereby, we discovered that NPY is anchored to the membrane through interaction of the phospholipids with the long and hydrophobic side-chains of residues of the C-terminal helix.

Here, we examine the structure and dynamics of [Ala^{31}, Pro^{32}]-NPY bound to DPC micelles by ^{1}H NMR and analysis of ^{15}N-relaxation data. The results are compared with the solution structure of [Ala^{31}, Aib^{32}]-NPY and wild-type NPY. We find that Y_5 receptor-selectivity is most probably related to the destabilization of the α-helical conformation at the C-terminal tetrapeptide, as shown for [Ala^{31}, Aib^{32}]-NPY in aqueous solution as well as for [Ala^{31}, Pro^{32}]-NPY bound to DPC micelles. The structure of [Ala^{31}, Pro^{32}]-NPY differs from the fold of NPY in aqueous

solution in two ways: Firstly, as already observed in the case of NPY bound to DPC micelles, the C-terminal tyrosine-amide is placed closer to the membrane-water interface of the micelles. Secondly, the C terminus of [Ala^{31}, Pro^{32}]-NPY adopts a large and flexible loop that is differently anchored to the membrane by residues 30 and 36. In contrast, in native NPY a regular α-helical turn is found, which is anchored by residues 32 and 36. Implications of these findings for a possible alternative binding mode at the Y_5 receptor are discussed.

4.2. Results

We have defined the experimental conditions for the determination of the structure and dynamics of [Ala^{31},Pro^{32}]-NPY highly similarly to those described for wild-type pNPY (Bader *et al.*, 2001) thereby allowing a direct comparison of the data. In doing so, diagnostic structural properties of [Ala^{31},Pro^{32}]-NPY that might be typical for selectivity at the Y_5 receptor can possibly be identified.

In the presence of 300 mM DPC at pH 6.0, wild-type pNPY is monomeric and bound to the micelles. However, in spite of the elevated pH, only the amide protons of the first three N-terminal residues were significantly affected by exchange broadening. Moreover, the α-helix became stabilized and the signal dispersion was increased due to the presence of polar and charged headgroups. For many peptide hormones like opioids and neurokinins (Schwyzer, 1986; Schwyzer, 1987), parathyroid hormone (Pellegrini & Mierke, 1999b) and cholecystokinin (Moroder *et al.*, 1993; Pellegrini & Mierke, 1999a) a pathway for receptor binding that includes membrane association as an initial step has been proposed. We therefore

felt encouraged to conduct our studies in a membrane-mimicking environment.

The chemical shifts of the proton resonances were assigned according to standard methodology (Wüthrich, 1986). The assignments for the N-terminal residues Tyr^{1}–Arg^{19} were supported by the fact that they were nearly perfectly identical to the values found for NPY on DPC micelles (Bader *et al.*, 2001). The residue-specific nitrogen frequencies could subsequently be determined using [^{15}N,^{1}H]-HSQC and NOE-relayed [^{15}N,^{1}H]-HSQC-correlation maps. Again, the resonances of residues Tyr^{1}-Arg^{19} were very similar in both peptides (Figure 4.1 CDE).

Secondary chemical shifts

Wishart *et al.* (1991) found a strong relationship between chemical shifts and the protein conformation, and the chemical shift index (CSI) introduced by them has been recognized as a simple and rapid method to assign secondary structure elements solely based on the analysis of the chemical shifts. For proteins in a α-helical conformation it was discovered that the ^{1}H NMR chemical shift of the $C_{\alpha}H$ proton of all 20 naturally occurring amino acids experience a mean upfield shift of 0.39 ppm with respect to the values encountered in disordered (random coil) conformations. This relationship, which was originally based on empirical (statistical) data could later on be theoretically validated by *ab inito* quantum-mechanical calculations of H^{N} and ^{15}N chemical shifts (deDios, 1996). For ^{15}N nuclei, major factors determining the chemical shift are χ^{1} side-chain conformations, direct (and to a lesser amount indirect) effects due to hydrogen bonding as well as the electrostatic field of the protein. According to the CSI protocol of Wishart *et al.* (1992), [Ala^{31},Pro^{32}]-NPY is uniquely folded into a α-helical conformation between residues

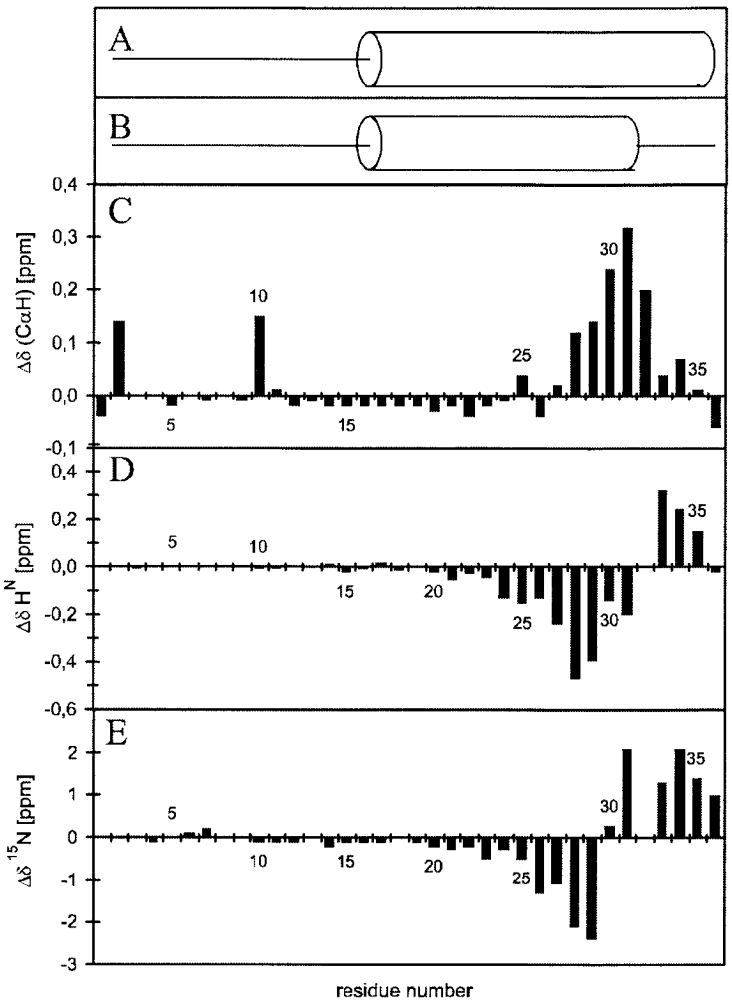

Figure 4.1 (A) Secondary structure of NPY on DPC micelles according to Bader *et al.* (2001). (B) Secondary structure of [Ala^{31}, Pro^{32}]-NPY on DPC micelles (this work). (C) Secondary chemical shift differences for the CαH, (D) for the H^N, (E) for the ^{15}N resonance between [Ala^{31}, Pro^{32}]-NPY and NPY bound to DPC micelles. The secondary chemical shift deviations of the CαH, the H^N protons and ^{15}N of NPY, respectively, were subtracted from the corresponding values of [Ala^{31}, Pro^{32}]-NPY. Sequence-corrected values were used for the calculation of the ^{15}N secondary chemical shift deviations (Braun *et al.*, 1994). .

Asp^{16}–Ala^{31} (Figure 4.1 B) (for a complete listing of the proton chemical shifts and their deviations from the corresponding random coil values (the so-called secondary chemical shifts) see the supplementary material), a finding which is clearly confirmed by NOE and supported by ^{15}N

relaxation data (S^2>0.5) (see below).

Based upon a comparison of secondary chemical shifts of $C_\alpha H$, H^N and ^{15}N resonances as derived from the Y_5 receptor-selective mutant [Ala^{31}, Pro^{32}]-NPY and from wild-type NPY we recognize that: (1) Consecutive downfield differences in the secondary chemical shifts of the $C_\alpha H$ proton larger than 0.1 ppm are observed only in the segment Asn^{29}-Arg^{33}, indicating a local perturbation/destabilization of the secondary structure with respect to the α-helix which is normally found in wild-type NPY at this segment (Figure 4.1 C). (2) We noticed downfield secondary chemical shifts for the amide protons of [Ala^{31}, Pro^{32}]-NPY on the hydrophobic side following a periodic pattern. A similar pattern was discovered for pNPY bound to DPC micelles (Bader *et al.*, 2001) and was interpreted to indicate interactions of the phospholipid headgroups with the amide protons and/or weaker intramolecular hydrogen bonding of the lipid-exposed backbone amide protons (Zhou *et al.*, 1992; Wishart *et al.*, 1991). Moreover, it has been reported in literature that secondary chemical shifts of amide protons in α-helical conformations are often found to be periodic in amphiphilic helices (Kuntz *et al.*, 1991). (3) Interestingly, when directly comparing the resonance positions of [Ala^{31}, Pro^{32}]-NPY with wild-type NPY, increasing upfield secondary chemical shift differences are found for both the H^N and the corresponding ^{15}N resonances in the region of Tyr^{21}-Asn^{29} (Figure 4.1 DE). We contribute this effect to a stabilization of the α-helix in that segment of the polypeptide chain. This stabilizing effect is also evident from the scalar $^3J_{HN\alpha}$ couplings and the generalized order parameters S^2 (*vide supra*). The decrease of the absolute value for residues Leu^{30} and Ala^{31} most likely reflects an indirect effect (deDios, 1996) due to the loss of hydrogen bonds of the corresponding carbonyl oxygens to amide protons from residues further down the sequence. (4) Pronounced downfield secondary chemical shift differences are found at Arg^{33}/Gln^{34} for both H^N and ^{15}N reso-

nances, which is attributed to increased flexibility at the C terminus of the mutant. It may also be due to an increased distance to the charged headgroups of the phospholipids. Again, this finding is further supported by coupling constants and relaxation data (see below).

Interresidual NOEs and coupling constants

Except for unresolved cross-peaks between the residue pairs 19/20, 21/22 and 24/25 all of the possible H^N_i / H^N_{i+1} sequential NOEs were observed in the segment 14-31, which is indicative for a well-structured peptide in helical conformation (Wüthrich, 1986). In full agreement with this suggestion, many H^α_i / H^N_{i+3} and H^α_i / H^β_{i+3} NOE connectivities are present throughout this region (Figure 4.2). Interestingly, both types

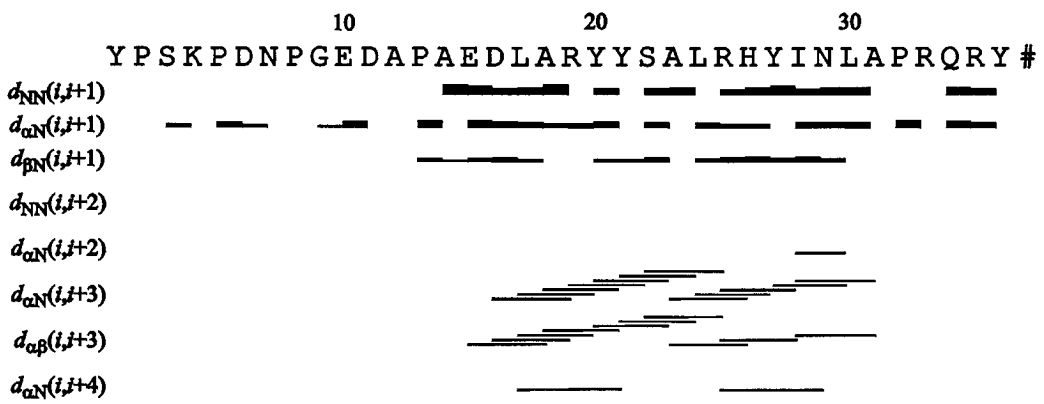

Figure 4.2 Summary of the meaningful distances as derived from the interresidual NOEs between the backbone H^N, H^α and H^β of [Ala^{31}, Pro^{32}]-NPY on DPC micelles.

of (*i*,*i*+3) NOE crosspeaks are missing between residues 26 and 29, replaced by an H^α_{25} / H^N_{29} NOE. On the contrary, an H^α_i / H^N_{i+2} NOE is found between residues 29 and 31. This is compatible with the view that the two subsequent α-helical turns as found in wild-type NPY are modified to form a wider turn between residues 25 and 29 and a more narrow one between 28 and 31 in the mutant, possibly due to different

side-chain/membrane interactions (see below). Any medium-range NOEs are completely lacking at the C-terminal pentapeptide, suggesting this segment to be in a more extended rather than helical conformation.

Figure 4.3 shows the CD spectra of NPY and the mutant each of them

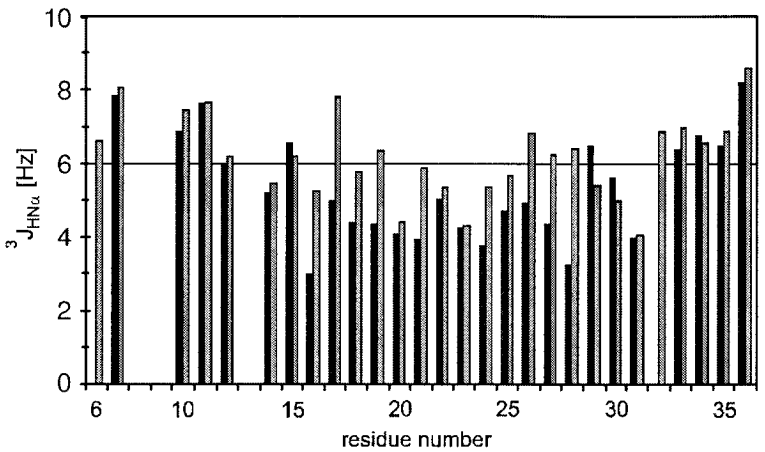

Figure 4.3 Comparison of the vicinal $^3J_{HN\alpha}$ coupling constants between [Ala^{31}, Pro^{32}]-NPY (black bars) and NPY (shaded bars) bound to DPC micelles.

on DPC micelles at pH 6.0 and 37°C. Both curves indicate a maximum at 192 nm and a minimum at 209 nm. A second local minimum at 220 nm indicating the presence of α-helical conformation, is clearly less intense in the mutant compared to wild-type NPY. Again, this demonstrates the reduction of helicity upon substitution of Ile^{31}-Thr^{32} by Ala-Pro and supports the results obtained for another Y_5 receptor-selective mutant, [Ala^{31}, Aib^{32}]-NPY, studied in aqueous solution (Cabrele *et al.*, 2000).

A major difference between NPY and [Ala^{31}, Pro^{32}]-NPY concerns the values adopted by the vicinal $^3J_{HN\alpha}$ coupling constants of residues 16 – 28, all of which are in the range of 3-5 Hz and correspond to ϕ-angles similar to those found in stable α-helices (Karplus, 1963; Wang & Bax, 1996). Most of them are significantly higher in wild-type NPY, some even around 6 Hz (Bader *et al.*, 2001). This gives evidence for a rigidified backbone conformation of residues 16-28 in the Y_5 receptor-selective mutant.

Values > 6 Hz for the N-terminal residues as well as for the C-terminal tetrapeptide are similar in NPY and the mutant and they indicate rotationally averaged ϕ-angles usually encountered in more flexible segments (Figure 4.4).

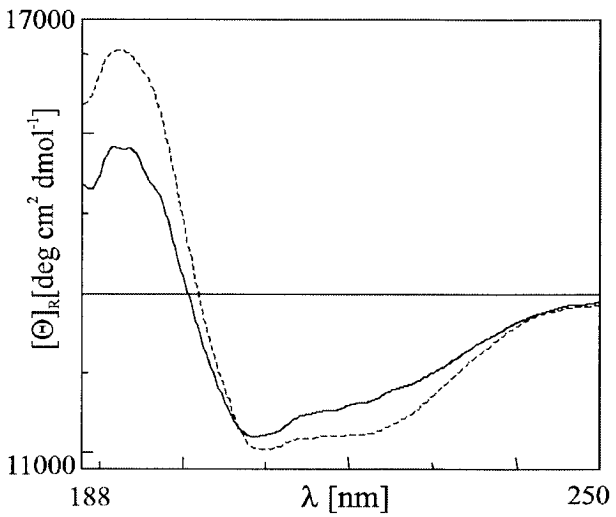

Figure 4.4 CD spectra of 50 μM [Ala^{31}, Pro^{32}]-NPY (—) and NPY (---) in the presence of 10 mM DPC micelles.

Three-dimensional structure

Some 30 low-energy three-dimensional structures were generated using a total of 67 intra-residual, 67 sequential and 73 medium-range (*i-j* = 2, 3, 4) meaningful upper-limit distance restraints and 145 dihedral angle restraints. The structures were calculated with molecular dynamics in torsion angle space using a simulated annealing protocol as implemented in the program DYANA (Güntert *et al.*, 1997), followed by an energy minimization with the AMBER (Weiner *et al.*, 1986) force field. The 17 lowest NMR-energy term structures out of this set were further surveyed. They contained no distance violations larger than 0.15 Å . Statistical information on the structure calculation is provided in the supple-

mentary material. The residue-specific atomic root mean square deviation (RMSD) for the backbone heavy atoms decreased from 26.7 at Tyr^{1} to 1.3 at Asp^{16} and was < 1.0 in the region between Leu^{17} and Leu^{30}. At the C terminus it increased to 12.7 at Tyr^{36}. All the structures were α-helical in the segment between Asp^{16} and Leu^{30} (Figure 4.5). Best convergence of

Figure 4.5 Backbone atoms (Cα, N and C) of 17 minimized structures for [Ala^{31}, Pro^{32}]-NPY on DPC micelles, superimposed over the backbone atoms of residues Tyr^{21}-Asn^{29}.

the resulting structures was observed for the region between Tyr^{21} and Asn^{29} with a RMSD of 0.26(±0.10) Å for the backbone heavy atoms and 1.35(±0.37) Å for all heavy atoms, respectively. In most of the structures nearly all residues between Glu^{15} and Leu^{30} were involved in either (*i*,*i*+4) or (*i*,*i*+3) hydrogen bonds. Hence, the results from the tertiary structure calculation supported the suggestions based upon NOE pattern and chemical shift analysis. These findings are in accordance with the results from NMR relaxation measurements that showed a highly flexible N terminus, a stable helical segment consisting of residues Leu^{17} to Leu^{30} and a decrease in stability at the C terminus. The nearly complete lack of NOEs in the C-terminal pentapetide results in a highly disordered C ter-

minus. However, as shown by spin-label experiments (see below), the Tyr^{36}-amide comes into proximity of the membrane and can therefore be considered as being restrained to 2D diffusion on the micelle surface, rather than randomly diffusing in 3D space.

Topological orientation

The membrane-integrating 5-doxyl-stearic acid was added at a concentration of approximately 1 spin-label/micelle. The doxyl-group that contains an unpaired electron, becomes located in the vicinity of the headgroups at the micelle surface (Brown *et al.*, 1981) and thereby leads to enhanced relaxation rates of nuclei closer than about 10 Å to the spin-label. The resulting reduction in signal intensity was estimated from the relative peak volumes in a [^{15}N,^{1}H]-HSQC spectra recorded before and after addition of the spin-label. Furthermore, the results from these experiments were compared to the results obtained for wild-type NPY (Bader *et al.*, 2001) (Figure 4.6). A nearly identical pattern of relative intensities for both peptides is found at the N terminus up to residue 15. The 3-4 residue periodicity for the amount of reduction in signal intensity, which was also noticed in the case of NPY bound to DPC micelles and which is typical for helices associated parallel to the micelle surface, is observed in the segment 17-29. Local minima in signal intensity upon addition of 5-doxylstearate agree perfectly for residues 17, 21, 24/25 and 29. However, the signal intensity of Ile^{28} and Asn^{29} are very similarly affected in wt-NPY, whereas in [Ala^{31},Pro^{32}]-NPY the remaining signal intensity of Ile^{28} is three times larger than for Asn^{29} after addition of the spin-label. On the contrary, the signal of Leu^{30} is reduced to about the same extent as for Asn^{29} in wt-NPY. These findings suggest that membrane anchoring is no longer mediated by Ile^{28}/Asn^{29} as observed in NPY but rather shifts to Asn^{29}/Leu^{30} in the mutant.

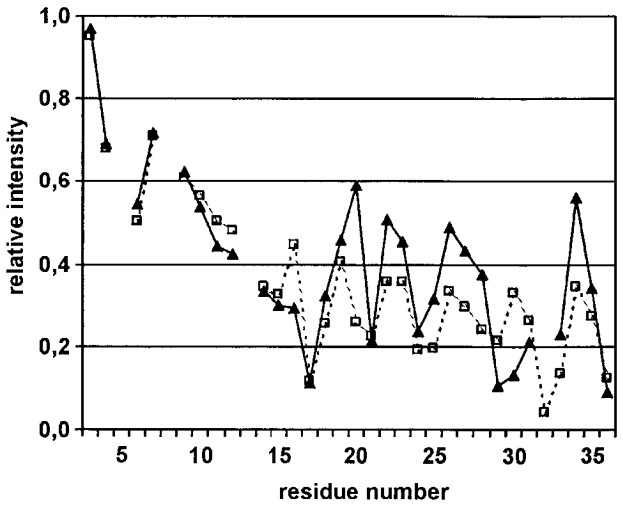

Figure 4.6 Comparison of the residual relative signal intensity in [^{15}N,^{1}H]-HSQC spectra between [Ala^{31}, Pro^{32}]-NPY (–▲–) and NPY (--▫--) bound to DPC micelles upon addition of 5 mM of the spin-labeled 5-doxylstearic acid.

Conclusions drawn from the chemical shift differences and from NOE data support the view that the most dramatic perturbation of the conformation is localized around residues 29/30. Apparently, many signals of nuclei in the helical segment comprising residues 17-28 are reduced to a lesser extent in the mutant compared to NPY. We therefore argue that the mean distance of these residues to the spin-label is larger due to a weaker membrane-association. Alternatively, the orientation of [Ala^{31}, Pro^{32}]-NPY may be better defined on the membrane such that certain protons are fixed in a position opposite to the membrane surface further away from the spin-label for most of the time. The latter argument implies that wt-NPY slightly wobbles about its helical axis when bound to the membrane. The weak reductions at the C terminus, especially for Gln^{34}, might be attributed to the already proposed increased flexibility in that segment. However, it has to be emphasized that the Tyr^{36}-amide belongs to the residues that are affected by the spin-label in both NPY and the Y_5 receptor-selective peptide to the largest extent. Thus, although the mutant is speculated to be more flexible between Arg^{33}-Tyr^{36}, the C

terminus cannot be considered to diffuse randomly in the aqueous environment but rather seems to be anchored onto the micelle surface.

Amide proton H/D exchange

By measuring the proton-deuterium exchange time-course for pNPY we previously found that nearly all peaks in a 2D [^{15}N,^{1}H]-HSQC spectrum had vanished only 10 minutes after addition of D_2O to a lyophilized sample, except for the signals of residues Leu^{24}, Arg^{25}, Tyr^{27}, Ile^{28} and Ile^{31}. Moreover, the signal of Ile^{28} was still strong after more than 70 minutes at 37°C, indicating that the most persistent contacts between NPY and the membrane surface are mediated by residues in the C-terminal half of the helix (Bader *et al.*, 2001). In [Ala^{31},Pro^{32}]-NPY, only the four peaks of residues 21 (Tyr), 24, 25 and 28 are still visible after 10 minutes. Moreover, in the mutant the most efficient shielding from solvent access is now observed for residue Leu24, which only disappears after 40 minutes of measurement. Obviously, the main association points with the membrane are shifted towards the N-terminal half of the helix in the mutant, whereas the lack of anchoring residues in positions 31 and 32 lead to a lower affinity of [Ala^{31},Pro^{32}]-NPY to DPC micelles.

Backbone-dynamics

To further characterize the [^{31}Ala,^{32}Pro]-NPY/DPC system we have probed the dynamics of the molecule using ^{15}N relaxation. The latter supplies information on the magnitude of motions of ^{1}H,^{15}N bond vectors in a coordinate system that is synchronized to overall tumbling. The present analysis is based on ^{15}N R_1 and R_2 relaxation rates recorded at both 500 and 600 MHz as well as ^{15}N{^{1}H}-NOE data at 500 MHz on a 1 mM uni-

formly ^{15}N labeled [Ala^{31},Pro^{32}]-NPY sample.

At 500 MHz, the average R_1 values for Lys^4-Ala^{14} and Asp^{16}-Tyr^{36} were 1.62 ± 0.11 Hz and 1.99 ± 0.12 Hz, respectively. R_2 is 2.12 ± 0.31 Hz at Lys^4-Ala^{12}, is 4.44 Hz at Ala^{14}, and increases to 10.0 up to residue Arg^{19}. It is 9.98 ± 1.34 Hz at Tyr^{20}-Ile^{31} and drops to 5.29 ± 0.60 Hz at the C-terminal tetrapeptide. At Lys^4-Ala^{14}, the heteronuclear NOE, which very sensitively reflects changes in rigidity, is negative (in the range of –8.38 and 0), adopts values from 0.36 to 0.67 between Asp^{16} and Tyr^{20} and is > 0.6 for almost all residues between Tyr^{21}-Ile^{28} (0.67 ± 0.07). Towards the C terminus, the value of the NOE steadily decreases from a value of 0.59 at Asn^{29} to 0.10 at Tyr^{36}. Due to problems in the peak volume integrations of residue 15, the corresponding relaxation rate constants could not be determined. The local fluctuations of the R_1 and R_2 data measured at 600 MHz are qualitatively very similar to the 500 MHz parameters (data not shown). Compared to wild-type NPY on DPC micelles, the R_1(500) are on average 22% (± 8 %) higher than those of the mutant, but the local fluctuations of the data are again very similar (Figure 4.7). The R_2(500) rates are similar for both peptides within ±1 Hz at nearly all residues between Lys^4-Ile^{28}. However, in the C-terminal segment comprising Asn^{29}-Tyr^{36} they are systematically lower in the mutant by 2 – 3.75 Hz, indicating increased flexibility for that part of the backbone. In accordance with the R_2 rates, systematically lowered NOEs (between -0.12 and -0.32) are found at the C-terminal hexapeptide Leu^{30}-Tyr^{36}.

Similarly to our analysis for wt-NPY bound to DPC micelles (Bader *et al.*, 2001), we calculated the correlation time for overall tumbling, the generalized order parameters and effective correlation times for internal motions on one or two different time-scales according to the Model-Free approach (Lipari & Szabo, 1982a; Lipari & Szabo, 1982b; Clore *et al.*, 1990). The first estimate of the overall (isotropic) rotational correlation

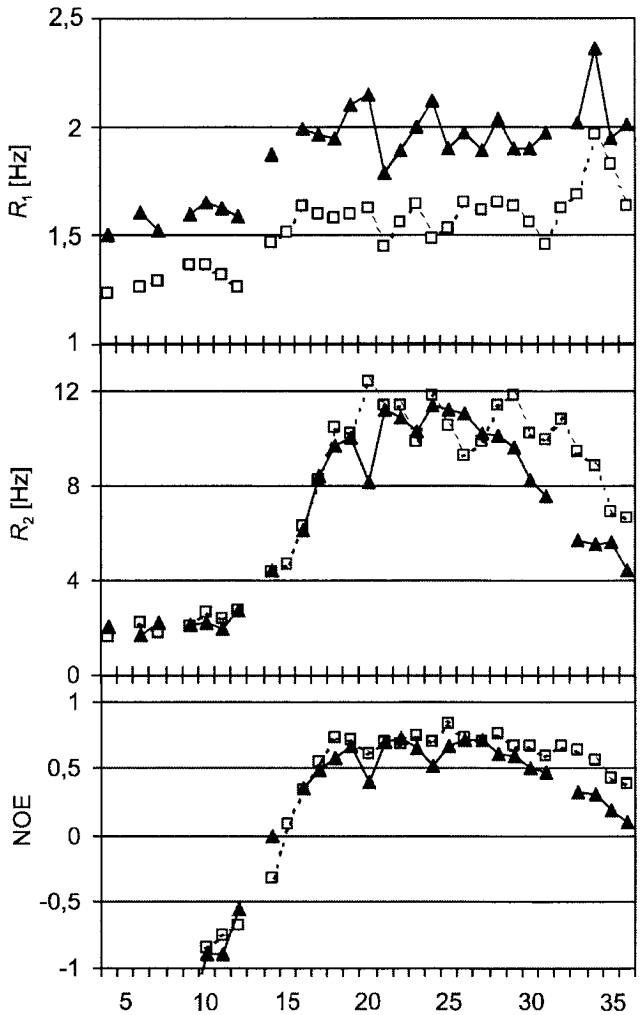

Figure 4.7 Comparison of the ^{15}N-relaxation rate constants R_1, R_2 and $^{15}N\{^1H\}$-NOEs between [Ala^{31}, Pro^{32}]-NPY (–▲–) and NPY (--▫--) bound to DPC micelles, determined at 500 MHz, vs. the residue number.

time was obtained from the average value of R_2/R_1 nuclei for residues in the segment 21-29, for which the heteronuclear $NOE_{(500)}$ was larger than 0.6 (Kay *et al.*, 1989). These are $(R_2/R_1)_{500}$ = 5.49 (± 0.48) and $(R_2/R_1)_{600}$ = 8.04 (± 0.90), corresponding to correlation times τ_c of 8.17 ± 0.43 and 8.48 ± 0.56, respectively. Fixing τ_c = 8.2 ns, as estimated from the 500 MHz data, we selected the internal motional parameters S^2, S_f^2, S_s^2, t_e and R_{ex}, respectively, according to the statistical approach initially described by Mandel *et al.* (1995). Fitting to one of the proposed models was well pos-

sible for almost all residues, except Asp[11], Ala[12], Asp[16] and Asn[29], for which the sum-squared error residuals exceeded the 95% confidence interval of the χ^2-distribution slightly. However, replacement of the selected models by any of the more complex ones did not significantly improve the fits. Finally, the motions of residues Lys[4]-Asn[7] as well as Leu[17]-Leu[30] were described by the SMF, whereas the EMF was applied for fitting the relaxation data of the helix-capping residues Gly[9]-Asp[16] and Ile[31]-Tyr[36]. A small chemical exchange contribution of 1.8 Hz had to be introduced at Leu[24]. A complete listing of the parameter from the fit is given in the supplementary materials.

After the final optimization, the overall rotational correlation time was at 8.22 (± 0.09) ns, compared to the value of 8.96(± 0.10) ns as determined for wt-NPY bound to DPC micelles. The values of the derived generalized order parameter are similar for the N-terminal residues up to Arg[19] (Figure 4.8). However, systematically higher values of S^2 are

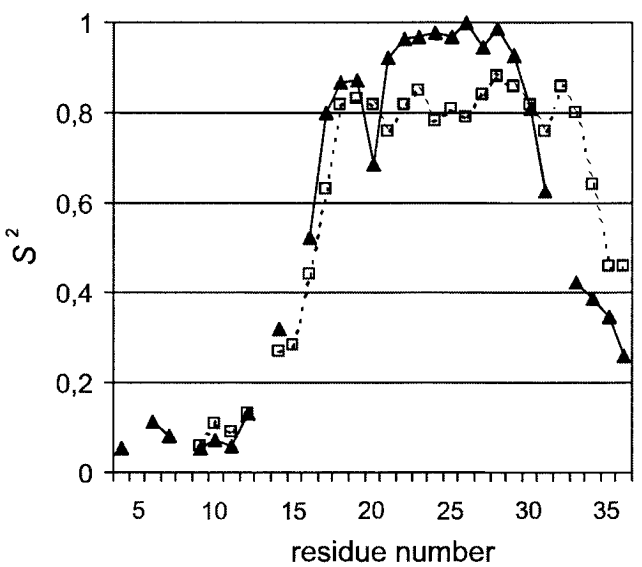

Figure 4.8 Comparison of the generalized order parameters S^2 between [Ala[31], Pro[32]]-NPY (–▲–) and NPY (--▫--) bound to DPC micelles, as determined from ^{15}N relaxation measurements.

encountered in the segment of residues Tyr^{21}-Asn^{29} of the Y_5 receptor-selective mutant, in which the backbone is almost perfectly rigid (S^2=0.96±0.03), compared to a mean order parameter of S^2=0.82 ± 0.04 between Ala^{18} and Arg^{33} for wt-NPY (Bader *et al.*, 2001). On the contrary, corresponding S^2 values are between 0.11 and 0.38 lower for Ala^{31}-Tyr^{36} in the mutant than in wt-NPY. Thus, the dipeptide [Ala^{31}, Pro^{32}] increases the flexibility mostly at the location of its introduction thereby confirming NOE and chemical shift data as well as coupling constants. On the other hand, the loss of rigidity of the mutant at the C terminus is counterbalanced by increased stability of the central part of the helix. Again, we speculate, that this fact might be due to a better anchoring and a more well-defined orientation of [Ala^{31}, Pro^{32}]-NPY on the membrane.

4.3. Discussion

Interest in Y_1 and Y_5 receptor subtypes has recently been steered by the fact that they are supposed to mediate the orexigenic action of NPY (Gehlert, 1999) and therefore present interesting targets for the design of anti-obesity drugs. The newly developed class of Y_5receptor-selective mutants (Cabrele *et al.*, 2000; Cabrele *et al.*, 2001; Cabrele *et al.*, *accompanying paper*), some of which could be shown to act as agonists, provide important tools to study the pharmacological role of this receptor subtype. Accordingly, [Ala^{31}, Aib^{32}]-NPY has served to demonstrate the importance of the Y_5 receptor in the stimulation of food intake (Cabrele *et al.*, 2000).

Of course, structure-based drug design would tremendously benefit from the knowledge of the peptide conformation in its receptor-bound

form. However, the difficulties in expression, purification and reconstitution of functional GPCRs have so far prevented direct structure determinations of ligand-GPCR complexes either by NMR or X-ray crystallography. Very recently, the conformation of the pituitary adenylate cyclase activating polypeptide mutant PACAP(1-21)-NH_2, bound to its GPCR has been solved using 2D transferred nuclear Overhauser effect spectroscopy (Inooka *et al.*, 2001). In their investigation Inooka *et al.* discovered that the C-terminal region comprising residues 8-21 forms a α-helix. This structure is very similar to that of micelle-bound PACAP (RMSD < 1 Å). However, a β-coil element for residues 3-7 of the N terminus exists only in the receptor-bound state, thereby producing a hydrophobic patch which is essential for receptor binding.

We believe that the observations on PACAP and our results presented in this work can be nicely explained within the framework of the message-address concept which was introduced by Schwyzer in his Membrane Compartments Theory (Schwyzer, 1986; Schwyzer, 1995). Accordingly, the amphipathic helical portion of PACAP and similarly of other peptide hormones serves as the address to target the molecule to the membrane surface. They do so by providing necessary contacts to the membrane through hydrophobic residues that intercalate into the lipid interior. These interactions stabilize the helix only in vicinity of a membrane such that otherwise unstructured peptides adopt a unique fold. The hormone then diffuses two-dimensionally laterally along the membrane surface in search of its receptor. Finally, receptor recognition and binding might go hand in hand with a conformational change (induced fit) at selected portions of the molecule (the so-called message) allowing for specific interactions between the ligand and the receptor. Such a two-step ligand transportation model (Inooka *et al.*, 2001) is supposed to be entropically favourable, since only a few dihedral angles in the flexible part of the molecule become conformationally restricted upon receptor

binding. Because of the mechanism that involves membrane association as a first step moderate to high affinity of the hormone to the membrane is required. High affinity binders display high on-rates and low-off rates for membrane binding. It has recently been emphasized that the two events are controlled by different mechanisms (see Selzer *et al.*, 2000, and references cited therein). High on-rates require far-reaching forces and are therefore promoted through favorable electrostatic forces. Low off-rates are most efficiently achieved through multiple hydrophobic contacts. In view of this concept NPY as well as the mutant are optimized in both respects: The C-terminal helix comprises hydrophobic membrane-surface exposed residues as well as positively charged Arg residues.

In close analogy to PACAP, the secondary structure of NPY can be characterized by a C-terminal α-helix (residues Asp^{16}-Tyr^{36}) and a completely flexible N terminus (Bader *et al.*, 2001; Cowley *et al.*, 1992; Monks *et al.*, 1996). Recently, we determined the structure, orientation and backbone dynamics of NPY on DPC micelles (Bader *et al.*, 2001). We found that the presence of the phospholipid membrane stabilizes the α-helix and induces a conformational change at the C-terminal tetrapeptide compared to the unligated solution structure of NPY. In our view Thr^{32} and Tyr^{36}-NH_2 anchor NPY on the membrane such that Arg^{33} and Arg^{35} are placed in the aqueous phase but still positioned close to the membrane surface. In doing so, they are able to make contacts to the receptor as a part of the message (see below). Similarly, the central part of the amphiphilic helix (residues 16-31) serves as the address targeting and orientating NPY on the membrane surface, whereas the N terminus is most probably another part of the message at some receptor subtypes.

In the presented class of NPY mutants (Cabrele *et al., accompanying paper*), selectivity in binding to the Y_5 receptor with retained high affinity is achieved through introduction of the dipeptide [Ala^{31}, Xxx^{32}] with Xxx being either Aib, Pro or Hyp just next to the C-terminal message

sequence. In order to understand the selective recognition of these mutants by only one receptor subtype on a structural level, we focus our analysis in the following on differences between [Ala^{31}, Pro^{32}]-NPY and wt-NPY with respect to their structure and dynamics in the presence of the membrane mimicking dodecylphosphocholine micelles.

Summarizing our results we find: (1) None of the measured data are indicative of significant differences with respect to structure or dynamics for the N-terminal residues 1-20 between NPY and the mutant. (2) Chemical shift data and $^{3}J_{HN\alpha}$ coupling constants as well as generalized order parameters determined from ^{15}N relaxation parameters clearly demonstrate a rather rigid backbone between residues Tyr^{21}-Asn^{29} in the mutant, while NPY exhibits some residual flexibility. Such an increase in rigidity of the helix might compensate for the entropic gain of the C-terminal pentapeptide sequence. Alternatively, more extended helices that are stably anchored to micelle surfaces need to become more flexible in order to accommodate for the surface bend and the fact that there is little long-range order of the lipid molecules. (3) We have identified a slightly altered membrane-anchoring mode in the mutant. The anchoring residues were recognized by their proximity to the membrane-integrating spin-label and displayed largest levels of signal reduction at residues 17, 21, 24, 29/30 and 36. Hence, the anchor at residue 28/29 in wt-NPY is shifted to residue 29/30 in the mutant. Moreover, the absolute differences between minima and maxima were more pronounced than in wt-NPY. We propose that the orientation of [Ala^{31}, Pro^{32}]-NPY with respect to the membrane surface may be very well defined whereas wt-NPY slightly wobbles about its helical axis. Moreover, a proton-deuterium exchange experiments shows a faster overall exchange kinetics in the mutant. The most efficient shielding from the solvent is observed for the amide proton of Leu^{24} in the mutant. We therefore propose that the principal site mediating membrane association is shifted from Ile^{28} in wt-

NPY to Leu^{24}/Tyr^{21} in the mutant, possibly due to the substitution of membrane anchoring residues Ile^{31}-Thr^{32}. In combination with the significantly lower overall correlation time of [Ala^{31}, Pro^{32}]-NPY we suggest a weaker membrane affinity constant for this type of NPY mutants. (4) Finally, we notice the lack of $H_{\alpha N}$ (*i*, *i*+3) NOEs between residues 26 and 29. Together with the fact that the membrane anchor is shifted by one position towards the C terminus in this part we propose a π-helical turn for the mutant at the end of the helix rather than an α-helix. (5) As mentioned above, the increased rigidity in the central helix of the mutant is compensated by a much more flexible C-terminal pentapeptide. The positions of the mutations present starting points after which the regular secondary structure is interrupted. This is evident from lowered order parameters, the lack of medium-range NOEs and from secondary chemical shifts which are more close to the random coil values for [Ala^{31}, Pro^{32}]-NPY. However, Tyr^{36}-NH_2 is apparently again in close vicinity to the membrane, a fact that is obvious from the signal reductions for protons of this moiety observed in the spin-label experiment, and hence the C terminus folds back onto the membrane surface. This interpretation is further supported by decreasing secondary chemical shift differences of H^N and CαH protons between the mutant and NPY.

In the following we would like to comment briefly on two points of interest. Firstly, the more pronounced differences between minima and maxima of signal reductions in the spin-label experiment add further evidence for a more stable helix in the segment comprising residues Tyr^{21}-Asn^{29} in the mutant. Any residual flexibility will allow (membrane-averted) protons of the hydrophilic side of the helix to approach the spin-label more closely for some time. Since the effect of the spin-label depends on the sixth power of the distance this will have a remarkable effect on the observed signal reductions and will level off the differences to some extent. Secondly, a contradiction seems to exist between the

steady decrease of the generalized order parameter S^2 towards the C terminus and the statement that the C-terminal Tyr36-NH_2 group serves as a membrane anchor. However, we like to emphasize that the spin-label only probes the distance to the membrane surface. In accordance with both data we propose that the C-terminal tetrapeptide segment diffuses freely in two dimensions along the membrane surface around its anchor point at residue 29/30. In doing so, the order parameter will decrease in the observed fashion but the membrane anchor will keep the last residue still close to the surface. In that context it is of interest to notice that the order parameter decreases more slowly at the C-cap of the helix than at the N-cap which can be explained by the additional terminal anchor. Finally, a change in the orientation (as is expected by introduction of D-Pro instead of Pro at position 32) abolishes any binding affinity for the Y_5 receptor. In an attempt to visualize these statements, we propose a model for the conformation at the C terminus as shown in Figure 4.9. To sum-

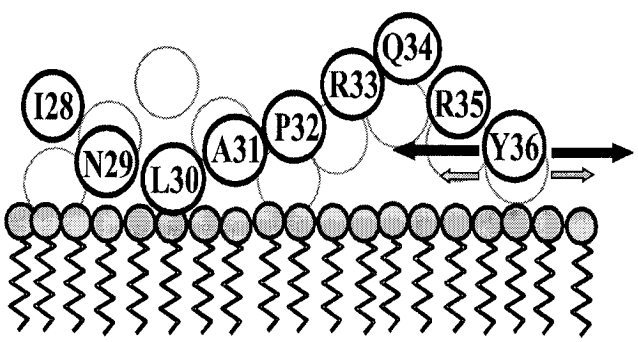

Figure 4.9 Model for the topological orientation of the C-terminal loop of [Ala^{31}, Pro^{32}]-NPY on the dodecylphosphocholine micelle surface. The corresponding spatial arrangements of residues of NPY are shown in grey for comparison.

marize, the pentapeptide Ala^{31}-Arg^{35} can be considered as a flexible loop being anchored to the membrane through residues Asn^{29}/Leu^{30} as well as through Tyr^{36}-NH_2.

In summary we draw the following scenario of the events that finally

lead to receptor recognition of NPY and subtype selective mutants: In a first step, the hydrophobic side of the amphiphilic helix of NPY binds to the membrane. Considering the fact that in the presence of DPC micelles only a single set of resonances is observed in the $^{15}N,^{1}H$ correlation map and that all NOE data can be fitted to a single structure without problems we conclude that it is the membrane-bound form that predominates and makes the inital receptor contact. Moreover, removal of the hormone from the membrane is energetically unfavorable. Minakata *et al.* (1989) had designed five amphiphilic NPY models with multiple substitutions on the hydrophobic side of the helix between residues 13-32. From their data they had demonstrated that the surfactant properties of NPY result from its potential to form amphiphilic secondary structures and not from specific amino acid sequences in this region. In one of the peptides they changed three hydrophobic residues by leucines and three tyrosines by phenylalanines. Although this changed the conformation and self-association in solution, this peptide showed nevertheless 20% of the potency of NPY in inhibiting the electrically stimulated contractions of the rat *vas deferens*. Hence, the main role of the hydrophobic residues might be anchoring on the membrane rather than specific interactions with the receptor. We suggest, that upon binding to the membrane, some residues on the hydrophilic side are pre-positioned so that receptor recognition is facilitated. These are for instance Arg^{33} and/or Arg^{35}, that may not be substituted by alanine without dramatic or complete loss of activity at the Y receptors, respectively (Beck-Sickinger *et al.*, 1994; McCrea *et al.*, 2000; Eckard *et al.*, 2001). In the Y_5 receptor selective mutants these residues are exposed to the aqueous environment in a wider loop anchored by residues 29/30 and 36 on the membrane. In NPY, Arg^{33} and Arg^{35} are placed in the aqueous compartment as well, but in a regular α-helical turn anchored to the membrane by residues 32 and 36. As a consequence the basic residues are more flexible in the mutant and their distance from the

membrane, water interface is larger on average. During the initial contact with the receptor, these charged residues are likely to form an electrostatic attraction with basic residues from the receptor loops, *e.g.* a salt-bridge, that may very favorably contribute to the free energy of binding and hence increase the affinity to the receptor. Selzer *et al.* (2000) succeeded in the design of faster associating protein complexes by incorporating charged residues in the vicinity of the binding interface, based on the fact that the rate of association can be increased by favourable electrostatic interactions. Similarly, we speculate that the presented class of NPY mutants is attracted only by the Y_5 receptor subtype due to a favourable distribution of negatively charged residues. Such a favorable electrostatic attraction due to a Arg-Asp interaction was observed by Giragossian & Mierke (2001) in their structure of CCK-8 bound to the DPC-anchored CCK-receptor. Once, NPY or the mutants have been guided into close vicinity of residues from the loop, other contacts in the receptor,ligand complex which triggers the intracellular signal may be formed via induced fit. We like to emphasize that our view is important for the *inital* contact and that further data on the receptor,ligand complex are required. However, Inooka *et al.* (2001) have recently discovered, that the membrane bound conformation of the peptide PACAP is very similar to the conformation in the complex.

4.4. Materials and Methods

Materials

$^{15}NH_4Cl$ was purchased from Martek (Columbia, USA), deuterated DPC-d_{38} (99%-d), and methanol-d_3 were ordered from Cambridge Isotope Laboratories (Andover, Massachusets, USA). 5-doxylstearic acid was bought from Aldrich (Buchs, Switzerland). Isotopically non-enriched DPC was obtained from Avanti Polar Lipids (Alabaster, AL, USA). Oligonucleotide primers were synthesized by Microsynth GmbH (Balgach, Switzerland).

Peptide synthesis

Isotopically non-enriched peptide [Ala^{31}, Pro^{32}]-pNPY was prepared by solid-phase peptide synthesis using Fmoc (9-fluorenylmethoxycarbonyl) protection group strategy on a robot system (Syro, MultiSynTech, Bochum), as described (Cabrele *et al., accompanying paper*). In order to obtain the peptide amide, 4-(2',4'-dimethoxyphenyl- Fmoc-aminomethyl)phenoxy resin was used as polymeric support (Novabiochem, Läufelingen, Switzerland). The purity and the molecular weight were checked by reversed-phase HPLC (column C-18, 3x125mm, 5mm, flow 0.6ml/min, gradient 20% acetonitrile to 70% acetonitrile in water/trifluoroacetic acid (100:0.1) within 30 min) and electron spray ionization (ESI) - mass spectrometry (MS) (SSQ710, Finnigan, San Jose, CA), respectively.

Cloning, expression, and purification of uniformly ^{15}N enriched [Ala^{31}, Pro^{32}]-pNPY

Starting from the plasmid pUBK19/NPY-G (Bader *et al.*, 2001) that contains the pNPY-Gly DNA fused to the nucleotide sequence of N-terminally decahistidine-tagged yeast ubiquitin (Ub) (Kohno *et al.*, 1998), the double mutations I31A/T32P were introduced by site-directed mutagenesis using the

QuikChange Mutagenesis Kit (Stratagene). The two complementary primers required in this method (Weiner *et al.*, 1994) were chosen as follows: forward: 5′-CGCTGCGTCACTACATCAACCTGGCTCCGCGTCAGCGTTACGGGTGAT-AGTCG-3′ and reverse: 5′-CGACTATCACCCGTAACGCTGACGCGGAGC-CAGGTTGATGTAGTGACGCAGCG-3′. For the selection of DNA bearing the mutation, methylated and hemimethylated DNA was digested with *Dpn*I (New England Biolabs) and subsequently transformed into *Escherichia coli* XL2-Blue strain (Stratagene). The sequence of the resultant plasmid pUBK19/{AP}-NPY-G was confirmed using dideoxy-sequencing.

Expression of uniformly ^{15}N-labeled H_{10}-Ub-[Ala^{31}, Pro^{32}]-NPY-G was performed in the E. coli BL21 (DE3) strain on M9 minimal medium with $^{15}NH_4Cl$ as the sole nitrogen source as described previously (Bader *et al.*, 2001). Isolation under denaturing conditions (6 M guanidine hydrochloride, 50 mM Tris pH 8.0, 100 mM NaCl, 1 mM β-mercaptoethanol), purification (using Ni^{2+} affinity chromatography including on-column refolding by continuously decreasing the guanidine concentration of the refolding buffer from 6 M to 0 M), and cleavage of the fusion protein by use of ubiquitin hydrolase was done according to the protocol by Kohno (Kohno *et al.*, 1998). The separation of [Ala^{31}, Pro^{32}]-NPY-G from H_{10}-Ub was achieved on a Ni^{2+}-NTA-Agarose column (Qiagen, Basel, Switzerland) followed by desalting of the eluate using Sep-Pak Plus C_{18} cartridges (10% acetonitrile to 50% acetonitrile in 0.1% trifluoroacetic acid in steps of 10%/10 ml each). The C-terminal α-amidation of [Ala^{31}, Pro^{32}]-NPY-G using peptidylglycine α-amidating enzyme (EC 1.14.17.3; Unigene Laboratories, Fairfield, NJ., USA) was performed as described previously (Bader *et al.*, 2001). Completeness of the reaction was checked by electrospray ionization mass spectrometry upon reversed phase C_{18} chromatography purification.

CD spectroscopy

CD spectra were recorded on a JASCO J-720 spectropolarimeter over the range of 180 – 250 nm at 37°C using a water-jacketed 5-mm sample cell. The peptide concentration was 50 mM in the presence of 10 mM DPC in water at pH 6.0. The response time was set to 2 sec at a scan speed of 20 nm/min. The sensitivity range was at 10 mdeg, the step resolution at 0.2 nm and the band-width at 2 nm. The background-spectrum due to the detergent was subtracted from the spectra of the peptide-containing solutions. High frequency noise was reduced by

application of a low-path Fourier transform filter. Each measurement was performed four times. The ellipticity is expressed as mean residue molar ellipticity $[\Theta]_R$ in deg cm^2 $dmol^{-1}$. The helix-content was estimated according to method of Chen *et al.* (1974).

NMR spectroscopy

The NMR spectra used for the assignment of proton chemical shifts and derivation of distance and dihedral angle restraints were measured using samples containing 2.5 mM [Ala^{31}, Pro^{32}]-pNPY, 300 mM dodecylphosphocholine-d_{38} in either 10% D_2O/90% H_2O or 99% D_2O at pH 6.0 (uncorrected pH meter reading) and 37°C on a Bruker Avance 600 MHz spectrometer. For measurements of ^{15}N relaxation data uniformly ^{15}N enriched (>99%) [Ala^{31}, Pro^{32}]-pNPY was used at a concentration of 1.0 mM in the presence of 300 mM DPC-d_{38} in 10% D_2O/90% H_2O at 37°C. The pH was adjusted to 6.0 and data were recorded on both a Bruker Avance 500 and a Bruker Avance 600 instruments operating at nitrogen frequencies of 50.68 MHz and 60.81 MHz, respectively. Proton chemical shifts were referenced relative to the water line ($\delta(H_2O)$ = 4.63 ppm at 310 K) and nitrogen shifts were referenced indirectly to liquid NH_3 (Live *et al.*, 1984). The spectra were processed using the Bruker XWINNMR-2.1 software and transferred into the XEASY (Bartels *et al.*, 1995) program. Peak volumes were integrated within the program SPSCAN that uses lineshape-deconvolution of signals for proper integration of partially overlapping peaks.

For the identification of the amino acid spin systems a clean TOCSY (Griesinger *et al.*, 1988) experiment with a mixing time of 12 ms utilizing continuous-wave presaturation of the water resonance was recorded. NOESY experiments (Macura & Ernst; 1980, Kumar *et al.*, 1980) incorporating a filter scheme for zero-quantum suppression (Otting, 1990) with a mixing time of 75 ms was used for both the sequence-specific sequential resonance assignment and the determination of upper proton,proton distance limits required for the structure calculation. Water suppression was obtained using the WATERGATE sequence (Piotto *et al.*, 1992). Scalar $^3J_{HN\alpha}$ coupling constants were derived from inverse Fourier transformation of in-phase NOESY peaks involving H^N protons (Szyperski *et al.*, 1992).

The assignment of nitrogen frequencies and relaxation experiments were derived from [^{15}N,^1H]-HSQC (Bodenhausen & Ruben, 1980) experiments utiliz-

ing the sensitivity enhancement element (Palmer *et al.*, 1991a; Kay *et al.*, 1992) and water-flip back methodology (Grzesiek & Bax, 1993). The assignment of the proton, nitrogen correlation maps was significantly supported by information from a 150 ms NOE-relayed [^{15}N,^{1}H]-HSQC experiment.

Relaxation measurements were performed as described (Bader *et al.*, 2001). In essence, proton-detected versions of Carr-Purcell-Meiboom-Gill (R_2), inversion-recovery (R_1) and steady-state ^{15}N{^{1}H} heteronuclear Overhauser effect sequences were used. Water-suppression in all these experiments was achieved through application of pulsed-field gradients in coherence-selection schemes. For R_1 and R_2 experiments recycle delays of 2.2 s and for the ^{15}N{^{1}H}-NOE delays of 3.2 sec were applied. For R_1 (R_2) experiments 16 (32) scans were accumulated for each increment and 64 scans for each increment in the ^{15}N{^{1}H}-NOE. The R_1 series used the following relaxation delays: 0.03, 0.12, 0.21, 0.76, 1.23, 1.99 and 3.00 seconds. The R_2 series was run with the following delay settings: 0.004, 0.012, 0.02, 0.04, 0.1, 0.2, 0.4, 0.6 seconds. Buildup of the NOE was achieved through a pulse train of 120 degree proton pulses separated by 5 ms over a period of 3 seconds.

Spin-label experiment

The orientation of [Ala^{31}, Pro^{32}]-NPY with respect to the membrane surface was determined by measuring the effect of the micelle-integrating 5-doxyl-stearic acid on relaxation of the backbone ^{1}H^{N} and ^{15}N^{HN} signals through distance-dependent electron-,nuclear-spin relaxation as observed in a [^{15}N,^{1}H]-HSQC spectrum. The methodology has been described for wild-type pNPY in Bader *et al.* (2001). The intensities of the cross-peaks before and after addition of the spin-label were determined and compared.

Hydrogen exchange

For the measurement of proton-deuterium exchange of the amide protons, a protonated ^{15}N-[Ala^{31},Pro^{32}]-NPY sample was dissolved in D_2O and 2D [^{15}N,^{1}H]-HSQC spectra were recorded at different time intervals. Thereby, the

disappearance of the ^{15}NH was monitored 10, 40, and 70 minutes, respectively, upon addition of the solvent.

Structure calculation

The structure calculation was performed by restrained molecular dynamics in torsion angle space using a simulated annealing protocol as implemented in the program DYANA (Güntert *et al.*, 1997), similar to the procedure described previously for pNPY (Bader *et al.*, 2001). From a total of 622 unambiguously assigned NOE cross-peaks and 26 $^3J_{HN\alpha}$ coupling constants (of which only those 16 were included that were indicative of non-rotationally averaged torsion angles, *i.e.*, < 6 Hz), 207 meaningful upper distance limits, as well as 145 ϕ, ψ, χ^1, and χ^2 torsion angle restraints were derived. In no case it was possible to obtain stereospecific assignments. The final DYANA calculation was performed with 100 randomized starting structures, and the 30 DYANA conformers with the lowest target function were further refined using the AMBER (Weiner *et al.*, 1986) force-field as implemented in the program OPAL (Luginbühl *et al.*, 1996). The quality of the final 17 energy-minimized conformers with NMR energies less than 3 kcal/mol was checked in the range of residues 17-29 using the program PROCHECK-NMR (Laskowski *et al.*, 1996). The figures were prepared with the program MOLMOL (Koradi *et al.*, 1996). The NMR ensemble of 17 energy-minimized conformers has been deposited in the Research Collaboratory for Structural Bioinformatics PDB code 1ICY.

Relaxation data analysis

Relaxation rate constants R_1, R_2 and NOE enhancements including their associated uncertainties were determined as previously described for wild-type pNPY (Bader *et al.*, 2001). The parameters were interpreted by application of the modelfree-approach (Lipari & Szabo, 1982a; Lipari & Szabo, 1982b; Clore *et al.*, 1990) using the Modelfree (version 4.01) software package (Palmer *et al.*, 1991b; Mandel *et al.*, 1995). We followed the previously described protocols for estimation of the initial overall rotational correlation time, selection of model-free parameters for adequate description of the experimental relaxation data and

optimization of the motional parameters (Bader *et al.*, 2001). The statistical approach suggested by Mandel *et al.* (1995) was applied, and the following models were used in the fitting procedure: (1) S^2; (2) S^2, τ_e; (3) S^2, R_{ex}, (4) S^2, τ_e, R_{ex}; (5) S^2_f, S^2_s, τ_e. Experimental errors for R_1 and R_2 at both applied fields were approx. 3% as determined from duplicated measurements. For large negative values of the $^{15}N\{^1H\}$-NOE saturation-transfer mediated effects due to more elevated water-amide proton exchange at pH=6 lead to largely erroneous values of the heteronuclear NOE and hence the data for residues 4, 6 and 7 were excluded from the analysis. Otherwise, the error was calculated from estimates of the baseplane noise in the spectra and set to approx. 10% or at minimum 0.1 for NOE values between –1 and +1.

4.5. References

Bader, R., Bettio, A., Beck-Sickinger, A. G. & Zerbe, O. (2001). Structure and dynamics of micelle-bound neuropeptide Y: Comparison with unligated NPY and implications for receptor selection. *J. Mol. Biol.* **305,** 307-329.

Bartels, C., Xia, T.-h., Billeter, M., Güntert, P. & Wüthrich, K. (1995). The program XEASY for computer-supported spectral analysis of biological macromolecules. *J. Biomol. NMR* **6,** 1-10.

Beck-Sickinger, A. G. & Jung, G. (1995). Structure-activity relationships of neuropeptide Y analogues with respect to Y_1 and Y_2 receptors. *Biopolymers* **37,** 123-142.

Beck-Sickinger, A. G., Wieland, H. A., Wittneben, H., Willim, K. D., Rudolf, K. & Jung, G. (1994). Complete L-alanine scan of neuropeptide Y reveals ligands binding to Y_1 and Y_2 receptors with distinguished conformations. *Eur. J. Biochem.* **225,** 947-958.

Blundell, T. L., Pitts, J. E., Tickle, I. J., Wood, S. P. & Wu, C.-W. (1981). X-ray analysis (1.4 Å resolution) of avian pancreatic polypeptide: Small globular protein hormone. *Proc. Natl Acad. Sci. USA* **78,** 4175-4179.

Bodenhausen, G. & Ruben, D. J. (1980). Natural abundance nitrogen-15 NMR by enhanced heteronuclear spectroscopy. *Chem. Phys. Lett.* **69,** 185-189.

Braun, D., Wider, G. & Wüthrich, K. (1994). Sequence-corrected ^{15}N "random coil" chemical shifts. *J. Am. Chem. Soc.* **116,** 8466-8469.

Brown, L. R., Bösch, C. & Wüthrich, K. (1981). Location and orientation relative to the micelle surface for glucagon in mixed micelles with dodecylphosphocholine: EPR and NMR studies. *Biochim. Biophys. Acta* **642,** 296-312.

Cabrele, C. & Beck-Sickinger, A. G. (2000). Molecular characterization of the ligand-receptor interaction of the neuropeptide Y family. *J. Pept. Sci.* **6,** 97-122.

Cabrele, C., Langer, M., Bader, R., Wieland, H. A., Doods, H. N., Zerbe, O. & Beck-Sickinger, A. G. (2000). The first selective agonist for the neuropeptide YY_5 receptor increases food intake in rats. *J. Biol. Chem.* **275,** 36043-36048.

Cabrele, C., Wieland, H. A., Langer, M., Stidsen, C. & Beck-Sickinger, A. G. (2001). Y-receptor affinity modulation by the design of pancreatic polypeptide/neuropeptide Y chimera led to Y_5-receptor ligands with picomolar affinity. *Peptides,* in press.

Chen, Y. H., Yang, J. T. & Chau, K. H. (1974). Determination of the helix and beta form of proteins in aqueous solution by circular dichroism. *Biochemistry* **13,** 3350-3359.

Clore, G. M., Driscoll, P. C., Wingfield, P. T. & Gronenborn, A. M. (1990). Analysis of the backbone dynamics of interleukin-1 beta using two- dimensional inverse detected heteronuclear ^{15}N-^{1}H NMR spectroscopy. *Biochemistry* **29,** 7387-7401.

Cowley, D. J., Hoflack, J. M., Pelton, J. T. & Saudek, V. (1992). Structure of neuropeptide Y dimer in solution. *Eur. J. Biochem.* **205,** 1099-1106.

Criscione, L., Rigollier, P., Batzl-Hartmann, C., Rueger, H., Stricker-Krongrad, A., Wyss, P., Brunner, L., Whitebread, S., Yamaguchi, Y., Gerald, C., Heurich, R. O., Walker, M. W., Chiesi, M., Schilling, W., Hofbauer, K. G. & Levens, N. (1998). Food intake in free-feeding and energy-deprived lean rats is mediated by the neuropeptide Y_5 receptor. *J. Clin. Invest.* **102,** 2136-2145.

Darbon, H., Bernassau, J. M., Deleuze, C., Chenu, J., Roussel, A. & Cambillau, C. (1992). Solution conformation of human neuropeptide Y by ^{1}H nuclear magnetic resonance and restrained molecular dynamics. *Eur. J. Biochem.* **209,** 765-771.

deDios, A. C. (1996). Ab initio calculations of the NMR chemical shift. *Prog. Nucl. Magn. Reson. Spectrosc.* **29,** 229-278.

Dumont, Y., Martel, J. C., Fournier, A., St-Pierre, S. & Quirion, R. (1992). Neuropeptide Y and neuropeptide Y receptor subtypes in brain and peripheral tissues. *Prog. Neurobiol.* **38,** 125-167.

Eckard, C. P., Cabrele, C., Wieland, H. A. & Beck-Sickinger, A. G. (2001). Molecular characterisation of NPY receptors using synthetic peptides and anti-receptor antibodies. *Molecules,* in press.

Giragossian, C. & Mierke, D. F. (2001). Intermolecular interactions between cholecystokinin-8 and the third extracellular loop of the cholecystokinin A receptor. *Biochemistry,* in press.

Gehlert, D. R. (1998). Multiple receptors for the pancreatic polypeptide (PP-fold) family: physiological implications. *Proc. Soc. Exp. Biol. Med.* **218,** 7-22.

Gehlert, D. R. (1999). Role of hypothalamic neuropeptide Y in feeding and obesity. *Neuropeptides* **33,** 329-338.

Griesinger, C., Otting, G., Wüthrich, K. & Ernst, R. R. (1988). Clean TOCSY for ^{1}H spin system identification in macromolecules. *J. Am. Chem. Soc.* **110,** 7870-7872.

Grzesiek, S. & Bax, A. (1993). The importance of not saturating H_2O in protein NMR. Application to sensitivity enhancement and NOE measurements. *J. Am. Chem. Soc.* **115,** 12593-12594.

Güntert, P., Mumenthaler, C. & Wüthrich, K. (1997). Torsion angle dynamics for NMR structure calculation with the new program DYANA. *J. Mol. Biol.* **273,** 283-298.

Henry, G. D. & Sykes, B. D. (1994). Methods to study membrane protein structure in solution. *Methods Enzymol.* **239,** 515-535.

Inooka, H., Ohtaki, T., Kitahara, O., Ikegami, T., Endo, S., Kitada, C., Ogi, K., Onda, H., Fujino, M. & Shirakawa, M. (2001). Conformation of a peptide ligand bound to its G-protein coupled receptor. *Nat. Struct. Biol.* **8,** 161-165.

Kanatani, A., Ito, J., Ishihara, A., Iwaasa, H., Fukuroda, T., Fukami, T., MacNeil, D. J., Van der Ploeg, L. H. & Ihara, M. (1998). NPY-induced feeding involves the action of a Y_1-like receptor in rodents. *Regul. Pept.* **75-76,** 409-415.

Karplus, M. (1963). Vicinal proton coupling in nuclear magnetic resonance. *J. Am. Chem. Soc.* **85,** 2870-2871.

Kay, L. E., Keifer, P. & Saarinen, T. (1992). Pure absorption gradient enhanced heteronuclear single-quantum correlation spectroscopy with improved sensitivity. *J. Am. Chem. Soc.* **114,** 10663 - 10665.

Kay, L. E., Torchia, D. A. & Bax, A. (1989). Backbone dynamics of proteins as studied by ^{15}N inverse detected heteronuclear NMR spectroscopy: application to staphylococcal nuclease. *Biochemistry* **28,** 8972-8979.

Kohno, T., Kusunoki, H., Sato, K. & Wakamatsu, K. (1998). A new general method for the biosynthesis of stable isotope-enriched peptides using a decahistidine-tagged ubiquitin fusion system: an application to the production of mastoparan-X uniformly enriched with ^{15}N and $^{15}N/^{13}C$. *J. Biomol. NMR* **12,** 109-121.

Koradi, R., Billeter, M. & Wüthrich, K. (1996). MOLMOL: a program for display and analysis of macromolecular structures. *J. Mol. Graph.* **14,** 51-55, 29-32.

Kumar, A., Ernst, R. R. & Wüthrich, K. (1980). A two-dimensional nuclear Overhauser enhancement (2D NOE) experiment for the elucidation of complete proton,proton cross-relaxation networks in biological macromolecules. *Biochem. Biophys. Res. Com.* **95,** 1-6.

Kuntz, I. D., Kosen, P. A. & Craig, E. C. (1991). Amide chemical shifts in many helices in peptides and proteins are periodic. *J. Am. Chem. Soc.* **113,** 1406-1408.

Laskowski, R. A., Rullmannn, J. A., MacArthur, M. W., Kaptein, R. & Thornton, J. M. (1996). AQUA and PROCHECK-NMR: programs for checking the quality of protein structures solved by NMR. *J. Biomol. NMR* **8,** 477-486.

Lauterwein, J., Bösch, C., Brown, L. R. & Wüthrich, K. (1979). Physicochemical studies of the protein-lipid interactions in melittin-containing micelles. *Biochim. Biophys. Acta* **556,** 244-264.

Lipari, G. & Szabo, A. (1982a). Model-free approach to the interpretation of nuclear magnetic resonance relaxation in macromolecules. 1. Theory and range of validity. *J. Am. Chem. Soc.* **104,** 4546-4559.

Lipari, G. & Szabo, A. (1982b). Model-free approach to the interpretation of nuclear magnetic resonance relaxation in macromolecules. 2. Analysis of experimental results. *J. Am. Chem. Soc.* **104,** 4559-4570.

Live, D. H., Davis, D. G., Agosta, W. C. & Cowburn, D. (1984). Observation of 1000-fold enhancement of ^{15}N NMR via proton-detected multiple-quantum coherences: Studies of large peptides. *J. Am. Chem. Soc.* **106,** 6104-6105.

Luginbühl, P., Güntert, P., Billeter, M. & Wüthrich, K. (1996). The new program OPAL for molecular dynamics simulations and energy refinements of biological macromolecules. *J. Biomol. NMR* **8,** 136-146.

Macura, S. & Ernst, R. R. (1980). Elucidation of cross-relaxation in liquids by two-dimensional NMR spectroscopy. *Mol. Phys.* **41,** 95-117.

Mandel, A. M., Akke, M. & Palmer, A. G., 3rd. (1995). Backbone dynamics of *Escherichia coli* ribonuclease HI: correlations with structure and function in an active enzyme. *J. Mol. Biol.* **246,** 144-163.

McCrea, K., Wisialowski, T., Cabrele, C., Church, B., Beck-Sickinger, A. G., Kraegen, E. & Herzog, H. (2000). 2-36[K^4,$RYYSA^{19-23}$]PP a novel Y_5-receptor preferring ligand with strong stimulatory effect on food intake. *Regul. Pept.* **87,** 47-58.

Michel, M. C., Beck-Sickinger, A., Cox, H., Doods, H. N., Herzog, H., Larhammar, D., Quirion, R., Schwartz, T. & Westfall, T. (1998). XVI. International Union of Pharmacology recommendations for the nomenclature of neuropeptide Y, peptide YY, and pancreatic polypeptide receptors. *Pharmacol. Rev.* **50,** 143-150.

Minakata, H., Taylor, J. W., Walker, M. W., Miller, R. J. & Kaiser E. T. (1989). Characterization of amphiphilic secondary structures in neuropeptide Y through the design, synthesis, and study of model peptides. *J. Biol. Chem.* **264,** 7907-7913.

Monks, S. A., Karagianis, G., Howlett, G. J. & Norton, R. S. (1996). Solution structure of human neuropeptide Y. *J. Biomol. NMR* **8,** 379-390.

Moroder, L., Romano, R., Guba, W., Mierke, D. F., Kessler, H., Delporte, C., Winand, J. & Christophe, J. (1993). New evidence for a membrane-bound pathway in hormone receptor binding. *Biochemistry* **32,** 13551-13559.

Opella, S. J. (1997). NMR and membrane proteins. *Nat. Struct. Biol.* **4,** 845-848.

Opella, S. J., Kim, Y. & McDonnell, P. (1994). Experimental nuclear magnetic resonance studies of membrane proteins. *Methods Enzymol.* **239,** 536-560.

Otting, G. (1990). Zero-quantum suppression in NOESY and experiments with a z-filter. *J. Magn. Reson.* **86,** 496-508.

Palmer, A. G., 3rd., Cavanagh, J., Wright, P. E. & Rance, M. (1991a). Sensitivity improvement in proton-detected two-dimensional heteronuclear correlation NMR spectroscopy. *J. Magn. Reson.* **93,** 151-170.

Palmer, A. G., 3rd., Rance, M. & Wright, P. E. (1991b). Intermolecular motion of a zinc finger DNA-binding domain from xfin characterized by proton-detected natural abundance ^{13}C heteronuclear NMR spectroscopy. *J. Am. Chem. Soc.* **113,** 4371-4380.

Pellegrini, M. & Mierke, D. F. (1999a). Molecular complex of cholecystokinin-8 and N-terminus of the cholecystokinin A receptor by NMR spectroscopy. *Biochemistry* **38,** 14775-14783.

Pellegrini, M. & Mierke, D. F. (1999b). Structural characterization of peptide hormone/receptor interactions by NMR spectroscopy. *Biopolymers* **51,** 208-220.

Piotto, M., Saudek, V. & Sklenar, V. (1992). Gradient-tailored excitation for single-quantum NMR spectroscopy of aqueous solutions. *J. Biomol. NMR* **2,** 661-665.

Rudolf, K., Eberlein, W., Engel, W., Wieland, H. A., Willim, K. D., Entzeroth, M., Wienen, W., Beck-Sickinger, A. G. & Doods, H. N. (1994). The first highly potent and selective non-peptide neuropeptide Y Y_1 receptor antagonist: BIBP3226. *Eur. J. Pharmacol.* **271,** R11-13.

Sargent, D. F. & Schwyzer, R. (1986). Membrane lipid phase as catalyst for peptide-receptor interactions. *Proc. Natl Acad. Sci. U S A* **83,** 5774-5778.

Schwyzer, R. (1986). Molecular mechanism of opioid receptor selection. *Biochemistry* **25,** 6335-6342.

Schwyzer, R. (1987). Membrane-assisted molecular mechanism of neurokinin receptor subtype selection. *EMBO J.* **6,** 2255-2259.

Schwyzer, R. (1995). 100 years lock-and-key concept: are peptide keys shaped and guided to their receptors by the target cell membrane? *Biopolymers* **37,** 5-16.

Selzer, T., Albeck, S. & Schreiber, G. (2000). Rational design of faster associating and tighter binding protein complexes. *Nat. Struct. Biol.* **7,** 537-541.

Stanley, B. G. & Leibowitz, S. F. (1985). Neuropeptide Y injected in the paraventricular hypothalamus: a powerful stimulant of feeding behavior. *Proc. Natl Acad. Sci. U S A* **82,** 3940-3943.

Szyperski, T., Güntert, P., Otting, G. & Wüthrich, K. (1992). Determination of scalar coupling constants by inverse Fourier transfomation of in-phase multiplets. *J. Magn. Reson.* **99,** 552-560.

Tatemoto, K. (1982). Neuropeptide Y: complete amino acid sequence of the brain peptide. *Proc. Natl Acad. Sci . U S A* **79,** 5485-5489.

Wang, A. & Bax, A. (1996). Determination of the backbone dihedral angles phi in human ubiquitin from reparametrized Karplus equations. *J. Am. Chem. Soc.* **118,** 2483-2494.

Weiner, M. P., Costa, G. L., Schoettlin, W., Cline, J., Mathur, E. & Bauer, J. C. (1994). Site-directed mutagenesis of double-stranded DNA by the polymerase chain reaction. *Gene* **151,** 119-123.

Weiner, P. K., Kollman, P. A., Nguyen, D. T. & Case, D. A. (1986). An all-atom force field for simulations of proteins and nucleic acids. *J. Comput. Chem.* **7,** 230-252.

Wieland, H. A., Engel, W., Eberlein, W., Rudolf, K. & Doods, H. N. (1998). Subtype selectivity of the novel nonpeptide neuropeptide Y Y_1 receptor antagonist BIBO 3304 and its effect on feeding in rodents. *Br. J. Pharmacol.* **125,** 549-555.

Wishart, D. S., Sykes, B. D. & Richards, F. M. (1991). Relationship between nuclear magnetic resonance chemical shift and protein secondary structure. *J. Mol. Biol.* **222,** 311-333.

Wishart, D. S., Sykes, B. D. & Richards, F. M. (1992). The chemical shift index: a fast and simple method for the assignment of protein secondary structure through NMR spectroscopy. *Biochemistry* **31,** 1647-1651.

Wüthrich, K. (1986). *NMR of Proteins and Nucleic Acids*, Wiley, New York.

Zhou, N. E., Zhu, B.-Y., Sykes, B. D. & Hodges, R. S. (1992). Relationship between amide proton chemical shifts and hydrogen bonding in amphipathic alpha-helical peptides. *J. Am. Chem. Soc.* **114,** 4320-4326.

4.6. Supplementary Materials

Table S1

Chemical shifts for [Ala31, Pro32]-pNPY on DPC micelles[a]

Residue	N	H^N	H^α	H^β	others
Tyr 1	-	-	4.47	3.04, 3.20	δH 7.20, 7.20; εH 6.88, 6.88
Pro 2	-		4.46	2.00, 2.30	γCH_2 1.96, 1.96; δCH_2 3.31, 3.72
Ser 3	117.1	8.32	4.45	3.87, 3.87	
Lys 4	123.9	8.22	4.66	1.72, 1.83	γCH_2 1.45, 1.45; δCH_2 1.73, 1.73; εCH_2 3.00, 3.00
Pro 5	-		4.41	1.92, 2.28	γCH_2 2.01, 2.01; δCH_2 3.60, 3.80
Asp 6	120.4	8.32	4.52	2.59, 2.62	
Asn 7[b]	119.3	8.17	4.99	2.65, 2.80	δNH_2 6.86, 7.60
Pro 8	-		4.42	1.92, 2.28	γCH_2 2.01, 2.01; δCH_2 3.76, 3.76
Gly 9	109.3	8.34	3.94, 3.94		
Glu 10	120.8	8.03	4.30	2.07, 2.10	γCH_2 2.22, 2.22
Asp 11	121.7	8.32	4.61	2.58, 2.66	
Ala 12	125.6	8.12	4.58	1.34	
Pro 13	-		4.42	1.92, 2.28	γCH_2 2.01, 2.01; δCH_2 3.65, 3.76
Ala 14	123.8	8.38	4.24	1.41	
Glu 15	120.1	8.28	4.24	2.01, 2.08	γCH_2 2.29, 2.29
Asp 16	121.5	8.18	4.44	2.62, 2.67	
Leu 17	120.7	8.39	4.16	1.82, 1.82	γH 1.64; δCH_3 0.93, 0.98
Ala 18	121.1	8.04	4.03	1.52	
Arg 19	119.6	7.96	4.10	1.75, 1.84	γCH_2 1.45, 1.52; δCH_2 3.14, 3.14
Tyr 20	120.3	7.98	4.42	3.09, 3.09	δH 7.02, 7.02; εH 6.78, 6.78
Tyr 21	119.7	8.34	4.30	3.16, 3.16	δH 7.05, 7.05; εH 6.77, 6.77
Ser 22	114.3	8.29	3.99	3.96, 4.02	
Ala 23	124.5	7.78	4.23	1.63	
Leu 24	118.8	8.09	4.17	1.83, 1.83	γH 1.63; δCH_3 0.94, 0.98
Arg 25	117.7	8.16	3.83	1.69, 1.78	γCH_2 1.44, 1.53; δCH_2 3.05, 3.05
His 26	117.4	7.81	4.30	3.12, 3.20	δ^2H 6.43; ε^1H 8.12
Tyr 27	117.6	7.96	4.20	2.99, 3.11	δH 7.13, 7.13; εH 6.83, 6.83
Ile 28	117.3	8.09	3.87	1.97	γCH_2 1.27, 1.68; γCH_3 0.95; δCH_3 0.85
Asn 29	118.2	7.74	4.58	2.77, 2.83	δNH_2 6.82, 7.49
Leu 30	120.4	7.63	4.27	1.67, 1.71	γH 1.57; δCH_3 0.80, 0.83
Ala 31	123.6	7.82	4.40	1.39	
Pro 32	-		4.45	2.01, 2.28	γCH_2 2.07, 2.07; δCH_2 3.60, 3.80
Arg 33	119.9	8.26	4.22	1.79, 1.88	γCH_2 1.66, 1.66; δCH_2 3.20, 3.20
Gln 34	119.5	8.22	4.23	1.99, 2.06	γCH_2 2.32, 2.32; εNH_2 6.80, 7.44
Arg 35	120.3	8.08	4.18	1.83, 1.83	γCH_2 1.66, 1.66; δCH_2 3.10, 3.10
Tyr 36	120.1	7.91	4.51	2.86, 3.09	δH 7.10, 7.10; εH 6.79, 6.79
NH_2	107.5	6.99, 7.38			

[a] 2.5 mM in 300 mM DPC/90% H_2O/10% ^2H_2O at 37°C and pH 6.0. Chemical shifts are referenced to the water frequency at 37°C (4.63 ppm). ^{15}N chemical shifts are referenced to liquid $^{15}NH_3$ via the proton chemical shift scale.

[b] Chemical shifts are given for Pro8 in trans conformation.

Table S2

^{15}N relaxation parameters for [Ala31, Pro32]-pNPY on DPC micelles[a]

Magnetic field	500 MHz						600 MHz			
Residue	R_1 [Hz]	σ (R_1)	R_2 [Hz]	σ (R_2)	NOE	σ_{NOE}	R_1 [Hz]	σ (R_1)	R_2 [Hz]	σ (R_2)
Lys 4	1.50	0.18	2.04	0.46	-8.38	0.84	1.27	0.07	1.91	0.13
Asp 6	1.60	0.10	1.67	0.76	-2.05	0.21	1.28	0.09	2.68	0.20
Asn 7	1.52	0.09	2.18	0.40	-3.23	0.32	1.28	0.07	2.29	0.13
Gly 9	1.59	0.08	2.15	0.26	-1.37	0.20	1.31	0.08	2.11	0.07
Glu 10	1.65	0.08	2.17	0.22	-0.90	0.20	1.35	0.08	2.41	0.06
Asp 11	1.62	0.08	1.94	0.26	-0.89	0.20	1.28	0.08	2.35	0.23
Ala 12	1.58	0.08	2.68	0.22	-0.56	0.20	1.27	0.08	3.31	0.33
Ala 14	1.87	0.10	4.44	0.36	0	0.20	1.48	0.08	5.12	0.16
Asp 16	1.99	0.11	6.14	0.53	0.36	0.10	1.58	0.10	8.00	0.50
Leu 17	1.96	0.14	8.40	0.85	0.49	0.07	1.45	0.08	9.71	0.19
Ala 18	1.94	0.14	9.71	0.75	0.58	0.06	1.47	0.07	n.d.	n.d.
Arg 19	2.10	0.17	10.0	1.00	0.67	0.07	1.57	0.08	10.75	0.23
Tyr 20	2.15	0.14	8.13	0.53	0.40	0.04	1.61	0.05	8.93	0.16
Tyr 21	1.79	0.15	11.24	1.26	0.70	0.07	1.53	0.11	11.11	0.25
Ser 22	1.89	0.14	10.87	1.18	0.73	0.07	1.36	0.10	11.91	0.28
Ala 23	2.00	0.19	10.31	0.85	0.66	0.07	1.43	0.09	11.91	0.28
Leu 24	2.12	0.18	11.36	1.29	0.53	0.05	1.52	0.13	14.71	0.43
Arg 25	1.90	0.18	11.24	1.77	0.68	0.07	1.42	0.11	12.35	0.61
His 26	1.97	0.34	10.99	1.93	0.72	0.07	1.84	0.20	12.35	0.61
Tyr 27	1.89	0.20	10.20	1.67	0.71	0.07	1.51	0.12	11.49	0.53
Ile 28	2.04	0.18	10.10	1.63	0.61	0.06	1.57	0.10	12.05	0.58
Asn 29	1.90	0.19	9.62	1.29	0.59	0.06	1.47	0.08	11.24	0.25
Leu 30	1.90	0.14	8.20	0.94	0.51	0.05	1.41	0.09	9.90	0.39
Ala 31	1.97	0.14	7.52	0.57	0.48	0.05	1.52	0.08	8.33	0.28
Arg 33	2.02	0.12	5.68	0.26	0.33	0.03	1.52	0.08	6.41	0.16
Gln 34	2.36	0.19	5.50	0.85	0.32	0.03	1.74	0.15	6.33	0.16
Arg 35	1.94	0.16	5.59	0.62	0.19	0.10	1.66	0.11	5.59	0.19
Tyr 36	2.01	0.12	4.41	0.40	0.10	0.10	1.62	0.08	4.74	0.40

[a] 1 mM in 300 mM DPC/90% H_2O/10% ^2H_2O at 37°C and pH 6.0. No values are available for the N-terminal residue Ser 3 due to fast H^N exchange.

Table S3

Backbone dynamical parameters for [Ala31, Pro32]-pNPY bound to DPC micelles[a]

Residue	S^2	dS^2	τ_e [ps]	$d\tau_e$ [ps]	S_s^2	dS_s^2	S_f^2	dS_f^2	R_{ex}	dR_{ex}	$\chi^{2\,b}$
Lys 4	0.05	0.01	401	47							0.60
Asp 6	0.11	0.02	451	60							3.90
Asn 7	0.08	0.01	426	44							1.63
Gly 9	0.05	0.01	643	66	0.06	0.01	0.90	0.05			3.64
Glu 10	0.07	0.01	799	88	0.08	0.01	0.84	0.05			5.37
Asp 11	0.06	0.02	808	90	0.07	0.02	0.81	0.05			7.88
Ala 12	0.13	0.02	882	115	0.17	0.03	0.77	0.05			6.14
Ala 14	0.32	0.03	1100	219	0.38	0.03	0.84	0.05			4.99
Asp 16	0.52	0.05	1323	251	0.59	0.04	0.89	0.04			5.51
Leu 17	0.80	0.02	141	38							3.53
Ala 18	0.87	0.03	147	63							0.47
Arg 19	0.87	0.03	1065	423							1.76
Tyr 20	0.69	0.02	1022	101							6.84
Tyr 21	0.92	0.02									3.02
Ser 22	0.96	0.02									5.31
Ala 23	0.97	0.02									7.51
Leu 24	0.98	0.06							1.89	0.58	2.50
Arg 25	0.97	0.04									5.52
His 26	1.00	0.04									3.15
Tyr 27	0.94	0.03									1.58
Ile 28	0.99	0.03									9.89
Asn 29	0.93	0.02									12.81
Leu 30	0.81	0.02	125	34							2.51
Ala 31	0.63	0.04	1297	200	0.71	0.03	0.88	0.03			1.36
Arg 33	0.42	0.03	1437	97	0.51	0.03	0.83	0.02			6.13
Gln 34	0.39	0.04	1596	105	0.42	0.04	0.92	0.04			3.40
Arg 35	0.35	0.03	1348	174	0.41	0.03	0.86	0.04			0.41
Tyr 36	0.26	0.03	1354	154	0.31	0.04	0.83	0.04			2.89

[a] The parameters are obtained applying the following models: (1) S^2, (2) S^2, $\tau_e = \tau_f$, (3) S^2, R_{ex}, (4) S^2, $\tau_e = \tau_f$, R_{ex}, (5) S_f^2, S^2, $\tau_e = \tau_s$.

[b] χ^2 values are calculated as the sum-sqared error residuals. The theoretical values for the 95% confidence interval of the χ^2-distribution are 9.49, 7.81, and 5.99 for one, two, and three motional parameters, respectively.

Table S4

Statistical information for the structure-calculation of the micelle-bound [Ala31, Pro32]-pNPY

Distance restraints	Total	207
	Intra-residual	67
	Inter-residual	140
	Sequential (i - j = 1)	67
	Medium (i - j = 2, 3, 4)	73
RMSD[a] (Å)	Leu17-Asn29 backbone[b]	0.41 ± 0.14
	Leu17-Asn29 all heavy atoms	1.84 ± 0.39
	Tyr21-Asn29 backbone	0.26 ± 0.10
	Tyr21-Asn29 all heavy atoms	1.35 ± 0.37
Structure check[c] (Average %)	Leu17-Asn29	98.6/0
	Tyr1-Tyr36	61.6/1.5
NOE constraint violations	Number ≥ 0.1 Å	0.80 ± 0.79
	Maximum (Å)	0.13 ± 0.04
Dihedral angle constraint violations	Number ≥ 2.5 degrees	0.07 ± 0.25
	Maximum	1.17 ± 0.94
AMBER energies (kcal/mol)[d]	Total	-1949 ± 714
	Van der Waals	203 ± 345
	Electrostatic	-1297 ± 252

[a] Atomic root mean square deviation calculated by superimposing the corresponding region of the 17 minimized structures referenced by the mean coordinates.

[b] N, Cα, C´ atoms.

[c] Percentage of the ϕ, φ angles falling within the most favoured/disallowed Ramachandran regions for the 17 refined structures.

[d] AMBER energies are given as the sum of solute-solute and solute-water interactions. Energies of water-water interactions are neglected.

Seite Leer /
Blank leaf

Chapter 5

Towards a Peptide Model Mimicking the Third Extracellular Loop of a Neuropeptide Y Receptor

5.1. Introduction

The rational drug design would of course mostly profit from high-resolution structures of the target. Furthermore, structural information of the ligand/receptor complex could reveal conformational changes that take place upon ligand binding (induced fit). However, especially for the membrane associated G protein coupled receptors the structural characterization is currently limited to theoretical models. Many GPCR transmembrane domains have been modelled on the basis of the structure of the bacteriorhodopsin helices (Henderson *et al.*, 1990), but this will at best lead to models that have a qualitative value, and clearly are too imprecise to be used as a basis for drug design. The recently solved first structure of a GPCR (bovine rhodopsin) (Palczewski *et al.*, 2000) provides a better template, but rational drug design is still inconceivable.

The difficulties in gaining structural data of transmembrane receptors are primarily due to insufficient over-expression, problems with its purification, concentration, and with the preparation of fully reconstituted receptors in membrane environments. Concerning X-ray crystallography techniques, the rate-limiting step is the crystallization of the solubilized

receptors. On the other hand, the upper size of about 30-50 kDa that was limiting NMR structure determination until the TROSY methodology was introduced few years ago excluded the application of NMR in that area.

A different approach was followed by several authors. Based on site-directed mutagenesis and cross-linking studies it became clear, that peptide ligands mainly bind to the extracellular domains of their target receptors. For the structural studies of these interactions, it would therefore be sufficient to model the receptor by the ectopic amino-acids. Evidence for the structural similarity of an isolated receptor fragment with the corresponding part of the full-length receptor was obtained from both biological as well as NMR studies. The solution structures of three peptides each containing the sequence of one of the turns, that are defined in a recent crystal structure of bacteriorhodopsin (Lücke *et al.*, 1999) , namely the CD, DE and FG loops, were determined. The structures of the peptides, as measured in DMSO by NMR, closely resembled the structures of the corresponding turns in the high resolution structure of the intact protein (Katragadda *et al.*, 2000). König *et al.* (1989) nicely demonstrated that three peptides, corresponding to the second, third and a putative fourth cytoplasmic loop (in the carboxy-terminal sequence) of rhodopsin were able to compete with metarhodopsin II for G_t binding exhibiting K_d values in the 2 mM range and even displayed a pairwise synergistic competition effectiveness. The conclusion can be drawn from these experiments that the cytoplasmic loops of a G protein coupled receptor reflect the structure of the corresponding segment in the parent protein.

As outlined above, spectroscopic investigations of well-designed fragments of a receptor can be assumed to provide a reliable method for the identification of the structural features of the loops and termini of the receptor. A number of NMR studies of linear and cyclic peptides, corre-

sponding to the natural sequence of the intra- and extracellular loops of receptors, has been reported (Table 5.1)

Table 5.1 NMR studies reported for loop-domains of receptors (and/or the complex with their ligands)

receptor domain/ligand	intermol. NOEs	ligand cross-linking	reference
i3 (bovine rhodopsin)			Yeagle *et al.*, 1995b
C terminus (bovine rhodopsin)			Yeagle *et al.*, 1995a
N terminus (PTH1 R)/PTH	none	yes	Pellegrini *et al.*, 1998
N terminus (CCK_A R)/CCK-8	3	yes	Pellegrini & Mierke, 1999
i3 (PTH1 receptor)/PTH			Pellegrini *et al.*, 1996; Mierke *et al.*, 1996
e1 (PTH1 receptor)/PTH	n.d.	yes	Piserchio *et al.*, 2000
e3 (CCK_A receptor)/CCK-8	5	yes	Giragossian & Mierke, 2001

We chose the e3-loop of the Y receptors as a starting point for our investigations of possible interactions of NPY with a receptor fragment. From analysis of hydropathicity plots, the loop length is estimated to consist of approx. 12 amino acid residues and is with it the shortest among e1-3 (e1, e2 consist of approx. 19 and 32 residues, respectively). This limited size is well-suited both for the synthesis and for the subsequent NMR studies. A further rational for choosing a loop stems from ligand binding data of a series of Y_1 receptor mutants in which aspartic acid and glutamic acid residues present in putative extracellular domains were systematically replaced by alanines. In contrast to mutations in the N-terminal domain, substitution of acidic residues present in the three extracellular loops resulted in proteins unable to bind NPY (Walker *et al.*, 1994).

In the design of the receptor fragment, Mierke and co-workers considered it important to incorporate a sufficient number of amino acids of the adjacent TM helices to act as anchors, tethering the loop to the lipid/micelle environment and providing the naturally occuring topological orientation. In the first part of this work, we followed a similar strategy. We synthesized N-terminally acetylated and C-terminally amidated peptides, whose sequences were derived from the e3-loops of three different Y receptors. All these peptides additionally incorporated 2-4 amino acids of the adjacent TM helices at their termini. In the second part, we took a slightly different approach. We chose a lipopeptide as a model compound, whose peptidic part comprises the native peptide sequence of the loop spanning amino acids, whereas the transmembrane helices are mimicked by hydrocarbon chains (Figure 5.1).

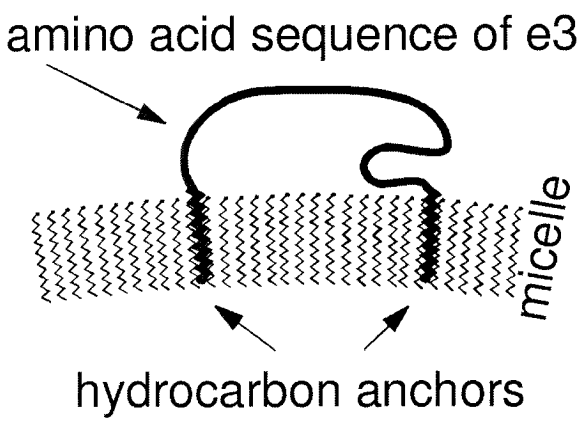

Figure 5.1 Schematic representation of the lipopeptide, anchored to a micelle by its hydrocarbon tails.

Here we describe the solid-phase synthesis of a series of peptides derived from the e3-loops of several Y receptor subtypes. Different solvents were tested for their ability to give high-quality NMR spectra. Moreover, some molecules were modified by the coupling of hydrocarbon-chains to their N and C termini. Strategies for the purification of these highly hydrophobic peptides and for NMR sample preparation in mixed micelles are presented. Specific binding of NPY to the loop models can be detected using [^{15}N,^{1}H]-HSQC spectroscopy utilizing ^{15}N-labeled

NPY. In principle, this method would allow to detect even very weak binding (K_d > 1mM).

5.2. Results and Discussion

Characterization of N-acetylated and C-terminally amidated peptides derived from the e3-loops of three Y receptor subtypes

In an effort to describe the interaction of NPY with the human Y_1 receptor, Sautel *et al.* (1996) found a cluster of residues in the third extracellular loops, which could not be mutated to alanine without significantly reducing the binding of NPY, namely Asn^{283}, Phe^{286} and Asp^{287}, Trp^{288} and His^{298} (arrows in Figure 5.2). Moreover, receptors with alanine mutations at positions Asn^{283}, Phe^{286} and Asp^{287} additionally showed reduced binding for the nonpeptide antagonist BIBP 3226. Mutations at other positions tested (Thr^{280}, Thr^{284}, Asn^{289}, His^{290} and Gln^{291}) did not affect the binding of NPY or BIBP 3226.

Therefore, the third extracellular loop of the Y_1 receptor is a prime candidate for being involved in direct ligand contacts. However, results from mutational studies could never completely exclude the possibility, that the loss of affinity is due to indirect effects like lower receptor efficacy or destabilization of the active state. In particular, molecular dynamics simulation of NPY Y_1 receptor interactions suggested that Asp^{199}, Asp^{103} and Asp^{286} (the latter of which is located in the e3-loop) in the receptor interact, respectively, with Lys^4, Arg^{33} and Arg^{35} of NPY (Sylte *et al.*, 1999).

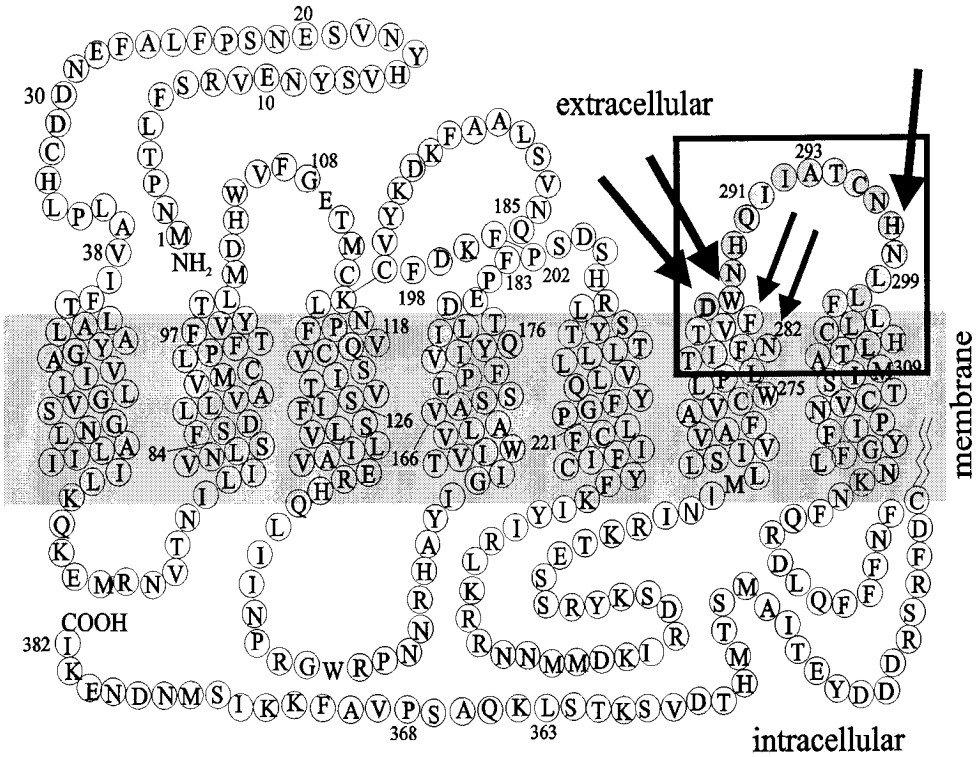

Figure 5.2 Model of the Y_1 receptor. The e3-loop is boxed. Ala-mutations in this region, that result in a significant loss of affinity for NPY are indicated by arrows. From Sautel *et al.* (1996).

Interestingly, the third extracellular loop of another familiy 1a GPCR, the CCK_A receptor, has recently been recognized to be involved in forming contacts to the ligand CCK-8. By observing intermolecular NOEs between CCK-8 and the CCK_A receptor-fragment (329-357), it became evident that the C-terminus of the ligand is in close proximity to transmembrane helix VI (Giragossian & Mierke, 2001). This is in agreement with biological data: Site-directed mutagenesis of Asn^{333} and Arg^{336} residues in this region, and the reciprocal mutations of Asp^{32} and the carboxamide of CCK had established the biological importance of these residues in binding (Kennedy *et al.*, 1997).

On the other hand, results from one receptor type may not be directly translated to another ligand/receptor system. Since the extracellular loops are the recognition sites for the ligands, these domains are expected

to reflect the whole variety of selective ligand/receptor interactions in their amino acid sequences and secondary/tertiary structures.

Table 5.2 presents an alignment of the amino acid sequences of the third extracellular loops for rhodopsin, as derived from the recently published crystal structure (Palczewski *et al.*, 2000), the CCK_A receptor and the Y_1, Y_2 and Y_5 receptors, demonstrating complete sequence diversity between the different receptor systems and a sequence identity of only one amino acid between the different subtypes in the family of the Y receptors. Even more importantly, the e3-loops of rhodopsin and the Y receptors are of largely different length thereby complicating modelling approaches based on the crystal structure of the former.

To check for possible interactions between the third extracellular loop of the Y receptors with NPY, we synthesized a series of peptides derived from the Y_1, Y_2, and the Y_5 receptors (Table 5.3). The loop-sequences

Table 5.3 Amino acid sequences of N-acetylated and C-terminally amidated peptides derived from the e3-loop[a]

Peptide number	Source	Sequence
1	Y_1 (283-302)	*Ac--NTVF***DWNHQIIATCNHN***LLF-NH*$_2$
2	Y_2 (282-301)	*Ac-FQLAV***DIDSQVLDLKEYK***LI--NH*$_2$
3	Y_5 (282-301)	*Ac-FHVVT***DFNDNLISNRHFK***LV--NH*$_2$

a. TM-domains or putative TM-domains are indicated in *italics*, the e3-loop sequences are written in **bold**.

were chosen such that a few residues from the potential C terminus and N terminus of the adjacent TM VI and TM VII, respectively, would help to anchor the peptides to the micelles. For this reason charged termini were avoided by acetylation of the N terminus and cleaving the peptide from a rink amide resin in form of the C-terminal amide.

Table 5.2 Amino acid sequences of the e3-loops of rhodopsin, the CCK_A and the Y receptors[a]

Receptor	Sequence
bovine rhodopsin (265-296)	*CWLPYAGVAFYIF*----THQGSDFGP----*IFMTIPAFFAK*
human CCK_A (325-361)	*CWMPIFSANA*--WRAYDTASAERRLSG--*TPISFILLLSYT*
human Y_1 (275-311)	*CWLPLTIFNTVF*--**D**WNHQIIATCNHN--*LLFLLCHLTAMI*
mouse Y_1 (274-310)	*CWLPLTIFNTVF*--**D**WNHQIIATCNHN--*LLFLLCHLTAMI*
frog Y_1 (270-306)	*CWLPFFIFNLVF*--**D**WNHEAVATCNHN--*LLFLICHLTAMI*
pig Y1 (275-311)	*CWLPLTIFNTVF*--**D**WNHQIIATCNHN--*LLFLLCHLTAMI*
human Y_2 (275-311)	*SWLPLHAFQLAV*--**D**IDSQVLDLKEYK--*LIFTVFHIIAMC*
human Y4 (277-313)	*LWLPLHVFNSLE*--**D**WHHEAIPICHGN--*LIFLVCHLLAMA*
human Y_5 (275-311)	*SWMPLHLFHVVT*--**D**FNDNLISNRHFK--*LVYCICHLLGMM*

a. TM-domains or putative TM-domains are represented in *italics*, the conserved Asp^{289} within the e3-loop of the Y receptor-family is written in **bold**, and the transition sites or putative transition sites between the e3-domain and the transmembrane domains are indicated by hyphens (--).

Peptide **1** was hardly soluble in almost any organic solvent or aqueous solutions at either acidic or basic conditions. A NOESY-spectrum measured in DMSO revealed several sequential H^N-H^N cross-peaks, that are characteristic for the presence of a helical conformation. However, the complete absence of any medium range NOEs indicates that, although temporary turns might build up, a persistent and stable helix is absent.

In contrast, peptides **2** and **3** were fairly soluble in mixtures of organic solvent and water. Mixed micelles of peptide and dodecylphosphocholine were prepared according to the protocol by Killian *et al.* (1994) (see Materials and Methods for details). A number of conditions of varying pH and addition of physiological concentrations of sodium chloride were screened with respect to the effect on the line-width in 1D ^{1}H NMR spectra. Although the solutions were perfectly clear at a concentration of 1-2 mM peptide in 300 mM DPC, we observed very broad line-widths in all samples, indicating higher aggreagates of the peptides and/or the micelles. Moreover, within one hour at room temperature, the solutions adopted a gel-like consistency, except for peptide **2** at a pH around 4.

Considering, that Giragossian & Mierke (2001) found stable conditions for measuring CCK_A-R(329-357), we compared the primary sequences of the CCK_A-, the Y_1/Y_2 and Y_5-fragments with respect to the distributions of charged residues within the peptides (Table 5.4).

Whereas in CCK_A-R(329-357) positively as well as negatively charged residues are equally distributed in the first and second half of the loop region, peptide **1** is very poor in charges, and peptides **2** and **3** bear positive charges only towards their C terminus, whereas the N terminus is negatively charged. Therefore, aggregation might be driven by hydrophobic interactions in peptide **1**, and by electrostatic interactions in peptides **2** and **3** due to an anti-parallel arrangement in which positive and negative charges compensate. Further support of this hypothesis is

Table 5.4 Potential charge distribution within CCK_A-R(329-357) and peptides 1-3 at pH 6[a].

Peptide	Sequence
CCK_A-R (329-357)	*IFSANA***WRAYDTASAERRLSG***TPISFILL* 0000000+00-0000-++00000000000
Peptide 1 (e3 of Y_1)	*NTVF***DWNHQIIATCNHN***LLF* 0000-000000000000000
Peptide 2 (e3 of Y_2)	*FQLAV***DIDSQVLDLKEYK***LI* 00000-0-0000-0+-0+00
Peptide 3 (e3 of Y_5)	*HVVT***DFNDNLISNRHFK***LVY* 0000-00-00000+00+000

a. TM-domains or putative TM-domains are indicated in *italics*, the e3-loop sequences are written in **bold**.

obtained by the observation that introduction of positively charged residues concomitantly at the N and C termini of a lipopeptide derived from peptide 1 results in a construct that is well soluble in hexafluoroisopropanol (HFP) allowing to obtain 1D ^{1}H NMR spectra of satisfactory quality when prepared as mixed micelles with DPC (see below). Although high amounts of salt may reduce those ionic interactions by compensating the charges, such conditions would also weaken the interactions with NPY and thereby prevent the verification of the model.

Synthesis of a lipopeptide mimicking the third extracellular loop of the Y_1 receptor

In the second part of this chapter, we describe the synthesis of a lipopeptide, derived from the e3-loop, with hydrocarbon chains attached to its N and C termini. The latter mimick the adjacent TM domains and should anchor the peptide to a membrane. Since peptides from the native

sequence of the e3-loop of the Y_1-receptor are almost insoluble in all solvents except for DMSO, we synthesized a peptide, derived from the sequence of residues 283-299, but substituted the N-terminal Asn^{283} and the C-terminal His^{298} by a lysine. The C-terminal asparagine could not be mutated, because this side-chain serves to anchor the assembling peptide chain on the rink amide resin during the solid-phase peptide synthesis. After the chain assembly, palmitic acid was coupled to the N terminus, and hexadecylamine was linked to the free carboxy-terminus. An ESI-MS spectrum of the purified lipopeptide is shown in Figure 5.3.

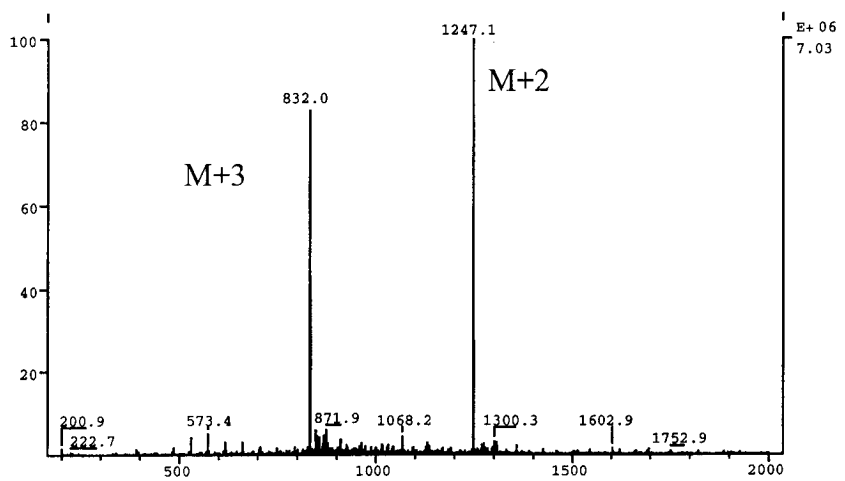

Figure 5.3 ESI-MS spectrum of purified $C_{15}H_{31}$(CO-NH)-KTVFDWNHQII-ATCNKN-(CO-NH)-$C_{16}H_{33}$. M_{theor}=2493.2; M_{exp}=2492.8.

Again, mixed micelles of lipopeptide and DPC were prepared according to Killian *et al.* (1994), however, including 10 mM DTT in the aqueous phase in order to avoid oxidation of the cysteine. Figure 5.4 shows a 1D ^{1}H-NMR spectrum of the backbone amide, as well as aromatic and side-chain amide protons of the peptide. Compared to a surface-associated peptide like NPY, the line-widths are slightly broader. This is not surprising, since we expect the lipopeptide to be integrated and tightly bound to the micelle. It can also not be excluded safely, that one lipopeptide is link-

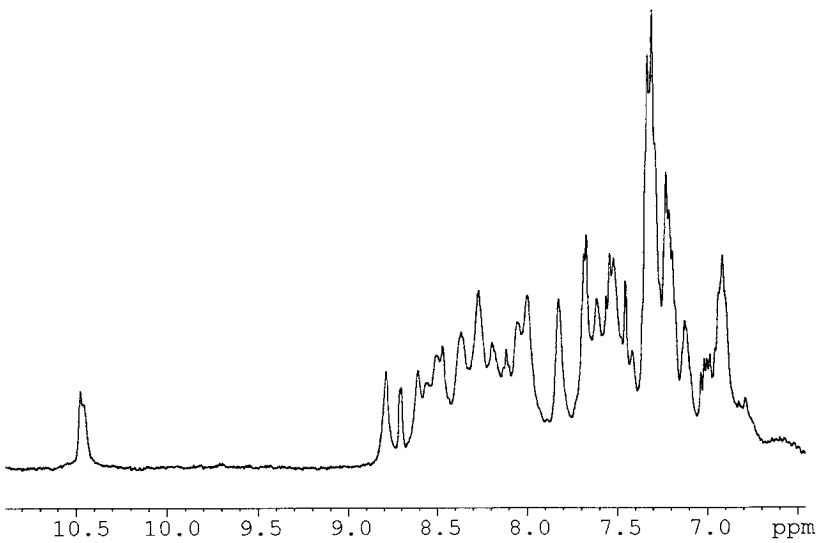

Figure 5.4 1D ^{1}H NMR spectrum of 0.5 mM lipopeptide, derived from the e3-loop of the Y_1 receptor, measured in 150 mM DPC-d38 at pH 6.0 and 37°C. The expansion shows backbone H^N, as well as aromatic and side-chain H^N protons. Especially well-resolved is the indole H^N of Trp6 (corresponding to Trp288 in the Y_1 receptor) at 10.5 ppm.

ing two different micelles by inserting the N-terminal palmitic group into micelle A and the C-terminal hexadecyl-moiety into micelle B. If this turned out to be true, the orientations of the two hydrocarbon should therefore be constrained in future constructs, *e.g.* by cyclization of the peptide.

Binding of ^{15}N-labeled NPY to the receptor-loop construct was tested by looking for changes in the positions of [^{15}N,^{1}H]-HSQC peaks due to chemical shift perturbation upon binding to the receptor fragment. However, the HSQC-spectra of NPY in the absence (Figure 5.5 A) and in the presence (Figure 5.5 B) of the lipopeptide revealed perfectly identical peak positions. Since this method is very sensitive and allows the detection of very weak binding, we conclude, that NPY has no affinity towards this single loop construct. Of course, we have to keep in mind, that the sequence of the peptide is changed at two positions (N283K, H297K), which alters the net charge of the loop fragment from -1 to +2. Consider-

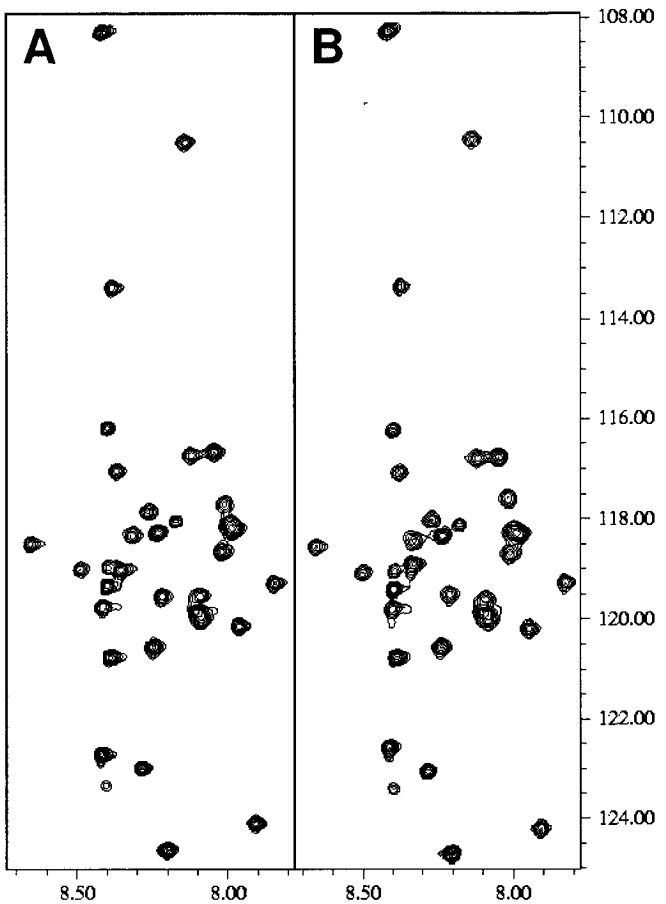

Figure 5.5 [^{15}N,^{1}H]-HSQC spectra of 0.1 mM ^{15}N-labeled pNPY in 150 mM DPC/H_2O at pH 6.0 and 37°C (A) in the absence of, and (B) in the presence of 0.5 mM lipopeptide, respectively.

ing that NPY is suggested to interact with the e3-loop primarily *via* its positively charged C terminus, this could lead to electrostatic repulsion of the ligand rather than attraction. Finally, one disadvantage of this approach concerns the lacking knowledge of the transition sites between transmembrane and loop domains. The loop-sequences as designed for the e3-loop of the CCK_A receptor by Mierke *et al.* include five to six amino acids of the adjacent TM regions, which is sufficient to act as a tethering point, embedding the peptide in the micelle. In contrast to our lipopep-

tide, in which the membrane helices are mimicked and substituted by hydrocarbon chains, Mierke's peptides are unconstrained for the partitioning of the residues in the membrane, the fixed charge and the aqueous compartments. Therefore, the precise knowledge of the locations of the transition sites between the loop domain and the adjacent transmembrane domains might be a prerequisite before subsituting the membrane-embedded helices by hydrocarbon chains.

5.3. Materials and Methods

Materials

Deuterated DPC-d38 (99%-d) and DL-1,4-dithiothreitol-d10 (98%-d) were ordered from Cambridge Isotope Laboratories (Andover, Massachusets, USA).

The *N*-(9-fluorenylmethoxycarbonyl, Fmoc)-protected natural amino acid residues were purchased from Alexis (Läufelingen, Switzerland). Side-chain protecting groups were: *tert*-butyl for Asp, Glu, Ser, Thr, and Tyr, Boc for Lys, trityl for Asn, Gln and His, 2,2,5,7,8-pentamethylchroman-6-sulphonyl (Pmc) for Arg. The 4-(2',4'-dimethoxyphenyl-Fmoc-aminomethyl)-phenoxy (Rink Amide)-resin and Fmoc-aspartic acid α-4-{N-[1-(4,4-dimethyl-2,6-dioxocyclohexylidene)-3-mehylbutyl]-amino} benzyl ester (Fmoc-Asp-ODmab) were obtained from Novabiochem (Läufelingen, Switzerland). *N*-hydroxybenzotriazole (HOBt), *O*-(7-azabenzotriazol-1-yl)-1,1,3,3-tetramethyluronium hexafluorophosphate (HATU) and *N*-diisopropylethylamine (DIPEA) were purchased from Fluka (Buchs, Switzerland). *N*, *N*'-diisopropylcarbodiimide (DIC) was bought from Aldrich (Buchs, Switzerland).

Solid-phase peptide synthesis

All peptides were prepared by solid-phase peptide synthesis using Fmoc (9-fluorenylmethoxycarbonyl) protection group strategy on a robot system (Syro, MultiSynTech, Bochum). Generally, a double coupling procedure with tenfold excess Fmoc-amino acid, HOBt, DIC in DMF (2×40 minutes) was chosen during peptide chain assembly. Fmoc-deprotection was achieved by 40% piperidine in DMF for three minutes, 20% piperidine for seven minutes and 40% piperidine for five minutes. The peptides were either studied in their C-terminally amidated and N-terminally acetylated form or upon attachment of hydrocarbon chains at the N- and C-termini. N-acetylation was attained by exposure to a 10-fold excess of acetic acid anhydrid and DIPEA in DMF for ten minutes. In order to obtain the peptide amide, 4-(2',4'-dimethoxyphenyl-Fmoc-aminomethyl)phenoxy (rink amide-) resin was used, anchored to a polymer matrix consisting of polystyrene-1% divinylbenzene (30 mg, 15 µmol). The peptide amides were cleaved from the resin with trifluoroacetic acid/thioanisole/thiocresol 90/5/5 within three hours and subsequently precipitated using ice-cold diethyl ether. The cysteine-containing peptides derived from the e3-loop of the Y_1 receptor were cleaved using trifluoroacetic acid/thioanisole/ethanedithiol 90/7/3. The synthesis of the peptides that were subsequently subjected to N- and C-terminal attachments of hydrocarbon-chains, started by manually coupling of (C-terminally protected) Fmoc-Asp-ODmab to the rink amide-resin (which results in a C-terminal asparagine after cleavage from the resin). A tenfold excess of Fmoc-Asp-ODmab, HOBt, DIC in DMF was applied for 1 hour. Then, a tenfold excess of DIPEA was added to the reaction mixture and shaken for another 24 hours at room temperature. After the chain assembly and Fmoc-deprotection, palmitic or caprylic acid was coupled to the N terminus. Again, a tenfold excess of the fatty acid, HOBt, DIC in DMF was added and shaken for one hour. Upon addition of a tenfold excess of DIPEA the reaction mixture was shaken over night. Dmab-deprotection was achieved in 2% hydrazine/DMF and monitored by measuring the absorption at λ=290 nm. Hexadecylamine was coupled to the free carboxy-terminus in DMF containing stochiometric amounts of hexadecylamine, HATU and a two-fold excess of DIPEA. The reaction was for 1 hour and repeated twice. The lipopeptides were cleaved from the resin as described above, but precipitated using cold water instead of diethyl ether.

Since the C-terminal coupling of the hydrocarbon-amine never exceeded a 50%-effectiveness, it was necessary to separate the desired products containing

two hydrocarbon chains from the lipopeptides that were only modified at their N terminus. This was achieved by application of Sephadex reversed-phase tC2 columns (Waters) and 1-butanol/methanol as solvent system (a similar strategy had been applied to preparations of Glycophorin-A, Prion (110-137), and fibroblast growth factor receptor (368-397), see Glover *et al.*, 1999). The percentage of organic solvents were concomitantly increased in steps of 5%, and the product eluted with 25% 1-butanol/ 25% methanol. The purity was checked using electron spray ionisation mass spectrometry. The yield was approximately 10%.

NMR spectroscopy

We followed the general protocol of Killian *et al.* (1994) for the preparation of mixed micelles of hydrophobic peptides and sodium dodecyl sulphate (SDS), however, used dodecylphosphocholine (DPC) instead of SDS. Probably the most important step in this protocol is deaggregation of the peptide. In many cases this happens by dissolving the peptide in trifluoroethanol (TFE) or hexafluoroisopropanol (HFP). Killian even recommends to dissolve the peptides firstly in TFA and dry under a stream of nitrogen, which we omitted. Instead we dissolved 1 mg of the lipopeptide directly in 250 µl HFP. The completely clear peptide solution was added to an equal volume of an aqueous solution containing 150 mM DPC-d38 and 10 mM of DL-1,4-dithiothreitol-d10 (DTT). Water was added to yield a 8:1 ratio of water to HFP by volume. The sample was vortexed and lyophilized by rapid freezing in liquid nitrogen. After lyophilization the dry sample was rehydrated with 90% H_2O/10% D_2O and the pH adjusted to 6.0. NMR data were recorded at 310 K on a Bruker DRX-500 spectrometer. [^{15}N,^{1}H]-HSQC experiments utilized pulsed-field gradients for coherence selection and quadrature detection with square-shaped gradients of 25 G/cm/lms for labeling nitrogen coherences. The gradients were followed by delays of 200 µs to allow to recover from gradients. Furthermore, the sensitivity enhancement element of Rance and Palmer was added to the standard sequences (Palmer *et al.*, 1991; Kay *et al.*, 1992), together with water-flip back methodology (Grzesiek & Bax, 1993). They were recorded with data matrices of 15 ppm (^{1}H) * 30 ppm (^{15}N) spectral widths with 2048(F2)*150(F1) complex time domain data points. Data were extended once in F1 by linear prediction, zero-filled and processed with 70° shifted sine-bell window functions in ω2 and ω1

prior to the 2D FT. A digital low-pass filter was applied to reduce the residual water line (Marion *et al.*, 1989).

5.4. References

Giragossian, C. & Mierke, D. F. (2001). Intermolecular interactions between cholecystokinin-8 and the third extracellular loop of the cholecystokinin A receptor. *Biochemistry*, in press.

Glover, K. J., Martini, P. M., Vold, R. R. & Komives, E. A. (1999). Preparation of insoluble transmembrane peptides: glycophorin-A, prion (110-137), and FGFR (368-397). *Anal. Biochem.* **272,** 270-274.

Grzesiek, S. & Bax, A. (1993). The importance of not saturating H_2O in protein NMR. Application to sensitivity enhancement and NOE measurements. *J. Am. Chem. Soc.* **115,** 12593-12594.

Henderson, R., Baldwin, J. M., Ceska, T. A., Zemlin, F., Beckmann, E. & Downing, K. H. (1990). Model for the structure of bacteriorhodopsin based on high-resolution electron cryo-microscopy. *J. Mol. Biol.* **213,** 899-929.

Katragadda, M., Alderfer, J. L. & Yeagle, P. L. (2000). Solution structure of the loops of bacteriorhodopsin closely resembles the crystal structure. *Biochim. Biophys. Acta* **1466,** 1-6.

Kay, L. E., Keifer, P. & Saarinen, T. (1992). Pure absorption gradient enhanced heteronuclear single-quantum correlation spectroscopy with improved sensitivity. *J. Am. Chem. Soc.* **114,** 10663-10665.

Kennedy, K., Gigoux, V., Escrieut, C., Maigret, B., Martinez, J., Moroder, L., Frehel, D., Gully, D., Vaysse, N. & Fourmy, D. (1997). Identification of two amino acids of the human cholecystokinin-A receptor that interact with the N-terminal moiety of cholecystokinin. *J. Biol. Chem.* **272,** 2920-2926.

Killian, J. A., Trouard, T. P., Greathouse, D. V., Chupin, V. & Lindblom, G. (1994). A general method for the preparation of mixed micelles of hydrophobic peptides and sodium dodecyl sulphate. *FEBS Lett.* **348,** 161-165.

König, B., Arendt, A., McDowell, J. H., Kahlert, M., Hargrave, P. A. & Hofmann, K. P. (1989). Three cytoplasmic loops of rhodopsin interact with transducin. *Proc. Natl Acad. Sci. USA* **86,** 6878-6882.

Lücke, H., Schobert, B., Richter, H. T., Cartailler, J. P. & Lanyi, J. K. (1999). Structure of bacteriorhodopsin at 1.55 A resolution. *J. Mol. Biol.* **291,** 899-911.

Marion, D., Ikura, M. & Bax, A. (1989). Improved solvent suppression in one- and two-dimensional NMR spectra by convolution of time-domain data. *J. Magn. Reson.* **84,** 425-430.

Mierke, D. F., Royo, M., Pellegrini, M., Sun, H. & Chorev, M. (1996). Peptide mimetic of the third cytoplasmic loop of the PTH/PTHrP receptor. *J. Am. Chem. Soc.* **118,** 8998-9004.

Palczewski, K., Kumasaka, T., Hori, T., Behnke, C. A., Motoshima, H., Fox, B. A., Le Trong, I., Teller, D. C., Okada, T., Stenkamp, R. E., Yamamoto, M. & Miyano, M. (2000). Crystal structure of rhodopsin: A G protein-coupled receptor. *Science* **289,** 739-745.

Palmer, A. G., Cavanagh, J., Wright, P. E. & Rance, M. (1991). Sensitivity improvement in proton-detected two-dimensional heteronuclear correlation NMR spectroscopy. *J. Magn. Reson.* **93,** 151-170.

Pellegrini, M., Bisello, A., Rosenblatt, M., Chorev, M. & Mierke, D. F. (1998). Binding domain of human parathyroid hormone receptor: from conformation to function. *Biochemistry* **37,** 12737-12743.

Pellegrini, M. & Mierke, D. F. (1999). Molecular complex of cholecystokinin-8 and N-terminus of the cholecystokinin A receptor by NMR spectroscopy. *Biochemistry* **38,** 14775-14783.

Pellegrini, M., Royo, M., Chorev, M. & Mierke, D. F. (1996). Conformational characterization of a peptide mimetic of the third cytoplasmic loop of the G-protein coupled parathyroid hormone/parathyroid hormone related protein receptor. *Biopolymers* **40,** 653-666.

Piserchio, A., Bisello, A., Rosenblatt, M., Chorev, M. & Mierke, D. F. (2000). Characterization of parathyroid hormone/receptor interactions: structure of the first extracellular loop. *Biochemistry* **39,** 8153-8160.

Sautel, M., Rudolf, K., Wittneben, H., Herzog, H., Martinez, R., Munoz, M., Eberlein, W., Engel, W., Walker, P. & Beck-Sickinger, A. G. (1996). Neuropeptide Y and the

nonpeptide antagonist BIBP 3226 share an overlapping binding site at the human Y_1 receptor. *Mol. Pharmacol.* **50,** 285-292.

Sylte, I., Andrianjara, C. R., Calvet, A., Pascal, Y. & Dahl, S. G. (1999). Molecular dynamics of NPY Y_1 receptor activation. *Bioorg. Med. Chem.* **7,** 2737-2748.

Walker, P., Munoz, M., Martinez, R. & Peitsch, M. C. (1994). Acidic residues in extracellular loops of the human Y_1 neuropeptide Y receptor are essential for ligand binding. *J. Biol. Chem.* **269,** 2863-2869.

Yeagle, P. L., Alderfer, J. L. & Albert, A. D. (1995a). Structure of the carboxy-terminal domain of bovine rhodopsin. *Nat. Struct. Biol.* **2,** 832-834.

Yeagle, P. L., Alderfer, J. L. & Albert, A. D. (1995b). Structure of the third cytoplasmic loop of bovine rhodopsin. *Biochemistry* **34,** 14621-14625.

Seite Leer /
Blank leaf

Curriculum Vitae

Personal:

Name:	Reto Bader
Date of birth:	April 25, 1971
Place of birth:	Bern, Switzerland
Citizenship:	Olten (SO), Switzerland
Marital status:	single

Education:

1978 – 1982	Primarschule Herrenschwanden
1982 – 1986	Sekundarschule Uettligen/Untergymnasium Bern-Neufeld
1986 – 1990	Gymnasium Bern-Neufeld, Typus B
1991 – 1996	Undergraduate studies in biology at the University of Bern emphasis: biochemistry
1995 – 1998	Undergraduate studies in mathematics at the University of Bern
1995 – 1996	Diploma thesis at the Department of Chemistry and Biochemistry at the University of Bern (Prof. B. Erni & Dr. B. Blum) subject: *RNA-Editing in Trypanosomatid Protozoa: In vitro Formation of a gRNA-mRNA Chimeric Putative Intermediate* degree: Dipl. Biol.
1998 – 2001	Ph. D. thesis at the Institute of Pharmaceutical Sciences at the ETH Zürich (Proff. G. Folkers, A. G. Beck-Sickinger & Dr. O. Zerbe) subject: *Structural Aspects of Neuropeptide Y: Implications of the Membrane-bound State for Receptor Recognition and Subtype Selection Studied by NMR.* degree: Dr. sc. nat. ETH

Publications

Cabrele, C., Langer, M., Bader, R., Wieland, H. A., Doods, H. N., Zerbe, O. & Beck-Sickinger, A. G. (2000). The First Selective Agonist for the Neuropeptide YY_5 Receptor Increases Food Intake in Rats. *J. Biol. Chem.* **275**, 36043-36048.

Bader, R., Lerch, M., Folkers, G. & Zerbe, O. (2000). Using Structural Information of Peptides, Derived from NMR Spectroscopy, in Pharmaceutical Chemistry. *Chimia* **54**, 627-632.

Bader, R., Bettio, A., Beck-Sickinger, A. G. & Zerbe, O. (2001). Structure and Dynamics of Micelle-bound Neuropeptide Y: Comparison with Unligated NPY and Implications for Receptor Selection. *J. Mol. Biol.* **305**, 307-329.

Bader, R., Rytz, G., Lerch, M., Beck-Sickinger, A. G. & Zerbe, O. (2001). The Key Motif to Gain High Affinity and Selectivity at the Neuropeptide Y_5-Receptor II: Solution Structure and Dynamics of [Ala^{31},Pro^{32}]-NPY. In preparation.